Roles of BRCA1 and BRCA2 in DNA Replication and Genome Stability

Jutta Zimmer

Lincoln College



A thesis submitted to the University of Oxford for the degree of Doctor of Philosophy

Trinity Term 2017

CRUK and MRC Oxford Institute for Radiation Oncology

Department of Oncology

University of Oxford

Contents

Acknowledgements VI

Abstract VII

Declaration VIII

Nomenclature VIII

Abbreviations IX

List of figures XV

List of tables XVII

1 Introduction 18

1.1 Breast cancer 18

1.2 Implications of BRCA1 and BRCA2 in cancer 21

1.3 Genomic instability 24

1.4 G-quadruplexes 26

1.5 Replication initiation 31

1.6 Replication stress 35

1.7 DNA damage response 45

1.8 Non-homologous end joining 48

1.9 Homologous recombination 50

1.10 Fanconi anaemia pathway 53

1.11 BRCA1 and BRCA2 in genomic stability 57

1.12 Strategies for targeting BRCA-deficient cells and tumours 61

1.13 Study aims 66

2 Materials and methods 67

2.1 Cell lines and culture conditions 67
2.2 Generation of spheroids 69
2.3 RNAi transfection 70
2.4 Cell viability assay 70
2.5 Clonogenic survival assay 71
2.6 Drug treatments 72
2.7 Fluorescence-activated cell sorting (FACS) 72
2.8 5-ethynyl-2'-deoxyuridine (EdU) incorporation 73
2.9 Mitotic index determination 73
2.10 Annexin V assay 74
2.11 Senescence-associated β-galactosidase assay 75
2.12 Metaphase spreads preparation 75
2.13 Immunofluorescence 76
2.14 Alkaline single-cell gel electrophoresis comet assay 77
2.15 DNA fibre assay 78
2.16 Immunoblotting 79
2.17 Antibodies 80
2.18 Statistical analysis 82

3 Targeting BRCA1 and BRCA2 deficiencies with G4-interacting compounds 83

3.1 Introduction 83
3.2 G4 stabiliser pyridostatin decreases viability of BRCA1- and BRCA2-deficient cells 84
3.3 Pyridostatin causes G2/M cell cycle arrest 88

3.4 Pyridostatin slows replication fork progression 89
3.5 Nascent DNA at pyridostatin-stalled forks is degraded in an MRE11-dependent manner 92
3.6 MRE11 nuclease inhibition does not rescue pyridostatin sensitivity 93
3.7 Pyridostatin-induced DNA damage can be repaired independently of BRCA2 95
3.8 POLQ is not required to prevent or repair pyridostatin-induced DNA damage 98
3.9 Olaparib-resistant BRCA1-deficient cells are sensitive to pyridostatin 102
3.10 Discussion 104

4 FANCD2 limits replication stress and genomic instability in cells lacking BRCA2 108

4.1 Introduction 108
4.2 FANCD2 and BRCA2 protect stalled replication forks via distinct mechanisms 109
4.3 FANCD2 limits replication fork progression in BRCA2-deficient cells 110
4.4 Loss of FANCD2 causes DNA damage accumulation in cells lacking BRCA2 112
4.5 FANCD2 and BRCA2 are synthetic lethal 116
4.6 Depletion of FANCD2 hypersensitises BRCA2-deficient cells to PARP inhibition 119
4.7 Discussion 120

5 Characterisation of a novel MRE11 inhibitor with activity on cell models for BRCA2 deficiency 124

5.1 Introduction 124
5.2 MU147 exhibits lower cytotoxicity than mirin 125
5.3 MU147 decreases MRN-dependent DNA end resection 126
5.4 MU147 slows DNA damage repair without affecting ATM activation .. 129
5.5 MU147 prevents MRE11 nuclease-mediated degradation of nascent DNA at stalled forks in cells lacking BRCA2 132
5.6 MU147 decreases survival of BRCA2-deficient cells and spheroids .. 134
5.7 Discussion 137
6 Discussion 139
7 References 154
8 Appendices 204
8.1 Conference proceedings 204
8.2 Publications arising from this work 206
8.3 Original copyright notices 239

Acknowledgements

I thank my supervisors Dr. Madalena Tarsounas and Dr. Anderson Ryan for giving me the opportunity to pursue my DPhil studies under their guidance. It has been a very valuable experience that allowed me to develop my academic and scientific skills immensely. I am grateful for having been able to attend and present my work at multiple international meetings and the many chances to integrate in the scientific community. I would also like to thank Cancer Research UK for funding my DPhil studies and therefore making this work possible. A special thanks goes to Lincoln College that has provided a second home for me. In particular, I would like to thank Prof. Bass Hassan and Dr. Louise Durning for their infinite support.

Thanks to all past and present lab members for all the discussions, troubleshooting and fun! Thank you, Johanna and Xianning, for the fruitful collaborations and for reading my thesis in the end. My research also greatly benefited from assistance with microscopy by Graham Brown.

A special thanks to Dr. Fedor Nikulenkov and Prof. Lumir Krejci for interesting discussions and productive collaboration!

Lastly, I want to thank my family and friends! A big thanks to my family for their support and confidence in me! My studies and experience in Oxford would not have been possible without them. Most importantly, I want to thank Gijs for his endless support at all times. You gave me so much love, strength and confidence. Thank you for always being there for me and believing in me.

Abstract

Genomic instability is a hallmark of cancer. The tumour suppressors BRCA1 and BRCA2 play key roles in genome integrity by promoting homologous recombination DNA repair and replication fork stability. Deficiency in these functions has been described as the Achilles heel of BRCA-defective tumours. This provides an important rationale for further exploring the roles of BRCA1 and BRCA2 in DNA replication and genome stability.

G-quadruplexes, alternative DNA structures formed by guanine-rich single-stranded DNA, represent natural replication fork barriers. This study demonstrates that treatment with the G-quadruplex-stabilising compound pyridostatin selectively decreases viability of BRCA1- and BRCA2-deficient cells by inducing replication stress and DNA damage.

Furthermore, this work identifies a new role of the Fanconi anaemia protein FANCD2 in limiting replication fork progression and genomic instability in human cancer cells lacking BRCA2. This function of FANCD2 is vital for BRCA2-deficient cell survival and affects treatment responses.

Finally, the data presented here reveal a synthetic lethal interaction between MRE11 nuclease and BRCA2. Characterisation of a novel chemical MRE11 nuclease inhibitor with activity on 2D and 3D cell culture models for BRCA2 deficiency highlights the clinical relevance for the use of MRE11 inhibitors for targeting BRCA2-deficient tumours.

In summary, this report describes novel roles of BRCA1 and BRCA2 relevant for selective targeting of BRCA-deficient tumour cells.

Declaration

I declare that the work presented in this thesis is wholly my own, except where stated otherwise, and that no portion of this work has been presented previously for another qualification at this or any other University.

Nomenclature

Human genes are denoted in upper case italic lettering (e.g. *BRCA2*).

Mouse genes are italicised with the first letter in uppercase and the remaining letters in lowercase (e.g. *Brca2*).

Human and mouse proteins are denoted in upper case lettering (e.g. BRCA2).

Species are denoted in italic lettering (e.g. *Caenorhabditis elegans*).

Abbreviations

˚C	degree(s) Celsius
2D	two-dimensional
3D	three-dimensional
53BP1	p53-binding protein 1
911	complex formed by RAD9, RAD1 and HUS1
A-NHEJ	alternative non-homologous end joining
ALT	alternative lengthening of telomeres
AML	acute myeloma leukaemia
ATM	ataxia telangiectasia mutated protein
ATR	ataxia telangiectasia and RAD3-related protein
ATRIP	ATR-interacting protein
BIR	break-induced replication
BLM	Bloom's syndrome protein
BRCA	breast cancer susceptibility protein, e.g. BRCA1
BSA	bovine serum albumin
C-NHEJ	classical non-homologous end joining
C. elegans	*Caenorhabditis elegans*
Cas9	CRISPR-associated protein 9
CDC	cell division cycle protein, e.g. CDC25A
CDK	cyclin-dependent kinase, e.g. CDK1
CDT1	chromatin-licensing and DNA replication factor 1
CFS	common fragile site(s)
CHD4	chromodomain helicase DNA-binding protein 4
ChIP-seq	chromatin immunoprecipitation sequencing
CHK	checkpoint kinase, e.g. CHK1
CIN	chromosomal instability
CldU	5-chloro-2′-deoxyuridine

cm	centimetre(s)
CMG	complex formed by CDC45, MCM2-7 and GINS
CO_2	carbon dioxide
CPT	camptothecin
CtIP	CTBP-interacting protein
D-loop	displacement loop
DAPI	4',6-diamidino-2-phenylindole
DDK	DBF4-dependent kinase
DDR	DNA damage response
dH_2O	distilled water
DMEM	Dulbecco's modified Eagle medium
DMSO	dimethyl sulphoxide
DNA	deoxyribonucleic acid
DNA-PK	DNA-dependent protein kinase
DNA-PKcs	DNA-dependent protein kinase catalytic subunit
DNA2	DNA replication helicase 2
DOG1	deletions of guanine-rich DNA
DOX	doxycycline
DPC	DNA-protein crosslink
DSB	double strand break
dsDNA	double-stranded DNA
DTT	dithiothreitol
ECL	enhanced chemiluminescence
EDTA	ethylene diamine tetraacetic acid
EdU	5-ethynyl-2'-deoxyuridine
EME1	essential meiotic structure-specific endonuclease 1
ER	oestrogen receptor
ERCC	excision repair cross-complementing, e.g. ERCC1
ETAA1	Ewing's tumour-associated antigen 1

EXO1	exonuclease 1
FA	Fanconi anaemia
FAAP24	Fanconi aneamia-associated protein 24
FACS	fluorescence-activated cell sorting
FAN1	Fanconi-associated nuclease
FANC	Fanconi anaemia group protein, e.g. FANCA
FBH1	F-box DNA helicase 1
FBS	foetal bovine serum
g	gravity
G-rich	guanine-rich
G4	G-quadruplex
GAPDH	glyceraldehyde 3-phosphate dehydrogenase
GEN1	GEN1, Holliday junction 5' flap endonuclease
GINS	complex formed by SLD5, PSF1, PSF2, and PSF3
h	hour(s)
HCl	hydrochloric acid
HER2	human epidermal growth factor receptor 2
HR	homologous recombination
HRP	horseradish peroxidase
hTERT	human telomerase reverse transcriptase
HU	hydroxyurea
IB	immunoblotting
ICL	interstrand crosslink
IdU	5-iodo-2′-deoxyuridine
IF	immunofluorescence
IgG	immunoglobulin G
IR	ionising radiation
K	lysine, e.g. K164
KAP1	KRAB-associated protein 1

kDa	kilo Dalton(s)
LIG	DNA ligase, e.g. LIG1
M	molar
mA	milliampere(s)
MCM	minichromosome maintenance complex component, e.g. MCM2
MDC1	mediator of DNA damage checkpoint 1
mg	milligram(s)
MHF1/2	FANCM-associated histone fold protein 1/2
MI	mirin
min	minute(s)
mL	millilitre(s)
mM	millimolar
MRE11	meiotic recombination protein 11
MRE11i	MRE11 inhibitor
MRI	magnet resonance imaging
MRN	complex formed by MRE11, RAD50 and NBS1
MSI	microsatellite instability
MU	MU147
MUS81	MUS81, structure-specific endonuclease
NBS1	Nijmegen breakage syndrome protein
NHEJ	non-homologous end joining
nm	nanometre(s)
nM	nanomolar
ORC	origin recognition complex
PAGE	polyacrylamide gel electrophoresis
PARP	poly (ADP-ribose) polymerase, e.g. PARP1
PARPi	PARP inhibitor
PBS	phosphate buffered saline
PCNA	proliferating cell nuclear antigen

PDS	pyridostatin
Pg	P-glycoprotein
PIF1	PIF1, 5’-3’ DNA helicase
POL	polymerase, e.g. POLQ
PR	progesterone receptor
pre-IC	pre-initiation complex
pre-RC	pre-replication complex
PrimPol	primase-polymerase, DNA-directed
PTIP	Pax transactivation domain-interacting protein
RAD	radiation resistance protein, e.g. RAD50
RECQL4	RECQ like helicase 4
REV1	REV1, DNA-directed polymerase
REV7	MAD2L2, mitotic arrest deficient-like 2
RFC	replication factor C
RIF1	RAP1-interacting factor 1
RMI1	RecQ-mediated genome instability protein 1
RNA	ribonucleic acid
RNF8/168	ring finger protein 8/168
ROS	reactive oxygen species
RPA	replication protein A
RT	room temperature
RTEL1	regulator of telomere elongation helicase 1
S	serine, e.g. S4
SDS	sodium dodecyl sulphate
SEM	standard error of the mean
shRNA	small hairpin RNA
siRNA	small interfering RNA
SLX4	SLX4, structure-specific endonuclease
SMARCAL1	SWI/SNF-related matrix-associated actin-dependent regulator of chromatin subfamily A-like protein 1

SMC1	structural maintenance of chromosomes protein 1
SSA	single strand annealing
SSB	single strand break
ssDNA	single-stranded DNA
T	threonine, e.g. T68
TLS	translesion synthesis
TMEJ	polymerase theta-mediated end joining
TNBC	triple negative breast cancer
TOPBP1	DNA topoisomerase II-binding protein 1
TOPIIIα	topoisomerase IIIα
TP53	tumour protein p53
Tris	tris (hydroxymethyl) aminomethane
UBE2T	ubiquitin-conjugating enzyme E2T
V	volt
WHO	World Health Organisation
WRN	Werner's syndrome protein
XLF	XRCC4-like factor
XRCC	X-ray repair complementing defective repair in Chinese hamster cells, e.g. XRCC2
ZRANB3	zinc finger RANBP2-type containing 3
µL	microlitre(s)
µm	micrometre(s)
µM	micromolar
γH2AX	phosphorylated histone H2AX

List of figures

Figure 1.1. Topologies of G4 structures. 27

Figure 1.2. Initial steps of DNA replication. 33

Figure 1.3. Restart of stalled replication forks by repriming and translesion synthesis or template switching. 37

Figure 1.4. Stalled fork restart by fork reversal. 41

Figure 1.5. Restart of collapsed forks by break-induced replication. 42

Figure 1.6. NHEJ pathways of DSB repair. 49

Figure 1.7. HR pathway of DSB repair. 51

Figure 1.8. SSA pathway of DSB repair. 53

Figure 1.9. FA pathway of ICL repair. 56

Figure 2.1. *BRCA2* disruption in the BRCA2-deficient DLD1 cell line. 68

Figure 2.2. Mechanism of DOX-inducible shRNA expression. 69

Figure 3.1. BRCA status of RPE1 and DLD1 cell lines. 84

Figure 3.2. G4 stabilisation by pyridostatin decreases viability of BRCA1- and BRCA2-deficient human cells. 87

Figure 3.3. Pyridostatin induces G2/M arrest in BRCA2-deficient cells. 88

Figure 3.4. Pyridostatin decreases replication progression. 91

Figure 3.5. Pyridostatin causes stalled forks that are degraded by MRE11. 93

Figure 3.6. Inhibition of MRE11 nuclease activity is insufficient to rescue pyridostatin-induced BRCA2-deficient cell killing. 94

Figure 3.7. Pyridostatin-induced DNA breakage is repaired in cells lacking BRCA2. 96

Figure 3.8. DNA breaks are resolved after release from pyridostatin in BRCA2-deficient cells. 97

Figure 3.9. Release from pyridostatin does not induce cell cycle arrest. 98
Figure 3.10. POLQ knockdown does not affect pyridostatin sensitivity. 99
Figure 3.11. POLQ is not required to prevent pyridostatin-induced DNA damage. 101
Figure 3.12. Olaparib-resistant BRCA1-deficient cells exhibit pyridostatin sensitivity. 103
Figure 4.1. FANCD2 and BRCA2 prevent degradation of nascent DNA at stalled replication forks via distinct mechanisms. 110
Figure 4.2. FANCD2 restricts replication in cells lacking BRCA2. 111
Figure 4.3. FANCD2 prevents DNA damage accumulation in BRCA2-deficient cells. 113
Figure 4.4. Loss of FANCD2 promotes apoptosis in cells lacking BRCA2. 114
Figure 4.5. FANCD2 depletion triggers cell death in cells lacking BRCA2. 115
Figure 4.6. FANCD2 loss induces senescence in BRCA2-depleted primary cells. 116
Figure 4.7. Depletion of FANCD2 using siRNAs in H1299 and MDA-MB-231 cell lines harbouring DOX-inducible shRNA against BRCA2. 117
Figure 4.8. FANCD2 is required for BRCA2-deficient cell survival. 118
Figure 4.9. FANCD2 dysfunction increases olaparib sensitivity of BRCA2-deficient cells. 120
Figure 5.1. MU147 is less toxic to cell viability than mirin. 126
Figure 5.2. Mirin and MU147 prevent phosphorylation of RPA on S4/8 in response to ionising radiation. 127
Figure 5.3. MU147 but not mirin decreases phosphorylation of RPA on S4/8 in response to camptothecin-induced DNA damage. 128

Figure 5.4. Mirin and MU147 delay DNA damage repair. 130
Figure 5.5. Mirin and MU147 do not affect ATM activation upon DNA damage. 131
Figure 5.6. Mirin and MU147 do not affect mitotic entry after ionising radiation. 132
Figure 5.7. Mirin and MU147 prevent MRE11-mediated degradation of nascent DNA at stalled forks in BRCA2-deficient cells. 133
Figure 5.8. MRE11 inhibition reduces BRCA2-deficient cell survival. 134
Figure 5.9. Growth of BRCA2-deficient spheroids is inhibited by chemical PARP and MRE11 inhibitors. 136
Figure 6.1. Model for G4-induced lethality in the context of BRCA deficiency. 140

List of tables

Table 1. Compounds. 72
Table 2. Primary antibodies. 80
Table 3. Secondary antibodies. 81

1 Introduction

DNA lesions, thousands of which occur spontaneously in each cell every day, continuously threaten genome integrity. Double strand breaks (DSBs), the most deleterious type of DNA breakage, arise spontaneously during DNA replication due to natural impediments that block replication fork progression, for example unusual DNA structures such as G-quadruplexes (G4s). Whilst occasional genetic alterations are beneficial for the long-term survival of a species, maintaining the genetic information encoded in DNA is essential for survival of the individual. Therefore, cells employ numerous mechanisms to assure faithful genome duplication and accurate repair of DNA damage occurring in their genomes. Failure of these pathways leads to genomic instability, a hallmark of cancer (Negrini *et al.*, 2010).

1.1 Breast cancer

Cancer, a disease that is characterised by the rampant outgrowth of abnormal cells, is a major cause of death worldwide (World Health Organisation (WHO), 2017). While breast cancer is the top cancer in women in the world (WHO, 2017), the incident rate of male breast cancers is estimated below 1 in 100,000 (Ly *et al.*, 2013). The survival rate of breast cancer varies greatly in different parts of the world ranging from less than 40% in low income countries to around 80% in high income countries (Coleman *et al.*, 2008). The differences in survival rates may be linked to variations in health care standards across countries worldwide (Coleman *et al.*, 2008). Multiple risk factors for breast cancer have been documented. One well-known risk factor is increasing age (Lacey *et al.*,

2009; Siegel *et al.*, 2016). Furthermore, the risk of developing breast cancer is elevated by personal or family history of cancer (Collaborative Group on Hormonal Factors in Breast, 2001; Lacey *et al.*, 2009). Mutations in certain genes, particularly in the tumour suppressors breast cancer susceptibility gene 1 (*BRCA1*) and 2 (*BRCA2*), strongly predispose individuals to breast cancer (see section 1.2). Additionally, reproductive factors are associated with an increased risk in developing breast cancer. This includes extended exposure to endogenous oestrogens by early menarche, late menopause and late childbirth as well as exogenous hormones by oral contraceptives and hormone replacement therapy (Lacey *et al.*, 2009; Ritte *et al.*, 2012). Environmental and lifestyle factors such as lack of physical activity, poor diet and frequent consumption of alcohol can also contribute to an elevated risk of developing breast cancer (Chen *et al.*, 2011; Danaei *et al.*, 2005; Pizot *et al.*, 2016). In fact, 21% of all breast cancer deaths worldwide have been attributed to these modifiable risk factors (Danaei *et al.*, 2005).

Importantly, early detection is key to improve cancer outcome and survival (Anderson *et al.*, 2008). Breast cancer can be detected by breast screening using X-rays (mammograms), ultrasound or magnet resonance imaging (MRI) (Shah *et al.*, 2014). If a suspicion for cancer exists, a biopsy is performed to isolate tissue and investigate the cells microscopically. After breast cancer diagnosis, certain tests are performed to determine the stage of the cancer, prognosis and type of treatment (Yeo *et al.*, 2014). Examples of factors evaluated in these tests include Ki-67, oestrogen receptor (ER), progesterone receptor (PR) and human epidermal growth factor receptor 2 (HER2). Ki-67

expression is indicative of the proliferation rate of cancer cells, whilst ER, PR and HER2 are important determinants for treatment decisions.

Local therapies for breast cancer include surgery and radiotherapy (Turner *et al.*, 2008a). These treatments are most commonly used for early stage cancers. Systemic therapies like chemotherapy, hormone therapy and targeted therapy are administered through the blood stream (Turner *et al.*, 2008b). Chemotherapeutic agents include cytotoxic compounds that induce DNA damage, prevent DNA/RNA synthesis or interfere with cell division (Anampa *et al.*, 2015; Palumbo *et al.*, 2013). Hormone therapy manipulates the endocrine system either by inhibiting hormone synthesis, antagonising hormone receptors or supplementing with specific hormones (Abdulkareem *et al.*, 2012; Jones *et al.*, 2004), and targeted therapy inhibits growth-promoting factors (Palumbo *et al.*, 2013). Additionally, prophylactic therapy with tamoxifen has been administered to women with a high risk for developing breast cancer (Nazarali *et al.*, 2014), which lowers incidents of the disease by 38% (Cuzick *et al.*, 2003).

Between 10-20% of breast cancers are triple negative defined by the absence of ER, PR and HER2 overexpression (Anders *et al.*, 2009). Patients with triple negative breast cancer (TNBC) have an overall poor prognosis. This can be linked to the aggressive pathological features of TNBC (Dent *et al.*, 2007) and the higher rate of early reoccurrence and distal metastasis to brain and lungs compared to other types of breast cancers (Dent *et al.*, 2009; Sorlie *et al.*, 2001). A disproportionally large part of breast cancer mortality is caused by TNBC (Schneider *et al.*, 2008). Treatment options are limited as TNBC do not respond to established hormonal therapy or HER2-targeted therapies. Instead, they are usually treated with a combination of surgery, radiotherapy,

targeted therapy and chemotherapy (Wahba *et al.*, 2015). Additionally, studies on the benefits of various adjuvant and neoadjuvant chemotherapies are being performed (Liedtke *et al.*, 2008; Wahba *et al.*, 2015). One promising approach for targeting TNBC is exploiting their similarity to *BRCA*-related tumours (Wahba *et al.*, 2015). Given that poly (ADP-ribose) polymerase (PARP) inhibitors have proven effective in *BRCA*-associated cancers (Tutt *et al.*, 2010), efficacy of this class of compounds in TNBC is currently being assessed in clinical trials (for example see ClinicalTrials.gov identifier: NCT02401347, NCT02498613, NCT02657889).

A study by Gonzalez-Angulo *et al.* (2011) identified *BRCA* mutations in 19.5% of TNBC patients with 15.6% attributed to *BRCA1* and 3.9% to *BRCA2*. Another study reported that 20% of TNBC had somatic or germ line mutations in *BRCA1* or *BRCA2* (Cancer Genome Atlas, 2012). Therefore, women diagnosed with TNBC may benefit from *BRCA1* and *BRCA2* genetic testing (Greenup *et al.*, 2013; Phuah *et al.*, 2012).

1.2 Implications of BRCA1 and BRCA2 in cancer

BRCA1 and *BRCA2* were identified as breast cancer susceptibility genes in the mid 1990s (Miki *et al.*, 1994; Wooster *et al.*, 1995). Despite *BRCA1* and *BRCA2* mutations accounting for only 2-3% of all breast cancers (Ford *et al.*, 1995; Newman *et al.*, 1997), mutations in other susceptibility genes are detected in even less cases (Wooster *et al.*, 2003). Mutations in *BRCA1* or *BRCA2* are found in 25% of hereditary breast and ovarian cancers (Kast *et al.*, 2016). In ovarian cancers, germ line mutations in *BRCA1* and *BRCA2* are evident in 9%

and 8% of cases, respectively, and somatic mutations in either one of these genes in another 3% (Cancer Genome Atlas Research, 2011). Analysis of 507 women with breast tumours revealed 47 cases with germ line mutations in homologous recombination (HR) genes including *BRCA1* and *BRCA2* (Cancer Genome Atlas, 2012). With sequencing technologies advancing, more than 25 genes have been linked to familial breast and/or ovarian cancer risk (Nielsen *et al.*, 2016).

Strikingly, a germ line mutation in one copy of the tumour suppressor genes *BRCA1* or *BRCA2* that impairs their normal function is sufficient to predispose women to breast and ovarian cancer (Peto *et al.*, 1999). While the general risk of women for developing breast cancer is about 12%, the risk in *BRCA1* and *BRCA2* mutation carriers is up to 65% and 49% respectively, by age 70 years (Antoniou *et al.*, 2003; Chen *et al.*, 2007). For ovarian cancer, the average risk is estimated to be 1.3%, and is increased to up to 40% in *BRCA1* and 18% in *BRCA2* mutation carriers (Antoniou *et al.*, 2003; Chen *et al.*, 2007). Individuals with heterozygous mutations in *BRCA1* or *BRCA2* have 82% lifetime risk of breast cancer, as well as 54% and 23% risk of ovarian cancer, respectively (King *et al.*, 2003). A recent study by Kuchenbaecker *et al.* (2017) estimated a breast cancer risk of 72% for *BRCA1* and 69% for *BRCA2* mutation carriers, by age 80 years. For ovarian cancer, *BRCA1* mutations were associated with a risk of 44% and *BRCA2* mutations with a risk of 16% (Kuchenbaecker *et al.*, 2017).

The tissue- and gender-specific tumour suppression mediated by BRCA1 and BRCA2 is not fully understood thus far. Studies suggest that a role of BRCA1 in hormone expression and signalling could be an important parameter (Hu, 2009). Nonetheless, *BRCA1* and *BRCA2* mutations also relate to elevated

risk of pancreatic, stomach, laryngeal, fallopian tube, and prostate cancer (Roy *et al.*, 2012; Venkitaraman, 2009).

Chromosomal abnormalities are a hallmark of BRCA-defective cells (Gretarsdottir *et al.*, 1998; Patel *et al.*, 1998; Tirkkonen *et al.*, 1997; Xu *et al.*, 1999b; Yu *et al.*, 2000) and a common feature of genomic instability (see section 1.3). Consistently, loss of BRCA1 or BRCA2 function causes severe proliferation defects and p53-dependent checkpoint activation leading to early embryonic lethality in mice (Ludwig *et al.*, 1997; Sharan *et al.*, 1997; Suzuki *et al.*, 1997). Therefore, it may seem paradoxical that mutations in *BRCA1* or *BRCA2* are associated with cancer predisposition in humans. However, *BRCA* heterozygosity is not lethal (Hakem *et al.*, 1996; Ludwig *et al.*, 1997; Suzuki *et al.*, 1997). Therefore, it is likely that, during tumourigenesis, checkpoint inactivation occurs before loss of the second *BRCA* allele (Goggins *et al.*, 2000). In line with this concept, mutations in tumour suppressor genes *TP53*, ataxia telangiectasia mutated (*ATM*) and checkpoint kinase 2 (*CHK2*) comply with loss of BRCA function in tumourigenesis (Crook *et al.*, 1998; Phillips *et al.*, 1999; Ramus *et al.*, 1999; Sullivan *et al.*, 2002; Tommiska *et al.*, 2008).

Recapitulation of the cancer susceptibility associated with BRCA deficiency has been attempted using mouse models. However, heterozygous *Brca* mutations are insufficient to induce cancer predisposition in these systems. Nonetheless, concomitant p53 dysfunction promotes tumour formation in mammary gland epithelium conditionally deleted in *Brca1* or *Brca2* (Jonkers *et al.*, 2001; Xu *et al.*, 1999a). Consistently, the frequency of *TP53* mutations is higher in breast cancers with germ line mutations in *BRCA1* or *BRCA2* compared to sporadic breast cancers (Greenblatt *et al.*, 2001). Little is known

about other tumour induction mechanisms upon loss of BRCA tumour suppressor functions. Nonetheless, Skoulidis *et al.* (2010) demonstrated that a heterozygous pathogenic *Brca2* truncation results in tumour formation in a murine $Kras^{G12D}$ model, irrespective of p53 status.

BRCAness is a term commonly used for the phenotype displayed by cancers defective in HR. Tumours with BRCAness share molecular features with *BRCA*-mutated tumours and in turn exhibit similar responses to therapies. Besides BRCA1 and BRCA2, dysfunction in HR-related factors including ataxia telangiectasia and RAD3-related protein (ATR), ATM, CHK1/2, Fanconi anaemia group protein A (FANCA), FANCC, FANCD2, Nijmegen breakage syndrome protein (NBS1), radiation resistance protein 51 (RAD51) and RAD54 has been shown to display similar treatment responses (McCabe *et al.*, 2006). HR-deficient tumours have been reported to harbour characteristic mutation signatures caused by the use of error-prone DNA repair mechanisms (Moynahan *et al.*, 2001; Tutt *et al.*, 2001; Xia *et al.*, 2001). Whole-genome analysis could therefore help to identify tumours with BRCAness. The structural rearrangement signatures of BRCAness are thought to allow for prediction of the patient's response to various chemotherapies (Watkins *et al.*, 2014). Importantly, BRCAness features likely stem from extreme genomic instability.

1.3 Genomic instability

Genomic instability is a characteristic of most cancers, defined as an increased propensity for the acquisition of mutations (Lee *et al.*, 2016a). Various forms of genomic instability exist including chromosomal instability (CIN), microsatellite

instability (MSI) and elevated frequency of base pair mutations (Negrini *et al.*, 2010). CIN, a phenomenon that is defined by continuous changes in chromosome structure and number over time (Nowell, 1976), is the most common kind of genomic instability in tumours (Negrini *et al.*, 2010). A second form of genomic instability, MSI, is characterised by the expansion or contraction of repetitive sequences in microsatellites (Fishel *et al.*, 1993; Leach *et al.*, 1993). The cause of genomic instability remains a subject of debate. Two key models have been proposed: the mutator hypothesis and the oncogene-induced replication stress model. The classic mutator hypothesis states that mutations in caretaker genes trigger genomic instability in precancerous lesions, which causes higher mutation rates and drives tumourigenesis (Loeb, 1991; Loeb *et al.*, 1974; Nowell, 1976). Caretaker genes or tumour suppressor genes are essential to maintain genomic instability and are often involved in the DNA damage response (Kinzler *et al.*, 1997). The oncogene-induced replication stress model postulates that genomic instability caused by oncogene activation is linked to DNA replication stress (Cleaver, 2005). This model is supported by the fact that common fragile sites (CFS), which are hotspots of replication stress (Durkin *et al.*, 2007), are preferentially affected by genomic instability upon oncogene activation (Bartkova *et al.*, 2005; Bartkova *et al.*, 2006; Di Micco *et al.*, 2006; Gorgoulis *et al.*, 2005; Tsantoulis *et al.*, 2008). Furthermore, there is evidence that a dysfunctional mitotic checkpoint could contribute to genomic instability (Kops *et al.*, 2005; Lee *et al.*, 2016a). Defects in this checkpoint, which ensures proper segregation of metaphase chromosomes, cause CIN phenotypes (Jeganathan *et al.*, 2007; Michel *et al.*, 2001; Rao *et al.*, 2005). Moreover, telomere erosion has been proposed to induce genomic instability in

cancer (Artandi *et al.*, 2000). In healthy cells, age-associated telomere shortening triggers senescence (Bodnar *et al.*, 1998). However, upon failure of this process, telomere attrition can cause CIN thereby driving cancer development (Artandi *et al.*, 2000; Davoli *et al.*, 2010; Hastie *et al.*, 1990; O'Sullivan *et al.*, 2002; Rudolph *et al.*, 2001). Besides the DNA-end replication problem, synthesis of telomeric DNA is complicated by the formation of non-canonical DNA conformations including G4s (Gilson *et al.*, 2007).

1.4 G-quadruplexes

G4s are secondary DNA structures formed spontaneously by DNA sequences consisting of stretches of guanines (G-tracts) separated by other bases (Gellert *et al.*, 1962). Stacks of G-quartets, square planar arrangements of four Hoogsteen-bond guanines, are stabilised by monovalent cations such as Na^+ and K^+ to allow the formation of four-stranded helical structures (Mergny *et al.*, 2005). The topology of G4 structures is very diverse (Figure 1.1). Intramolecular G4s are formed by a single DNA strand, whereas intermolecular G4s are formed by two or four DNA strands in a parallel or antiparallel orientation (Burge *et al.*, 2006; Patel *et al.*, 2007). G4 topology and stability is determined by the number of G-quartets as well as the loop length and composition formed by non-guanine bases (Risitano *et al.*, 2004; Vorlickova *et al.*, 2005; Wang *et al.*, 1993).

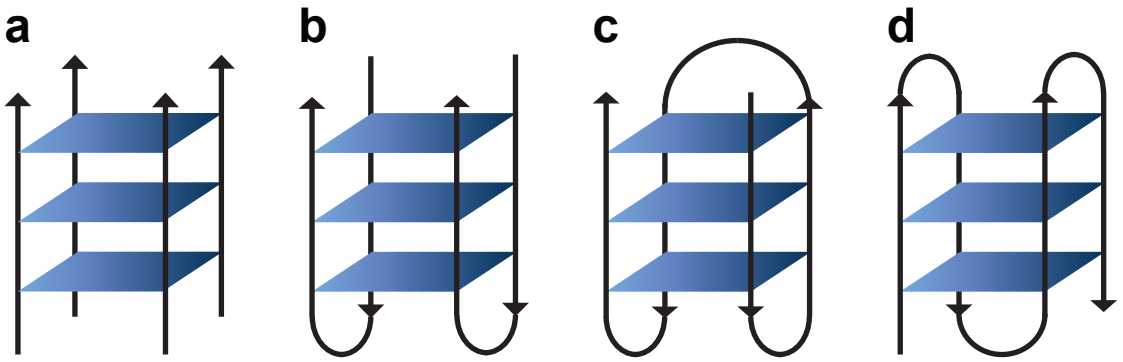


Figure 1.1. Topologies of G4 structures.
(**a**) Tetramolecular parallel structure. (**b**) Bimolecular antiparallel structure with adjacent parallel strands. (**c**) Unimolecular antiparallel structure with alternating parallel strands. (**d**) Unimolecular antiparallel structure with adjacent parallel strands and a diagonal loop. Adapted from Huppert (2008) with permission from The Royal Society of Chemistry.

In the late 1980s, telomeres were the first biologically relevant genomic sites found to adopt G4 configurations (Henderson *et al.*, 1987; Sen *et al.*, 1988; Sundquist *et al.*, 1989). The telomeric ends of chromosomes are substrates for G4 formation due to their repetitive TTAGGG sequence ending with a guanine-rich (G-rich) 3' overhang. In more recent years, computational analyses of the human genome detected more than 300,000 sites with G4-forming potential using the consensus sequence $G_{\geq 3}N_{1\text{-}7}G_{\geq 3}N_{1\text{-}7}G_{\geq 3}N_{1\text{-}7}G_{\geq 3}$ (Huppert *et al.*, 2005; Todd *et al.*, 2005). However, a different algorithm predicted that the number of sequences capable of G4 formation is significantly higher (Bedrat *et al.*, 2016). Importantly, a newly developed experimental G4-seq technique identified more than 700,000 G4 structures genome-wide (Chambers *et al.*, 2015).

Despite their abundance, G4s possess the potential to cause genomic instability due to their ability to obstruct replication fork progression (Lopes *et al.*, 2011; Paeschke *et al.*, 2011; Ribeyre *et al.*, 2009). Additionally, G4-forming DNA sequences are highly recombinogenic and mutagenic (Cahoon *et al.*, 2009; Piazza *et al.*, 2010; Ribeyre *et al.*, 2009), a characteristic related to

tumourigenesis (De *et al.*, 2011). Indeed, G4s have been linked to cancer development due their affiliation with oncogenes, tumour suppressors and somatic copy number alterations (Chambers *et al.*, 2015).

Thus, G4 formation has to be tightly regulated to preserve genome stability. The Bloom's (BLM) and Werner's (WRN) syndrome helicases are thought to remove G4s during DNA replication due to their G4-unwinding capacity *in vitro* (Fry *et al.*, 1999; Huber *et al.*, 2002; Mohaghegh *et al.*, 2001; Sun *et al.*, 1998). Elegant studies in *Caenorhabditis elegans* (*C. elegans*) suggest that the DOG1 helicase resolves G4s in order to prevent G4-associated genomic instability (Cheung *et al.*, 2002). Introduction of a G4 sequence into the *C. elegans* genome was highly mutagenic and DOG1 was required to prevent genomic rearrangements at G4 sites (Kruisselbrink *et al.*, 2008). Castillo Bosch *et al.* (2014) showed in *Xenopus* egg extracts that the vertebrate DOG1 homologue FANCJ is crucial for dismantling G4s to allow replication through these structures. Consistently, human FANCJ preferentially unwinds G4s *in vitro* (London *et al.*, 2008; Wu *et al.*, 2008). Supporting a role of FANCJ in G4 resolution, patient cells expressing a truncated form of FANCJ lacking the helicase domain accumulate deletions in the proximity of G4-forming sequences (London *et al.*, 2008). Furthermore, human cells depleted in FANCJ exhibit impaired proliferative capacity and elevated levels of DNA damage and apoptosis upon treatment with the G4-interacting compound telomestatin (Wu *et al.*, 2008). However, FANCJ knockout mouse cells are not sensitive to G4-stabilising agents (Matsuzaki *et al.*, 2015). In DT40 chicken cells, FANCJ mediates epigenetic stability by coordinating the actions of BLM, WRN and the Y-family polymerase REV1 (Sarkies *et al.*, 2012). REV1 is required for effective

replication of G4-forming sequences (Sarkies *et al.*, 2010), which can be linked to its ability to disrupt G4 structures *in vitro* (Eddy *et al.*, 2014). Additionally, PrimPol mediates restart of DNA replication downstream of G4s through its primase and polymerase function (Schiavone *et al.*, 2016). At chromosome ends, regulator of telomere length 1 (RTEL1) counteracts telomeric G4 assembly to prevent telomere fragility (Vannier *et al.*, 2012). While work in yeast first described a role of PIF1 helicase in suppressing G4-associated genome instability (Lopes *et al.*, 2011; Paeschke *et al.*, 2013; Paeschke *et al.*, 2011; Ribeyre *et al.*, 2009), human PIF1 seems to play a similar role (Rodriguez *et al.*, 2012; Sanders, 2010).

In line with the challenges G4 structures present during various cellular processes, stabilisation of G4s induces DNA breaks (Rodriguez *et al.*, 2012). In worms, the main mechanism for repair of these lesions is provided by polymerase theta (Polθ)-mediated end joining (TMEJ) (Koole *et al.*, 2014). Additionally, HR has been implicated in the repair of G4-associated DSBs in various organisms including *Neisseria gonorrhoeae*, *C. elegans* and *Saccharomyces cerevisiae* (Cahoon *et al.*, 2009; Lopes *et al.*, 2011; Ward *et al.*, 2007; Youds *et al.*, 2006). However, which repair pathways are activated in response to G4-induced DNA damage in human cells has not been studied extensively. Depletion of human translesion polymerases eta (Polη) and kappa (Polκ) sensitises cells to G4-stabilising compound telomestatin (Betous *et al.*, 2009) implicating translesion synthesis in the replication of G4 structures in human cells. Furthermore, a study by McLuckie *et al.* (2013) suggests that defects in non-homologous end joining (NHEJ) and HR enhance cell survival defects synergistically with chemical G4 stabilisation. Nonetheless, the

contribution of HR and other pathways to the prevention and repair of G4-associated DNA damage remains to be fully elucidated. This will be important to improve our understanding of HR involvement in preserving genome stability specifically in the context of G4s, which may be relevant for developing therapies for the treatment of HR-defective tumours.

In this regard, the distinct physiochemical and structural characteristics of G4s are key for the design of chemical G4 ligands and structure-specific antibodies. These reagents have proven useful in visualising G4s *in vivo* and studying their biological functions (Biffi *et al.*, 2013; Henderson *et al.*, 2014; Lam *et al.*, 2013; Muller *et al.*, 2010; Schaffitzel *et al.*, 2001).

Rodriguez *et al.* (2012) demonstrated that the G4-interacting small molecule pyridostatin causes replication- and transcription-dependent DNA damage. During transcription and replication, the DNA duplex is transiently unwound giving rise to single-stranded DNA (ssDNA). Thus, these processes provide an opportunity for the formation of G4s. Importantly, chromatin immunoprecipitation sequencing (ChIP-seq) analysis confirmed that the DNA damage marker phosphorylated histone variant H2AX (γH2AX) was associated with DNA sequences predicted to have G4-forming potential (Rodriguez *et al.*, 2012). Therefore, G4 stabilisation by pyridostatin interferes with transcription and replication ultimately causing DNA breakage. Notably, a structure-specific antibody enabled visualisation of G4s in cancer cells and tumours (Biffi *et al.*, 2013; Biffi *et al.*, 2014). G4 foci formation was elevated in S phase cells and increased upon pyridostatin treatment. Altogether, these studies suggest that G4-stabilising compounds and structure-specific antibodies allow for selective tracing of G4 structures, an important feature of druggable targets.

Importantly, the location of G4s is non-random. G4s are enriched in functional regions in the genome such as 5' untranslated regions and splicing sites (Chambers *et al.*, 2015). The conserved presence of G4s in biologically significant genomic regions suggests that G4 formation may have vital regulatory functions. Indeed, the biological relevance of G4s has become increasingly evident. Studies show that G4 formation influences processes including gene expression and replication initiation. For example, a G4 in the promoter of the *MYC* oncogene acts as a silencer element (Siddiqui-Jain *et al.*, 2002). On the contrary, a genome-wide study by Hansel-Hertsch *et al.* (2016) discovered that endogenous G4s in promoters are associated with elevated transcription levels. Interestingly, G4 motifs are highly enriched at replication origins, especially at frequently used ones (Besnard *et al.*, 2012; Cayrou *et al.*, 2011; Cayrou *et al.*, 2012), and have been shown to be required for replication initiation *in vivo* (Valton *et al.*, 2014).

1.5 Replication initiation

DNA replication is a process that duplicates the genome before cell division occurs. The replication machinery, the so-called replisome, is a complex consisting of specialised proteins that ensure accurate and efficient replication during each round of the cell cycle (Leman *et al.*, 2013). In brief, the double-stranded DNA (dsDNA) is unwound by the replicative helicase generating a replication fork with two ssDNA template strands. DNA polymerases then synthesise a new DNA strand complementary to each original DNA template strand. The replication process enables copying of each DNA helix in a cell into

two DNA helices, where one strand originates from the parental duplex DNA and the other one is the nascent antiparallel strand. This mechanism is called semiconservative replication, a process that is highly conserved from prokaryotes to eukaryotes (Meselson *et al.*, 1958). Despite the antiparallel nature of duplex DNA, all DNA polymerases incorporate nucleotides with 5' to 3' directionality (Hubscher *et al.*, 2000). Polymerase epsilon (Polε) continuously synthesises the leading strand (Pursell *et al.*, 2007), while the lagging strand is synthesised in discontinuous stretches of 100–200 base pairs, known as Okazaki fragments (Okazaki *et al.*, 1968), by polymerase delta (Polδ) (Nick McElhinny *et al.*, 2008). The replicative primase polymerase alpha (Polα) synthesises RNA-DNA hybrid primers at replication origins to initiate replication of the leading strand as well as on the 5' end of each Okazaki fragment (Hubscher *et al.*, 2000).

Replication activation includes two distinct steps: origin licensing and firing. During origin licensing, the pre-replication complex (pre-RC) site is recognised and during origin firing, DNA synthesis is initiated (Fragkos *et al.*, 2015). Importantly, origin usage is flexible (Cayrou *et al.*, 2011) and licensing of an origin does not necessarily imply firing of that origin (DePamphilis, 1993; Taylor, 1977). How licensed origins are chosen remains to be elucidated (Mechali, 2010). Nonetheless, there are various reasons why the uncoupling of licensing and firing is crucial. Firstly, the two-step mechanism is important to limit replication to once per cell cycle and avoid re-replication. Secondly, it allows for adaptation of DNA replication to structural organisation of chromosomes, cell cycle progression, cell growth conditions, DNA damage, gene expression and cell identity (Fragkos *et al.*, 2015).

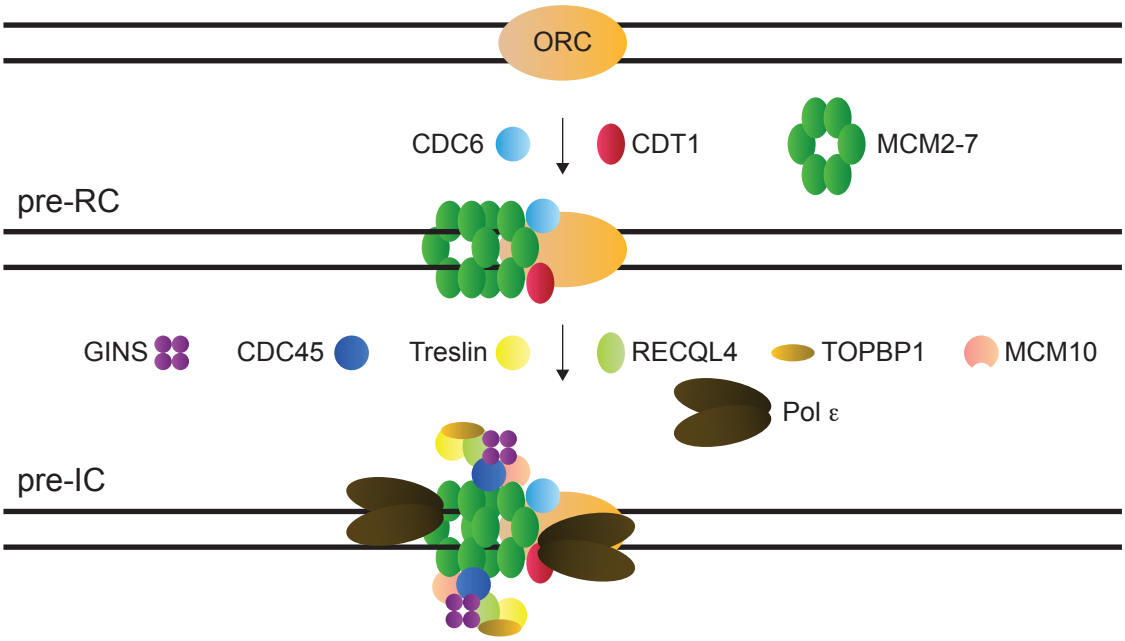


Figure 1.2. Initial steps of DNA replication.
After binding of ORC to a replication origin, CDC6 and CDT1 are recruited. Loading of a double hexamer of MCM2-7 completes the formation of the pre-replication complex (pre-RC) and licensing of the origin. Upon stimulation by CDK and DDK, the pre-initiation complex (pre-IC) is assembled. This involves binding of GINS, CDC45, Treslin, RECQL4, TOPBP1, MCM10 and Pol ε to the pre-RC.

The first step of origin licensing is the binding of the origin recognition complex (ORC) to the replication origin (Figure 1.2). ORC consists of six subunits (ORC1-ORC6). In vertebrates, ORC6 only interacts weakly with the ORC1-ORC5 complex despite being required for DNA synthesis (Prasanth *et al.*, 2002; Siddiqui *et al.*, 2007; Thomae *et al.*, 2011; Vashee *et al.*, 2003). In G1 phase, chromatin-licensing and DNA replication factor 1 (CDT1) and cell division cycle protein 6 (CDC6) bind to origins of replication and recruit MCM2-7 (Cook *et al.*, 2004). Double hexamers of MCM2-7 are loaded (Evrin *et al.*, 2009; Gambus *et al.*, 2011; Remus *et al.*, 2009) leading to the formation of the pre-RC (Figure 1.2) that licenses the origin. Once replication origins are licensed, relicensing during the same S phase is prevented by interaction of CDT1 with its inhibitor

Geminin (Tada *et al.*, 2001; Wohlschlegel *et al.*, 2000) as well as ORC1 and CDT1 ubiquitination and degradation (Li *et al.*, 2003; Mendez *et al.*, 2002; Nishitani *et al.*, 2006; Takeda *et al.*, 2005). Additionally, several other initiation factors are inactivated by phosphorylation. For example, CDC6 and MCM proteins are phosphorylated and subsequently translocated from the nucleus into the cytoplasm (Coverley *et al.*, 2000; Delmolino *et al.*, 2001; Nguyen *et al.*, 2000; Petersen *et al.*, 1999).

Licensed origins can be fired at the onset of S phase through multiple phosphorylation events mediated by cyclin-dependent kinase (CDK) and DBF4-dependent kinase (DDK). This triggers formation of the pre-initiation complex (pre-IC, Figure 1.2) by binding of CDC45, GINS, DNA topoisomerase II-binding protein 1 (TOPBP1), REQL4, Treslin, MCM10 and Polε to the pre-RC (Fragkos *et al.*, 2015). The inactive MCM double hexamer is phosphorylated by DDK (Francis *et al.*, 2009; Sheu *et al.*, 2006; Sheu *et al.*, 2010; Sun *et al.*, 2014) leading to disassembly into two active hexamers (Costa *et al.*, 2014). This enables formation of the CMG complex, which consists of CDC45, MCM2-7 and GINS (Aparicio *et al.*, 2009; Moyer *et al.*, 2006). CDK-mediated phosphorylation of Treslin promotes its interaction with TOPBP1, a factor required for CMG helicase activation (Boos *et al.*, 2011; Kumagai *et al.*, 2010; Kumagai *et al.*, 2011). Finally, origin melting occurs and the duplex DNA is unwound by the CMG complex generating two divergent replication forks (Costa *et al.*, 2011; Ilves *et al.*, 2010). Coupling of the replicative helicase and polymerases allows for the formation of a centralised replisome, which is important to coordinate leading and lagging strand synthesis (Leman *et al.*, 2013). In yeast, the active CMG complex is coupled to Polε or Polδ through a process mediated by SLD2,

SLD3, SLD7, and DPB11 as well as CDK and DDK (Kamimura *et al.*, 1998; Kamimura *et al.*, 2001; Masumoto *et al.*, 2002; Tanaka *et al.*, 2007; Tanaka *et al.*, 2011; Zegerman *et al.*, 2007; Zou *et al.*, 1998). TOPBP1, RECQL4 and Treslin are the functional homologues of DPB11, SLD2 and SLD3, respectively (Kumagai *et al.*, 2010; Makiniemi *et al.*, 2001; Matsuno *et al.*, 2006). TOPBP1 is needed to load CDC45, RECQL4 and Polε onto chromatin (Hashimoto *et al.*, 2003; Matsuno *et al.*, 2006; van Hatten *et al.*, 2002). Hereof, Treslin interacts with TOPBP1 to recruit CDC45 (Kumagai *et al.*, 2010). Another important component of the replisome, replication factor C (RFC), recognises primer template junctions and loads proliferating cell nuclear antigen (PCNA) (Furukawa *et al.*, 2003; Tsurimoto *et al.*, 1990). PCNA forms a trimeric ring structure that interacts with the DNA polymerase to stabilise the interaction with the DNA template. Thus, the sliding clamp PCNA is an essential cofactor that improves processivity of the DNA polymerase (Chilkova *et al.*, 2007; Majka *et al.*, 2004).

1.6 Replication stress

Replication stress is a phenomenon defined by the slowing or stalling of the replication fork (Zeman *et al.*, 2014). Replication stress can originate not only from physical obstacles such as secondary DNA structures (e.g. G4s), RNA-DNA hybrids and DNA lesions but also from shortage of nucleotides, repetitive DNA sequences, fragile sites and oncogene-induced stress (Zeman *et al.*, 2014). Replication stress is usually associated with the formation of long ssDNA stretches coated by replication protein A (RPA). Accumulation of ssDNA is often

caused by uncoupling of the DNA polymerase and the replicative helicase (Pacek *et al.*, 2004). The ssDNA stretches adjacent to newly synthesised dsDNA at stalled forks represent a primer-template junction (Byun *et al.*, 2005). This structure leads to the activation of the replication stress response (see section 1.7) initiated by recruitment of the protein kinase ATR (MacDougall *et al.*, 2007; Zou *et al.*, 2003a). The two key signalling functions of ATR at stalled forks include checkpoint activation to inhibit cell cycle progression and suppression of late origin firing (Tercero *et al.*, 2001). Additionally, ATR assists in stabilising and restarting arrested forks (Trenz *et al.*, 2006). There are multiple ways, by which completion of DNA synthesis can be ensured. In most cases of replication fork stalling, ATR licenses firing of dormant origins as a compensatory mechanism to rescue stalled replication forks (Ge *et al.*, 2007; Woodward *et al.*, 2006).

However, replication fork restart is required if converging replication forks stall in an origin-poor region (Berti *et al.*, 2016; Cortez, 2015). Due to the discontinuous manner of lagging strand synthesis, bypass of lesions on the lagging strand does not pose a major challenge. On the contrary, repriming and resuming replication downstream of a lesion on the leading strand generates an unreplicated ssDNA gap (Elvers *et al.*, 2011; Heller *et al.*, 2006; Lopes *et al.*, 2006; Yeeles *et al.*, 2011). PrimPol has recently been shown to mediate repriming in eukaryotic cells. Its function as a primase and a polymerase enables *de novo* DNA synthesis initiation after fork stalling (Bianchi *et al.*, 2013; Garcia-Gomez *et al.*, 2013; Mouron *et al.*, 2013). This is associated with the formation of a ssDNA gap.

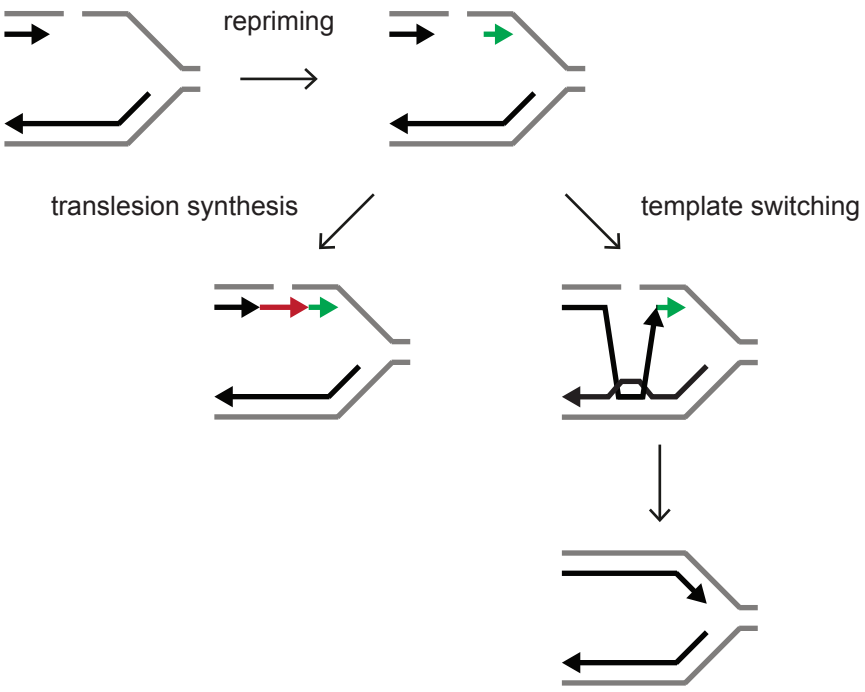


Figure 1.3. Restart of stalled replication forks by repriming and translesion synthesis or template switching.
DNA synthesis at a stalled fork is restarted by repriming (green arrow), which results in a ssDNA gap. This lesion is filled in by translesion synthesis or template switching as illustrated.

DNA damage tolerance mechanisms are required to prevent catastrophic accumulation of unresolved ssDNA gaps and collapse into DSBs (Berti *et al.*, 2016). Figure 1.3 shows how the ssDNA gap resulting from repriming can be filled in by postreplication repair through translesion synthesis or template switching (Karras *et al.*, 2010). PCNA ubiquitination is implicated in the choice between the two repair mechanisms (Hoege *et al.*, 2002). While monoubiquitinated PCNA triggers error-prone translesion synthesis, polyubiquitinated PCNA channels cells into template switching (Stelter *et al.*, 2003). PCNA is monoubiquitinated at its conserved lysine 164 (K164) residue by the concerted actions of E3 ubiquitin ligase RAD18 and its associated E2 ubiquitin-conjugating enzyme RAD6 (Hoege *et al.*, 2002; Kannouche *et al.*, 2004; Stelter *et al.*, 2003). Monoubiquitinated PCNA recruits translesion

polymerases to stalled forks to substitute for the replicative polymerase (Freudenthal *et al.*, 2010; Kannouche *et al.*, 2004; Watanabe *et al.*, 2004). Specialised translesion polymerases allow replication across DNA lesions at the risk of generating mutations (Waters *et al.*, 2009). Importantly, PCNA can further be polyubiquitinated at K63 by yeast E3 ubiquitin ligase RAD5 (Hoege *et al.*, 2002) or the human orthologues SHPRH (Motegi *et al.*, 2006; Unk *et al.*, 2006) and HLTF (Motegi *et al.*, 2008; Unk *et al.*, 2008). Through interaction with RAD18, RAD5 recruits the E2 ubiquitin-conjugating enzymes UBC13/MMS2 to activate template switching (Haracska *et al.*, 2004; Ulrich *et al.*, 2000). Recently, template switching was shown to also be promoted by the RAD9-RAD1-HUS1 (911) complex and exonuclease 1 (EXO1) (Karras *et al.*, 2013). Template switching is a mostly error-free mechanism that bypasses the lesion by sister chromatid pairing, i.e. using the newly synthesised strand as a template to fill the gap (Zhang *et al.*, 2005). However, rearrangements can arise from misalignment of repetitive DNA sequences (Goldfless *et al.*, 2006). Strand invasion into the homologous duplex is mediated by RAD51 nucleofilaments (Branzei *et al.*, 2008). Thus, sister chromatid junctions are formed by annealing the lesion-containing strand to the newly synthesised double-stranded chromatid forming a three-stranded duplex (Giannattasio *et al.*, 2014). This leads to the formation of a displacement loop (D-loop) that can be expanded through Polδ-dependent DNA synthesis (Torres-Ramos *et al.*, 1997; Vanoli *et al.*, 2010). Template switching structures are resolved by BLM helicase and topoisomerase III (Liberi *et al.*, 2005; Mankouri *et al.*, 2011). Furthermore, persistent sister chromatid junctions generated by template switching can be cleaved by MUS81 nuclease (Ashton *et al.*, 2011; Mankouri *et al.*, 2011).

Importantly, translesion synthesis and template switching activities are not limited to S phase but also promote lesion tolerance in G2/M phase (Karras *et al.*, 2010). Altogether, template switching is a key mechanism to prevent mutations triggering genomic instability (Gao *et al.*, 2017).

Another mechanism that mediates fork restart is fork reversal, a process that occurs in two steps (Figure 1.4; Neelsen *et al.* (2015)). Firstly, the replication fork is remodelled into a four-way structure by annealing of the nascent DNA strands. Secondly, the reversed fork is restarted. Fork reversal has been postulated to prevent replication across lesions, which induces DNA damage accumulation, and to expand the time for DNA repair of lesions (Neelsen *et al.*, 2013; Ray Chaudhuri *et al.*, 2012; Zellweger *et al.*, 2015). In this regard, Neelsen *et al.* (2015) describe fork reversal as "an 'emergency brake' that transiently protects replication forks in the face of DNA damage". In recent years, multiple proteins have been implicated in fork reversal. F-box DNA helicase 1 (FBH1) promotes fork reversal *in vitro* and catalyses fork regression *in vivo* (Fugger *et al.*, 2015). Additionally, RAD51 has been proposed to mediate reannealing of nascent DNA strands to promote fork reversal (Zellweger *et al.*, 2015). A recent study reported a role of BRCA2 and RAD51 in protecting nascent DNA at reversed forks from meiotic recombination protein 11 (MRE11)-mediated degradation and in recruiting Polα for replication resumption (Kolinjivadi *et al.*, 2017). Due to their DNA helicase and translocase activity, unwinding and nascent DNA annealing to reverse stalled replication forks can be performed simultaneously by RAD54, SMARCAL1 and ZRANB3 (Bugreev *et al.*, 2011; Ciccia *et al.*, 2009; Ciccia *et al.*, 2012; Vujanovic *et al.*, 2017). Polyubiquitinated PCNA plays an essential role in fork reversal by recruiting

ZRANB3 to stalled forks (Vujanovic *et al.*, 2017). After remodelling of the fork, the reversed fork can be restarted by two different mechanisms (Berti *et al.*, 2016). One depends on the concerted actions of PARP1 and RECQ1 (Berti *et al.*, 2013), and the other one relies on DNA replication helicase 2 (DNA2) and WRN (Thangavel *et al.*, 2015). During the former mechanism (Figure 1.4a), PARP1 stabilises reversed forks thereby controlling restart by RECQ1 (Berti *et al.*, 2013). Suppression of premature fork restart ensures time for DNA damage repair. Upon release of PARP1, the helicase activity of RECQ1 restores reversed forks by promoting branch migration to allow replication restart (Berti *et al.*, 2013; Zellweger *et al.*, 2015). During the latter mechanism (Figure 1.4b), DNA2 and WRN mediate restart by resecting the regressed arm of the reversed fork (Thangavel *et al.*, 2015). Berti *et al.* (2016) proposed two scenarios, by which DNA2-mediated resection could restart replication. SMARCAL1 could transform the reversed fork into a functional replication fork. This hypothesis is supported by the preference of SMARCAL1 to restart reversed forks with a 3' ssDNA tail (Couch *et al.*, 2013), a substrate generated by DNA2 and WRN (Thangavel *et al.*, 2015). Alternatively, the reversed fork could be restarted by a previously suggested HR-like mechanism (Petermann *et al.*, 2010b) that involves invasion of the 3' ssDNA overhang into the duplex ahead of the fork. This action could be mediated by RAD51. The resulting Holliday junction structure could be resolved by specific resolvases or dissolvases.

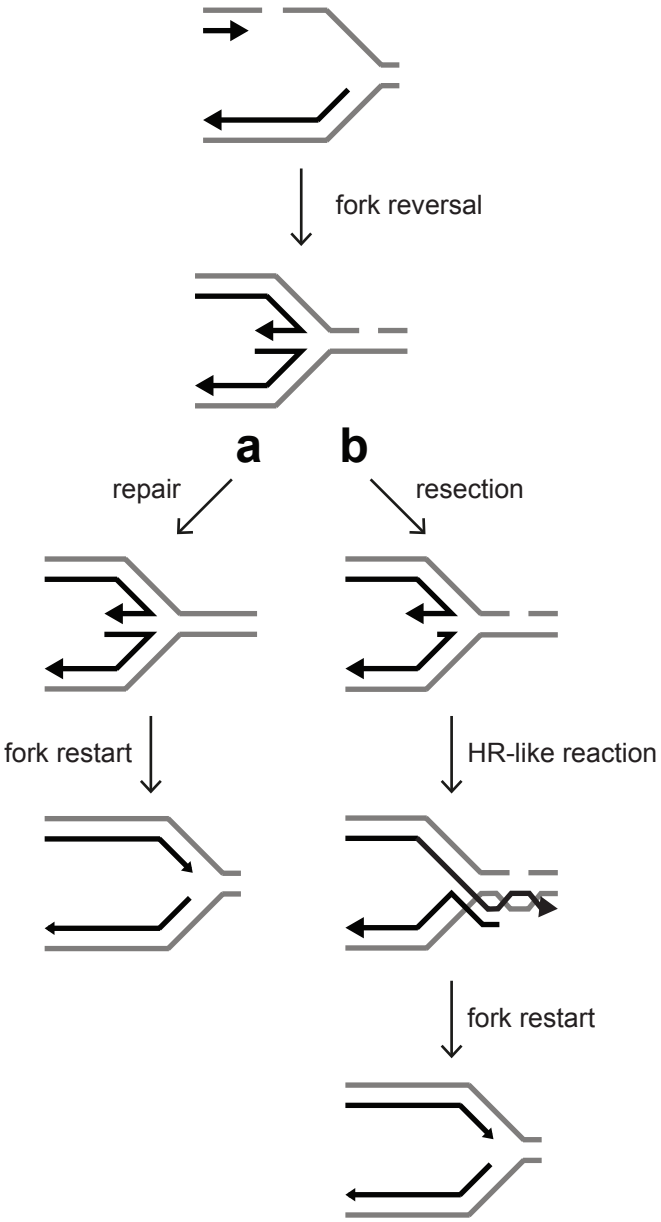


Figure 1.4. Stalled fork restart by fork reversal.
Upon fork reversal of a stalled fork, two mechanisms have been proposed to restart replication (Berti *et al.*, 2016). (**a**) Fork reversal allows time and space for repair of the lesion in front of the fork. Subsequently, the reversed fork is restored and restarted. (**b**) The 5' end of the regressed arm is resected. The resulting 3' overhang invades the duplex ahead of the fork in a HR-like reaction. After the Holliday junction structure has been resolved or dissolved, replication is restarted.

Failure to resume DNA synthesis leads to prolonged fork stalling, which can cause collapse of the replication fork associated with replisome disassembly and/or DSB formation (Zeman *et al.*, 2014). Since these events are not mutually exclusive, a collapsed fork can be defined more generally as a replication fork

devoid of the ability to perform DNA synthesis (Cortez, 2015). Persistently stalled or reversed forks can be cleaved by various nucleases. The structure-specific nuclease MUS81 has been shown to facilitate replication restart by cleaving stalled replication forks, generating a DSB (Hanada *et al.*, 2007). SLX4 also contributes to the collapse of stalled forks (Couch *et al.*, 2013). Alternatively, a one-ended DSB can result from replication fork 'run off' across a lesion ahead of the replication fork (Kuzminov, 2001).

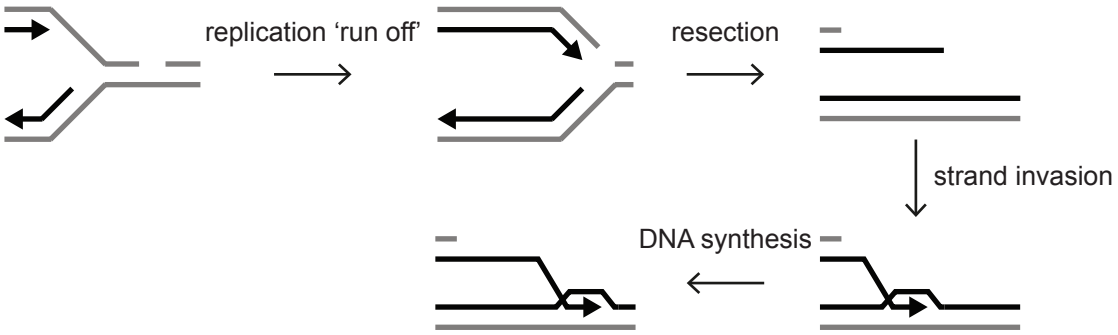


Figure 1.5. Restart of collapsed forks by break-induced replication.
A ssDNA nick is converted into a one-ended DSB by replication 'run off'. After resection, the nascent strand of the template duplex is invaded. Subsequently, DNA synthesis occurs through a migrating bubble.

One-ended DSBs associated with fork collapse can be repaired by break-induced replication (BIR) (Llorente *et al.*, 2008). Besides restarting broken replication forks (Costantino *et al.*, 2014; Hashimoto *et al.*, 2011), an essential function of BIR is the maintenance of chromosome ends in the absence of telomerase via a process called alternative lengthening of telomeres (ALT) (Dilley *et al.*, 2016; Lydeard *et al.*, 2007; Roumelioti *et al.*, 2016). In brief, BIR involves resection and invasion of the broken DNA strand into an intact homologous template, followed by DNA synthesis (Figure 1.5). BIR-associated DNA synthesis is different from conventional replication due to the lack of a

replication fork. Instead, DNA synthesis progresses via a migrating D-loop or bubble (Wilson *et al.*, 2013). Through strand invasion, the newly synthesised strand of the template duplex is displaced, which causes a conservative mode of DNA synthesis (Donnianni *et al.*, 2013; Saini *et al.*, 2013). Another characteristic of BIR is the uncoupling of leading and lagging strand synthesis (Saini *et al.*, 2013). The leading strand is synthesised by extension of the broken 3' end. This ssDNA accumulates behind the BIR bubble and is used as the template for lagging strand synthesis later (Saini *et al.*, 2013; Wilson *et al.*, 2013). However, the process of lagging strand synthesis in BIR remains to be elucidated. In yeast, all polymerases of the classic replication mechanism are involved in BIR, namely Polα, Polδ and Polε (Lydeard *et al.*, 2007). It is not well understood why cells require Polα during BIR since replication can be initiated from the 3' broken DNA end. Polδ, more specifically its subunit POLD3, is a key player in BIR (Costantino *et al.*, 2014; Lydeard *et al.*, 2007). While POLD3 is not essential for conventional DNA synthesis, it enables Polδ to replicate DNA via strand displacement (Smith *et al.*, 2009). Polε seems to be important for efficient BIR after its initiation (Lydeard *et al.*, 2007). However, its exact role is not fully understood yet. It is important to note that Dilley *et al.* (2016) discovered that Polα and Polε are not required for BIR-mediated telomere maintenance in human cells. The involvement of other factors of the conventional replisome remains controversial. A study in yeast reported that all normal replisome components are required during BIR except for the pre-RC factors ORC and CDC6 (Lydeard *et al.*, 2010). This can be explained by the fact that, in contrast to conventional replication, BIR is not initiated at an origin. However, more recent studies in yeast and human cells claim that the MCM

complex is dispensable for BIR (Dilley *et al.*, 2016; Wilson *et al.*, 2013). Interestingly, PIF1 helicase is needed to recruit Polδ to the D-loop and promote DNA synthesis through bubble migration (Wilson *et al.*, 2013).

BIR can be RAD51-dependent or -independent. The former more efficient mechanism relies on RAD51 filaments to perform a homology search and catalyse strand invasion (Davis *et al.*, 2004; Malkova *et al.*, 2005). RAD51-independent BIR is mutagenic because it uses microhomologies for annealing (Downing *et al.*, 2008). This mechanism is mediated by RAD52 and suppressed by RAD51 filaments (Downing *et al.*, 2008). In human cancer cell lines, RAD52- and POLD3-dependent BIR events have been detected upon oncogene-induced replication stress (Costantino *et al.*, 2014; Sotiriou *et al.*, 2016). Here, RAD52 plays an essential role in the repair of collapsed replication forks by BIR (Sotiriou *et al.*, 2016). Whether RAD51-dependent and -independent BIR exists in this context remains to be determined. Fork stalling at difficult-to-replicate fragile sites is resolved by RAD52-dependent BIR (Bhowmick *et al.*, 2016; Minocherhomji *et al.*, 2015). To promote POLD3-dependent DNA synthesis, stalled forks are cleaved by MUS81 in early mitosis (Minocherhomji *et al.*, 2015). This mechanism is crucial to counteract mitotic chromosome segregation problems (Minocherhomji *et al.*, 2015). Interestingly, another study, using the same setting, found that mitotic BIR was dependent on RAD52 but not BRCA2 or RAD51 (Bhowmick *et al.*, 2016). BIR-like DNA synthesis in mitosis has also been reported in the context of replication stress resulting from mutations in MCM4 or p53-independent expression of p21 (Galanos *et al.*, 2016; Luebben *et al.*, 2014). BIR is terminated by convergence with a replication fork approaching from the opposite direction or MUS81-mediated cleavage of the BIR

intermediates (Mayle *et al.*, 2015). Notably, BIR exhibits a high mutation rate (Deem *et al.*, 2011; Sakofsky *et al.*, 2014). This could be caused by exposure of ssDNA behind the bubble due to uncoupling of leading and lagging strand synthesis (Saini *et al.*, 2013) or by instability of the D-loop structure leading to template switching during BIR (Smith *et al.*, 2007).

Altogether, restart mechanisms of stalled or collapsed forks are crucial to ensure proper DNA replication of the entire genomic DNA of a cell. Failure of these processes is an important source of DNA damage accumulation including DSBs. Importantly, cells employ checkpoint responses upon replication stress and DNA damage to prevent genomic instability (Gaillard *et al.*, 2015; Zeman *et al.*, 2014).

1.7 DNA damage response

Among DNA lesions, DSBs are believed to be the most toxic as they do not leave a complementary strand that can be used as a template for repair. Moreover, DSBs generate chromosome breakage and rearrangement, both of which may trigger apoptosis or tumourigenesis (van Gent *et al.*, 2001). To prevent these detrimental consequences of DSBs, cells have evolved sophisticated surveillance mechanisms to safeguard their genomes.

The DNA damage response (DDR) is a cellular network that mediates DNA damage signalling and repair. A central component of the DDR are DNA damage checkpoints that induce transient cell cycle arrest allowing sufficient time for repair. This is essential to preserve genomic integrity and prevent transmission of DNA errors to daughter cells. The checkpoint kinases ATM and

ATR are essential factors of the DDR as they signal to cell cycle checkpoints and DNA repair pathways.

ATM is recruited to DSB sites upon sensing of broken DNA molecules by the MRE11-RAD50-NBS1 (MRN) complex (Lee *et al.*, 2005). In the absence of DNA damage, ATM remains an inactive dimer. Upon genomic insult, it becomes activated by autophosphorylation on serine 1981 (S1981) (Bakkenist *et al.*, 2003). ATM kinase activity provokes cell cycle arrest by p53 activation (Kastan *et al.*, 1992) and direct phosphorylation of CHK2 on threonine 68 (T68) (Ahn *et al.*, 2000; Matsuoka *et al.*, 2000; Melchionna *et al.*, 2000; Zhou *et al.*, 2000). CHK2 phosphorylates CDC25A, thereby silencing CDK2 activity and preventing G1/S transition (Falck *et al.*, 2001). Additionally, CHK2 has also been reported to inactivate CDC25C leading to G2 arrest due to CDK1 inactivity (Matsuoka *et al.*, 1998).

ATR is stimulated in response to stalled replication forks and resected DSBs. Hereof, the ssDNA-RPA complex recruits ATR via its partner protein ATRIP (Zou *et al.*, 2003a) and the RAD17 clamp loader to junctions between ssDNA and dsDNA. RAD17 in turn loads the PCNA-related 911 complex onto DNA (Zou *et al.*, 2003b). TOPBP1 binds to 911 and stimulates ATR kinase activity (Kumagai *et al.*, 2006). Recently, a second ATR-stimulatory mechanism mediated by Ewing's tumour-associated antigen 1 (ETAA1) has been described (Bass *et al.*, 2016; Feng *et al.*, 2016; Haahr *et al.*, 2016; Lee *et al.*, 2016b). ETAA1 binds to RPA and directly activates ATR kinase independently of TOPBP1. ATR induces activation of Claspin, which then binds and activates CHK1 (Chini *et al.*, 2003; Liu *et al.*, 2006). Mitotic entry in the presence of DNA

damage is prevented by phosphorylation of CDC25C by CHK1 (Peng *et al.*, 1997; Sanchez *et al.*, 1997).

While the original concept described a strict dependency of CHK1 on ATR and CHK2 on ATM, a crosstalk between these kinases has recently become apparent. For example, ATM has been shown to phosphorylate CHK1 in response to ionising radiation (Gatei *et al.*, 2003; Sorensen *et al.*, 2003), whilst CHK2 activation upon replication stress induced by DNA-crosslinking agent cisplatin depends on ATR (Pabla *et al.*, 2008).

After checkpoint activation, a cascade of DDR factor assembly is initiated by ATM, ATR and DNA-dependent protein kinase (DNA-PK)-dependent phosphorylation of histone variant H2AX on S139 (γH2AX) spanning megadaltons of DNA flanking each DSB (Burma *et al.*, 2001; Rogakou *et al.*, 1999; Rogakou *et al.*, 1998; Stiff *et al.*, 2004; Ward *et al.*, 2001). This signals the recruitment of downstream DDR factors like mediator of DNA damage checkpoint protein 1 (MDC1) and E3 ligase RNF8 (Huen *et al.*, 2007; Kolas *et al.*, 2007; Mailand *et al.*, 2007; Stucki *et al.*, 2005). Further ubiquitin signals by RNF168 finally orchestrate the recruitment of other ATM-related mediators including p53-binding protein 1 (53BP1) and BRCA1 (Doil *et al.*, 2009; Stewart *et al.*, 2009), which regulate DSB repair by NHEJ and HR.

The choice of DSB repair pathway depends on several parameters including the location and complexity of the break as well as the cell cycle status (Chapman *et al.*, 2012; Shibata *et al.*, 2011; Tsouroula *et al.*, 2016). During G1 phase, 53BP1 caps DSB ends and channels cells into NHEJ (Bothmer *et al.*, 2010). During S/G2 phase, BRCA1 competes with 53BP1 and assists in its removal (Bunting *et al.*, 2010; Chapman *et al.*, 2012) to allow DSB

end resection generating long 3' ssDNA overhangs that are substrates for HR (Dynan *et al.*, 1998; Heyer *et al.*, 2010).

1.8 Non-homologous end joining

Classical NHEJ (C-NHEJ) provides a rapid repair mechanism for DSBs by promoting potentially inaccurate ligation of the break ends (Figure 1.6a). C-NHEJ is initiated by rapid binding of the KU70-KU80 heterodimer to the DSB ends, upon which DNA-dependent protein kinase catalytic subunit (DNA-PKcs) is recruited and activated (Mari *et al.*, 2006; Uematsu *et al.*, 2007). The ATM-related kinase DNA-PKcs is responsible for keeping the DNA ends in close proximity and recruiting end-processing factors, such as Artemis, to cleave ssDNA overhangs (Ma *et al.*, 2002; Povirk *et al.*, 2007). Finally, DSB ends are ligated by the scaffold protein XRCC4, XRCC4-like factor (XLF) and DNA ligase 4 (LIG4) (Ahnesorg *et al.*, 2006; Grawunder *et al.*, 1997; Gu *et al.*, 2007).

While C-NHEJ is active throughout the cell cycle, alternative NHEJ (A-NHEJ; Figure 1.6b) functions mostly in S and G2 phase of the cell cycle, and is considered a backup pathway when DSB repair by C-NHEJ or HR fails (Verkaik *et al.*, 2002; Wang *et al.*, 2003; Wang *et al.*, 2005). This is likely to be due to the high rates of insertions, deletions and translocations caused by error-prone A-NHEJ (Simsek *et al.*, 2010; Zhang *et al.*, 2011). A-NHEJ relies on signalling by PARP1 (Audebert *et al.*, 2004; Mansour *et al.*, 2010), and 5'-3' DNA end resection mediated by the MRN complex (Dinkelmann *et al.*, 2009; Xie *et al.*, 2009) and CtBP-interacting protein (CtIP) (Bennardo *et al.*, 2008; Zhang *et al.*, 2011). While A-NHEJ has not been fully characterised to this date, it is believed

that microhomologies are commonly used to anneal the resected DSB ends. This process is facilitated by Polθ (also known as POLQ), a polymerase that also mediates repair synthesis (Chan *et al.*, 2010; Kent *et al.*, 2015), followed by LIG1- or LIG3-mediated ligation (Liang *et al.*, 2008; Paul *et al.*, 2013; Wang *et al.*, 2005).

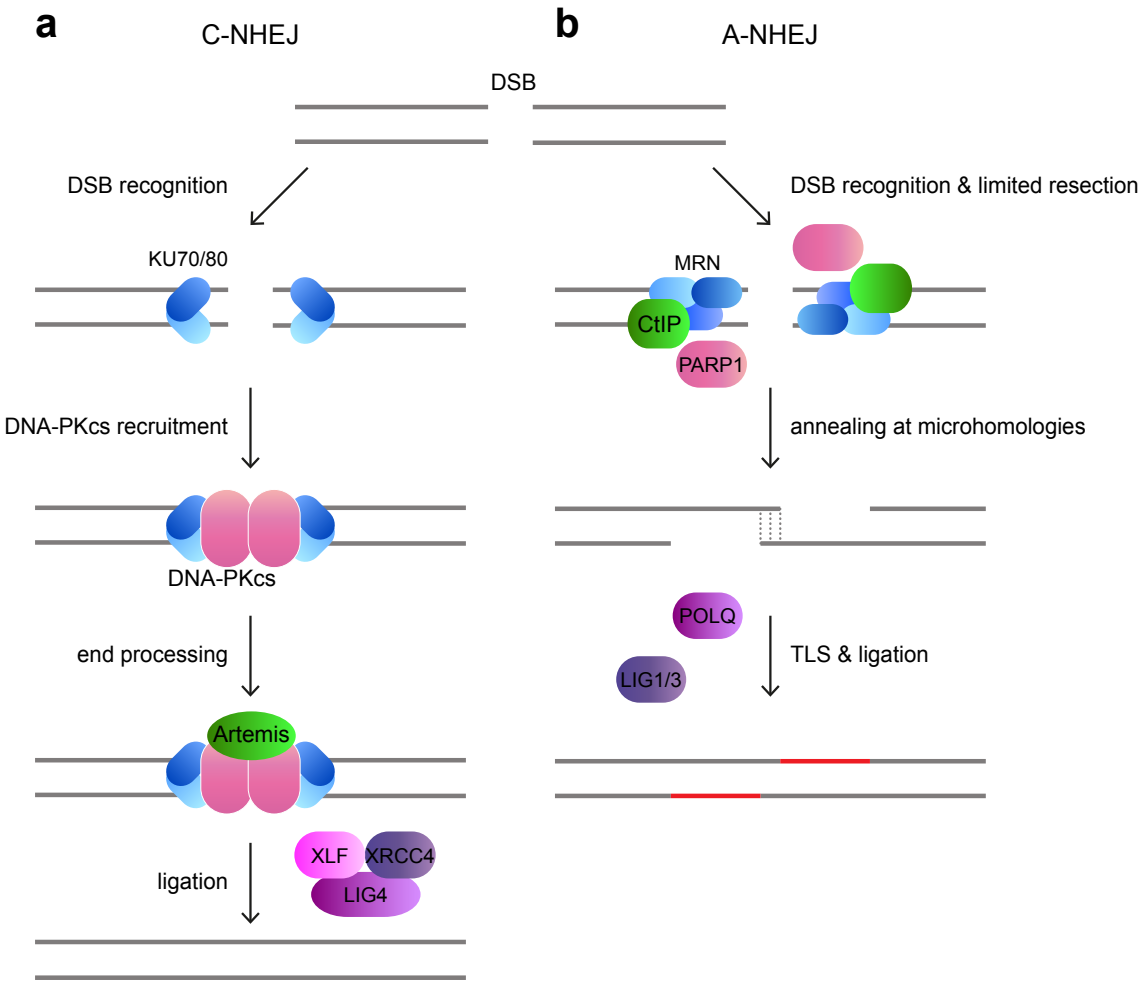


Figure 1.6. NHEJ pathways of DSB repair.
(**a**) During C-NHEJ, the DSB is recognised by KU70/80. After DNA-PKcs is recruited, the DSB ends are processed by various factors including Artemis. Finally, the ends are ligated by XRCC4, XLF and LIG4. (**b**) During A-NHEJ, the DSB is recognised and processed by various factors including PARP1, the MRN complex and CtIP. Using microhomologies, the DSB ends are annealed, gaps are filled in by POLQ-mediated translesion synthesis (TLS) and ligated by LIG1/3.

1.9 Homologous recombination

HR is an accurate repair pathway for DSBs in mammalian cells (Figure 1.7). In S and G2 phase of the cell cycle, elevated CDK1 levels promote DSB end resection (Ira *et al.*, 2004) initiated by the MRN complex (Shibata *et al.*, 2014; Tsubouchi *et al.*, 1998). Extensive end resection leading to long 3' ssDNA overhangs is carried out by multiple factors including nucleases CtIP, EXO1, DNA2 and BLM helicase (Nimonkar *et al.*, 2011; Nimonkar *et al.*, 2008; Sartori *et al.*, 2007). Shibata *et al.* (2014) recently proposed a two-step model for DSB resection, in which MRE11 endonuclease makes an upstream incision allowing exonucleolytic 3'-5' processing toward the DSB. These actions of MRE11 are coupled with the 5'-3' digestion of ssDNA by EXO1/BLM away from the DNA end. The generated exposed ssDNA is rapidly coated by RPA to prevent formation of secondary structures and protect from degradation (Chen *et al.*, 2013). The RAD51 recombinase is loaded onto the ssDNA overhangs by BRCA2 and the RAD51 paralogues RAD51B, RAD51C, RAD51D, XRCC2 and XRCC3 (Bishop *et al.*, 1998; Johnson *et al.*, 1999; Moynahan *et al.*, 2001; Tarsounas *et al.*, 2004; Yang *et al.*, 2005). RAD51 nucleofilament formation initiates the search and invasion into an intact, homologous dsDNA template (Baumann *et al.*, 1996; Sung, 1994; Sung *et al.*, 1995), most commonly provided by the newly replicated, identical sister chromatid (Johnson *et al.*, 2000). This results in the formation of a D-loop, which is converted into a double Holliday junction upon capture of the second DSB end (Bzymek *et al.*, 2010). After branch migration, Holliday junctions are cleaved by GEN1 (Ip *et al.*, 2008; Rass *et al.*, 2010) or MUS81-EME1 (Wyatt *et al.*, 2013), or dissolved by the BLM-TOPIIIα-RMI1 complex (Wu *et al.*, 2003).

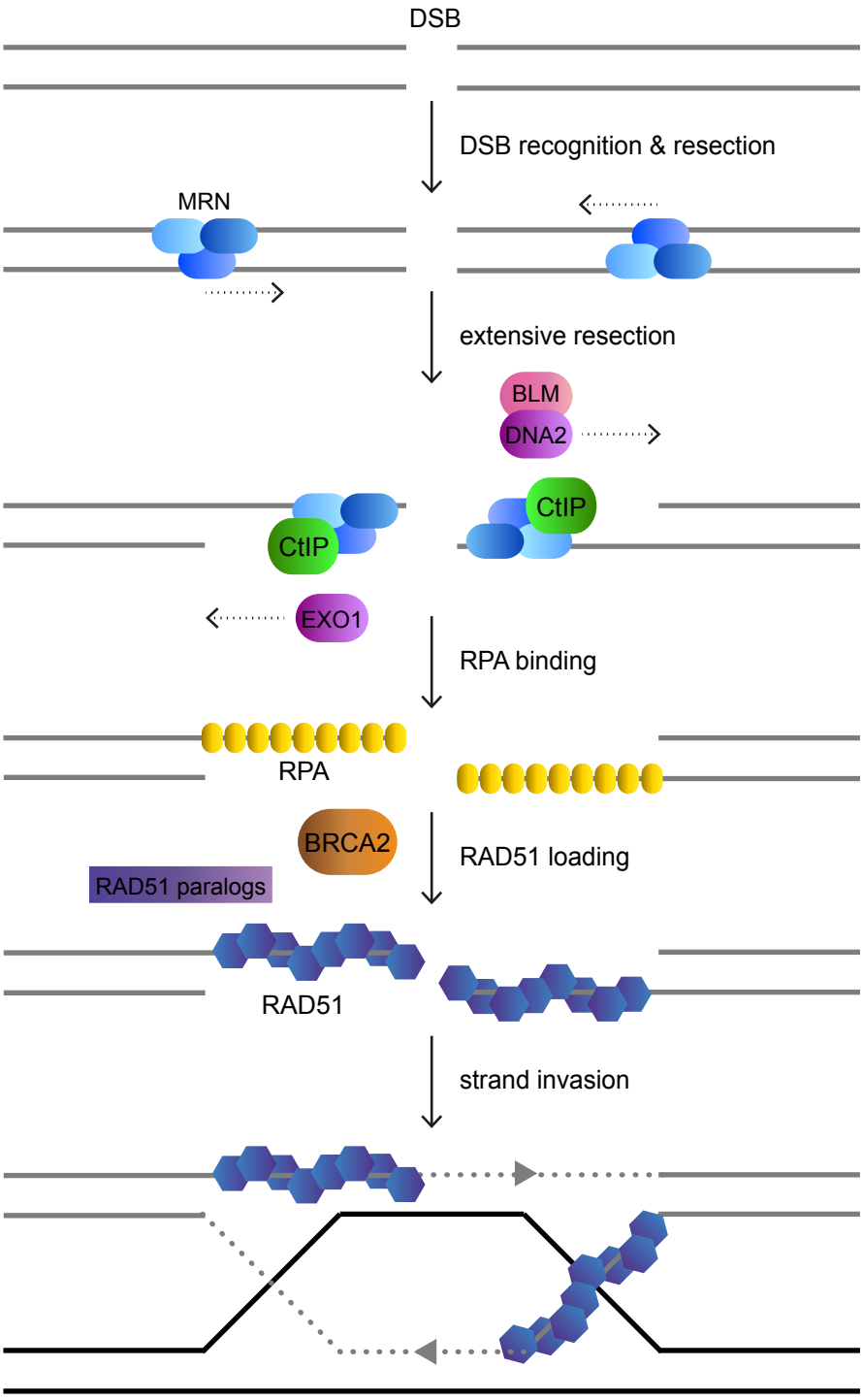


Figure 1.7. HR pathway of DSB repair.
HR is initiated by nucleolytic incisions in proximity to the DSB by the MRN complex. Extensive resection is carried out together with CtIP as well as BLM, DNA2 and EXO1. The thus generated ssDNA overhangs are coated by RPA and subsequently, RAD51 recombinase is loaded by BRCA2 and the RAD51 paralogs. The RAD51 nucleoprotein filament mediates strand invasion into an intact, homologous DNA duplex. Finally, the double Holliday junction is resolved by GEN1, MUS81-EME1 or BLM-TOPIIIα-RMI1 (not shown).

The long ssDNA tails generated by extensive resection are not only substrates for HR-mediated DSB repair but also for single strand annealing (SSA; Figure 1.8) (Paques *et al.*, 1999). After extensive resection of the DSB (see above), RAD52 anneals homologous ssDNA tails (Rothenberg *et al.*, 2008). Subsequently, non-complementary 3' flaps are cleaved by the nucleotide excision repair complex XPF–ERCC1 (Motycka *et al.*, 2004). While the mismatch repair complex MSH2–MSH3 is involved in processing ssDNA overhangs during SSA in yeast (Sugawara *et al.*, 1997), it seems to be dispensable for SSA in mammalian cells (Bennardo *et al.*, 2009). Despite end resection being most active in S/G2 phase of the cell cycle (Huertas *et al.*, 2008; Ira *et al.*, 2004), a DSB may be resected before synthesis of the respective sister chromatid. SSA can act at these breaks because, in contrast to HR, SSA does not use the sister chromatid as a template for repair (Bhargava *et al.*, 2016). Nonetheless, due to the mutagenic nature of SSA (Bhargava *et al.*, 2016), HR remains the preferable pathway for DSB repair in S/G2 phase.

Importantly, many HR factors have been implicated in the Fanconi anaemia (FA) pathway (Michl *et al.*, 2016b). For example, BRCA1 is required to disassociate the replicative CMG helicase from chromatin in the vicinity of DNA interstrand crosslinks (ICLs) to allow repair of such lesions by the FA pathway (Long *et al.*, 2014).

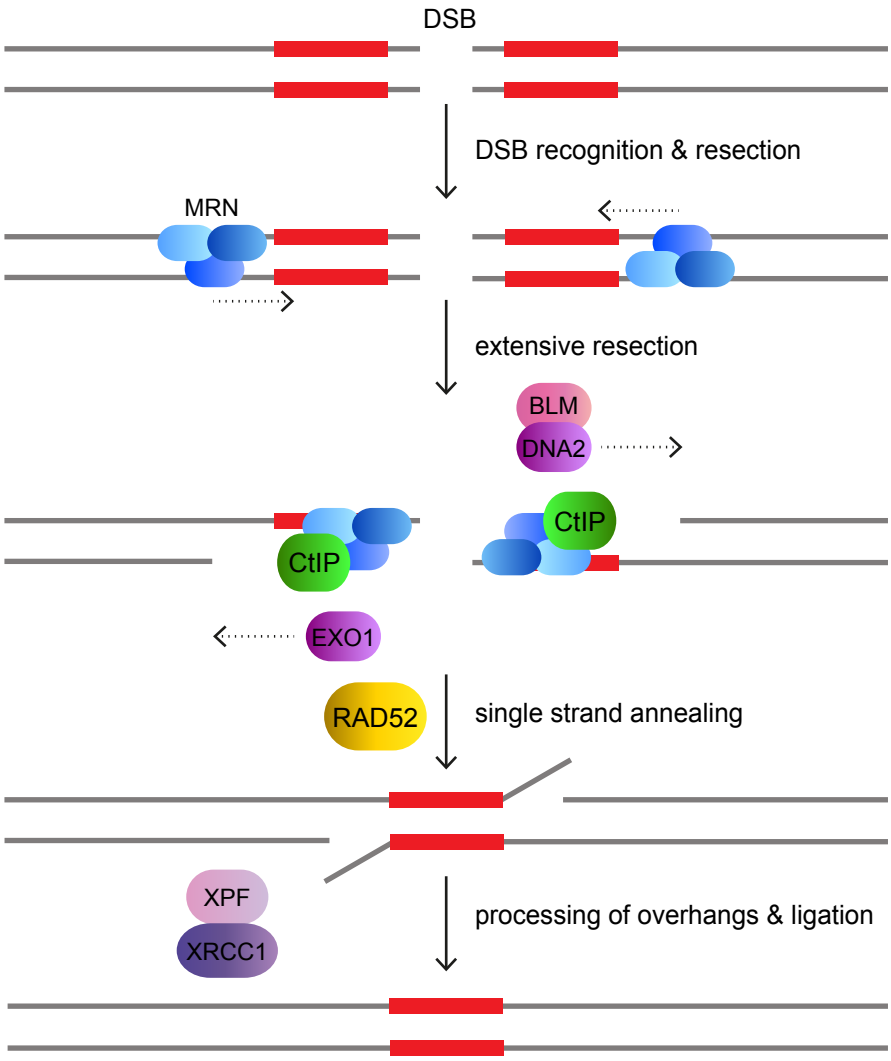


Figure 1.8. SSA pathway of DSB repair.
Resection is initiated by nucleolytic incisions near the DSB by the MRN complex. Long ssDNA tails are generated by extensive resection mediated by MRN, CtIP, BLM, DNA2 and EXO1. Complementary single strands are annealed by RAD52 and the resulting flaps are cleaved by XPF–XRCC1. Red boxes indicate regions of homology.

1.10 Fanconi anaemia pathway

The FA pathway repairs ICLs (Figure 1.9), toxic DNA lesions that obstruct transcription and replication by preventing separation of DNA strands. Metabolic by-products of ethanol, cigarette smoke and dietary fat can cause ICLs endogenously (Stone *et al.*, 2008). Similarly, many chemotherapeutic agents

such as platinum drugs and mitomycin C induce ICLs exogenously (Takahara *et al.*, 1995; Tomasz *et al.*, 1997).

In vitro studies suggest that converging replication forks are required to trigger ICL repair (Zhang *et al.*, 2015). ICLs are recognised by FANCM together with its interaction partners FA-associated protein 24 (FAAP24) and FANCM-associated histone fold protein 1/2 (MHF1/2). Subsequently, the FA core complex is recruited, which consists of 14 proteins (FANCA, FANCB, FANCC, FANCE, FANCF, FANCG, FANCL, FANCM, FANCT, FAAP20, FAAP24, FAAP100, MHF1 and MHF2) and activates the FANCI-FANCD2 complex. FANCI-FANCD2 is phosphorylated (Andreassen *et al.*, 2004; Ishiai *et al.*, 2008), and then monoubiquitinated by ubiquitin ligase subunit FANCL and the respective E2 ubiquitin-conjugating enzyme UBE2T (also known as FANCT) (Hira *et al.*, 2015; Miles *et al.*, 2015; Rickman *et al.*, 2015; Virts *et al.*, 2015). Monoubiquitinated FANCDI-FANCD2 is loaded onto the chromatin to mediate downstream reactions that resolve the ICL. Finally, eviction of the complex is achieved by sumoylation of FANCI-FANCD2 (Gibbs-Seymour *et al.*, 2015) and/or phosphorylation of FANCI (Sareen *et al.*, 2012).

Monoubiquitinated FANCI-FANCD2 controls unhooking of the ICL, which is initiated by nucleolytic incision at converged replication forks in proximity to the ICL (Knipscheer *et al.*, 2009). SLX4 (also known as FANCP (Kim *et al.*, 2011)) is recruited (Crossan *et al.*, 2011; Yamamoto *et al.*, 2011) and functions as a scaffold for several structure-specific endonucleases, such as ERCC4 (also known as XPF or FANCQ)-ERCC1, MUS81-EME1 and SLX1. ERCC4-ERCC1 is the main nuclease responsible for incisions that release the ICL (Hodskinson *et al.*, 2014; Klein Douwel *et al.*, 2014), while MUS81-EME1 and SLX1 play

rather redundant roles (Kim *et al.*, 2013). The nuclease FAN1 has also been implicated in making incisions adjacent to ICLs (Pizzolato *et al.*, 2015). However, a recent study showed that FANCD2-mediated FAN1 recruitment protects from genomic instability stemming from replication fork stalling, a function dispensable for ICL repair (Lachaud *et al.*, 2016).

After ICL unhooking, the lesion is bypassed by insertion of nucleotides opposite the ICL and extension of the nascent DNA strand by translesion synthesis. These actions rely on REV1 and polymerase zeta (Polζ) (Budzowska *et al.*, 2015; Sarkar *et al.*, 2006). The unhooked adduct is removed by nucleotide excision repair (Lage *et al.*, 2003), leaving an intact DNA double strand that can serve as a template for repair of the opposite strand by HR (Knipscheer *et al.*, 2009).

Importantly, FA proteins are pivotal for maintaining stalled replication fork stability (Schlacher *et al.*, 2012). FANCD2 or FANCA dysfunction results in MRE11-mediated degradation of nascent DNA at stalled forks. Importantly, the protective function of FANCD2 at stalled forks requires pathway activation through ubiquitination by the core complex. FANCD2 and FANCI have also been implicated in the restart of stalled replication forks in response to replication stress (Chaudhury *et al.*, 2013; Chen *et al.*, 2015).

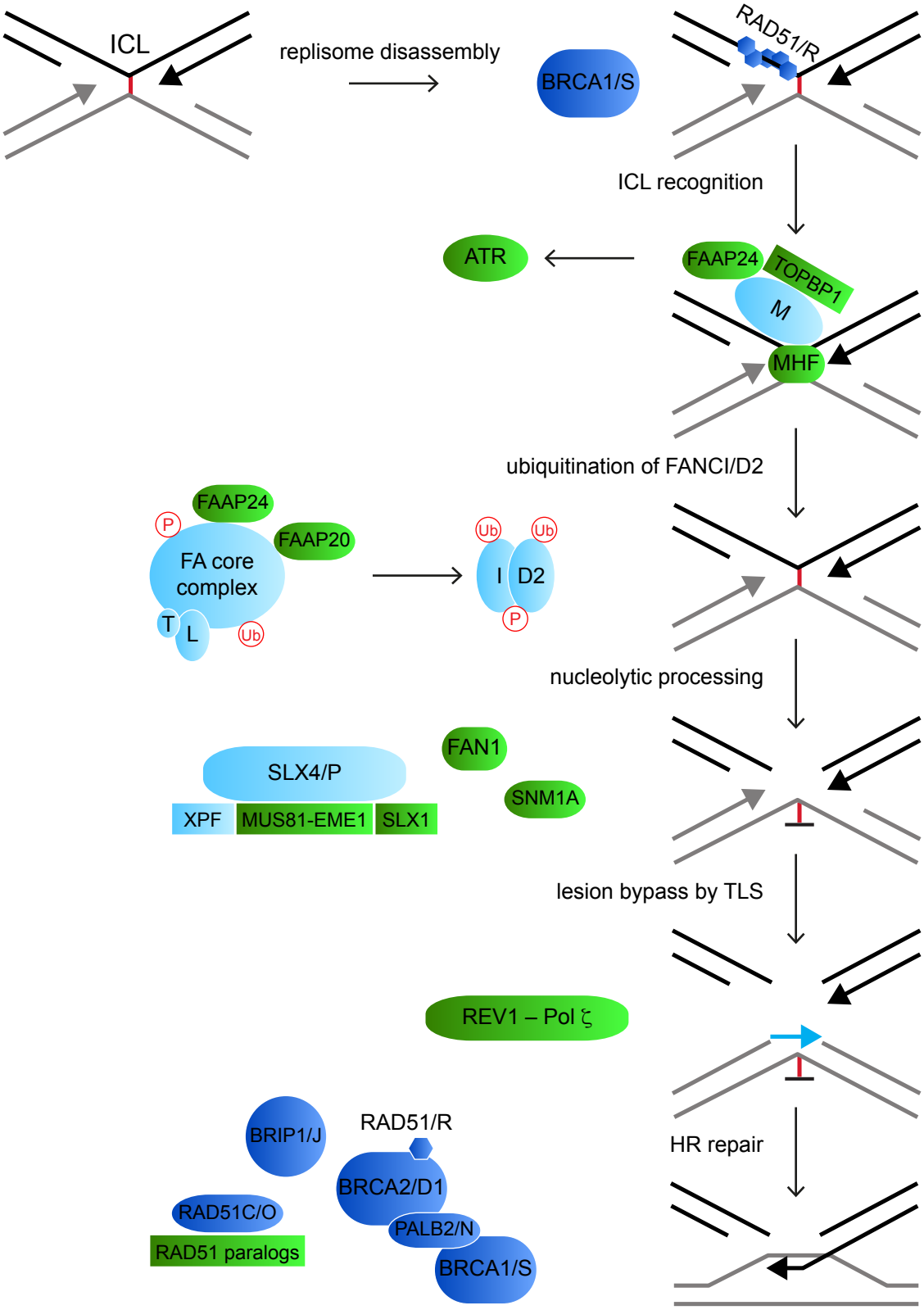


Figure 1.9. FA pathway of ICL repair.
Upon fork stalling, the replisome disassembles and the ICL is recognised. The FA core complex mediates ubiquitination of FANCI/D2. Nucleolytic incisions unhook the ICL generating a DSB. TLS restores an intact DNA double strand, a template for HR-mediated repair of the DSB. Light blue, FA proteins; dark blue, HR proteins; green, other proteins in the FA pathway. Adapted from Michl *et al.* (2016b).

FA is a rare autosomal recessive disease with 1-5 incidents per one million caused by biallelic mutations in a FA gene (Auerbach *et al.*, 2001; Verlander *et al.*, 1995). FA patients commonly display developmental abnormalities including skeletal malformations, hyper- or hypo-pigmentation and low birth weight (Wajnrajch *et al.*, 2001). Furthermore, life expectancy of these individuals is reduced to an average of 20 years due to progressive bone marrow failure and cancer susceptibility (Joenje *et al.*, 2001). More than one fifth of FA patients develop cancer (Kutler *et al.*, 2003), most commonly acute myeloma leukaemia (AML) (Rosenberg *et al.*, 2003). Other types of FA-associated cancers include tumours in liver, head and neck as well as gynecologic malignancies (Alter, 1996; Kutler *et al.*, 2003). One important feature of FA patient cells is their hypersensitivity to ICL-inducing agents such as cisplatin, mitomycin C and diepoxybutane (Auerbach *et al.*, 1976; Ishida *et al.*, 1982; Sasaki *et al.*, 1973; Weksberg *et al.*, 1979). In the absence of a functional FA pathway, ICLs result in chromosomal breakage and aberrations. Radial chromosomes are characteristic of FA-deficient cells and cause the extreme toxicity of crosslinking agents in FA patients (Auerbach *et al.*, 1989). Until today, this characteristic is being exploited for FA diagnostic tests (Pagano *et al.*, 2015).

1.11 BRCA1 and BRCA2 in genomic stability

Cells with BRCA1 or BRCA2 deficiency exhibit spontaneous DNA breaks and impaired proliferation (Patel *et al.*, 1998; Xu *et al.*, 1999b; Yu *et al.*, 2000). More precisely, BRCA2-deficient cells spontaneously accumulate chromosomal aberrations including triradial and quadradial structures, a typical feature of FA

dysfunction (Patel *et al.*, 1998). Additionally, gross chromosomal arrangements like translocations, deletions and chromosome fusions are characteristic of cells lacking BRCA2 (Yu *et al.*, 2000). Similar phenotypes are observed in the context of BRCA1 dysfunction (Xu *et al.*, 1999b). Importantly, these findings extend to human tumour cells of patients with *BRCA1* or *BRCA2* mutations (Gretarsdottir *et al.*, 1998; Tirkkonen *et al.*, 1997). Despite these hallmarks of BRCA deficiency, it remains unclear, which functions of BRCA1 and BRCA2 are essential for genome integrity and cell proliferation under physiological conditions.

It has been estimated that in dividing cells, 10 DSBs occur per day. These can stem from exposure to reactive oxygen species (ROS), ionising radiation or unintentional actions of nuclear enzymes (Lieber, 2010). ROS are generated as a metabolic by-product of oxidative respiration and can react with DNA. This can lead to nicks in the DNA that can form a DSB if they occur near each other. Furthermore, natural ionising radiation from the environment can create free radicals that damage DNA (Lomax *et al.*, 2013). Unintentional DSB formation can be caused by topoisomerase II, an enzyme that cleaves both strands of the DNA helix to relieve topological stress (Wang, 1996). If topoisomerase II fails to re-join the DNA ends, a DSB is generated (Adachi *et al.*, 2003). Since most commonly no homologous template is available for the repair of DSBs originating from these sources, NHEJ acts to repair such lesions (Lieber, 2010). Similarly, intentional DSBs for V(D)J recombination and class switch recombination are repaired by NHEJ (Ma *et al.*, 2002; Yan *et al.*, 2007). On the contrary, meiotic DSBs generated by SPO11 are resolved by HR (Keeney, 2008). Given the minor contribution of HR to the repair of endogenous DSBs, it

seems unlikely that the HR defect of BRCA-deficient cells causes their proliferative impediment under physiological conditions.

Importantly, BRCA1 and BRCA2 have been classified as FA components (Howlett *et al.*, 2002; Sawyer *et al.*, 2015). The FA pathway provides a key mechanism for ICL repair, with its dysfunction leading to hypersensitivity to ICL-inducing agents (see section 1.10). There are various endogenous sources of ICLs that accumulate mainly as a result of metabolic actions (Clauson *et al.*, 2013). It is important to note that the cellular tolerance of ICLs is extremely low. In repair-deficient cells, 20-40 ICLs are lethal (Phillips, 1996). This indicates the importance of efficient ICL repair to maintain cell viability.

Besides their essential roles in DSB and ICL repair, BRCA1 and BRCA2 are implicated in maintaining replication fork progression that can be hindered endogenously. Repetitive sequences and non-canonical B-DNA structures pose natural challenges to the replication machinery (Techer *et al.*, 2017). During transcription, the nascent RNA can form a RNA-DNA hybrid with the template DNA strand, a structure that can obstruct replication forks (Gan *et al.*, 2011). Furthermore, lesions on the template strand commonly induce replication fork stalling. Alternatively, the replisome can ‘skip’ over the lesion leaving a gap behind the fork (see section 1.6). BRCA1 and BRCA2 have been postulated to play an important role in template switching (Scully *et al.*, 2000; Venkitaraman, 2000; Wang *et al.*, 2000), a mechanism that allows replication past lesions or gaps behind the fork (see section 1.6). Importantly, Mazloum *et al.* (2009) demonstrated that fungal BRCA2 mediates template switching. Additionally, the authors of a recent study in chicken cells proposed that BRCA1 and BRCA2 prevent base substitution mutations through template switching (Zamborszky *et*

al., 2017). BRCA1 and BRCA2 are also required at stalled replication forks to protect nascent DNA from MRE11-mediated degradation (Chandramouly *et al.*, 2011; Schlacher *et al.*, 2011; Schlacher *et al.*, 2012; Ying *et al.*, 2012). Recently, it was shown that BRCA2-dependent RAD51 nucleoprotein filaments maintain stalled fork stability threatened by MRE11 nuclease (Kolinjivadi *et al.*, 2017). Furthermore, RAD51 interacts with Polα to ensure continuous DNA synthesis at these forks (Kolinjivadi *et al.*, 2017). Therefore, BRCA1 and BRCA2 play important roles in fork stability and restart. Defects in replication induce S phase checkpoint activation to prevent entry into G2 phase prior to completion of DNA synthesis (see section 1.7). If left unresolved, persistent replication-associated DNA damage can lead to proliferative arrest or cell death (Gaillard *et al.*, 2015). This suggests that the functions of BRCA1 and BRCA2 in DNA replication are essential to ensure cell proliferation.

Strikingly, BRCA1 and BRCA2 are tumour suppressor and mutations in either one of their genes elevates the risk of developing breast or ovarian cancer (see section 1.2). The dysfunction of BRCA1 or BRCA2 in the processes discussed above are thought to drive genomic instability and tumourigenesis. In this regard, BRCA1 and BRCA2 act as caretakers (Kinzler *et al.*, 1997). The inactivation of a caretaker gene destabilises the genome and therefore encourages mutations in other genes including so called gatekeeper genes that drive cancer development (Kinzler *et al.*, 1997). Nonetheless, the genomic instability features associated with BRCA1- and BRCA2-dysfunctional cancers can also be exploited therapeutically.

1.12 Strategies for targeting BRCA-deficient cells and tumours

Tumour cells lacking BRCA1 or BRCA2 function are deficient in HR-mediated DSB repair. This characteristic opens a therapeutic window for the development of strategies to specifically target and eliminate BRCA-deficient tumours. The genomic instability intrinsic to *BRCA*-mutated cells drives carcinogenesis but has also been described as the Achilles heel of these tumours (Rigakos *et al.*, 2012). Therapies for patients with *BRCA*-mutated tumours rely on the inefficient repair of DSBs induced by DNA-damaging agents. Platinum drugs such as cisplatin are commonly used as a chemotherapeutic agent for the treatment of BRCA-defective cancers. Platinum-based compounds induce DNA crosslinks (Rice *et al.*, 1988; Rudd *et al.*, 1995; Takahara *et al.*, 1995) that cannot be repaired effectively in the absence of HR. Multiple studies in human and mouse model systems for BRCA deficiency have demonstrated that cells lacking BRCA1 or BRCA2 function are more sensitive to platinum drugs than their *wildtype* counterparts (Bartz *et al.*, 2006; Bhattacharyya *et al.*, 2000; Evers *et al.*, 2008; Fedier *et al.*, 2003; Husain *et al.*, 1998). Importantly, BRCA-deficient breast and ovarian cancers are hypersensitive to cisplatin (Alsop *et al.*, 2012; Byrski *et al.*, 2009; Byrski *et al.*, 2014; Gorodnova *et al.*, 2015; Vencken *et al.*, 2011). However, tumours have been reported to acquire resistance to cisplatin through secondary intragenic mutations that restore functional BRCA (Sakai *et al.*, 2008; Swisher *et al.*, 2008).

In a pharmaceutical screen for compounds with selective cytotoxicity against BRCA2-deficient cells by Evers *et al.* (2010b), the three alkylating agents chlorambucil, melphalan and nimustine were identified. *In vivo*, these alkylators showed activity against BRCA2-deficient tumours, with melphalan

and nimustine achieving a longer relapse-free survival than cisplatin (Evers *et al.*, 2010b). The action of alkylating agents seems to extend to BRCA1-defective cancers as nimustine eradicated 100% of BRCA1-deficient tumours in genetically engineered mouse models (Evers *et al.*, 2010a). Strikingly, a platinum-resistant BRCA2-defective ovarian carcinoma was eliminated by treatment with melphalan and has not recurred for 26 years (Osher *et al.*, 2011). These findings suggest that alkylating agents may be worth considering for the treatment of *BRCA*-mutated tumours in the future.

Recently, the concept of synthetic lethality has been exploited for the search of novel therapies for BRCA-deficient tumours (Bryant *et al.*, 2005; Farmer *et al.*, 2005). Synthetic lethality describes a functional redundancy between two genes, where the loss of one or the other can be tolerated but the combined loss of both is lethal (Dobzhansky, 1946). Since HR provides a mechanism for the restart of stalled replication forks and repair of DSBs, cells lacking HR activities mediated by BRCA1 and BRCA2 rely on backup pathways to deal with these types of lesions. For example, PARP1 is required for single-strand break (SSB) repair (Satoh *et al.*, 1992) with its inhibition leading to accumulation of SSBs that cause replication fork stalling. When these forks fail to restart, SSBs are converted into DSBs, which rely on HR for repair. In BRCA-deficient cells, DSBs accumulate with detrimental consequences on cell survival. PARP1 and HR have also been implicated in the restart of stalled replication forks (Bryant *et al.*, 2009; Petermann *et al.*, 2010b), a function that likely contributes to the synthetic lethal interaction between PARP and BRCA (Farmer *et al.*, 2005; McCabe *et al.*, 2006). Evidence for activity in BRCA2-defective tumours has been provided for the PARP inhibitor olaparib (Domchek

et al., 2016; Fong *et al.*, 2009; Kaufman *et al.*, 2015; Matulonis *et al.*, 2016; Tutt *et al.*, 2010; van der Noll *et al.*, 2015) resulting in its approval for clinical use. However, efficacy of PARP inhibitors seems to be low in platinum-resistant cancers (Coleman *et al.*, 2015; Fong *et al.*, 2010). This indicates that PARP inhibitors will be unlikely to provide an alternative therapy for patients who have developed resistance against platinum-based treatments.

A common problem with treatment of *BRCA*-mutated tumours is the development of resistance to therapies. Driven by the genomic instability intrinsic to BRCA deficiency, intragenic secondary mutations in the *BRCA1* or *BRCA2* gene arise restoring expression of a functional *wildtype* protein. This mechanism has been reported to mediate resistance to both platinum drugs and PARP inhibitors (Barber *et al.*, 2013; Edwards *et al.*, 2008; Sakai *et al.*, 2009; Sakai *et al.*, 2008; Swisher *et al.*, 2008). A clinical study examining *BRCA*-mutated ovarian cancers identified a patient with a germ line *BRCA2* mutation who had developed platinum and PARP inhibitor resistance and exhibited 12 distinct *BRCA2* secondary reversion mutations (Patch et al., 2015). A significant correlation between the presence of secondary somatic mutations that restore BRCA and the response to platinum-based chemotherapy was observed in recurrent carcinomas. Twelve (92%) of 13 carcinomas with restored BRCA were platinum-resistant (Norquist et al., 2011). The authors of the study hypothesize that reversion mutations in *BRCA* occur as a result of DNA-damaging chemotherapy and/or the endogenous genomic instability in these tumours, and that platinum therapy provides selection pressure for resistant clones with restored BRCA function. Therefore, it will be crucial to develop

alternative treatment strategies that are less prone to the emergence of secondary reversion mutations.

In mouse models, PARP inhibitor resistance can be attributed to the increased expression of genes encoding P-glycoprotein (Pg) efflux transporters. However, resistance can be prevented by co-administering PARP inhibitor with a Pg inhibitor (Rottenberg *et al.*, 2008). Whether this concept can be applied in human patients, remains to be addressed.

Multiple studies report that loss of 53BP1 (Bunting *et al.*, 2010; Jaspers *et al.*, 2013), REV7 (Boersma *et al.*, 2015; Xu *et al.*, 2015), RIF1 (Chapman *et al.*, 2013; Escribano-Diaz *et al.*, 2013; Zimmermann *et al.*, 2013) or PTIP (Callen *et al.*, 2013; Wang *et al.*, 2014) restores HR capacity in BRCA1-deficient tumours by reactivating CtIP-mediated resection leading to PARP inhibitor resistance. However, whether loss of 53BP1 causes resistance to cisplatin or other drugs remains controversial (Bouwman *et al.*, 2010; Bunting *et al.*, 2012; Jaspers *et al.*, 2013). It is noteworthy that the response to crosslinking agents may be complicated by the dual role of BRCA1 in early recognition of the ICL as well as in the HR-mediated repair of the ICL-associated DSB (see section 1.10). Possibly due to the essential function of BRCA2 in loading RAD51 at DSB sites, the aforementioned mechanism does not provide resistance in BRCA2-deficient tumours.

Recently, a novel concept of drug resistance was proposed for BRCA2-deficient tumours. Ray Chaudhuri *et al.* (2016) suggest a link between replication fork stability and chemoresistance. MRE11-mediated degradation of nascent DNA at stalled forks in cells lacking BRCA2 can be prevented by down-regulation of CHD4, PTIP or PARP1 (Ding *et al.*, 2016; Ray Chaudhuri *et al.*,

2016). Importantly, HR capacity is not restored in these cells. Supporting a correlation between fork stability and drug resistance, BRCA2-deficient tumours that have acquired resistance to PARP inhibitors or cisplatin exhibit stable replication forks. However, fork stability in these tumours was not associated with reduced levels of PTIP or MRE11 (Ray Chaudhuri *et al.*, 2016). Future studies will have to elucidate the precise contribution of fork stability to the development of resistance to chemotherapeutic agents.

BRCA-deficient cells rely on DSB repair by POLQ-mediated A-NHEJ (Ceccaldi *et al.*, 2015; Mateos-Gomez *et al.*, 2015). POLQ prevents RAD51 assembly on ssDNA and promotes A-NHEJ in BRCA-deficient cells. These functions are mediated by the RAD51-binding domain and the polymerase domain of POLQ, respectively (Ceccaldi *et al.*, 2015; Mateos-Gomez *et al.*, 2015). However, the relative contribution of the two to the synthetic lethality between POLQ and BRCA remains to be elucidated. This will allow the design of specific chemical POLQ inhibitors to target BRCA deficiency. POLQ depletion hypersensitises BRCA-deficient cells to PARP inhibitor and cisplatin (Ceccaldi *et al.*, 2015) indicating potential combination therapies for *BRCA*-mutated cancers in the future.

A need for new strategies to target BRCA-defective tumours is undeniable, in particular to treat tumours that have acquired resistance to current therapies. One promising example is 6-thioguanine. This compound effectively kills BRCA-deficient tumours including those that have gained resistance through Pg induction or genetic reversion of the *BRCA2* gene (Issaeva *et al.*, 2010). Inspired by this finding, a phase II clinical trial on *BRCA*-mutated breast and ovarian tumours was initiated with 6-thioguanine prodrugs (Nicum *et al.*, 2014).

In summary, current treatments for *BRCA*-mutated cancers lack sufficient effectiveness and selectivity, and are susceptible to development of resistance. Therefore, novel approaches to target BRCA-defective tumours are needed.

1.13 Study aims

The objective of this work was to identify and investigate novel strategies to selectively target BRCA-deficient cancer cells. Firstly, we aimed to determine the effect of the G4-stabilising compound pyridostatin on BRCA1- and BRCA2-deficient cells (addressed in chapter 3). Secondly, we sought to investigate the interplay between the FA pathway and HR. We were particularly interested in the relationship between the key players FANCD2 and BRCA2 due to their essential roles in replication and DNA damage repair (addressed in chapter 4). Thirdly, we intended to explore a possible synthetic lethal interaction between MRE11 and BRCA2. Along this line, we sought to characterise a novel chemical inhibitor of MRE11 nuclease (addressed in chapter 5).

2 Materials and methods

2.1 Cell lines and culture conditions

All cell lines used in this study were adherent and cultivated as monolayers at 37˚C in 5% CO_2. Human colorectal adenocarcinoma DLD1 (parental and *BRCA2*-mutated, Horizon Discovery; Figure 2.1), primary fibroblast MRC-5 and osteosarcoma U2OS (both from American Type Culture Collection) cell lines were grown in Dulbecco's Modified Eagle's Medium (DMEM; Sigma-Aldrich #D5796) supplemented with 10% foetal bovine serum (FBS; Invitrogen #10270-106) and 1% penicillin-streptomycin (Sigma-Aldrich #P4333). Tetracycline-free FBS (Thermo Fisher Scientific #SH3007003) was used for human non-small cell lung carcinoma H1299 and breast adenocarcinoma MDA-MB-231 cells (both from American Type Culture Collection) expressing doxycycline (DOX)-inducible BRCA2 small hairpin RNA (shRNA) previously established in Dr. Tarsounas' lab (Zimmer *et al.*, 2016), in which efficient depletion of BRCA2 was achieved by addition of 2 μg/mL DOX (Sigma-Aldrich #D9891) to the media for 3 days. The mechanism underlying DOX-inducible shRNA expression is shown in Figure 2.2. Human retinal-pigmented epithelial RPE1 (hTERT Cas9 $p53^{\Delta}$ and hTERT Cas9 $p53^{\Delta}$ $BRCA1^{\Delta}$) cells were a gift from Dr. Daniel Durocher (Lunenfeld-Tanenbaum Research Institute, Toronto, Canada) and were grown in DMEM supplemented with 10% FBS, 1% penicillin-streptomycin and 2 μg/mL blasticidin (Thermo Fisher Scientific #A1113903) to select for Cas9 expression.

Cells were sub-cultured when they reached 70-80% confluence. To detach cells for passaging, cells were washed with phosphate buffered saline (PBS; Fisher Scientific #BR0014) and incubated with Trypsin-EDTA (Sigma-Aldrich

#T3924) at 37˚C for 5 minutes (min). Fresh media containing serum was added to neutralise trypsinisation. The cell concentration was determined using a haemocytometer.

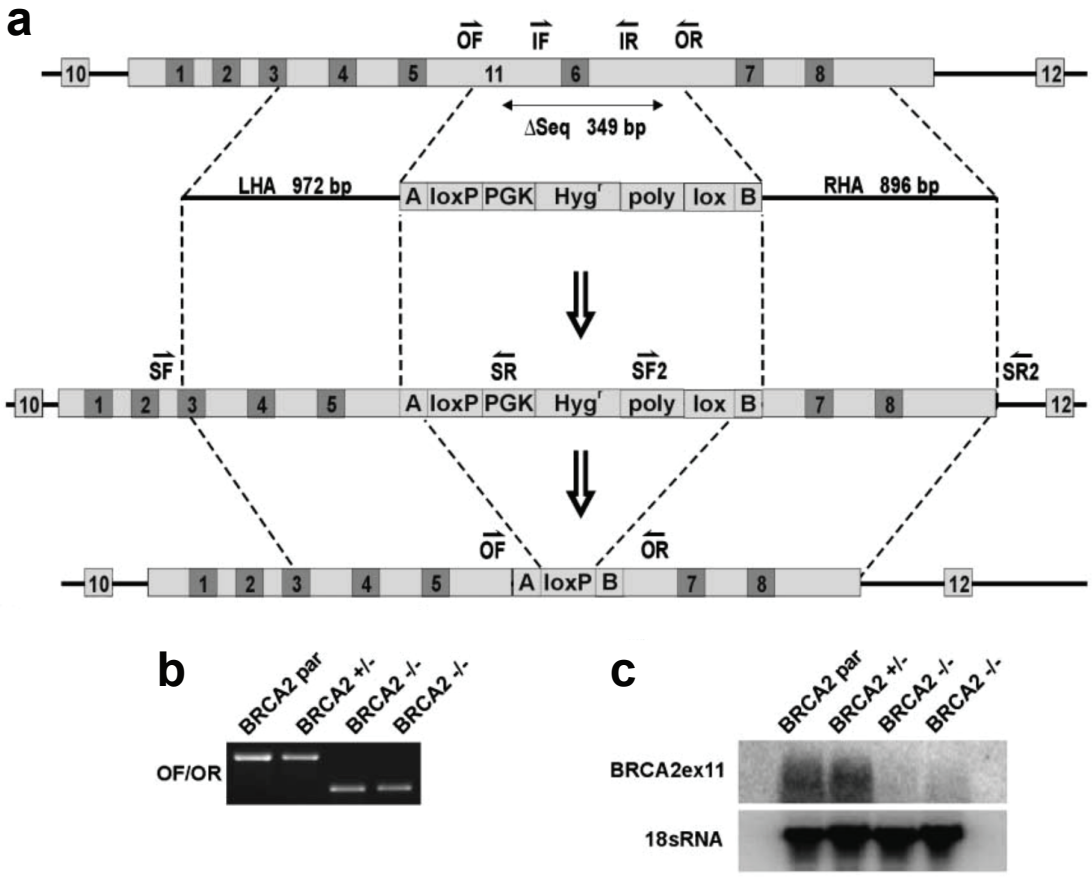


Figure 2.1. *BRCA2* disruption in the BRCA2-deficient DLD1 cell line.
(**a**) Scheme outlining the targeting strategy for *BRCA2* exon 11. Light grey boxes indicate exons and dark grey boxes indicate BRC repeats of *BRCA2*. OF and OR, primers outside the deleted sequence. IF and IR, primers inside the deleted sequence. SF, SR, SF2, and SR2, screening primer pairs. LHA and RHA, left and right homology arms. (**b**) PCR using genomic DNA of the parental cell line (BRCA2 par), heterozygous (BRCA2+/-) and homozygous (BRCA2-/-) knockout cell lines. (**c**) Northern blot detecting the *BRCA2* exon 11 mRNA transcript of cell lines in (**b**). Adapted from Hucl *et al.* (2008) with permission from the American Association for Cancer Research.

Quality Control of Horizon Discovery validated the *BRCA2* knockout in DLD1 cells (Figure 2.1) by genotyping using the following primers: TTT GAT GGT

CAA CCA GAA AGA A (forward primer) and TTC CAA ACT AAC ATC ACA AGG TG (reverse primer).

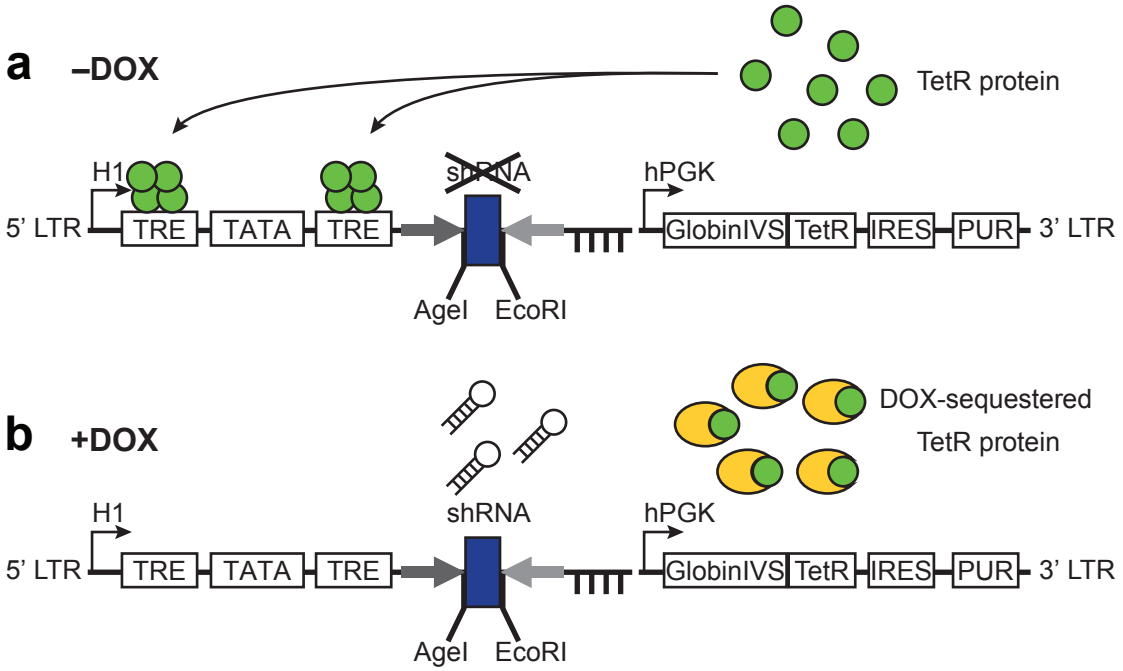


Figure 2.2. Mechanism of DOX-inducible shRNA expression.
(**a**) In the absence of DOX (–DOX), shRNA expression is repressed by constitutively expressed TetR protein, which binds to the TREs within the H1 promoter. (**b**) In the presence of DOX (+DOX), TetR protein is sequestered and the shRNA is expressed. GlobinIVS-TetR, GlobinIVS-Tet repressor fusion. H1, H1 promoter. hPGK, constitutive polymerase II hPGK promoter. IRES, internal ribosomal entry site. LTR, long terminal repeat. PUR, puromycin resistance gene. TATA, TATA box. TetR, Tet repressor. TRE, Tet-responsive element. Adapted from Wiederschain *et al.* (2009) with permission from Taylor & Francis.

2.2 Generation of spheroids

DLD1 cells (1 x 10^5 per well) were seeded in 96-well round bottom ultra low attachment plates (Sigma-Aldrich #CLS7007) and centrifuged at 210 x g for 10 min. Spheroids were cultured at 37°C and 5% CO_2. Drug treatment was initiated 4 days after seeding and fresh drug-containing media was replaced every 3 days. Images were acquired using a Nikon TE2000-E microscope, and spheroid volumes were determined using Matlab R2014a.

2.3 RNAi transfection

DLD1 (8 x 10^5) or H1299 (3 x 10^5) cells were reverse-transfected in 6 cm dishes (Greiner Bio-One #628160) using Dharmafect 1 (Dharmacon #T-2001) according to manufacturer's instructions. In brief, 5 µL Dharmafect reagent were added to 0.5 mL Opti-MEM reduced serum media (Thermo Fisher Scientific #31985062) and incubated at room temperature (RT) for 5 min. This solution was then mixed with 0.5 mL Opti-MEM reduced serum media containing small interfering RNA (siRNA), incubated at RT for 20 min and then added to the cell suspension. The media was replaced after 24 h of incubation at 37˚C. Depletion of the proteins of interest was complete 48 h after transfection, as determined by immunoblotting. 53BP1 (CAG GAC AGU CUU UCC ACG AAU), BRCA1 (CAG CAG UUU AUU ACU CAC UAA), POLQ (UUU CAU AUA AAC AUU CUG G) and MRE11 (GAG CAU AAC UCC AUA AGU A) siRNA with two-base deoxynucleotide overhangs as well as FANCD2 and BRCA2 siGENOME SMARTpool siRNA (used at 40 nM) were obtained from Dharmacon (#M-016376-02 and #M-003462-01), FANCD2 esiRNA (used at 20 nM) was obtained from Sigma-Aldrich (#EHU029261), and AllStars negative control siRNA was obtained from Qiagen (#1027281).

2.4 Cell viability assay

Cell viability was assessed using resazurin-based assays. Resazurin is a blue dye that is enzymatically reduced to red fluorescent resorufin in the mitochondria of viable cells. The reaction is detectable and quantifiable fluorometrically, and is considered a reliable readout for cell viability

(Czekanska, 2011). Cells seeded in triplicate at densities of 1,000 to 3,000 cells per well in 96-well plates (Corning #353072) were allowed to attach before growth media were replaced with drug-containing media. Cell viability was assessed by incubation with 10 µg/mL resazurin (Sigma-Aldrich #R7017) at 37°C for 2 h. Subsequently, fluorescence was measured at 544 nm using a plate reader (POLARstar Omega, BMG Labtech). Data were analysed using Prism software (GraphPad). Cell viability was expressed relative to untreated cells of the same cell line.

2.5 Clonogenic survival assay

Cells were plated in triplicate at densities between 200 and 4,000 cells per well in 6-well plates (Greiner Bio-One #657160), and drug treatment was initiated after cells had adhered. Colonies were stained with 0.5% crystal violet (Sigma-Aldrich #C6158) in 50% methanol (Thermo Fisher Scientific #M/3900) and 20% ethanol (Thermo Fisher Scientific #E/0600) in dH_2O after 10-14 days. Cell survival was expressed relative to untreated cells of the same cell line.

2.6 Drug treatments

Compounds used in this study are summarised in Table 1.

Table 1. Compounds.

Name	Target	Solvent	Supplier
Camptothecin	topoisomerase I	DMSO	Sigma-Aldrich (#C9911)
Hydroxyurea	ribonucleoside reductase	dH_2O	Sigma-Aldrich (#H8627)
KU55933	ATM	DMSO	Sigma-Aldrich (#SML1109)
Mirin	MRE11	DMSO	Sigma-Aldrich (#M9948)
MU147	MRE11	DMSO	Dr. Lumir Krejci
Olaparib	PARP1/2	DMSO	Selleckchem (#S1060)
Pyridostatin	G-quadruplexes	dH_2O	Sigma-Aldrich (#SML0678)

2.7 Fluorescence-activated cell sorting (FACS)

Cells were harvested by trypsinisation and centrifugation for 10 min at 300 x g. The supernatant was removed, and cells were washed in PBS and fixed in 70% ice-cold ethanol overnight at -20°C. Fixed cells were pelleted by centrifugation for 5 min at 300 x g followed by two washes in PBS. After incubation with 10 µg/mL RNase A (Sigma-Aldrich #R6513) for 5 min at RT, DNA was stained with 20 µg/mL propidium iodide (Sigma-Aldrich #P4864) and analysed using flow cytometry (FACSCalibur, Becton Dickinson). Data was acquired using CellQuest Pro (Becton Dickinson) and at least 10,000 events per condition and experiment were analysed using ModFit LT software (Verity Software House).

2.8 5-ethynyl-2'-deoxyuridine (EdU) incorporation

To label replicated DNA, cells seeded were incubated with 10 µM EdU for 45 min at 37°C and processed using the Click-iT EdU Alexa Fluor 647 Flow Cytometry Assay Kit (Thermo Fisher Scientific #C10634) according to manufacturer's instructions with modifications. In brief, cells were collected by trypsinisation, washed in 1% bovine serum albumin (BSA; Sigma-Aldrich #A7906) in PBS and fixed in 4% paraformaldehyde (Electron Microscopy Services #15710) in PBS for 15 min at RT. Cells were washed in 1% BSA in PBS and resuspended in 100 µL saponin-based permeabilisation and wash reagent. Subsequently, 100 µL Click-iT reaction cocktail containing copper sulfate, fluorescent dye azide and reaction buffer additive in PBS was added and cells were incubated for 30 min at RT. Cells were washed in saponin-based permeabilisation and wash reagent and resuspended in PBS containing 20 µg/ml propidium iodide and 10 µg/ml RNase A before samples were processed using flow cytometry (FACSCalibur, Becton Dickinson). Data was acquired using CellQuest Pro (Becton Dickinson) and at least 10,000 events per condition and experiment were analysed using FlowJo software (FlowJo, LLC).

2.9 Mitotic index determination

Cells were harvested by trypsinisation and fixed in 70% ice-cold ethanol overnight at -20°C, followed by rehydration in PBS. For phospho-histone H3 staining of mitotic cells, non-specific binding sites were blocked by washing in PBS supplemented with 2% FBS followed by incubation with an anti-phospho-H3 (S10) antibody (1:200, Abcam #ab5176) for 1 h. The cell pellet was washed

in 2% FBS in PBS and secondary antibody (anti-rabbit Alexa Fluor 488, 1:200, Invitrogen #R37116) was added for 1 h. After incubation with 10 µg/mL RNase A for 5 min at RT, DNA was stained with 20 µg/mL propidium iodide and analysed using flow cytometry (FACSCalibur, Becton Dickinson). Analysis of at least 10,000 events per condition and experiment was performed using CellQuest Pro (Becton Dickinson) and FlowJo software (FlowJo, LLC).

2.10 Annexin V assay

Apoptotic and dead cells were labelled with a FITC Annexin V/Dead Cell Apoptosis Kit (Thermo Fisher Scientific #V13241) according to the manufacturer's instructions.

Annexin V is a Ca^{2+}-dependent phospholipid-binding protein with a high affinity for phosphatidyl serine, which is situated on the cytoplasmic side of the plasma membrane in live cells. Upon apoptosis onset, phosphatidyl serine is translocated from the inner to the outer surface of the membrane. Exposed phosphatidyl serine can then detected and bound by Annexin V (Koopman *et al.*, 1994; van Engeland *et al.*, 1998).

Briefly, cells were harvested by trypsinisation, washed in PBS and resuspended in 100 µL Annexin-binding buffer. Then, 5 µL AlexaFluor 488 Annexin V and 1 µL propidium iodide working solution (100 µg/mL) were added. Cells were incubated for 15 min at RT, before 400 µL Annexin-binding buffer was added. Stained cells were immediately analysed by flow cytometry (FACSCalibur, Becton Dickinson). Live cells excluded staining. Early apoptotic cells bound Annexin V–FITC but excluded propidium iodide. Cells in necrotic or

late apoptotic stages were labelled with both Annexin V-FITC and propidium iodide. 20,000 events were analysed per condition and experiment using CellQuest Pro (Becton Dickinson) and FlowJo software (FlowJo, LLC).

2.11 Senescence-associated β-galactosidase assay

Expression of senescence-associated β-galactosidase was used as a biomarker of senescent cells (Dimri *et al.*, 1995). Cells were fixed with 2% formaldehyde and 0.2% glutaraldehyde (Sigma-Aldrich #G7526) for 10-15 min at RT and stained by incubation with freshly prepared staining solution (1 mg/mL X-Gal (Fisher Scientific #T-5062), 5 mM potassium ferrocyanide (Sigma-Aldrich #P9387), 150 mM NaCl (Fisher Scientific #S/31120/63), 2 mM $MgCl_2$ (VWR #25108.260) and 40 mM citric acid (Sigma-Aldrich #C83155), pH 6.0) at 37°C under atmospheric CO_2 levels. Staining was stopped after 6 h. Cells were examined using light microscopy.

2.12 Metaphase spreads preparation

Cells were arrested in metaphase using colcemid, which depolymerises microtubules and prevents spindle formation during mitosis (Yang *et al.*, 2010). Following 4-h incubation with 0.1 µg/mL colcemid (Life Technologies #15210-040), mitotic cells were collected by mitotic shake-off and swollen in pre-warmed hypotonic buffer (0.03 M sodium citrate (Thermo Fisher Scientific #BP327)) at 37˚C for 25 min. Three drops of freshly prepared fixative (3:1 mix of methanol and acetic acid (VWR #20103.330)) were added to the cells followed

by centrifugation at 650 x g for 10 min. Then, the supernatant was aspirated leaving 1 mL for resuspending the cells. After 11 mL of fixative were added, the cells were pelleted by centrifugation again. After resuspending the pellet in 250-500 µL fixative, the cells were dropped onto slides pre-soaked in 45% acetic acid and left to dry overnight. For Giemsa staining, metaphase spreads were incubated with 0.1 M phosphate buffer (pH 6.8; 0.1 M NaH_2PO_4 (VWR #102454R) and 0.1 M Na_2HPO_4 (VWR #102494C)) for 1 min, with 0.025% trypsin in 0.1 M phosphate buffer (pH 6.8) for 2 min and again in 0.1 M phosphate buffer (pH 6.8) for 1 min. Metaphase spreads were incubated with Giemsa (VWR #350864X) for 15 min, washed with dH_2O three times prior to mounting. Specimens were viewed with an inverted microscope (Leica DMI6000B) and fluorescence imaging workstation equipped with a HCX Plan-Apochromat 100x/1.4-0.7 oil objective. Images were acquired using a DFC350 FX R2 digital camera (Leica) and LAS-AF software (Leica). Quantifications were performed using ImageJ (National Institutes of Health, USA).

2.13 Immunofluorescence

Cells were washed in PBS and lysed in hypotonic solution (85.5 mM NaCl and 5 mM $MgCl_2$) for 5 min at RT. Next, cells were fixed with 4% paraformaldehyde for 10 min at RT and permeabilised in 4% paraformaldehyde supplemented with 0.03% SDS (National Diagnostics #EC-874). After washing in PBS with 0.4% Photoflo (Sigma-Aldrich #P7417) and blocking with antibody dilution buffer (1% goat serum (Sigma-Aldrich #G6767), 0.3% BSA, 0.005% Triton X-100 (Sigma-Aldrich #X100) in PBS), cells were incubated with primary antibody overnight at

RT. On the next day, cells were washed three times in PBS with 0.4% Photoflo and secondary antibody was added for 1 h. Following three washes as above, the coverslips were dried and mounted on microscope slides using Prolong Antifade Gold supplemented with DAPI (Thermo Fisher Scientific #P36931). Images were acquired and analysed as described for metaphase spreads.

2.14 Alkaline single-cell gel electrophoresis comet assay

DNA damage levels were assessed using alkaline comet assays, in which the intensity of the comet tail relative to the head is indicative of the extent of DNA damage. Comet assays were performed as previously described (Parsons *et al.*, 2009). In brief, 2 x 10^5 cells were embedded in 1% low-melting agarose in PBS on a microscope slide. Subsequently, the cells were lysed in buffer containing 2.5 M NaCl, 100 mM EDTA (Sigma-Aldrich #E9884), 10 mM Tris-HCl pH 10.5 (Fisher Scientific #BP152), 1% DMSO (Sigma-Aldrich #D8418) and 1% Triton X-100 for 1 h at 4˚C. To denature the DNA, the slides were incubated in cold electrophoresis buffer (300 mM NaOH (VWR #28245.298), 1 mM EDTA, 1% DMSO, pH >13) for 30 min in the dark. Following electrophoresis at 25 V and 300 mA for 25 min, the DNA was neutralised with 0.5 M Tris-HCl pH 8.0. After staining with SYBR Gold, specimens were viewed using a Nikon eclipse Ni-E microscope. Tail measurements were performed using the Komet 5.5 image analysis software (Andor Technology).

2.15 DNA fibre assay

DNA was labelled by addition 25 µM CldU (Sigma-Aldrich # C6891) or 250 µM IdU (Sigma-Aldrich #I7125) and incubation at 37°C. Cells were washed with warm PBS three times in between treatments with thymidine analogues CldU and IdU as well as hydroxyurea and pyridostatin. Cells were harvested by trypsinisation and 0.5 x 10^6 cells were resuspended in cold PBS. Next, 7 µL lysis buffer (200 mM Tris-HCl pH 7.4, 50 mM EDTA, 0.5% SDS) were mixed with 2 µL cell suspension on a microscopy slide and incubated horizontally for 7 min at RT. The DNA was spread by tilting the slide manually at an angle of 30°-45°. The air-dried DNA was fixed in methanol/acetic acid (3:1) for 10 min. Slides were then rehydrated in PBS twice for 3 min and the DNA was denatured in 2.5 M HCl (VWR #20252.244) for 1 h at RT. The slides were washed several times in PBS until a pH of 7-7.5 was reached, followed by incubation in blocking solution (2% BSA, 0.1% Tween 20 (Sigma-Aldrich #P7949), PBS; 0.22 µm filtered) for 40 min at RT and in primary antibodies (rat anti-CldU, 1:500 (Abcam #ab6326) and mouse anti-IdU, 1:100 (Becton Dickinson #347580)) for 2.5 h at RT. After five washes in PBS-Tween (0.2% Tween 20 in PBS) for 3 min and one short wash in blocking solution, the slides were incubated with the secondary antibodies (anti-rat Cy3, 1:300 (Jackson Immuno Research #712-165-153) and anti-mouse Alexa 488, 1:300 (Invitrogen #R37120)) for 1 h at RT. Subsequently, they were washed as before, air-dried and mounted in Prolong Antifade Gold (Thermo Fisher Scientific #P36930). Images were acquired and analysed as described for metaphase spreads.

2.16 Immunoblotting

Cells were harvested by trypsinisation and resuspended in appropriate amounts of SDS-PAGE loading buffer (0.16 M Tris-HCl pH 6.8, 4% SDS, 20% glycerol (MP Biomedical #193996), 0.01% bromophenol blue (Thermo Fisher Scientific #B392-5), 100 mM DTT (Thermo Fisher Scientific #BP172-5)). Samples were sonicated briefly (Ultrasonic Homogeniser 300VT, BioLogics Inc.), boiled at 70˚C for 10 min and centrifuged at 20,000 x g for 7 min. Relative protein concentrations were assessed using a spectrophotometer; equal amounts of protein were analysed by SDS-PAGE and immunoblotting. Samples were loaded onto Bis-Tris (Life Technologies #NP0302) or Tris-Acetate (Life Technologies #EA03752) gels and separated at 180 V in MOPS, MES or Tris-Acetate SDS running buffer (Life Technologies #NP0001, #NP0002 and #LA0041), respectively, using the XCell SureLock Mini-Cell system (Thermo Fisher Scientific #EI0001). Semi-dry transfer in transfer buffer (Life Technologies #NP00061) with 10% methanol was applied to transfer proteins onto a nitrocellulose membrane (GE Healthcare Life Sciences #10600001). To block non-specific binding sites, the membrane was incubated in blocking buffer (5% dried skimmed milk in PBS-Tween (0.05% Tween 20 in PBS)) for 1 h at RT. The protein of interest was detected by incubation with primary antibody (diluted in 2% BSA and 0.05% azide in PBS-Tween) overnight at 4˚C. The next day, the membrane was washed in PBS-Tween three times for 5 min at RT. After incubation with secondary antibody diluted in blocking buffer for 1 h at RT, the membrane was washed in PBS-Tween three times for 10 min at RT. Subsequently, ECL western blotting detection reagent (Thermo Scientific #1859701 & #1859698, Millipore #WBKLS0100 or GE Healthcare

#RPN2235V1/2) was used to detect proteins on X-ray films (Fujifilm #4741019289).

2.17 Antibodies

Primary and secondary antibodies used for immunoblotting (IB) and immunofluorescence (IF) are listed in Table 2 and Table 3.

Table 2. Primary antibodies.

Target, Name	Host	Dilution/Purpose	Target size (kDa)	Supplier
53BP1	rabbit	1:5,000 (IB/IF)	214	Novus Biologicals (NB100-304)
ATM pS1981, 10H11	mouse	1:1,000 (IB)	350	Cell Signaling (4526)
ATM, clone MAT3-4G10/8	mouse	1:5,000 (IB)	350	Sigma-Aldrich (A1106)
BRCA1	mouse	1:2,000 (IB)	220	Calbiochem (OP92)
BRCA2	mouse	1:2,000 (IB)	390	Calbiochem (OP95)
BrdU/ CldU	rat	1:500 (DNA fibre)		Abcam (ab6326)
BrdU/ IdU	mouse	1:100 (DNA fibre)		Becton Dickinson (347580)
CHK2 pT68	rabbit	1:1000 (IB)	62	Cell Signaling (2661)
FANCD2	rabbit	1:5,000 (IB)	166	Novus Biologicals (NB100-182)
GAPDH, 6C5	mouse	1:30,000 (IB)	37	Novus Biologicals (NB600-502)
H2AX, DR1016	rabbit	1:5,000 (IB)	13	Calbiochem

Table 2: Primary antibodies (continued).

Target, Name	Host	Dilution/Purpose	Target size (kDa)	Supplier
KAP1 pS824,	rabbit	1:1,000 (IB)	89	Bethyl Laboratories (A300-767A)
KAP1	rabbit	1:5,000 (IB)	100	Bethyl Laboratories (A300-274A)
MRE11	rabbit	1:5,000 (IB)	81	Novus Biologicals (NB100-142)
POLQ, 1B1	mouse	1:10,000 (IB)	198	Dr. J.-S. Hoffman
RPA2, 9H8	mouse	1:1,000 (IB)	29	Abcam (ab2175)
RPA32 pS4/S8	rabbit	1:4,000 (IB)	32	Bethyl Laboratories (A300-245A)
SMC1, BL308	rabbit	1:4,000 (IB)	160	Bethyl Laboratories (A300-055A)
γH2AX (S139), clone JBW301	mouse	1:4,000 (IB), 1:2,000 (IF)	15	Merck Millipore (05-636)

Table 3. Secondary antibodies.

Name	Type	Supplier
DAR Cy3	Cy3 donkey anti-rat IgG	Jackson Immuno Research (712-165-153)
GAM	goat anti-mouse polyclonal IgG-HRP	Dako (P0447)
GAM Alexa 488	Alexa Fluor 488 goat anti-mouse IgG	Invitrogen (R37120)
GAR	goat anti-rabbit polyclonal IgG-HRP	Dako (P0448)
GAR Alexa 546	Alexa Fluor 546 goat anti-rabbit IgG	Invitrogen (A-11035)

2.18 Statistical analysis

Statistical analysis was performed using Prism 6 software (GraphPad). Unpaired two-tailed *t*-tests, Mann-Whitney tests or chi-square tests were used in order to assess significant difference between samples. p values < 0.05 were considered to be statistically significant. Levels of statistical significance are indicated as follows: *, $p < 0.05$; **, $p < 0.01$; ***, $p < 0.001$; ****, $p < 0.0001$.

3 Targeting BRCA1 and BRCA2 deficiencies with G4-interacting compounds

3.1 Introduction

The diploid human genome consists of over 6 billion base pairs of DNA that have to be replicated trillions of times in a lifetime. Accurate and complete duplication of the DNA once per cell cycle is vital to maintain genome integrity. Telomeres, the natural ends of chromosomes, pose a serious challenge to accurate replication and are among the best-characterised sites with G4-forming potential due to their repetitive G-rich DNA sequence (Parkinson *et al.*, 2002). In line with the key function of these nucleoprotein complexes in protecting chromosome ends from degradation and fusion (McClintock, 1941; Palm *et al.*, 2008), telomere dysfunction leads to genomic instability (Blackburn, 2001). HR prevents telomere replication defects and telomere shortening (Badie *et al.*, 2010). Recently, BRCA2 was shown to inhibit telomere fragility specifically of the G-rich telomeric strand, which has G4-forming potential (Zimmer *et al.*, 2016).

Besides at telomeres, G4s have been detected at more than 700,000 distinct sites in the human genome (Chambers *et al.*, 2015). HR is known to be essential to prevent replication stress stemming from accumulation of unrepaired replication-associated DSBs (Arnaudeau *et al.*, 2001). Persistent G4s are potent replication barriers that can trigger replication stress (Bochman *et al.*, 2012), leading to DNA breakage, DDR activation and cell cycle arrest. In recent years, various chemical compounds have been shown to selectively bind and stabilise G4s with the small molecule pyridostatin being a potent

example (Muller *et al.*, 2010; Rodriguez *et al.*, 2008). Given the ability of G4s to induce replication stress and the vital role of HR in the repair of replication-associated DSBs, we hypothesised that G4 stabilisation may be particularly toxic in the context of HR deficiency with deleterious consequences on cell viability.

3.2 G4 stabiliser pyridostatin decreases viability of BRCA1- and BRCA2-deficient cells

To investigate the effect of G4 stabilisation in the context of BRCA1 and BRCA2 deficiency, we performed resazurin-based viability assays in BRCA1-proficient and -deficient RPE1 retinal pigmented epithelial cell lines as well as in BRCA2-proficient and -deficient DLD1 colorectal adenocarcinoma cell lines. The BRCA2 knockout in DLD1 cells was validated by sequencing of genomic DNA (by Quality Control, Horizon Discovery, see section 2.1). Lack of BRCA expression in RPE1 and DLD1 cell lines was confirmed by immunoblotting (Figure 3.1).

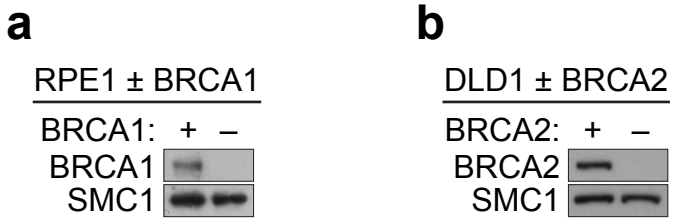


Figure 3.1. BRCA status of RPE1 and DLD1 cell lines.
BRCA1-proficient (+BRCA1) and -deficient (–BRCA1) RPE1 cells (**a**) and BRCA2-proficient (+BRCA2) and -deficient (–BRCA2) DLD1 cells (**b**) were immunoblotted as indicated. SMC1 was used as a loading control.

Based on its ability to preferentially kill BRCA-deficient cells, the PARP inhibitor olaparib was used as a control in the viability experiments (Bryant *et al.*, 2005; Farmer *et al.*, 2005). Treatment with olaparib for 6 days resulted in a dose-dependent reduction in viability of BRCA1- or BRCA2-deficient cells, whilst viability of the HR-proficient parental cell lines was hardly affected (Figure 3.2a and c). Interestingly, treatment with the G4-interacting compound pyridostatin for 6 days caused a marked decrease in viability of BRCA1-deficient RPE1 cells compared to their BRCA1-proficient counterparts (Figure 3.2b). Similarly, exposure of BRCA2-deficient DLD1 cells to pyridostatin induced a pronounced decrease in viability (Figure 3.2d). These data suggest that G4 stabilisation by pyridostatin selectively kills HR-defective cells.

It is important to note that the effect of pyridostatin in the context of BRCA1 deficiency was assessed in a non-transformed immortalised cell line (RPE1) while its effect on BRCA2-deficient cell viability was tested in a cancer cell line (DLD1). Non-transformed cell lines provide an important tool for genetic and cell biology studies. The limited life span of primary cells (Hayflick, 1965; Hayflick *et al.*, 1961) can be overcome by immortalisation. Cell lines immortalised by telomerase overexpression are thought to share more similarity with primary cells than with cancer cells (Lee *et al.*, 2004b). In line with this statement, hTERT-immortalised RPE1 cells are chromosomally stable with a diploid karyotype (Kuznetsova *et al.*, 2015; Thompson *et al.*, 2008), which makes them suitable for genetic manipulation. It is noteworthy that the RPE1 cell lines used in this study were deficient in p53, a characteristic that has been linked to genomic instability in these cells (Mardin *et al.*, 2015). Genomic instability is a common feature of cancers (see section

1.3). Cancer cell lines are the most widely used molecular models for cancer biology and anticancer therapies because they mimic certain characteristics of tumours (Gillet *et al.*, 2013). In contrast to normal cells, tumour-derived cells have adapted several genetic and epigenetic changes associated with carcinogenesis, tumour progression and drug treatment responses (Goodspeed *et al.*, 2016). Importantly, siRNA-mediated depletion of BRCA1 in DLD1 cells sensitised cells to olaparib and pyridostatin (Figure 3.12) consistent with the results obtained in RPE1 cells (Figure 3.2a and b).

Given that the difference in pyridostatin sensitivity between BRCA2-proficient and -deficient DLD1 cells was much clearer than between BRCA1-proficient and -deficient RPE1 cells, we decided to use the DLD1 cell lines as a model to further study the consequences of G4 stabilisation in the context of HR deficiency.

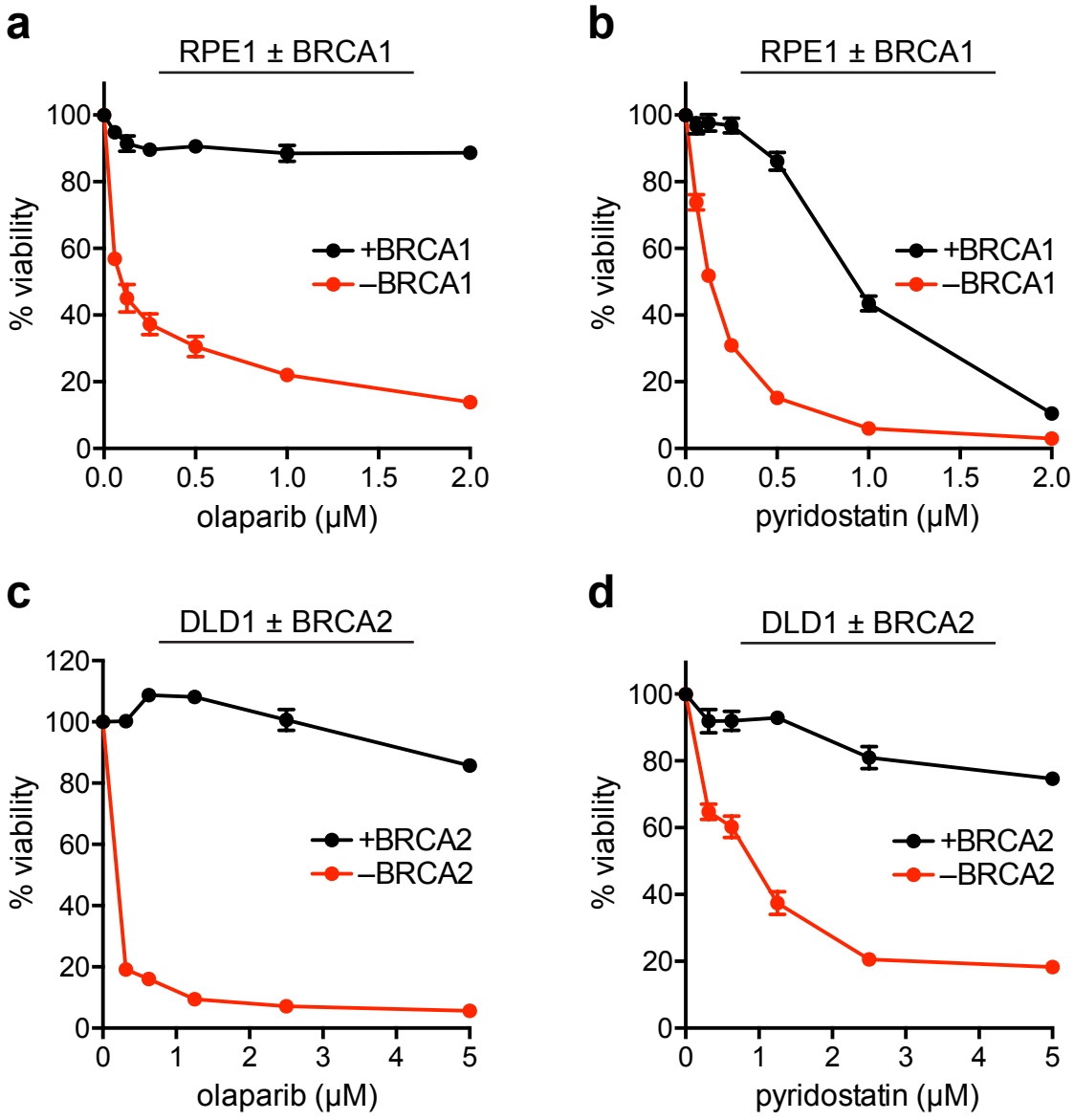


Figure 3.2. G4 stabilisation by pyridostatin decreases viability of BRCA1- and BRCA2-deficient human cells.
(**a** and **b**) Dose-dependent viability assays of BRCA1-proficient (+BRCA1) and -deficient (–BRCA1) RPE1 cells treated with indicated concentrations of olaparib (**a**) or pyridostatin (**b**) for 6 days. Graphs are representative of three independent experiments, each performed in triplicate. Error bars represent SEM of triplicate values obtained from a single experiment. (**c** and **d**) Dose-dependent viability assays of BRCA2-proficient (+BRCA2) and -deficient (–BRCA2) DLD1 cells treated with indicated concentrations of olaparib (**c**) or pyridostatin (**d**) for 6 days. Graphs are representative of three independent experiments, each performed in triplicate. Error bars represent SEM of triplicate values obtained from a single experiment.

3.3 Pyridostatin causes G2/M cell cycle arrest

The antiproliferative effect of pyridostatin has previously been linked to the accumulation of cells in the G2 phase of the cell cycle (Rodriguez *et al.*, 2012). Therefore, we sought to investigate whether the toxic effect of pyridostatin in cells lacking BRCA2 was associated with impaired cell cycle progression using FACS analysis (Figure 3.3).

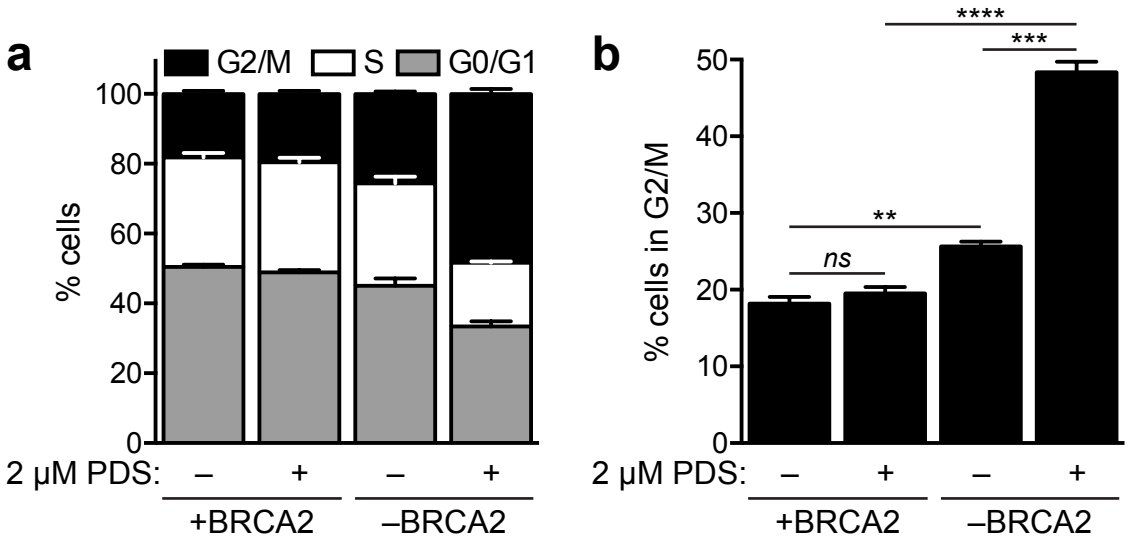


Figure 3.3. Pyridostatin induces G2/M arrest in BRCA2-deficient cells.
(**a**) Cell cycle distribution of BRCA2-proficient (+BRCA2) and -deficient (–BRCA2) DLD1 cells exposed to indicated treatments for two days. (**b**) Quantification of cells in G2/M phase of cells treated as in (**a**). At least 10,000 cells were analysed per condition and experiment. Error bars represent SEM of three independent experiments. *p* values were calculated using an unpaired two-tailed *t*-test (*ns*, non-significant; **, $p < 0.01$; ***, $p < 0.001$; ****, $p < 0.0001$). PDS, pyridostatin.

Untreated BRCA2-proficient and -deficient cells showed similar cell cycle distribution profiles with a mean of around 20 - 25% of cells in G2/M phase (Figure 3.3). The cell cycle profile of BRCA2-proficient cells remained unchanged after 48 h of treatment with 2 μM pyridostatin, whereas about 50% of BRCA2-deficient cells accumulated in G2/M, a significant increase

compared to untreated (p = 0.0026) or BRCA2-proficient pyridostatin-treated cells (p < 0.0001; Figure 3.3). These results indicate that the G2/M checkpoint is activated upon pyridostatin treatment specifically in BRCA2-deficient cells, leading to cell cycle arrest.

3.4 Pyridostatin slows replication fork progression

G4s are thought to assemble primarily during DNA replication when ssDNA is available (see section 1.4). Accordingly, DNA damage induced by pyridostatin has been shown to be replication-dependent (Rodriguez *et al.*, 2012). Both, reduced replication rates and increased origin firing are signatures of replicative stress (Zeman *et al.*, 2014). In order to define G4-induced replication stress in the context of BRCA2 deficiency, DNA fibre analyses were performed (Figure 3.4). BRCA2-proficient and -deficient DLD1 cells were labelled with consecutive 30-min pulses of the thymidine analogues CldU and IdU, respectively. Pyridostatin was added at a concentration of 2 μM during the second (IdU) pulse, and the ratio between IdU and CldU track length (hereafter called relative track length) was quantified. This allowed us to investigate the immediate effect of pyridostatin on replication dynamics.

A significant decrease in the relative track length was observed in pyridostatin-treated compared to untreated cells (p < 0.0001), an effect that was far more prominent in cells lacking BRCA2 (Figure 3.4a and c). Thus, pyridostatin is likely to promote persistent G4s that slow replication and/or cause DNA breakage that impede fork progression.

In response to replicative stress, dormant origins are fired to ensure completion of DNA replication during S phase (Ge *et al.*, 2007; Ibarra *et al.*, 2008; Woodward *et al.*, 2006). Possibly as a compensatory mechanism for hindered replication fork progression, pyridostatin treatment significantly increased origin firing ($p = 0.0243$), detected as green track only (Figure 3.4b). BRCA2-deficient cells displayed significantly elevated levels of origin firing compared to their BRCA2-proficient counterparts ($p = 0.0453$) indicative of the intrinsic replication stress associated with BRCA2 deficiency (Figure 3.4b). Strikingly, addition of pyridostatin further exacerbated this effect ($p = 0.0119$; Figure 3.4b). Altogether, pyridostatin-mediated G4 stabilisation caused signs of replication stress providing a possible explanation for the toxicity of pyridostatin in BRCA2-deficient cells.

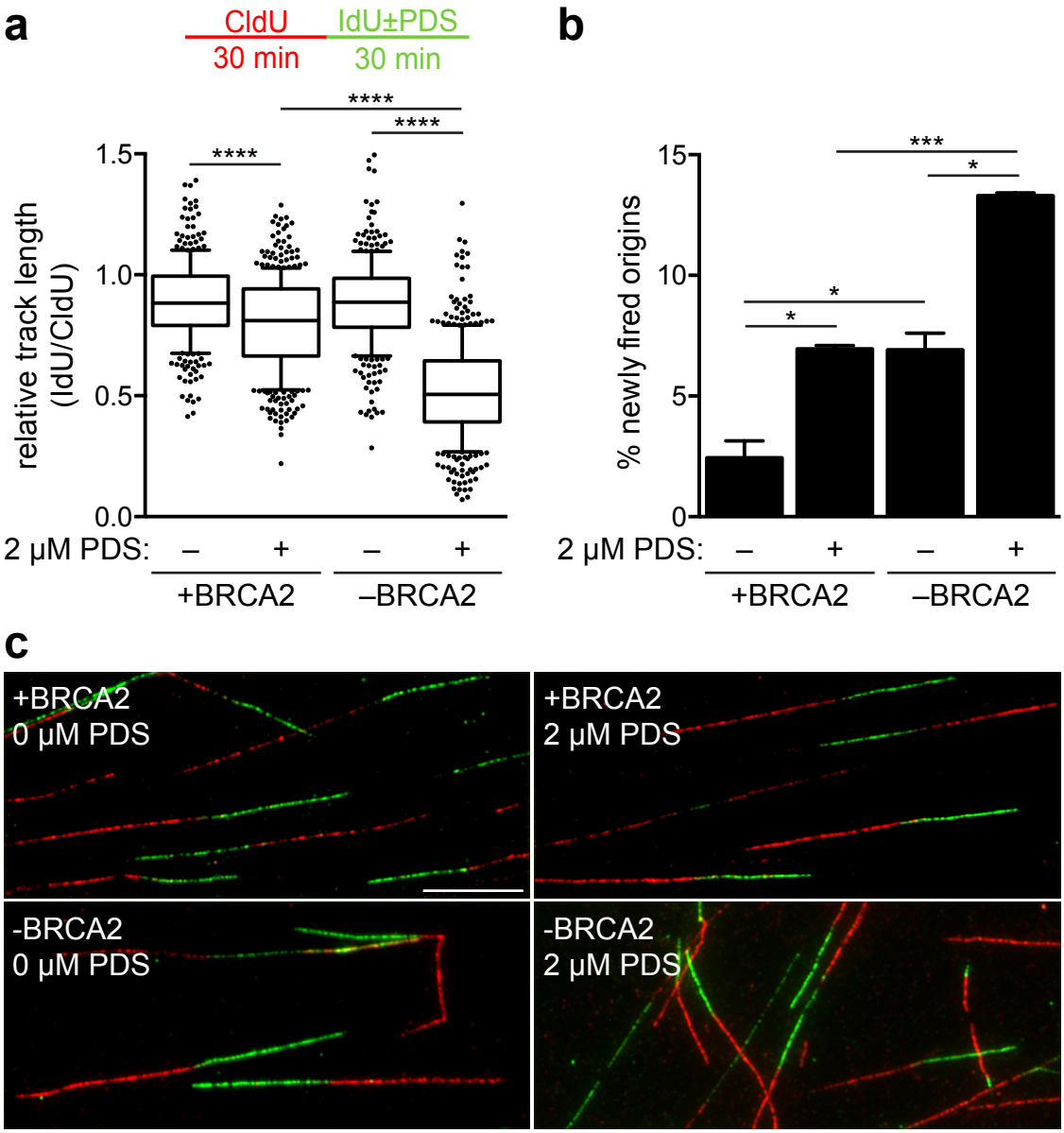


Figure 3.4. Pyridostatin decreases replication progression.
(**a**) BRCA2-proficient (+BRCA2) and -deficient (–BRCA2) DLD1 cells were processed for DNA fibre analysis as outlined in the inset followed by quantification of the relative replication track length (IdU/CldU). At least 150 fibres were quantified per condition and experiment. Middle line represents median, and the box extends from the 25th to 75th percentiles. The whiskers mark the 10th and 90th percentiles. *p* values were calculated using a Mann-Whitney test (*n*=2 independent experiments; ****, $p < 0.0001$). (**b**) Quantification of the frequency of newly fired origins in cells treated as in (**a**). At least 150 fibres were quantified per condition and experiment. Error bars represent SEM of two independent experiments. *p* values were calculated using an unpaired two-tailed *t*-test (*, $p < 0.05$; ***, $p < 0.001$). (**c**) Representative fibre images of cells treated as in (**a**). Scale bar, 10 μm. PDS, pyridostatin.

3.5 Nascent DNA at pyridostatin-stalled forks is degraded in an MRE11-dependent manner

Recently, Schlacher *et al.* (2011) identified a novel role for BRCA2 in protecting stalled replication forks from nucleolytic degradation by MRE11. In cells lacking BRCA2, depletion of the nucleotide pool by hydroxyurea leads to attrition of the nascent DNA strand, which is suppressed by treatment with mirin, a MRE11 nuclease inhibitor (Schlacher *et al.*, 2011). To investigate whether pyridostatin caused replication fork stalling similarly to hydroxyurea, we performed DNA fibre experiments (Figure 3.5). Replicated DNA was pulse-labelled with CldU and IdU for 30 min, after which cells were exposed to 2 mM hydroxyurea or 2 μM pyridostatin for 5 h. Attrition of the IdU track was used as a readout for degradation of nascent DNA at stalled forks.

Neither hydroxyurea nor pyridostatin had a drastic effect on the ratio between the IdU and CldU track length (relative track length) of BRCA2-proficient cells (Figure 3.5). However, both compounds induced a significant reduction in the relative track length of cells lacking BRCA2 ($p < 0.0001$), an effect that was reversed by addition of the MRE11 nuclease inhibitor mirin (Figure 3.5). This suggests that pyridostatin leads to stalling of replication forks and that BRCA2 is required to protect nascent DNA at pyridostatin-stalled forks from MRE11-mediated degradation.

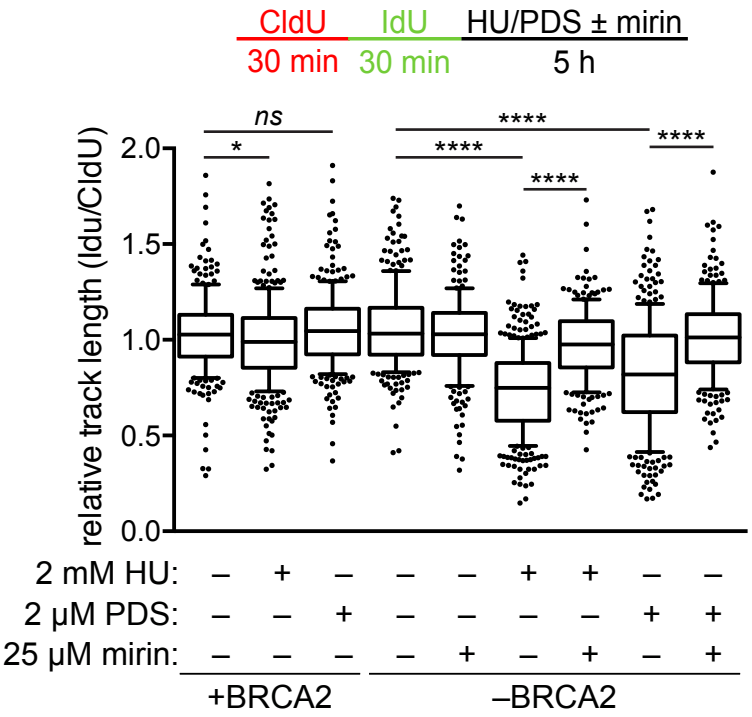


Figure 3.5. Pyridostatin causes stalled forks that are degraded by MRE11. BRCA2-proficient (+BRCA2) and -deficient (–BRCA2) DLD1 cells were processed for DNA fibre analysis as outlined in the inset followed by quantification of the relative replication track length (IdU/CldU). At least 50 fibres were quantified per condition and experiment. Middle line represents median, and the box extends from the 25th to 75th percentiles. The whiskers mark the 10th and 90th percentiles. *p* values were calculated using a Mann-Whitney test (*n*=3 independent experiments; *ns*, non-significant; *, $p < 0.05$; ****, $p < 0.0001$). HU, hydroxyurea. PDS, pyridostatin.

3.6 MRE11 nuclease inhibition does not rescue pyridostatin sensitivity

Replication fork stability has recently been proposed to confer resistance to chemotherapeutic agents in BRCA-deficient cells (Ray Chaudhuri *et al.*, 2016). Therefore, we sought to address whether pyridostatin toxicity in BRCA2-deficient cells could be attributed to loss of replication fork protection and subsequent MRE11-dependent fork degradation. We reasoned that chemical inhibition of MRE11 nuclease activity by mirin may thus promote resistance to G4 stabilisation by pyridostatin.

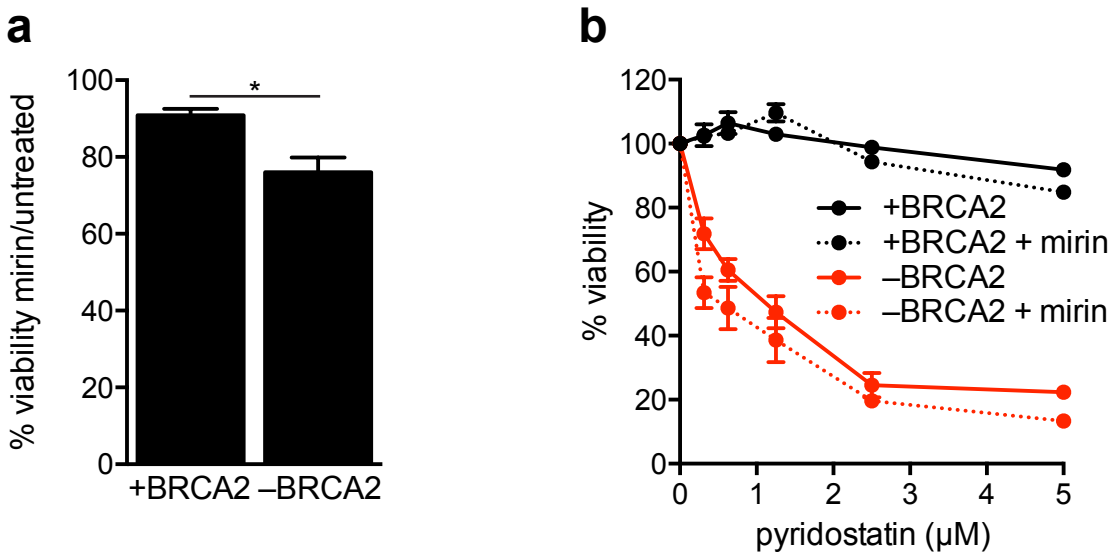


Figure 3.6. Inhibition of MRE11 nuclease activity is insufficient to rescue pyridostatin-induced BRCA2-deficient cell killing.
(**a**) Effect of 5 μM mirin on the viability of BRCA2-proficient (+BRCA2) and -deficient (–BRCA2) DLD1 cells after 6 days. (**b**) Dose-dependent viability assays of BRCA2-proficient (+BRCA2) and -deficient (–BRCA2) DLD1 cells treated with the indicated concentrations of pyridostatin in the presence (+mirin) or absence (-mirin) of 5 μM mirin for six days. Graphs are representative of three independent experiments, each performed in triplicate. Error bars represent SEM of triplicate values obtained from a single experiment. *p* values were calculated using an unpaired two-tailed *t*-test (*, $p < 0.05$)

We assessed toxicity of pyridostatin using resazurin-based assays when mirin was added at 5 μM, a concentration that mildly reduced cell viability (by about 10% for BRCA2-proficient and about 20% for BRCA2-deficient cells) within 6 days of treatment (Figure 3.6a). However, mirin did not alter the response to pyridostatin (Figure 3.6b), suggesting that MRE11 inhibition is insufficient to rescue the cell killing effect of pyridostatin in BRCA2-deficient cells.

3.7 Pyridostatin-induced DNA damage can be repaired independently of BRCA2

Replication stress is commonly associated with DNA breakage (Zeman *et al.*, 2014). Given the replication stress induced by pyridostatin in BRCA2-deficient cells, we next assessed if replication stress led to DNA damage in these cells.

Firstly, we monitored foci formation of the DNA damage markers γH2AX and 53BP1 after treatment with 2 μM pyridostatin for 16 h using immunofluorescence. A robust induction of both γH2AX and 53BP1 foci was observed in BRCA2-deficient cells after pyridostatin treatment, whilst foci induction in BRCA2-proficient cells was minor (Figure 3.7). This indicates that G4 stabilisation by pyridostatin causes DNA damage accumulation specifically in the context of BRCA2 deficiency.

Secondly, we asked whether pyridostatin-induced DNA damage could be repaired independently of BRCA2. Therefore, we treated cells with 2 μM pyridostatin for 16 h and quantified γH2AX and 53BP1 foci after releasing cells from pyridostatin into fresh media. The percentage of BRCA2-deficient cells exhibiting more than 20 γH2AX foci or more than 10 53BP1 foci was reduced significantly 72 h after release from pyridostatin ($p = 0.0007$ for γH2AX and $p = 0.0004$ for 53BP1; Figure 3.7).

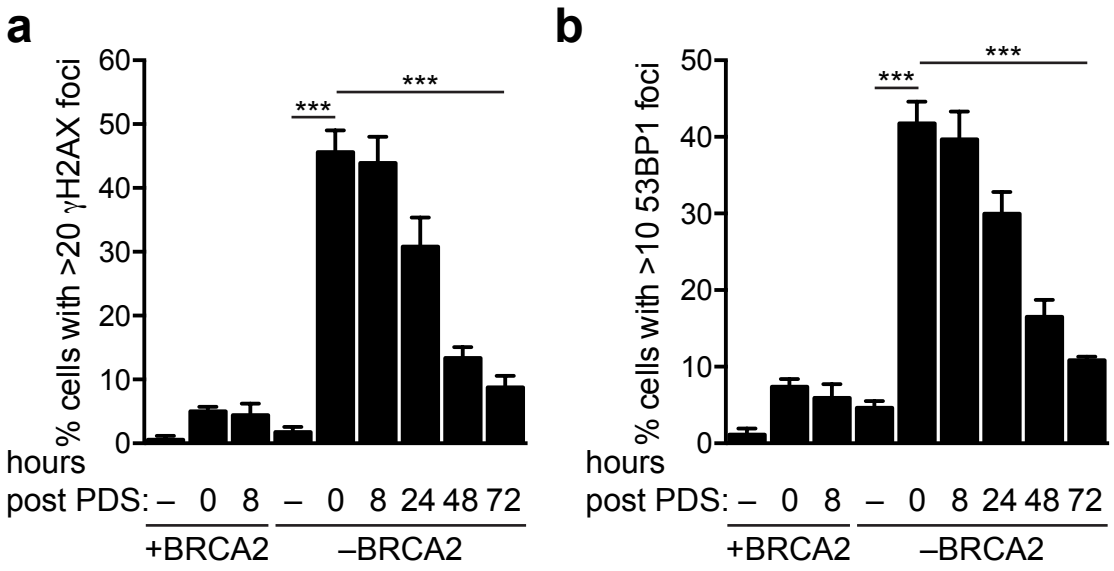


Figure 3.7. Pyridostatin-induced DNA breakage is repaired in cells lacking BRCA2.
(**a** and **b**) BRCA2-proficient (+BRCA2) and -deficient (–BRCA2) DLD1 cells were treated with 2 μM pyridostatin for 16 h and released into fresh media for indicated times. Shown are quantifications of cells with > 20 γH2AX foci (**a**) or > 10 53BP1 foci (**b**) assessed by immunofluorescence. At least 200 cells were analysed per condition and experiment. Error bars represent SEM of three independent experiments. *p* values were calculated using an unpaired two-tailed *t*-test (***, $p < 0.001$). PDS, pyridostatin.

To exclude the possibility that the decrease in γH2AX and 53BP1 foci was caused by a DNA damage signalling defect, alkaline comet assays were performed. Here, DNA damage levels were measured by comparing the percentage of tail DNA to total DNA in an individual cell. Pyridostatin induced a significant increase in tail DNA specifically in cells lacking BRCA2 ($p = 0.0107$) consistent with elevated DNA damage levels. DNA integrity was restored to levels of untreated cells 72 h after release from pyridostatin (Figure 3.8a and b). DNA breaks were also visualised using Giemsa-stained spreads of metaphase chromosomes. Upon pyridostatin treatment, increased numbers of chromosome aberrations were observed in BRCA2-deficient cells, which were resolved after release for 72 h (Figure 3.8c and d).

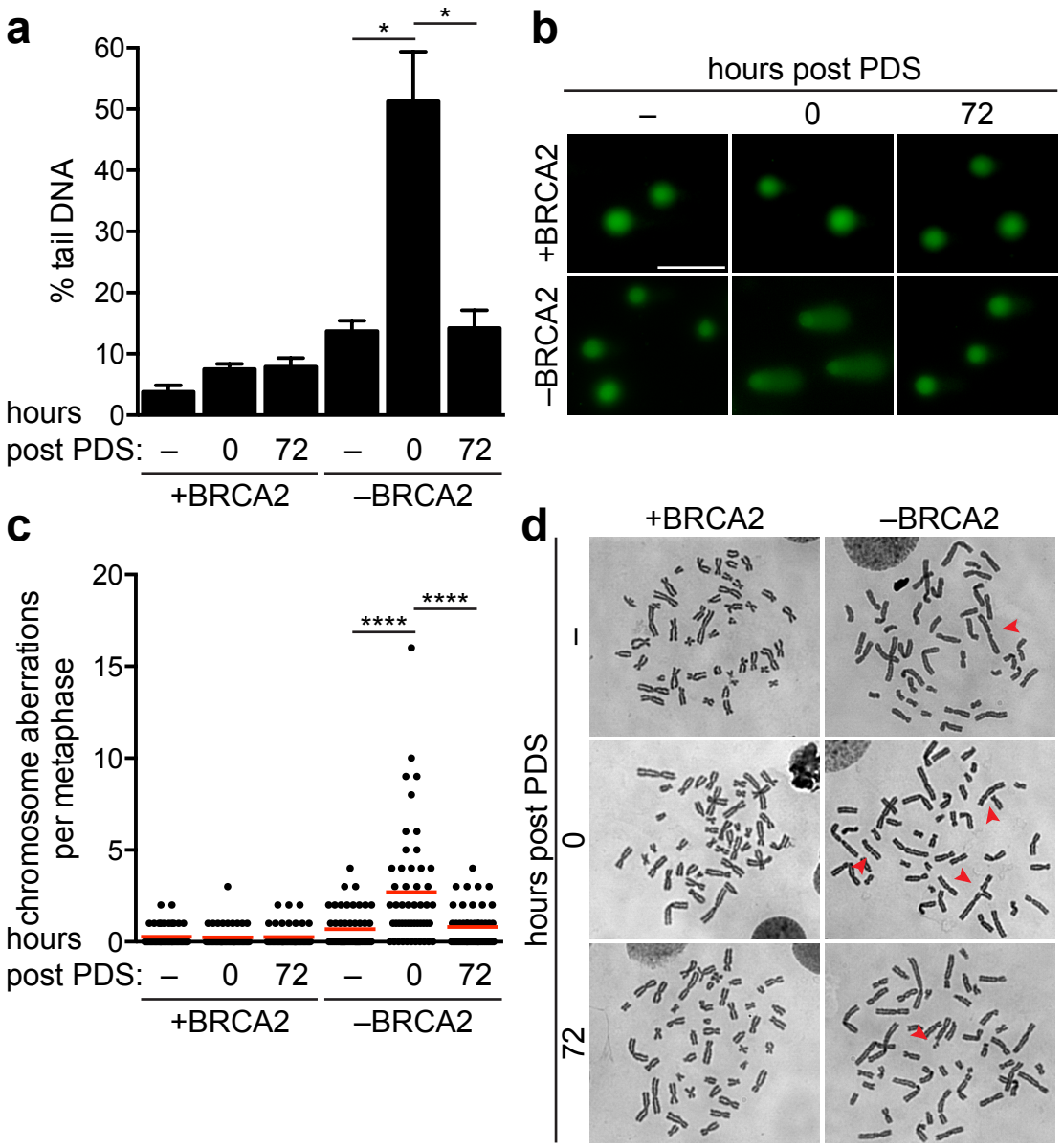


Figure 3.8. DNA breaks are resolved after release from pyridostatin in BRCA2-deficient cells.

(**a** and **b**) BRCA2-proficient (+BRCA2) and -deficient (–BRCA2) DLD1 cells were treated with 2 μM pyridostatin for 16 h, released into fresh media for 72 h and processed for alkaline comet assays. Shown is quantification of tail DNA (**a**) and representative images (**b**). 50 cells were analysed per condition and experiment. Error bars represent SEM of three independent experiments. *p* values were calculated using an unpaired two-tailed *t*-test (*, $p < 0.05$). Scale bar, 100 μm. (**c** and **d**) Metaphase spreads of cells treated as in (**a**) were prepared. Shown is quantification of chromosomal aberrations per metaphase (**c**) and representative images (**d**). Arrowheads point to aberrations. 50 metaphases were analysed. Each dot represents one metaphase. Red bars represent means. *p* values were calculated using a Mann-Whitney test (****, $p < 0.0001$). PDS, pyridostatin.

To assess whether BRCA2-deficient cells progressed normally through the cell cycle after release from pyridostatin, we performed FACS analysis. Indeed, cells did not arrest in a particular phase of the cell cycle after pyridostatin release (Figure 3.9). In summary, these data indicate that DNA damage induced by pyridostatin is repaired in the absence of BRCA2.

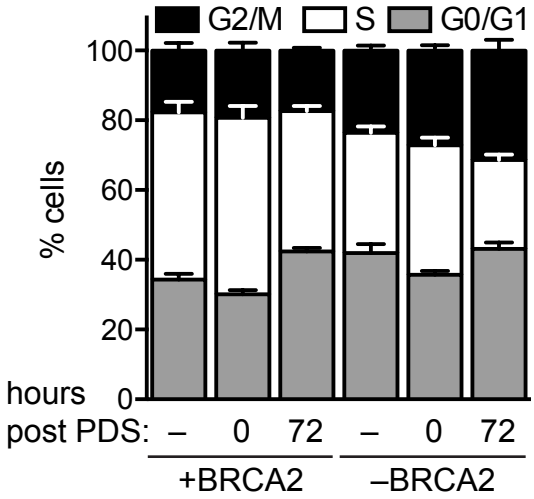


Figure 3.9. Release from pyridostatin does not induce cell cycle arrest.
BRCA2-proficient (+BRCA2) and -deficient (–BRCA2) DLD1 cells were treated with 2 μM pyridostatin for 16 h, released into fresh media for 72 h and processed for EdU incorporation followed by FACS analysis. Shown is cell cycle distribution. Error bars represent SEM of three independent experiments.

3.8 POLQ is not required to prevent or repair pyridostatin-induced DNA damage

In *C. elegans*, POLQ is required to prevent genomic instability stemming from stalled replication forks at endogenous G4s (Koole *et al.*, 2014). Thus, we reasoned that POLQ could play a role in repairing G4-induced DNA damage in human cells. To test this hypothesis, we depleted POLQ using siRNA in

BRCA2-proficient and -deficient DLD1 cells. Efficient knockdown of POLQ was confirmed using immunoblotting (Figure 3.10a).

Depletion of POLQ significantly reduced survival of BRCA2-deficient cells ($p < 0.0001$), while BRCA2-proficient cell survival was not affected (Figure 3.10b). However, POLQ ablation had no effect on pyridostatin sensitivity of BRCA2-proficient or -deficient cells in clonogenic survival assays (Figure 3.10c).

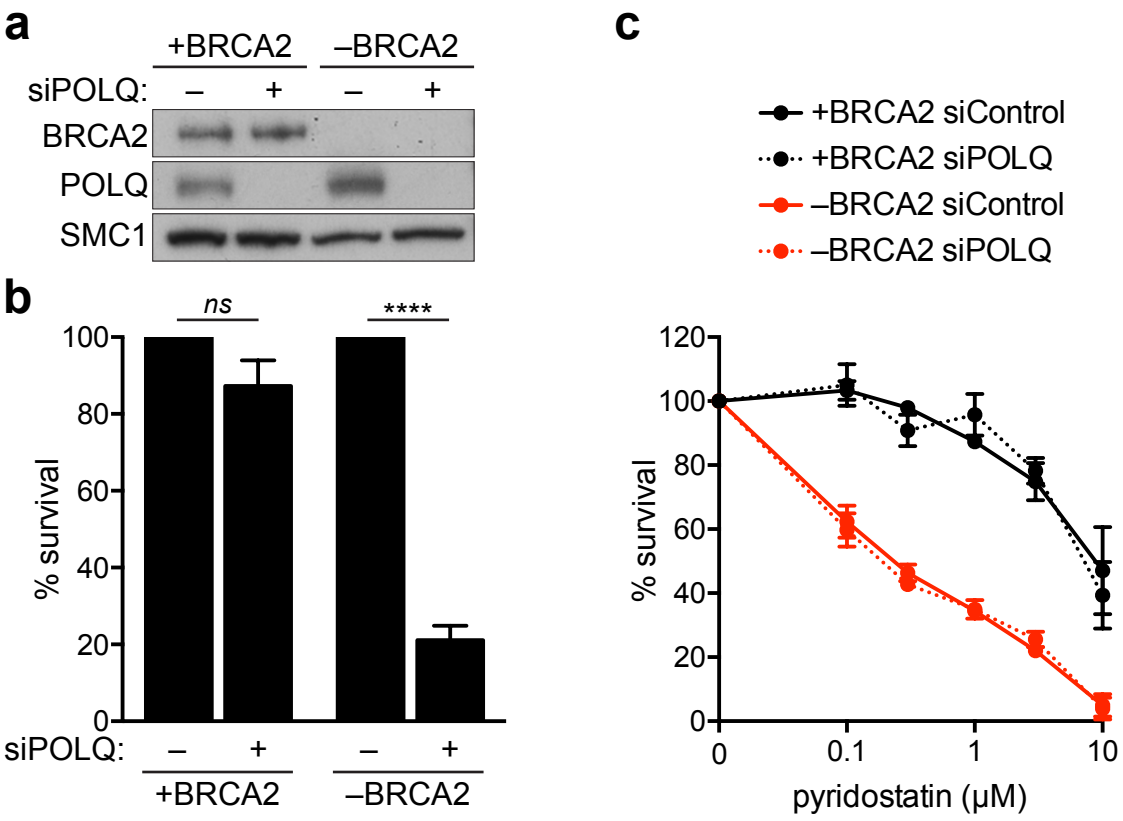


Figure 3.10. POLQ knockdown does not affect pyridostatin sensitivity.
(**a**) BRCA2-proficient (+BRCA2) and -deficient (–BRCA2) DLD1 cells transfected with control or POLQ siRNA were immunoblotted as indicated. SMC1 was used as a loading control. (**b**) Clonogenic survival assays of cells treated as in (**a**). Error bars represent SEM of three independent experiments. *p* values were calculated using an unpaired two-tailed *t*-test (*ns*, non-significant; ****, $p < 0.0001$). (**c**) Clonogenic survival assays of cells treated as in (**a**) and exposed to indicated concentrations of pyridostatin. Error bars represent SEM of three independent experiments.

Levels of γH2AX and 53BP1 foci, detected by immunofluorescence and indicative of DNA breakage, were not altered by POLQ depletion in BRCA2-proficient cells, neither in the absence nor in the presence of 2 μM pyridostatin for 16 h (Figure 3.11a and b). While loss of POLQ led to a significant increase in DNA damage in BRCA2-deficient cells (p = 0.0173 for γH2AX and p = 0.0339 for 53BP1), no additive effect was observed when cells were treated with pyridostatin (Figure 3.11a and b). A similar pattern was observed when DNA damage levels were estimated by comet assay (Figure 3.11c). Overall, these results indicate that POLQ is not required to prevent pyridostatin-induced DNA damage.

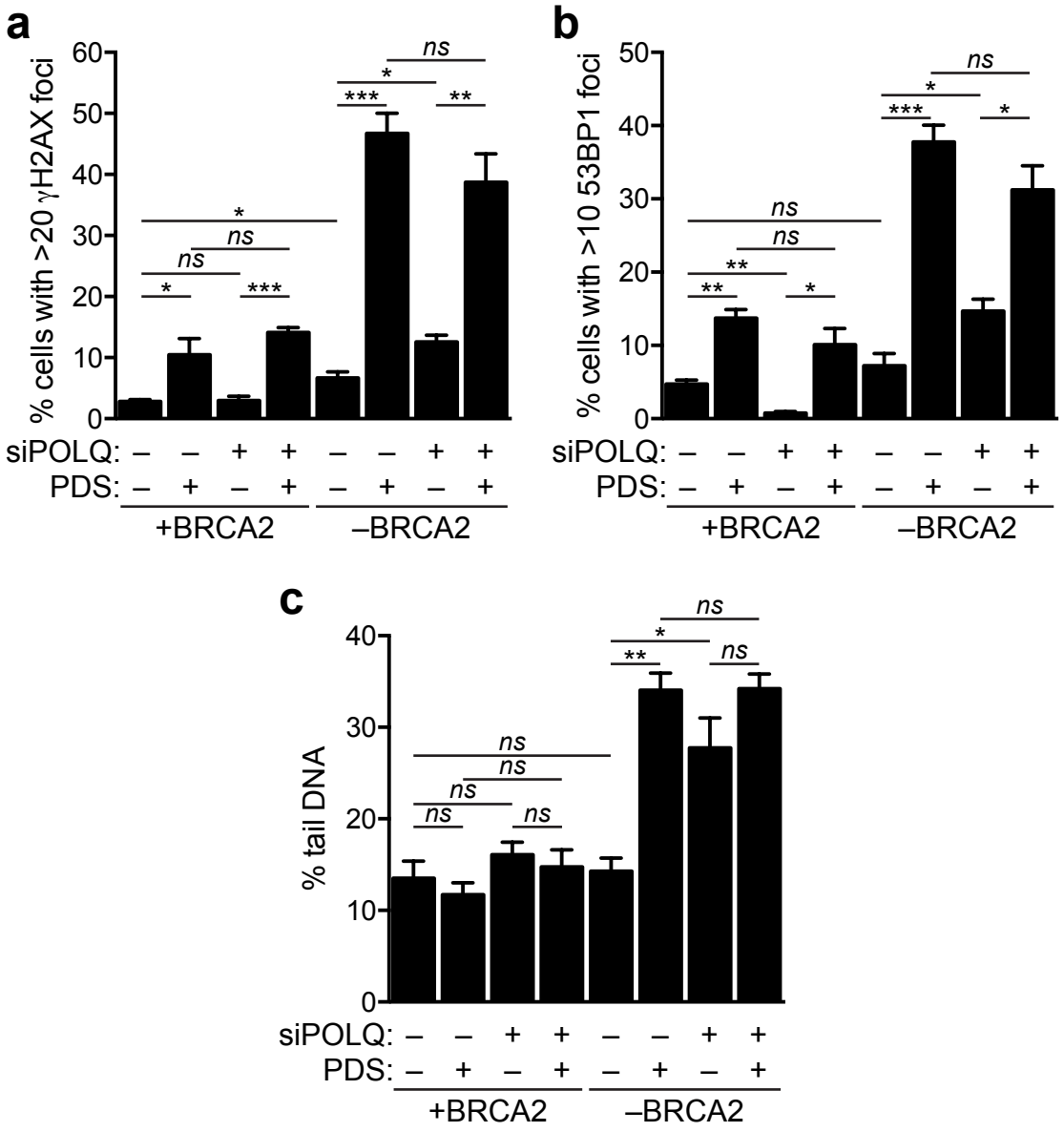


Figure 3.11. POLQ is not required to prevent pyridostatin-induced DNA damage. (**a** and **b**) BRCA2-proficient (+BRCA2) and -deficient (–BRCA2) DLD1 cells transfected with control or POLQ siRNA were treated with 2 μM pyridostatin for 16 h before processing for immunofluorescence. (**a**) Quantification of cells with > 20 γH2AX foci. (**b**) Quantification of cells with > 10 53BP1 foci. At least 200 cells were analysed per condition and experiment. Error bars represent SEM of three independent experiments. *p* values were calculated using an unpaired two-tailed *t*-test (*ns*, non-significant; *, $p < 0.05$; **, $p < 0.01$; ***, $p < 0.001$). (**c**) Cells treated as in (**a**) were processed for alkaline comet assay. Shown is quantification of tail DNA. 50 cells were analysed per condition and experiment. Error bars represent SEM of three independent experiments. *p* values were calculated using an unpaired two-tailed *t*-test (*ns*, non-significant; *, $p < 0.05$; **, $p < 0.01$). PDS, pyridostatin.

3.9 Olaparib-resistant BRCA1-deficient cells are sensitive to pyridostatin

In the clinic, the cure rates of cancer patients with dysfunctional BRCA1 or BRCA2 have been alleviated by the rapid development of drug resistance. One mechanism underlying PARP inhibitor resistance in BRCA1-deficient mouse mammary tumour cells is mediated by the concomitant loss of 53BP1 (Bunting *et al.*, 2010; Jaspers *et al.*, 2013).

To test whether this mechanism could be recapitulated in human cells, we performed clonogenic survival assays in DLD1 cells, in which BRCA1 and 53BP1 were depleted using siRNA. Expression of both BRCA1 and 53BP1 was abrogated by the respective siRNA as determined by immunoblotting (Figure 3.12a). Survival of BRCA1-depleted cells was significantly reduced by treatment with 0.1 μM olaparib for 24 h compared to control cells (p = 0.0033; Figure 3.12b). Depletion of 53BP1 resulted in a significant increase in survival of BRCA1-deficient cells treated with olaparib (p = 0.0218; Figure 3.12b). This was in line with 53BP1 ablation causing olaparib resistance in the context of BRCA1 deficiency. Next, we tested the sensitivity of olaparib-resistant BRCA1-deficient cells to pyridostatin. Treatment with 10 μM pyridostatin significantly decreased survival of BRCA1-depleted cells compared to control cells (p = 0.0001; Figure 3.12b). Strikingly, 53BP1 loss did not significantly improve survival of BRCA1-deficient cells in response to pyridostatin (p = 0.1044; Figure 3.12b). Regarding the slight, non-significant increase in survival observed in this context, it is important to consider that siRNA-mediated depletion of BRCA1 and 53BP1 has limitations regarding efficiency and duration of the protein knockdown. This may affect the results observed in the

clonogenic survival assays. Importantly, consistent with the data presented here, pyridostatin has been shown to sensitise olaparib-resistant *Brca1*-mutated mouse mammary tumour cells lacking 53BP1 (Zimmer *et al.*, 2016). Overall this suggests that BRCA1-deficient cells, including those refractory to PARP inhibitors, could be eliminated by G4-stabilising compounds.

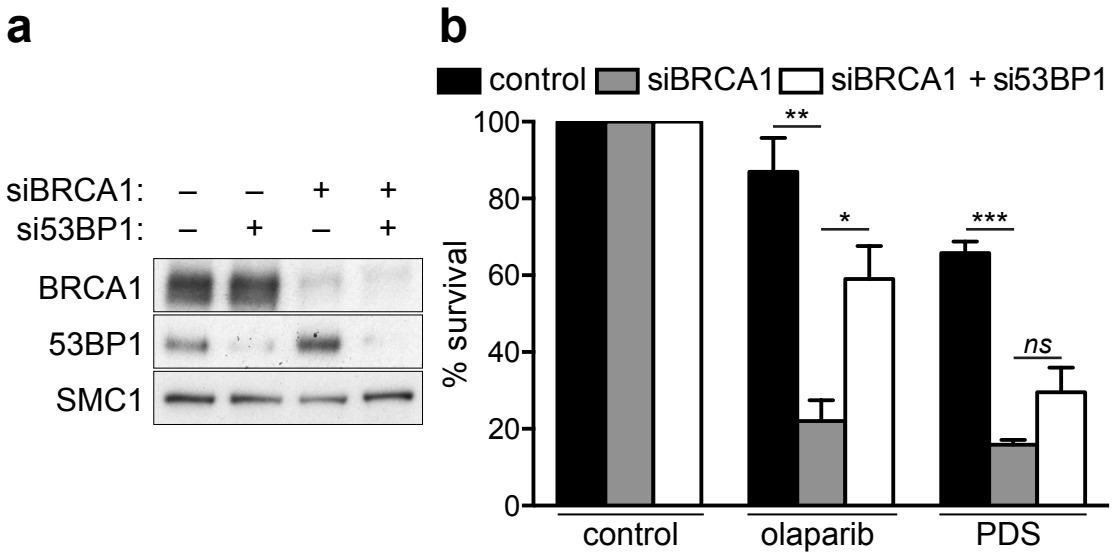


Figure 3.12. Olaparib-resistant BRCA1-deficient cells exhibit pyridostatin sensitivity.
(**a**) DLD1 cells were transfected with siRNA against BRCA1, 53BP1 or both and immunoblotted as indicated. SMC1 was used as a loading control. (**b**) Clonogenic survival assay of cells treated as in (**a**) and exposed to 10 μM pyridostatin or 0.1 μM olaparib for 24 h. Graphs shown are representative of two independent experiments, each performed in triplicate. Error bars represent SEM of triplicate values obtained from a single experiment. *p* values were calculated using an unpaired two-tailed *t*-test (*ns*, non-significant; *, $p < 0.05$; **, $p < 0.01$; ***, $p < 0.001$). PDS, pyridostatin.

3.10 Discussion

BRCA-deficient cells are known to be susceptible to replication stress-inducing and DNA-damaging agents (see section 1.12). G4-interacting compounds have been shown to stabilise G4 structures that obstruct replication fork progression. This leads to replication stress and in more severe cases DNA breakage (see section 1.4). Since BRCA1 and BRCA2 are key players in the cellular responses to replication stress and DNA damage (see section 1.11), we sought to investigate the impact of G4 stabilisation by the small molecule pyridostatin on BRCA1- and BRCA2-deficient cells.

Viability of cells lacking BRCA1 or BRCA2 was reduced by pyridostatin treatment (Figure 3.2) suggesting that G4 stabilisation provides a novel means for targeting BRCA deficiency. Furthermore, pyridostatin-treated BRCA2-deficient cells accumulated in G2/M phase of the cell cycle (Figure 3.3). The G2/M checkpoint is activated in response to damaged DNA after replication in order to prevent entry into mitosis and allow DNA damage repair (Lukas *et al.*, 2004). Thus, our data suggest that pyridostatin causes DNA damage likely during replication of BRCA2-deficient cells leading to G2/M cell cycle arrest. In agreement with this, replication fork progression was hindered by pyridostatin-mediated G4 stabilisation especially in BRCA2-deficient cells (Figure 3.4a and c). This coincides with a role of BRCA2 in the efficient replication of G4-forming sites in the genome. Our data demonstrate that G4 stabilisation by pyridostatin causes fork stalling (Figure 3.5). Several HR factors have been implicated in the restart of stalled or collapsed replication forks (Petermann *et al.*, 2010a). For example, RAD51 mediates reversal and restart of stalled forks (Petermann *et al.*, 2010b; Zellweger *et al.*, 2015). Therefore, we propose that

G4 stabilisation induces stalled forks that rely on BRCA2 to load RAD51 for restart of replication.

Nascent DNA at pyridostatin-stalled replication forks was degraded in the absence of BRCA2 in an MRE11-dependent manner (Figure 3.5). This is consistent with the previously described role of BRCA2 in protecting stalled replication forks (Schlacher *et al.*, 2011). Protection of nascent DNA at stalled forks from MRE11 nuclease-mediated degradation has recently been proposed to mediate drug resistance in BRCA-deficient cells (Ray Chaudhuri *et al.*, 2016). However, BRCA2-deficient cells remained sensitive to pyridostatin treatment despite inhibition of MRE11 nuclease activity by mirin (Figure 3.6b). There are multiple possible explanations for this. First and foremost, degradation of nascent DNA at pyridostatin-stalled replication forks may not cause the killing effect observed in cells lacking BRCA2. Alternatively, prolonged treatment with mirin may have off-target effects. MRE11 nuclease has multiple cellular functions and is not only responsible for resection at stalled forks (Stracker *et al.*, 2011).

After prolonged fork stalling, DSBs generated by collapse of replication forks are repaired by HR actions (Petermann *et al.*, 2010b; Saleh-Gohari *et al.*, 2005). In line with the concept that HR is responsible for repairing replication stress-associated DNA damage, treatment with pyridostatin for 16 h resulted in elevated levels of DNA damage markers in cells lacking BRCA2 (Figure 3.7). Nonetheless, pyridostatin-induced DNA damage was repaired within 72 h after release in BRCA2-deficient cells (Figure 3.7 and 3.8) suggesting that additional mechanisms act to prevent genomic instability arising from stabilised G4s. Inspired by work in *C. elegans* demonstrating that POLQ

maintains genome stability in the presence of G4s (Koole *et al.*, 2014), we investigated the role of POLQ in this context. POLQ depletion did not sensitise cells to pyridostatin (Figure 3.10c). Furthermore, no additive effect between pyridostatin and POLQ dysfunction on DNA damage was observed (Figure 3.11). Thus, our data indicate that POLQ does not play a role in preventing DNA damage caused by chemical G4 stabilisation. Nonetheless, it is possible that POLQ acts to bypass or resolve endogenous G4 structures in human cells. Chemical G4-interacting compounds may prevent recognition of G4 structures by POLQ. One possibility to test whether cells lacking POLQ accumulate G4s is by staining POLQ-depleted cells with a G4-specific antibody in an immunofluorescence experiment. It may also be interesting to perform whole-genome sequencing and search for POLQ signatures as previously described in *C. elegans* (Koole *et al.*, 2014; Roerink *et al.*, 2014).

In line with studies in mouse mammary tumour cell lines (Bunting *et al.*, 2010; Jaspers *et al.*, 2013), loss of 53BP1 in BRCA1-deficient human cells resulted in olaparib resistance (Figure 3.12b). Strikingly, these cells remained sensitive to pyridostatin (Figure 3.12b) suggesting that G4 stabilisation could provide a means to treat *BRCA*-mutated cancers that have developed resistance to PARP inhibition. In the context of BRCA1 deficiency, resistance to olaparib is mediated by re-activation of HR upon loss of 53BP1 (Bunting *et al.*, 2010). A clue regarding the mechanism underlying pyridostatin sensitivity of olaparib-resistant BRCA1-deficient cells came from immunofluorescence experiments performed in mouse mammary tumour cell lines (Zimmer *et al.*, 2016). Here, RAD51 foci were detected in response to olaparib and pyridostatin in BRCA1-proficient cells, in line with induction of HR.

Interestingly, while RAD51 foci were induced upon treatment with olaparib in BRCA1-, 53BP1-defective cells, no increase in RAD51 foci was observed following exposure to pyridostatin (Zimmer *et al.*, 2016). This suggests that these cells fail to re-activate HR upon pyridostatin treatment, which may contribute to their sensitivity to the compound. Whether our findings can be expanded to platinum drug-resistant BRCA-compromised tumours remains to be addressed.

In summary, our study identifies a novel role of BRCA2 in preventing G4-associated genome instability. The data presented suggest that chemical G4-stabilising compounds may provide powerful tools for the treatment of BRCA-defective tumours in the future.

4 FANCD2 limits replication stress and genomic instability in cells lacking BRCA2

4.1 Introduction

Tumour cells lacking BRCA2 are characterised by hypersensitivity to endogenous and exogenous sources of DNA damage and replication stress (Badie *et al.*, 2010; Zimmer *et al.*, 2016). This phenotype is related to the vital function of BRCA2 in HR and replication fork protection (see section 1.9). Similarly, the FA component FANCD2, which is best known for its role in ICL repair (see section 1.10), is required during DNA replication under stress conditions. Multiple studies have shown that FANCD2 coordinates various cellular responses to replication stress induced by exogenous agents (i.e. mitomycin C and hydroxyurea (Lachaud *et al.*, 2016; Lossaint *et al.*, 2013; Schlacher *et al.*, 2012)). Endogenous replication stress is a hallmark of BRCA2-deficient cells leading to genomic instability that fosters tumourigenesis. This prompted us to examine whether FANCD2 orchestrates replication stress tolerance in cells lacking BRCA2 as well as its impact on genome integrity and survival in the context of BRCA2 deficiency.

4.2 FANCD2 and BRCA2 protect stalled replication forks via distinct mechanisms

BRCA2 and FANCD2 play key roles in the repair of DSBs and ICLs (see sections 1.9 and 1.10). Additionally, the two proteins protect nascent DNA at stalled replication forks from MRE11 nuclease-mediated degradation (Schlacher *et al.*, 2011; Schlacher *et al.*, 2012). Here, we sought to address the functional interaction between these two factors during this process. To investigate fork stability in cells deficient in BRCA2 and FANCD2, H1299 cells harbouring DOX-inducible shRNA against BRCA2 were transfected with siRNA against FANCD2. Depletion of BRCA2 and FANCD2 was confirmed using immunoblotting (Figure 4.1a). Replication fork stability was assessed using DNA fibre assays, in which replicated DNA was labelled with CldU for 1 h followed by stalling replication by treatment with 2 mM hydroxyurea for 5 h.

Knockdown of FANCD2 or BRCA2 expression induced a significant shortening in replication tracks ($p < 0.0001$; Figure 4.1b), consistent with the previously reported function of the two factors in replication fork protection (Schlacher et al., 2011; Schlacher et al., 2012). An additional reduction in track length was observed upon concomitant loss of FANCD2 and BRCA2 suggesting increased levels of fork degradation (Figure 4.1b). These results indicate that FANCD2 and BRCA2 maintain fork stability via distinct mechanisms. Addition of the MRE11 nuclease inhibitor mirin partially restored track length in cells lacking both FANCD2 and BRCA2 (Figure 4.1b), implicating MRE11 as one of the nucleases mediating fork resection in this context.

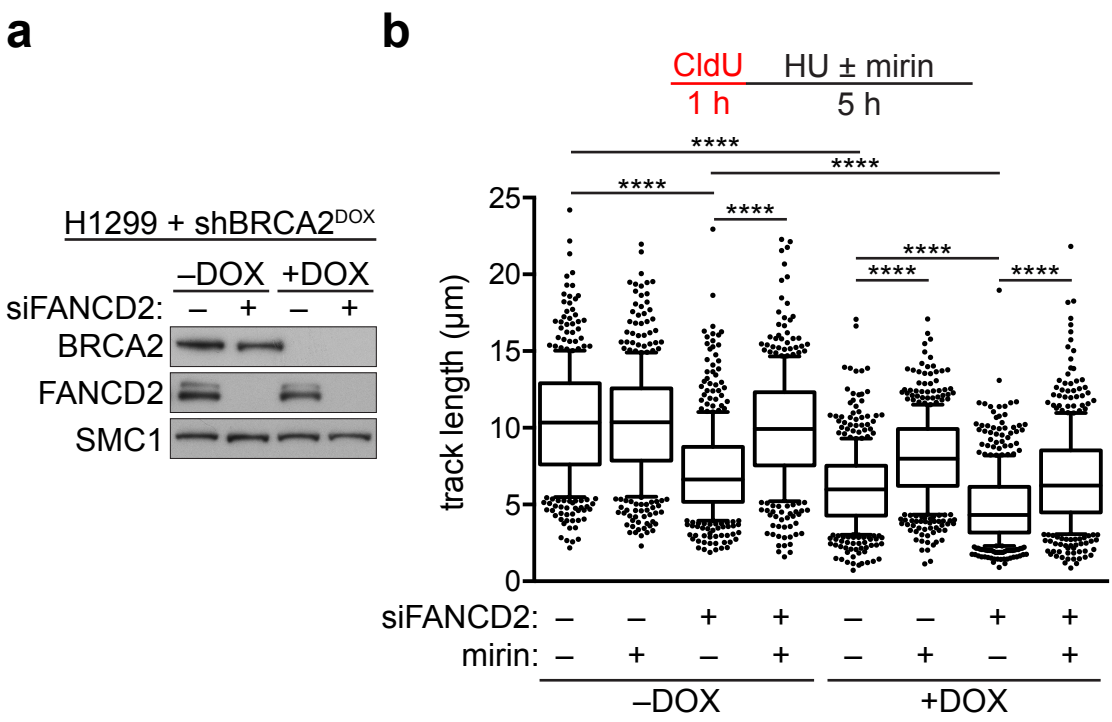


Figure 4.1. FANCD2 and BRCA2 prevent degradation of nascent DNA at stalled replication forks via distinct mechanisms.
(**a**) H1299 cells harbouring DOX-inducible shRNA against BRCA2 were transfected with control or FANCD2 siRNA and processed for immunoblotting after 72 h. SMC1 was used as a loading control. (**b**) Cells treated as in (**a**) were processed for DNA fibre analysis as outlined in the insets followed by quantification of the track length. At least 200 fibres were analysed per condition and experiment. Middle line represents median, and the box extends from the 25th to 75th percentiles. The whiskers mark the 10th and 90th percentiles. *p* values were calculated using a Mann-Whitney test (*n*=2 independent experiments; ****, $p < 0.0001$). HU, hydroxyurea. Data shown in this figure was generated in collaboration with Dr. Johanna Michl.

4.3 FANCD2 limits replication fork progression in BRCA2-deficient cells

FANCD2 has been implicated in a replisome surveillance mechanism that restrains DNA replication upon replication stress induced by hydroxyurea-mediated nucleotide depletion. This function of FANCD2 prevents accumulation of deleterious ssDNA gaps, sustains cell proliferation and protects from tumourigenesis (Lossaint *et al.*, 2013). To test whether FANCD2 limits DNA synthesis in the context of endogenous replication stress

associated with BRCA2 deficiency (Carlos *et al.*, 2013), we investigated replication dynamics in cells lacking FANCD2 and/or BRCA2 (Figure 4.2).

While depletion of BRCA2 decreased replication track length, simultaneous downregulation of FANCD2 and BRCA2 expression resulted in a track length similar to control cells (Figure 4.2). This suggests that FANCD2 restricts replication fork progression in BRCA2-deficient cells.

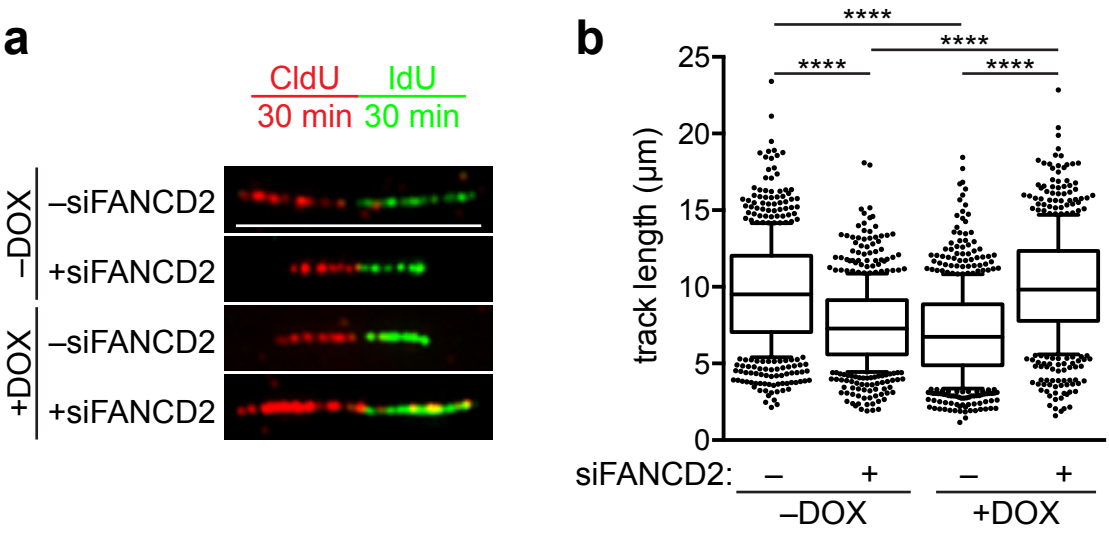


Figure 4.2. FANCD2 restricts replication in cells lacking BRCA2.
(**a** and **b**) H1299 cells harbouring DOX-inducible shRNA against BRCA2 were transfected with control or FANCD2 siRNA and processed for DNA fibre analysis as outlined in the insets. Shown are representative images (**a**) and quantification of the track length (**b**). At least 200 fibres were analysed per condition and experiment. Middle line represents median, and the box extends from the 25th to 75th percentiles. The whiskers mark the 10th and 90th percentiles. *p* values were calculated using a Mann-Whitney test (*n*=3 independent experiments; ****, $p < 0.0001$). Scale bar, 10 µm. Data shown in this figure was generated by Dr. Johanna Michl.

4.4 Loss of FANCD2 causes DNA damage accumulation in cells lacking BRCA2

Unrestrained replication has the potential to cause DNA damage accumulation (Zeman *et al.*, 2014). Thus, we sought to investigate the effects of concomitant abrogation of FANCD2 and BRCA2 on genome stability.

Spreads of mitotic chromosomes revealed significantly enhanced numbers of chromosomal aberrations in cells lacking FANCD2 and BRCA2 relative to cells lacking either one of the factors ($p < 0.0001$; Figure 4.3a and b). Consistently, levels of γH2AX foci that mark DNA damage sites were significantly elevated in FANCD2, BRCA2-depleted cells compared to single depletion of FANCD2 ($p = 0.0366$) or BRCA2 ($p = 0.0397$; Figure 4.3c). These results indicate that loss of FANCD2 triggers genomic instability in BRCA2-deficient cells.

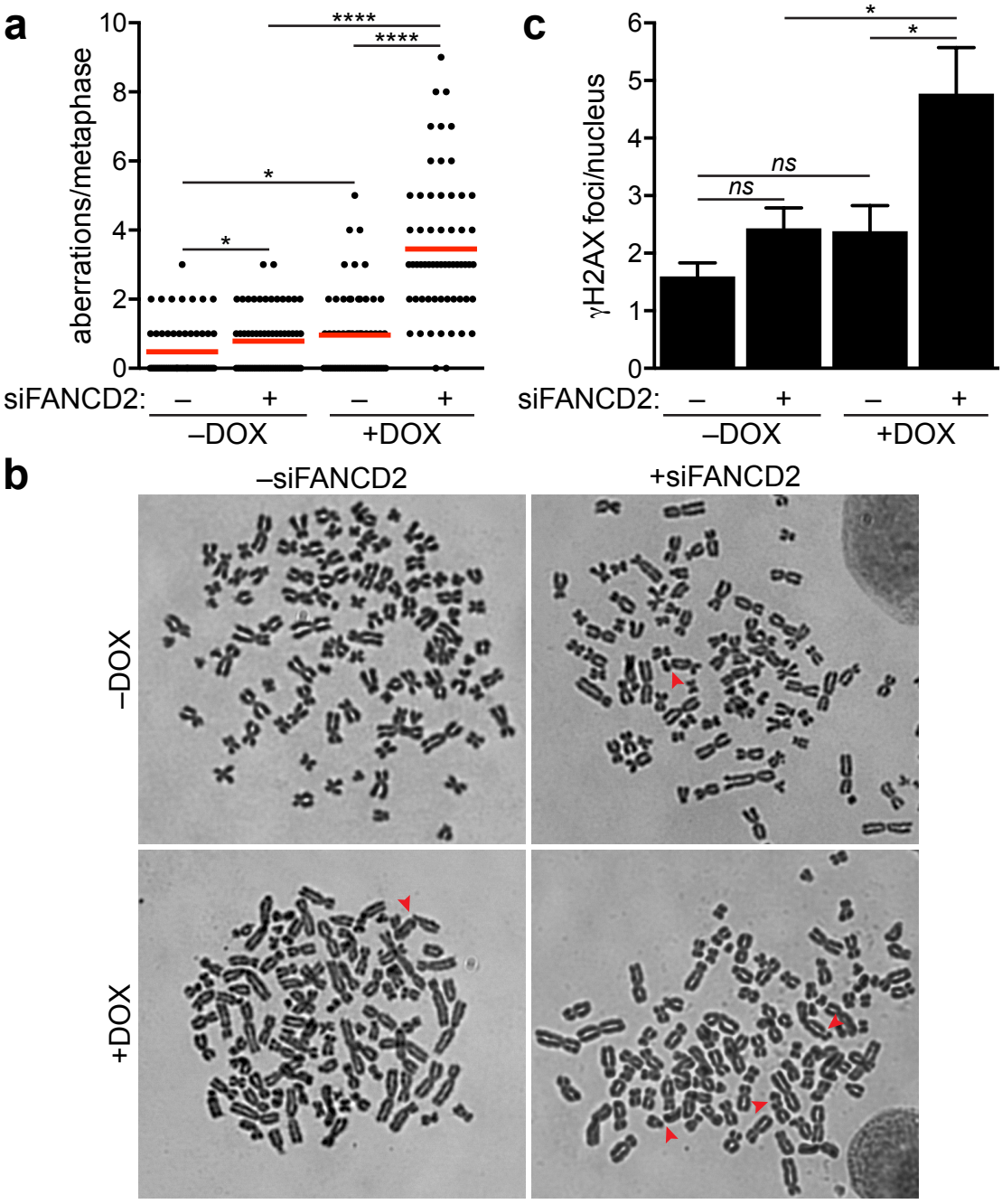


Figure 4.3. FANCD2 prevents DNA damage accumulation in BRCA2-deficient cells.

(**a**) H1299 cells harbouring DOX-inducible shRNA against BRCA2 were transfected with control or FANCD2 siRNA and metaphase spreads were prepared. Shown is the quantification of chromosomal aberrations per metaphase. 60 metaphases from two independent experiments were analysed. Each dot represents one metaphase. Red bars represent means. *p* values were calculated using a Mann-Whitney test (*,$p < 0.05$; ****, $p < 0.0001$). (**b**) Shown are representative images of cells processed as in (**a**). Arrowheads point to aberrations. (**c**) Cells treated as in (**a**) were processed for immunofluorescence. Shown is the quantification of γH2AX foci per nucleus. At least 100 cells were analysed per condition and experiment. Error bars represent SEM of three independent experiments. *p* values were calculated using an unpaired two-tailed *t*-test (*ns*, non-significant; *, $p < 0.05$). Data shown in this figure was generated in collaboration with Dr. Johanna Michl.

Damaged DNA activates the DDR, which can ultimately have deleterious consequences on cell fate by inducing senescence and apoptosis (Jackson *et al.*, 2009). Annexin V and β-galactosidase staining were used to assess whether the genomic instability associated with FANCD2 and BRCA2 deficiency promoted apoptosis and senescence, respectively.

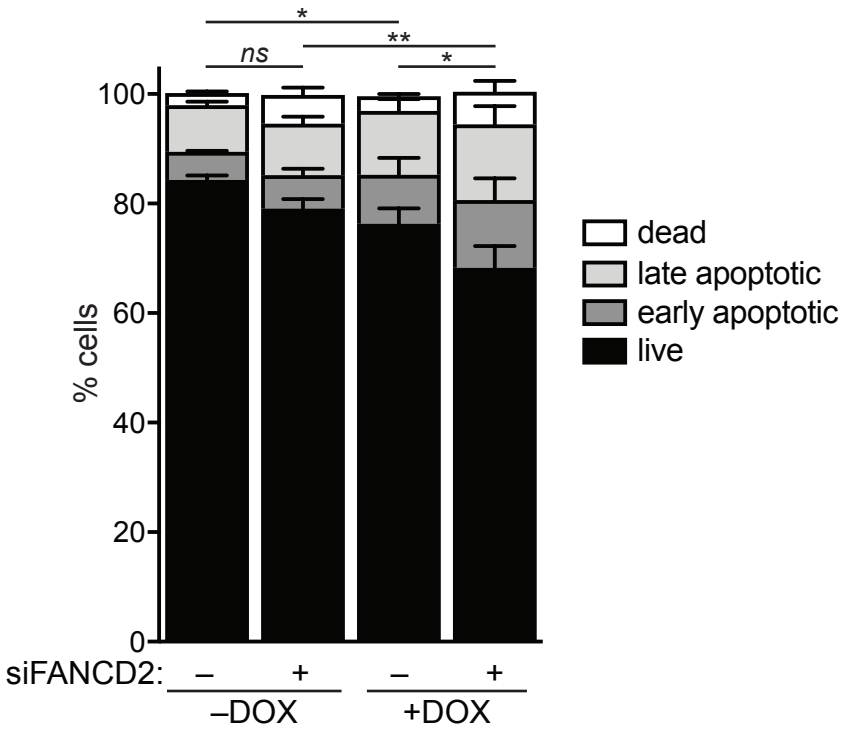


Figure 4.4. Loss of FANCD2 promotes apoptosis in cells lacking BRCA2.
H1299 cells harbouring DOX-inducible shRNA against BRCA2 were transfected with control or FANCD2 siRNA and processed for Annexin V staining followed by FACS analysis. 20,000 cells were analysed per condition and experiment. Error bars represent SEM of four independent experiments. *p* values were calculated using a chi-square test (*ns*, non-significant; *, $p < 0.05$; **, $p < 0.01$). Data shown in this figure was generated in collaboration with Dr. Johanna Michl.

An increase in apoptotic, Annexin V-binding cells was observed upon concomitant ablation of FANCD2 and BRCA2 relative to single depletion of FANCD2 or BRCA2 (Figure 4.4 and 4.5).

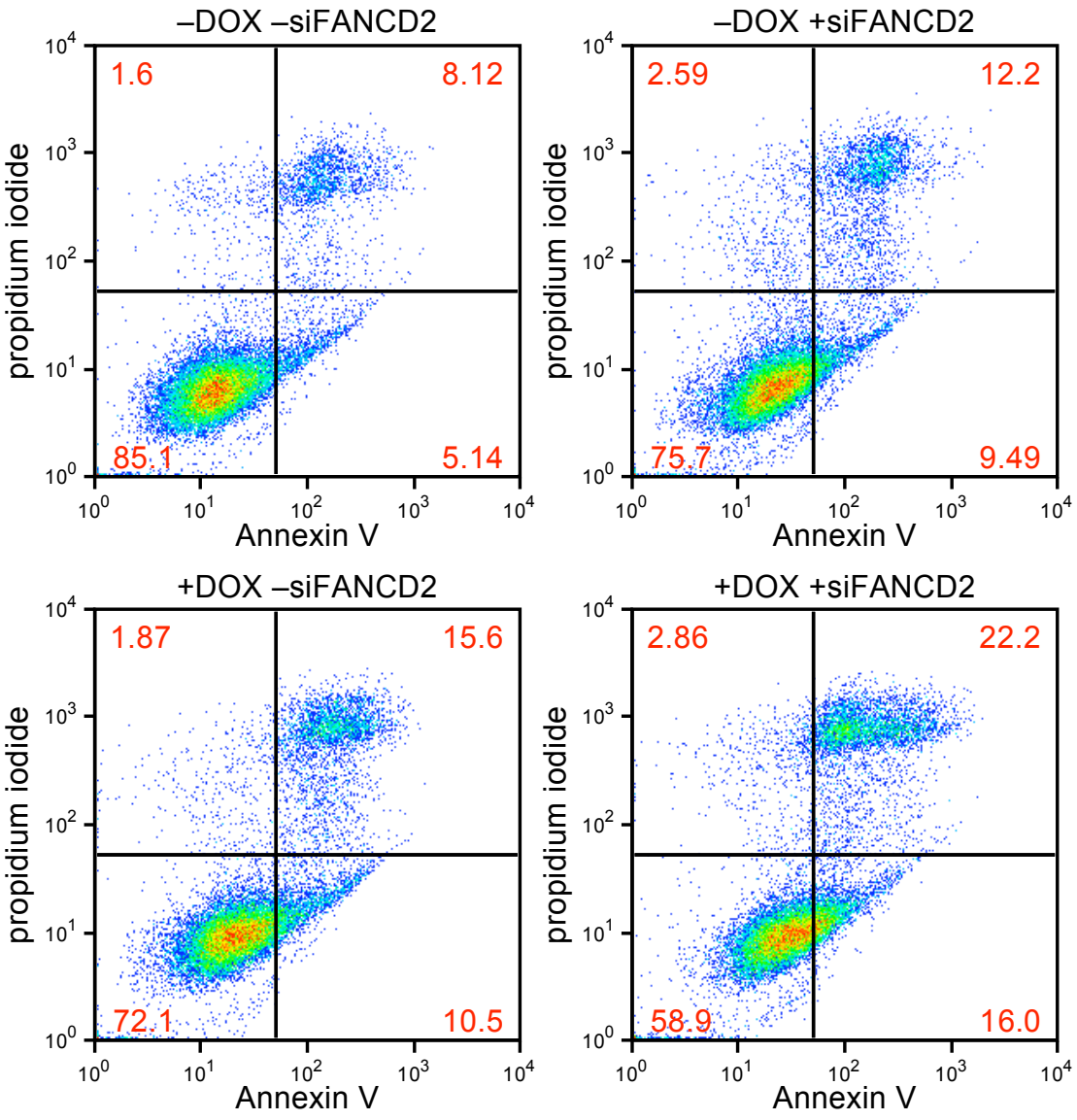


Figure 4.5. FANCD2 depletion triggers cell death in cells lacking BRCA2.
H1299 cells harbouring DOX-inducible shRNA against BRCA2 were transfected with control or FANCD2 siRNA and processed for Annexin V staining followed by FACS analysis. 20,000 cells were analysed per condition and experiment. Shown are representative plots of one experiment. Quantification of four independent experiments is shown in Figure 4.4. Data shown in this figure was generated in collaboration with Dr. Johanna Michl.

In primary MRC-5 human cells, efficient downregulation of FANCD2 and BRCA2 was achieved using siRNA (Figure 4.6a). Simultaneous depletion of FANCD2 and BRCA2 induced senescence significantly compared to knockdown of either FANCD2 (p = 0.0008) or BRCA2 (p < 0.0001), as monitored using β-galactosidase staining (Figure 4.6b and c).

In summary, these findings indicate that loss of FANCD2 causes apoptosis in BRCA2-depleted cancer cells and senescence in primary cells lacking BRCA2 expression.

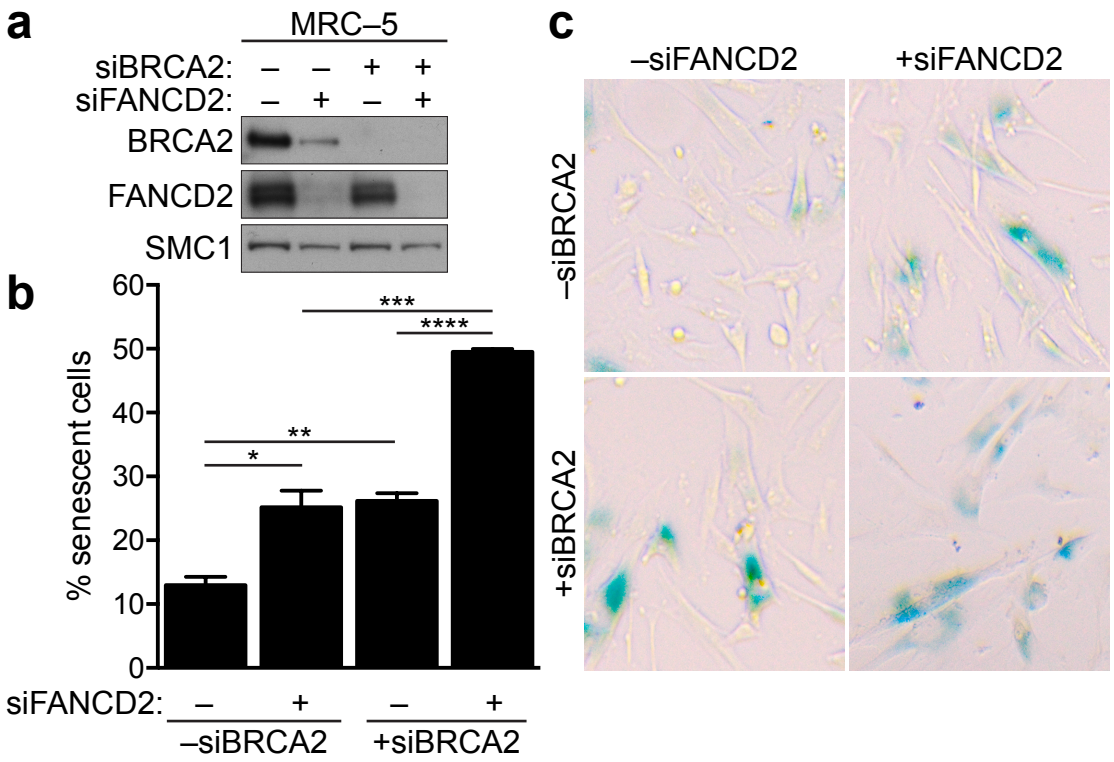


Figure 4.6. FANCD2 loss induces senescence in BRCA2-depleted primary cells. (**a**) MRC-5 cells transfected with siRNAs against BRCA2 and/or FANCD2 and cell extracts were processed for immunoblotting 48 h after transfection. SMC1 was used as a loading control. (**b**) Cells processed as in (**a**) were analysed by β-galactosidase staining. Shown is the quantification of positively stained, senescent cells. At least 400 cells were analysed per condition and experiment. Error bars represent SEM of three independent experiments. *p* values were calculated using an unpaired two-tailed *t*-test (*, $p < 0.05$; **, $p < 0.01$; ***, $p < 0.001$; ****, $p < 0.0001$). (**c**) Shown are representative images of cells processed as in (**b**). Data shown in this figure was generated in collaboration with Sibyl Bertrand and Dr. Johanna Michl.

4.5 FANCD2 and BRCA2 are synthetic lethal

Given that concomitant loss of FANCD2 and BRCA2 had deleterious consequences on cell fate, a potential synthetic lethality between FANCD2

and BRCA2 was investigated using clonogenic assays in H1299 and MDA-MB-231 cells harbouring DOX-inducible shRNA against BRCA2 transfected with two different FANCD2 siRNAs (Figure 4.7).

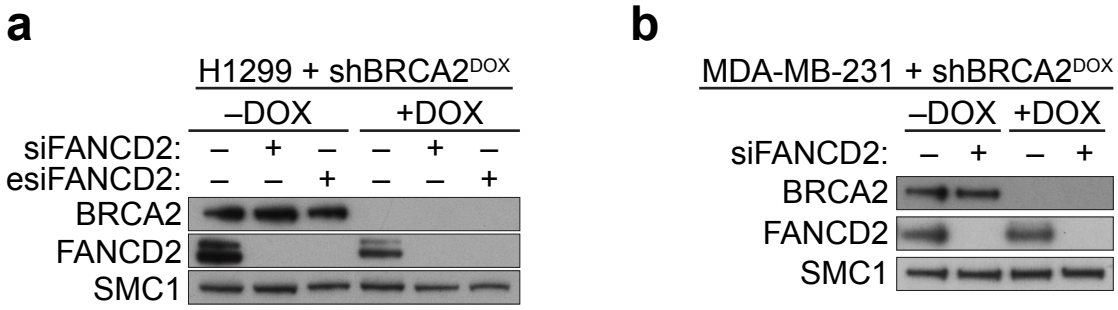


Figure 4.7. Depletion of FANCD2 using siRNAs in H1299 and MDA-MB-231 cell lines harbouring DOX-inducible shRNA against BRCA2.
(**a**) H1299 cells harbouring DOX-inducible shRNA against BRCA2 were transfected with two different siRNAs against FANCD2 and processed for immunoblotting 72 h after transfection. SMC1 was used as a loading control. (**b**) MDA-MB-231 cells harbouring DOX-inducible shRNA against BRCA2 were transfected with siRNA against FANCD2 and processed for immunoblotting 72 h after transfection. SMC1 was used as a loading control. Data shown in this figure was generated in collaboration with Dr. Johanna Michl.

While colony formation of BRCA2-proficient cells was hardly affected by FANCD2 depletion, survival of BRCA2-deficient cells was significantly impaired upon FANCD2 ablation ($p < 0.0001$ in Figure 4.8a; $p = 0.0005$ in Figure 4.8b; $p < 0.0001$ in Figure 4.8c). This suggests that FANCD2 is essential specifically for survival of cells lacking BRCA2 indicative of a synthetic lethal interaction between the two factors.

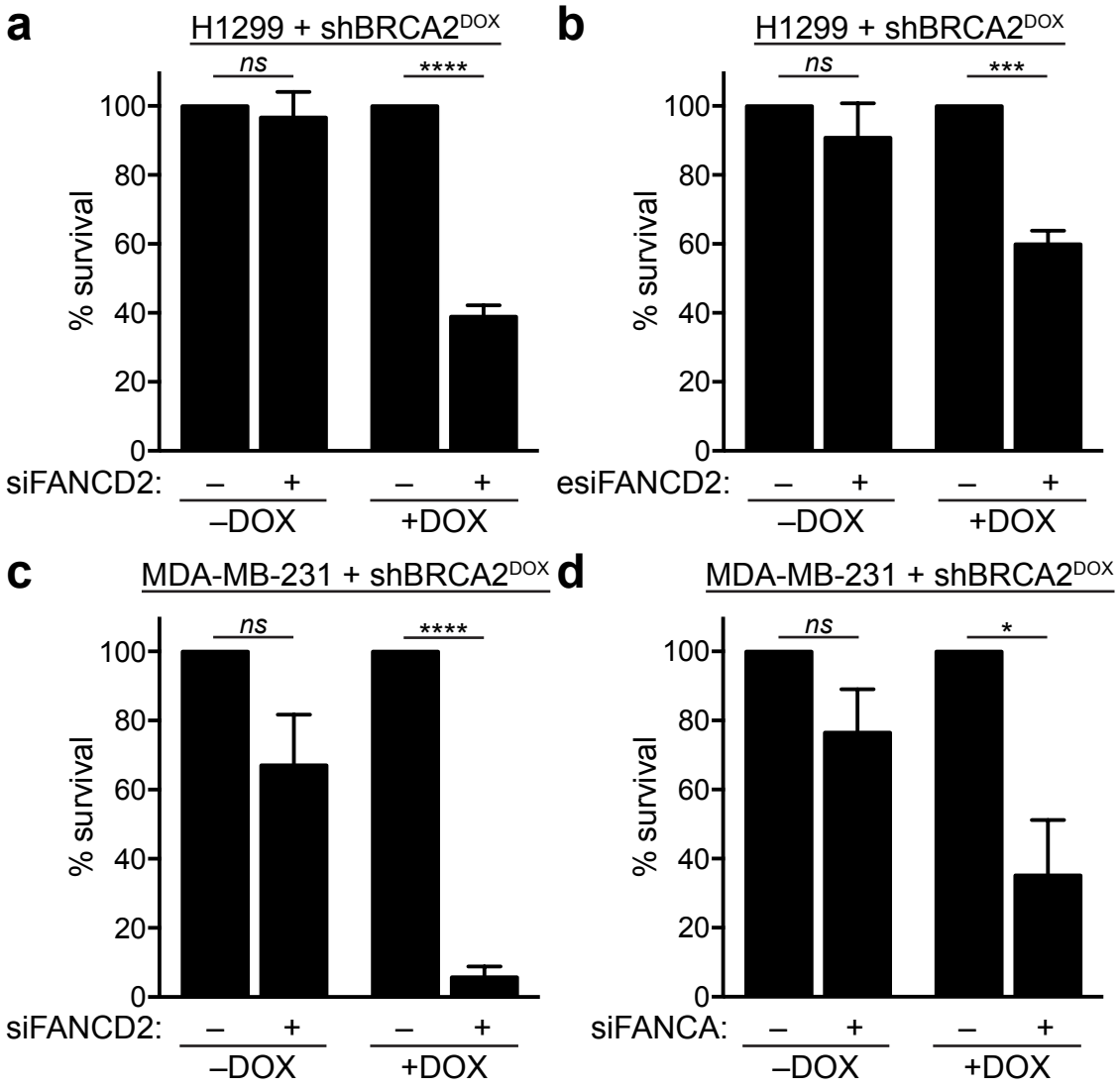


Figure 4.8. FANCD2 is required for BRCA2-deficient cell survival.
(**a** and **b**) Clonogenic survival assays of H1299 cells harbouring DOX-inducible shRNA against BRCA2 transfected with two different siRNAs against FANCD2. Error bars represent SEM of three independent experiments. *p* values were calculated using an unpaired two-tailed *t*-test (*ns*, non-significant; ***, $p < 0.001$; ****, $p < 0.0001$). (**c** and **d**) Clonogenic survival assays of MDA-MB-231 cells harbouring DOX-inducible shRNA against BRCA2 transfected with siRNAs against FANCD2 (**c**) or FANCA (**d**). Error bars represent SEM of three independent experiments. *p* values were calculated using an unpaired two-tailed *t*-test (*ns*, non-significant; *, $p < 0.05$; ****, $p < 0.0001$). Data shown in this figure was generated in collaboration with Dr. Johanna Michl.

Activation of FANCD2 through monoubiquitination mediated by the FA core complex is a crucial step in the FA pathway for ICL repair (Figure 1.9). Similarly, the protective role of FANCD2 at stalled replication forks is

dependent on its ubiquitination (Schlacher *et al.*, 2012). In contrast, the interaction of FANCD2 with MCM proteins under replication stress conditions does not require ubiquitination of FANCD2 (Lossaint *et al.*, 2013). Depletion of core complex component FANCA has previously been shown to inhibit FANCD2 ubiquitination (Andreassen *et al.*, 2004). Therefore, we used siRNA-mediated depletion of FANCA as a tool to estimate whether ubiquitination of FANCD2 was vital in the context of BRCA2 deficiency. Treatment with FANCA siRNA significantly reduced survival of BRCA2-deficient cells (p = 0.0154) without significantly affecting BRCA2-proficient survival (p = 0.1340; Figure 4.8d). This implies that FANCA and possibly its essential function in the ubiquitination of FANCD2 is crucial in cells lacking BRCA2.

4.6 Depletion of FANCD2 hypersensitises BRCA2-deficient cells to PARP inhibition

PARP inhibitors like olaparib provide an effective means for targeting BRCA2 deficiency (Bryant *et al.*, 2005). In contrast, FA patient cell lines do not seem to be sensitive to this class of compounds (Kim *et al.*, 2013). Nonetheless, we were interested to determine whether FANCD2 alters the response to olaparib-mediated PARP inhibition in BRCA2-deficient cells using clonogenic assays.

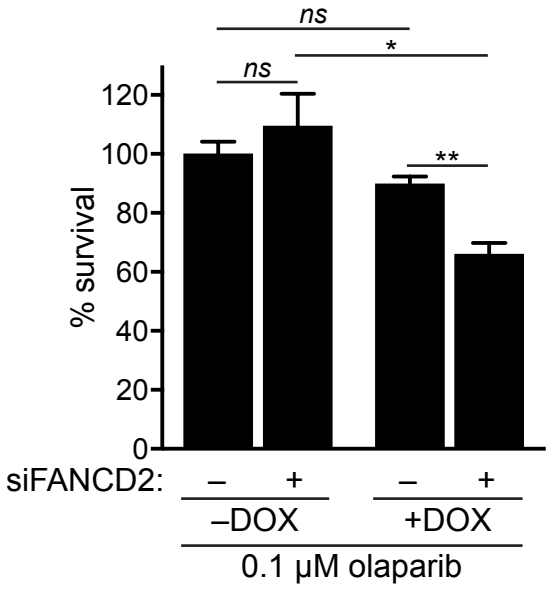


Figure 4.9. FANCD2 dysfunction increases olaparib sensitivity of BRCA2-deficient cells.
Clonogenic survival assays of H1299 cells harbouring DOX-inducible shRNA against BRCA2 transfected with FANCD2 siRNA and treated with 0.1 μM olaparib. Survival of olaparib-treated cells was expressed relative to DMSO-treated cells. Error bars represent SEM of three independent experiments. *p* values were calculated using an unpaired two-tailed *t*-test (*ns*, non-significant; *, $p < 0.05$; **, $p < 0.01$). Data shown in this figure was generated in collaboration with Dr. Johanna Michl.

Consistent with previous results (Kim *et al.*, 2013), olaparib was not toxic to FANCD2-depleted cells (Figure 4.9). While BRCA2-deficient cells exhibited a 10% decrease in survival in response to a low dose of olaparib, FANCD2 ablation significantly enhanced sensitivity of these cells ($p = 0.0056$; Figure 4.9). This suggests that FANCD2 affects the response of BRCA2-deficient cells to chemical PARP inhibition.

4.7 Discussion

In the past decades, it has become clear that there is substantial crosstalk between the FA and HR pathways of DNA damage repair given that increasing numbers of HR factors have been associated with FA (Michl *et al.*,

2016b). However, the functional interplay between FA and HR components in genomic instability, especially independently of ICL repair, has not been studied extensively thus far.

FANCD2 and BRCA2 have both been implicated in protection of stalled replication forks (Chaudhury *et al.*, 2013; Raghunandan *et al.*, 2015; Schlacher *et al.*, 2011; Schlacher *et al.*, 2012). Our study demonstrates that the two proteins promote this function via distinct mechanisms (Figure 4.1b). FANCD2 has been shown to limit replication fork progression in response to replication stress induced by hydroxyurea (Lossaint *et al.*, 2013). This inspired us to investigate the role of FANCD2 in the context of BRCA2 deficiency, which is associated with endogenous levels of replication stress (Carlos *et al.*, 2013). Similar to the response to hydroxyurea-induced replication stress, depletion of FANCD2 increased replication speed in BRCA2-deficient cells (Figure 4.2). We discovered that, in the absence of BRCA2, FANCD2 provides a protection mechanism against excessive DNA damage accumulation and chromosome aberrations (Figure 4.3), signs of genomic instability. In line with this, loss of FANCD2 induced apoptosis and senescence, and decreased survival specifically in BRCA2-compromised cells (Figure 4.4-4.6 and 4.8).

Future studies will be required to fully understand which function of FANCD2 promotes survival of BRCA-deficient cells. Our hypothesis is that FANCD2 is essential to restrict DNA synthesis and protect stalled replication forks to prevent genomic instability in the absence of BRCA2. Nonetheless, the contribution of ubiquitination of FANCD2 remains to be elucidated in more detail. Intriguingly, activation of FANCD2 by monoubiquitination is crucial for its protective function at stalled replication forks (Schlacher *et al.*, 2012) but

not for its interaction with the replisome to restrict DNA synthesis in the context of hydroxyurea-induced replication stress (Lossaint *et al.*, 2013). It will be interesting to investigate whether ubiquitination of FANCD2 is required to control DNA synthesis in BRCA2-deficient cells especially because our data suggests that the FA core complex component FANCA is required for BRCA2-deficient cell survival (Figure 4.8). This could be assessed by comparing the ability of *wildtype* FANCD2 and a ubiquitin mutant FANCD2 (K561R-FANCD2, Garcia-Higuera *et al.* (2001)) to complement the phenotypes observed upon FANCD2 depletion in cells lacking BRCA2.

It is believed that POLQ-mediated A-NHEJ provides a mechanism for the repair of collapsed forks in HR-compromised cells and thus essential for their survival (Ceccaldi *et al.*, 2015; Mateos-Gomez *et al.*, 2015). Kais *et al.* (2016) showed that, besides its function in fork stability, FANCD2 promotes A-NHEJ by recruiting CtIP and POLQ to DNA damage sites. However, it is unlikely that FANCD2 function in A-NHEJ is key for survival in the context of BRCA deficiency as depletion of other A-NHEJ factors (e.g. CtIP) is not lethal in BRCA-defective cells (Kais *et al.*, 2016). Importantly, loss of FANCI reduces survival of BRCA-deficient cells similarly to FANCD2 (Kais *et al.*, 2016). Given that both FANCI and FANCD2 regulate the restart of stalled replication forks in response to replication stress (Chaudhury *et al.*, 2013; Chen *et al.*, 2015), it is possible that this function is important to keep BRCA-deficient cells viable. In this regard, it will be interesting to investigate whether FANCD2 is essential only in the context of BRCA deficiency or also in tumours that display high levels of replication stress through other mechanisms, e.g. oncogene activation.

FANCD2 depletion hypersensitised BRCA2-deficient cells to PARP inhibition (Figure 4.9). Interestingly, overexpression of FANCD2 rescues stalled fork degradation in BRCA1-deficient cells and confers resistance to PARP inhibition (Kais *et al.*, 2016), linking the fork protective function of FANCD2 to PARP inhibitor sensitivity. A similar connection has recently been described for BRCA2, associating chemoresistance of BRCA2-deficient cells with replication fork stability (Ray Chaudhuri *et al.*, 2016). Whether FANCD2 expression levels correlate with the response of *BRCA*-mutated tumours to chemotherapeutic agents will be an interesting question to address.

Altogether, our data shed light onto the functional interaction between BRCA2 and FANCD2 in replication and genome maintenance. In the future, this could assist in understanding and treating the pathologies associated with BRCA2 and FANCD2 dysfunction.

5 Characterisation of a novel MRE11 inhibitor with activity on cell models for BRCA2 deficiency

5.1 Introduction

Cellular checkpoint responses coordinate DNA damage repair with cell cycle progression. Therefore, they play a vital role in the maintenance of genome integrity. The MRN complex is involved in multiple aspects of the DDR, including checkpoint activation and DSB repair. MRN acts as a DSB sensor and binds to broken DNA ends where it recruits and activates the ATM kinase (Lee *et al.*, 2004a). Subsequently, ATM promotes DSB repair by either HR or NHEJ (see section 1.7). Biochemically, the MRN complex displays not only DNA-binding and -end tethering activities, but also important nucleolytic functions (de Jager *et al.*, 2001; Williams *et al.*, 2008). It exhibits ssDNA and dsDNA endonuclease as well as 3'-5' dsDNA exonuclease activity (Paull *et al.*, 1998; Stracker *et al.*, 2011). These mediate the essential function of MRN in promoting DNA repair pathways that require resection of broken DNA ends: HR, SSA and A-NHEJ (Buis *et al.*, 2008; Chang *et al.*, 2017; Rass *et al.*, 2009; Williams *et al.*, 2008).

Functional studies of MRE11 have been limited by its essentiality for cell viability. As an alternative approach for defining cellular functions of MRE11, chemical inhibition of MRE11 nuclease activity has been attempted using mirin, currently the only commercially available MRE11 inhibitor (Dupre *et al.*, 2008). More recently, additional mirin derivatives with endo- and exonuclease-specific inhibitory activity against MRE11 have been identified (Shibata *et al.*, 2014). Recently, the novel compound MU147 was shown to inhibit MRE11

endo- and exonuclease *in vitro* (Fedor Nikulenkov and Lumir Krejci, unpublished). MU147 efficiently decreases endonuclease activity of purified MRN complex *in vitro*, while mirin does not (Fedor Nikulenkov and Lumir Krejci, unpublished). Furthermore, the *in vitro* inhibitory potential of MU147 on the exonuclease activity was more pronounced than that of mirin (Fedor Nikulenkov and Lumir Krejci, unpublished). MU147 could provide a powerful tool to study nuclease-independent functions of MRE11 given that it inhibits both nuclease activities of MRE11 *in vitro*. In this study, we aimed to characterise MU147 activity in cells. Furthermore, we sought to investigate the functional interaction between MRE11 and BRCA2.

5.2 MU147 exhibits lower cytotoxicity than mirin

Cellular toxicity, potentially caused by cross-reaction with other targets, is a general concern regarding mirin and other MRE11 inhibitors. Thus, cytotoxicity of MU147 was assessed in U2OS and H1299 cells using resazurin-based viability assays (Figure 5.1). Treatment for 3 days was chosen based on the duration of treatment needed in other cellular assays (Fedor Nikulenkov and Lumir Krejci, unpublished).

After treatment with increasing doses of MU147 or mirin up to 100 μM, viability of either cell line treated with MU147 was higher than their mirin-treated counterparts, especially at doses above 25 μM (Figure 5.1). This suggests that MU147 impairs cell viability to a lesser extent than mirin.

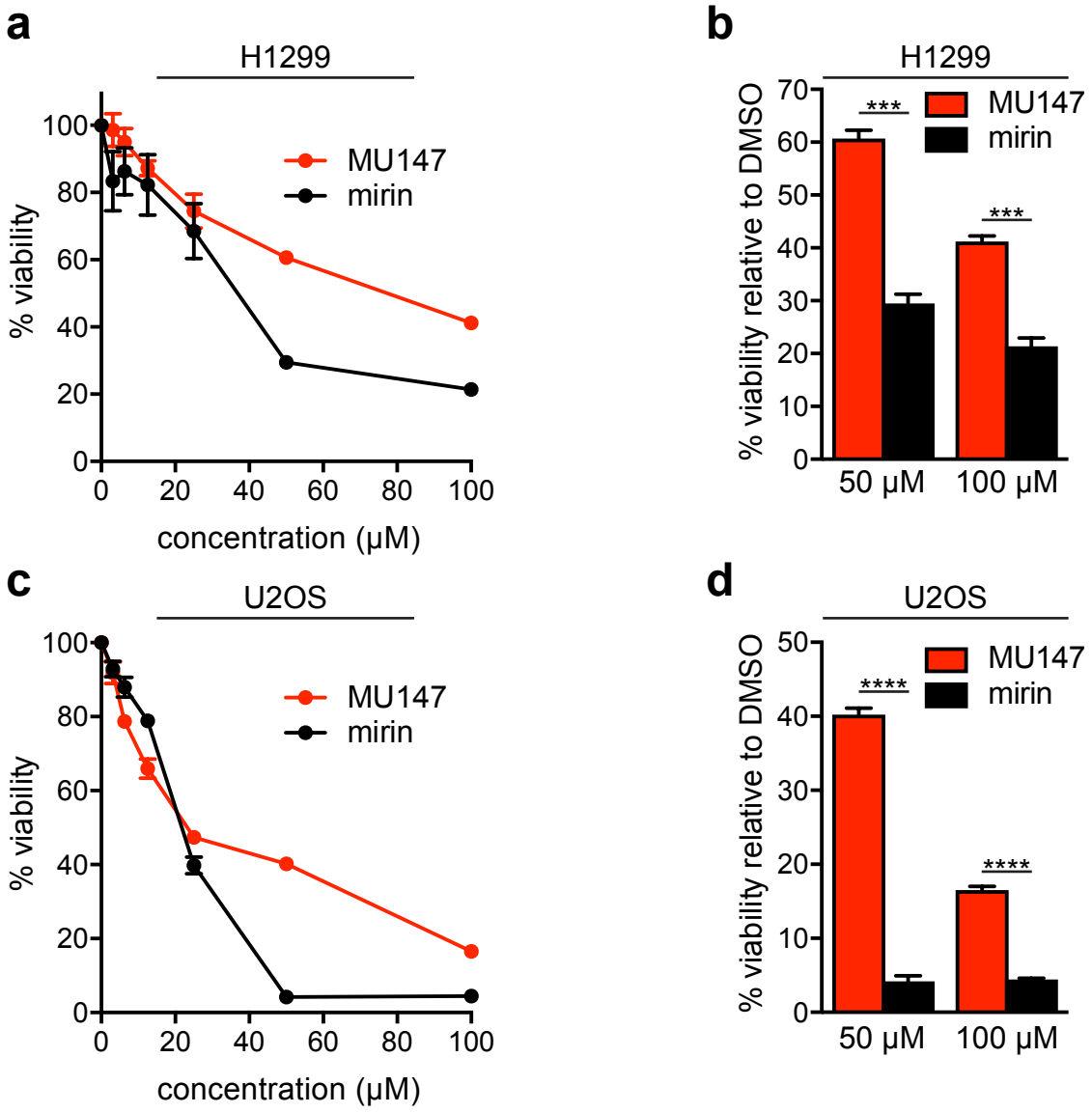


Figure 5.1. MU147 is less toxic to cell viability than mirin.
(**a** and **c**) Dose-dependent viability assays of H1299 (**a**) and U2OS (**c**) cells treated with indicated concentrations of mirin or MU147 for 3 days. The percentage of viability was normalised to DMSO-treated controls. Error bars represent SEM of three independent experiments. (**b** and **d**) Bar graphs of viability assays shown in (**a**) and (**c**) of H1299 (**b**) and U2OS (**d**) cells treated with 50 μM or 100 μM mirin or MU147. *p* values were calculated using an unpaired two-tailed *t*-test (***, $p < 0.001$; ****, $p < 0.0001$).

5.3 MU147 decreases MRN-dependent DNA end resection

A key function of MRE11 nuclease is during resection of DSB ends to allow DSB repair by HR or A-NHEJ (Rass *et al.*, 2009; Shibata *et al.*, 2014). Upon

DSB resection, RPA coats exposed ssDNA to protect it from degradation (Chen *et al.*, 2013). Using immunoblotting, we detected phosphorylation of RPA2 at S4 and S8, a widely used marker for ssDNA generated by DNA end resection (Bunting *et al.*, 2010).

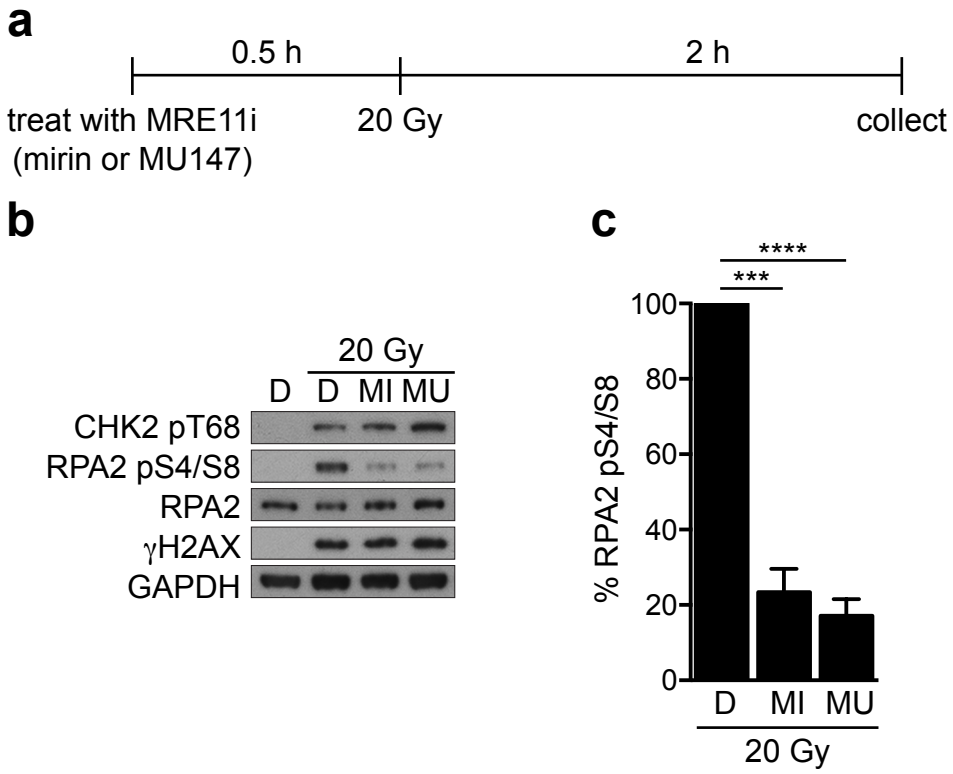


Figure 5.2. Mirin and MU147 prevent phosphorylation of RPA on S4/8 in response to ionising radiation.
(**a**) Timeline outlining experimental setup. U2OS cells were pre-treated with 50 μM mirin or MU147 for 30 min and irradiated with 20 Gy. Cells were processed for collected 2 h after irradiation. (**b**) Cells treated as in (**a**) were immunoblotted as indicated. GAPDH was used as a loading control. (**c**) Shown is the quantification of RPA2 pS4/S8 levels relative to GAPDH normalised to 20 Gy, DMSO-treated control of cells treated as in (**a**). Error bars represent SEM of three independent experiments. *p* values were calculated using an unpaired two-tailed *t*-test (***, $p < 0.001$; ****, $p < 0.0001$). D, DMSO. MI, mirin. MU, MU147.

After pre-treating the cells with 50 μM mirin or MU147, DNA damage was induced by 20 Gy ionising radiation or 1 μM topoisomerase I inhibitor camptothecin for 1h as confirmed by phosphorylation of histone variant H2AX

(γH2AX) and checkpoint kinase CHK2 (Figure 5.2 and 5.3). Ionising radiation induced phosphorylation of RPA at S4/S8 indicative of resection, which was significantly reduced by mirin (p = 0.0002) and MU147 (p < 0.0001; Figure 5.2).

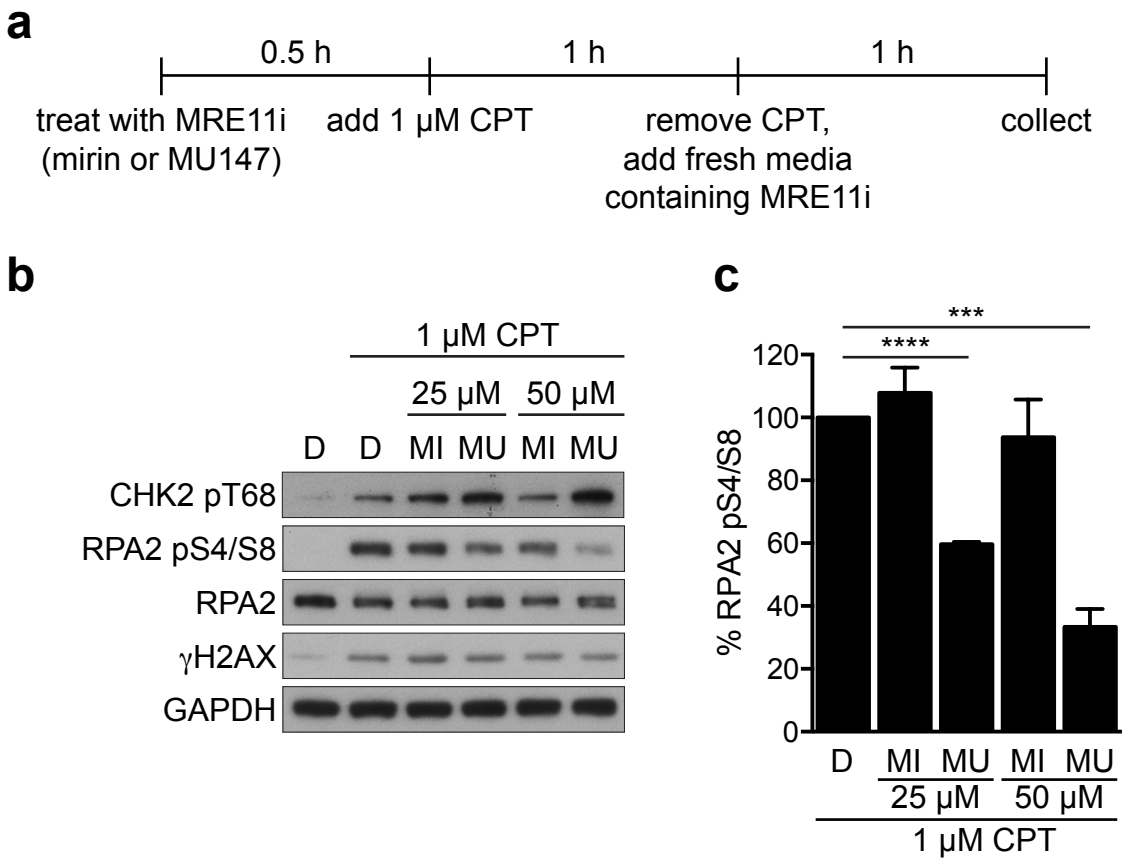


Figure 5.3. MU147 but not mirin decreases phosphorylation of RPA on S4/8 in response to camptothecin-induced DNA damage.
(**a**) Timeline outlining experimental setup. U2OS cells were pre-treated with mirin or MU147 for 30 min, followed by treatment with 1 μM CPT for 1 h. After CPT removal, cells were incubated for 1 h in the presence of mirin or MU147. (**b**) Cells treated as in (**a**) were immunoblotted as indicated. GAPDH was used as a loading control. (**c**) Shown is the quantification of RPA2 pS4/S8 levels relative to GAPDH normalised to CPT, DMSO-treated control of cells treated as in (**a**). Error bars represent SEM of three independent experiments. p values were calculated using an unpaired two-tailed t-test (***, p < 0.001; ****, p < 0.0001). CPT, camptothecin. D, DMSO. MI, mirin. MU, MU147.

Similarly to ionising radiation, camptothecin treatment resulted in a robust increase in phosphorylated RPA (Figure 5.3). However, mirin did not affect camptothecin-induced RPA phosphorylation at a concentration of 25 μM or 50 μM, whilst MU147 decreased phosphorylated RPA levels significantly in this context ($p < 0.0001$ for 25 μM and $p = 0.0003$ for 50 μM; Figure 5.3). Notably, phosphorylation of the checkpoint kinase CHK2 induced by ionising radiation and camptothecin was upregulated after MU147 treatment, possibly due to persistent DNA damage. Overall, our results suggest that MU147 inhibits resection and thus MRE11 nuclease activity effectively.

5.4 MU147 slows DNA damage repair without affecting ATM activation

Due to the major function of MRE11 in DNA damage repair, we next assessed the impact of mirin and MU147 on repair dynamics after camptothecin-induced damage. Cells were pre-treated with 100 μM mirin or MU147 and exposed to 1 μM camptothecin for 1 h. Subsequently, cells were released into fresh media containing mirin or MU147 and DNA damage levels were monitored by immunoblotting using an antibody against the DNA damage marker γH2AX (Figure 5.4).

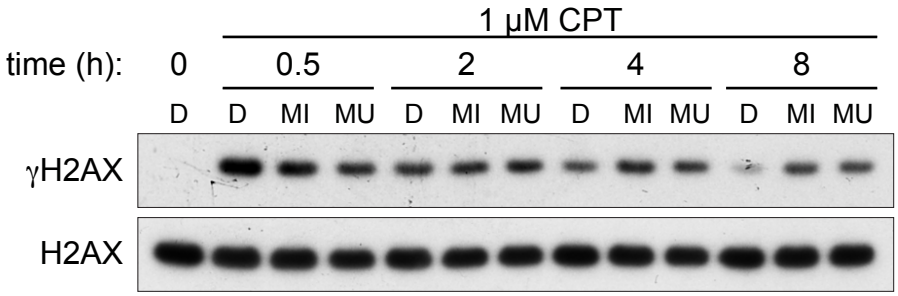


Figure 5.4. Mirin and MU147 delay DNA damage repair.
U2OS cells were pre-treated with 100 μM mirin or MU147 for 30 min, followed by treatment with 1 μM CPT for 1 h. After CPT removal, cells were incubated for indicated times in the presence of mirin or MU147. Cell extracts were fractionated and chromatin-bound fractions immunoblotted as shown. H2AX was used as a loading control. D, DMSO. MI, mirin. MU, MU147.

In control cells, the γH2AX signal decreased over time and disappeared around 8 h after camptothecin treatment suggesting that the DNA damage had been repaired. However, mirin or MU147 impaired DNA damage repair dynamics as indicated by persistent γH2AX expression (Figure 5.4).

To confirm that MU147 specifically inhibited resection without affecting initial signalling of DNA damage mediated by MRN-dependent ATM activation (Lee *et al.*, 2004a), we compared checkpoint responses after 10 Gy ionising radiation in cells pre-treated with 10 μM ATM inhibitor KU55933, 50 μM mirin or MU147 for 30 min (Figure 5.5).

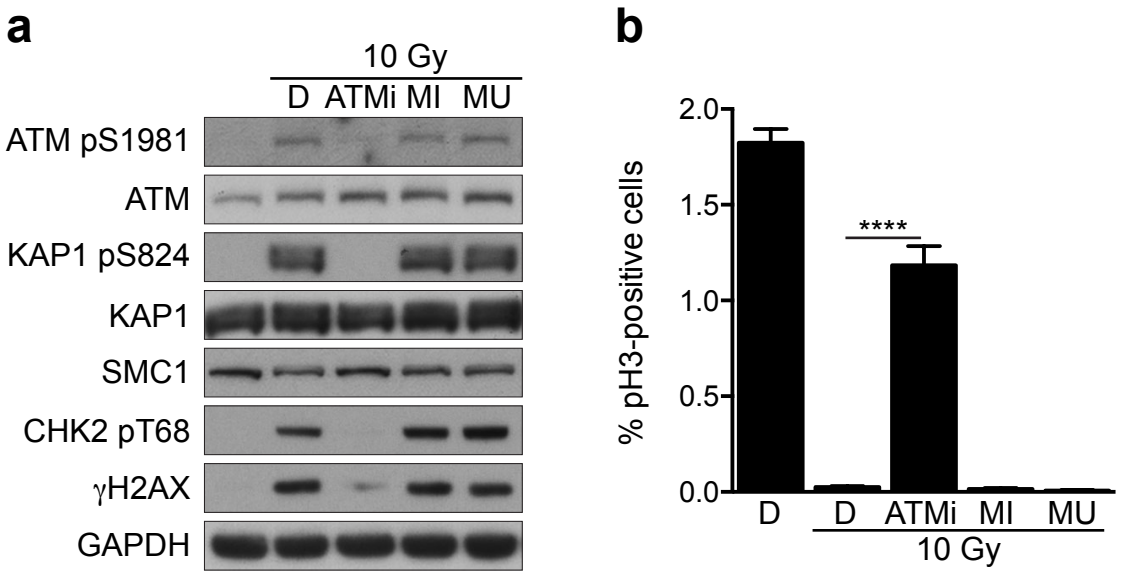


Figure 5.5. Mirin and MU147 do not affect ATM activation upon DNA damage. (**a**) U2OS cells were pre-treated with 10 μM ATMi (KU55933) or 50 μM mirin or MU147 for 30 min and irradiated with 10 Gy. Cells were processed for immunoblotting 2 h after irradiation and immunoblotted as indicated. GAPDH and SMC1 were used as loading controls. (**b**) Cells treated as in (**a**) were stained for pH3 4 h after irradiation and processed for FACS. Shown is the quantification of pH3-positive cells. At least 10,000 cells were analysed per condition and experiment. Error bars represent SEM of three independent experiments. *p* values were calculated using an unpaired two-tailed *t*-test (****, $p < 0.0001$). D, DMSO. MI, mirin. MU, MU147.

Exposure to ionising radiation induced phosphorylation of ATM and its downstream effectors KAP1, CHK2 and H2AX (Figure 5.5a). However, while KU55933 abrogated this response, mirin and MU147 had no impact on the activation of the MRN-activated DNA damage and checkpoint responses (Figure 5.5a). Consistently, cells exposed to mirin or MU147 failed to enter mitosis after ionising radiation indicative of an intact G2/M checkpoint, while cells treated with ATM inhibitor KU55933 showed increased mitotic entry as assessed by phosphorylation of histone H3 at S10 (Figure 5.5b and 5.6).

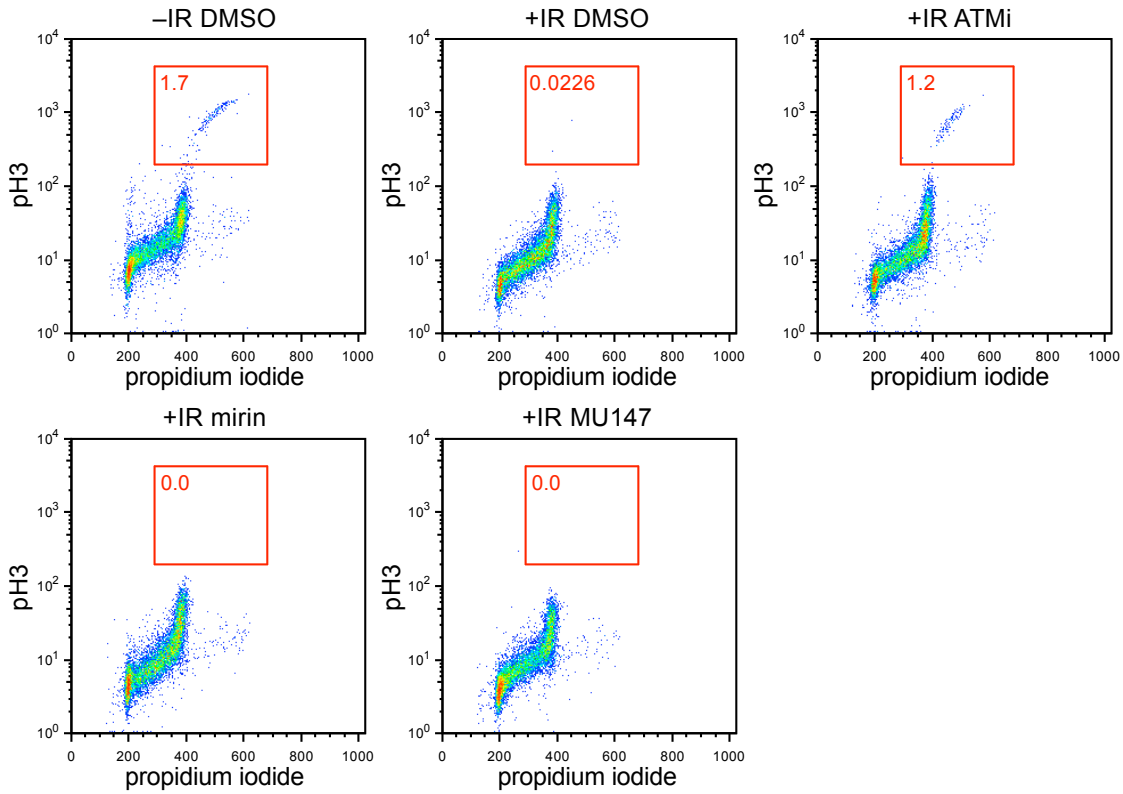


Figure 5.6. Mirin and MU147 do not affect mitotic entry after ionising radiation. U2OS cells were pre-treated with 10 μM ATMi (KU55933) or 50 μM mirin or MU147 for 30 min prior to irradiation (10 Gy, IR). Shown are representative FACS profiles of pH3-positive cells 4 h after irradiation.

5.5 MU147 prevents MRE11 nuclease-mediated degradation of nascent DNA at stalled forks in cells lacking BRCA2

Schlacher *et al.* (2011) reported that stalled forks are degraded by MRE11 nuclease in the absence of BRCA2. Following this model, we performed DNA fibre assays, in which replication tracks of BRCA2-proficient and -deficient DLD1 cells were labelled with IdU. Subsequently, replication forks were arrested by treatment with 2 mM hydroxyurea for 5 h in the presence or absence of 25 μM mirin or MU147 (Figure 5.7).

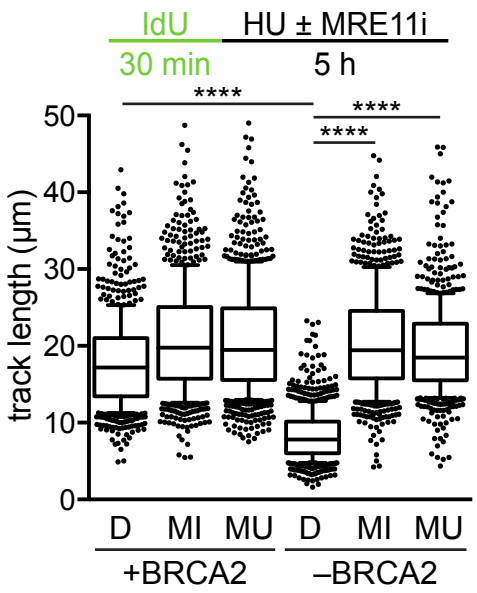


Figure 5.7. Mirin and MU147 prevent MRE11-mediated degradation of nascent DNA at stalled forks in BRCA2-deficient cells.
BRCA2-proficient (+BRCA2) and BRCA2-deficient (–BRCA2) DLD1 cells were processed for DNA fibre analysis as outlined in the inset followed by quantification of the replication track length. At least 200 fibres were analysed per condition and experiment. Middle line represents median, and the box extends from the 25th to 75th percentiles. The whiskers mark the 10th and 90th percentiles. *p* values were calculated using a Mann-Whitney test (*n*=3 independent experiments; ****, $p < 0.0001$). D, DMSO. HU, hydroxyurea. MI, mirin. MRE11i, MRE11 inhibitor. MU, MU147.

In line with previous reports, replication tracks were significantly shorter in BRCA2-deficient cells after hydroxyurea treatment compared to BRCA2-proficient cells ($p < 0.0001$; Figure 5.7). Importantly, both mirin and MU147 restored BRCA2-deficient track length to BRCA2-proficient levels (Figure 5.7) indicating that both compounds prevent MRE11-mediated degradation of nascent DNA at stalled forks in BRCA2-deficient cells.

5.6 MU147 decreases survival of BRCA2-deficient cells and spheroids

BRCA2-deficient V-C8 hamster cells have previously been reported to be sensitive to mirin (Ying *et al.*, 2012). This led us to assess the effect of mirin and MU147 on survival of BRCA2-proficient and -deficient human DLD1 cells (Figure 5.8). In clonogenic survival assays, a concentration of 10 μM was used to minimise cytotoxic effects of the compounds during the treatment for 24 h.

Treatment with 10 μM mirin or MU147 significantly reduced BRCA2-deficient cell survival compared to their DMSO-treated controls ($p = 0.0015$ for mirin and $p < 0.0001$ for MU147), while BRCA2-proficient cells remained unaffected (Figure 5.8). These results support a synthetic lethal interaction between MRE11 and BRCA2.

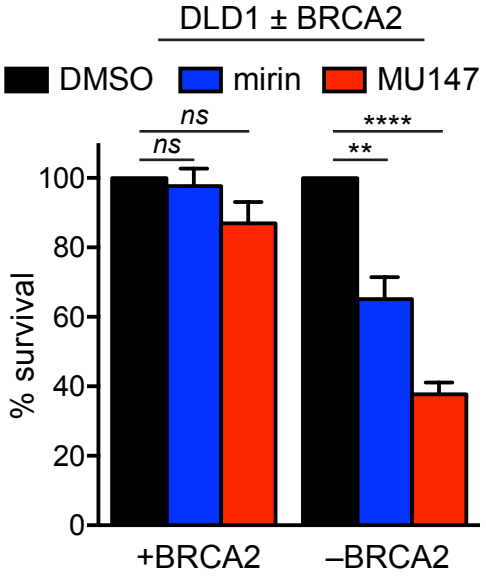


Figure 5.8. MRE11 inhibition reduces BRCA2-deficient cell survival.
Clonogenic survival assays of BRCA2-proficient (+BRCA2) and deficient (–BRCA2) DLD1 cells treated with 10 μM mirin or MU147 for 24 h. Error bars represent SEM of three independent experiments. *p* values were calculated using an unpaired two-tailed *t*-test (**, $p < 0.01$; ****, $p < 0.0001$).

To gain further insights into the pharmacological relevance of our findings, we used 3D cell culture spheroids as a model to simulate activity of our compounds on tumours (Figure 5.9). 3D cell cultures provide a powerful tool for *in vitro* evaluation of the anti-tumour effect and *in vivo* efficacy of drugs. This is because they harbour several common features of *in vivo* tumours such as cell-cell interaction, hypoxia, drug penetration, response and resistance, extracellular matrix and an inner necrotic core (Edmondson *et al.*, 2014; Mehta *et al.*, 2012).

Treatment with 2.5 μM PARP inhibitor olaparib specifically abrogated proliferation of BRCA2-deficient spheroids (Figure 5.9a and b). Strikingly, 25 μM mirin or MU147 effectively inhibited growth of BRCA2-deficient DLD1 spheroids while BRCA2-proficient counterparts were not affected (Figure 5.9c and d), highlighting their potential ability to kill BRCA2-deficient tumours.

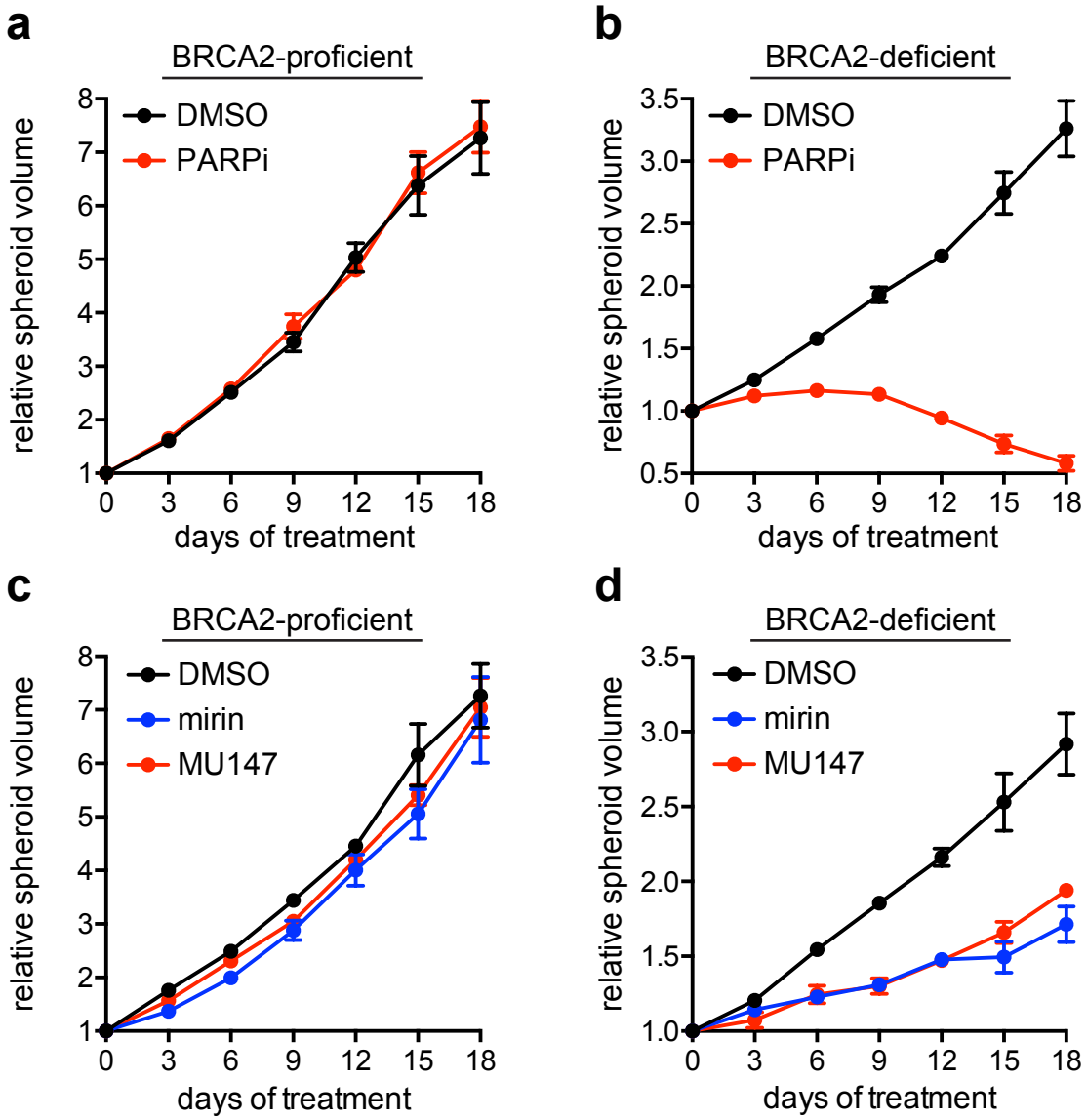


Figure 5.9. Growth of BRCA2-deficient spheroids is inhibited by chemical PARP and MRE11 inhibitors.
BRCA2-proficient (+BRCA2) and BRCA2-deficient (–BRCA2) DLD1 spheroids were treated with 2.5 μM PARPi (olaparib, **a** and **b**), 25 μM mirin or MU147 (**c** and **d**) for 18 days. Fresh drug-containing media were added every 3 days. Spheroid volumes were expressed relative to volumes when treatment was initiated. Graphs are representative of two independent experiments, each performed in triplicate. Error bars represent SEM of triplicate values obtained from a single experiment. PARPi, PARP inhibitor.

5.7 Discussion

MRE11 is a key factor in the DDR and essential for cell viability (Buis *et al.*, 2008). The MRE11 protein harbours DNA-binding domains and exhibits endo- and exonuclease enzymatic activity (Williams *et al.*, 2008). In this study, we establish the inhibitory effect of the compound MU147 on MRE11 nuclease activity (Figure 5.2, 5.3 and 5.7). Thus, we envision this compound to become a valuable tool for future studies of MRE11 function in cells. Our work demonstrates that MU147 attenuates DNA damage repair (Figure 5.4) without affecting ATM activation (Figure 5.5 and 5.6), which qualifies MU147 as an inhibitor of MRE11 nuclease activity. However, given that this compound has not yet fully been characterised, there are certain limitations that need to be considered. For instance, MU147 may have off-target effects on other nucleases. While the inhibitory action of the compound on other enzymes can be assessed *in vitro*, it is difficult to extrapolate such effects in cells. This is mainly due to the fact that the number of molecules of a specific enzyme in a cell is altered during cellular processes and problematic to define. Furthermore, cytotoxicity is a factor that may vary in different cell lines. Testing the effect of MU147 on viability in a large panel of cell lines at different doses would lead to a more accurate estimate of the cytotoxicity of the compound.

Using chemical inhibitors, we demonstrate a synthetic lethal interaction between MRE11 and BRCA2 (Figure 5.8). MRE11 plays a key role in A-NHEJ (Rass *et al.*, 2009; Xie *et al.*, 2009). Therefore, the mechanism underlying this synthetic lethality may stem from loss of A-NHEJ capacity by MRE11 inhibition, as it has previously been reported that cells compromised in HR rely on A-NHEJ for survival (Kais *et al.*, 2016; Mateos-Gomez *et al.*, 2015).

Furthermore, RAD52-mediated SSA may be disabled by inhibition of MRE11 nuclease leading to a decrease in BRCA2-deficient cell survival, as seen upon RAD52 dysfunction (Feng *et al.*, 2011). These hypotheses could be tested by assessing the impact of MRE11 inhibitors on A-NHEJ/SSA efficiency and investigating the relationship between A-NHEJ/SSA abrogation and MRE11 inhibition in the context of BRCA2 deficiency. The sensitivity of BRCA2-deficient cells and spheroids to mirin and MU147 (Figure 5.8 and 5.9) suggests a potential therapeutic application for MRE11 nuclease inhibitors for the treatment of BRCA2-deficient tumours.

All in all, this work contributed to the characterisation of a novel MRE11 nuclease inhibitor, MU147. Additionally, a synthetic lethal interaction between BRCA2 and MRE11 was described that could be exploited in the future for the treatment of cancer patients who carry a *BRCA2* mutation.

6 Discussion

Mutations in the *BRCA1* or *BRCA2* tumour suppressor genes greatly elevate the risk of cancer development (see section 1.2). Current therapies for *BRCA*-mutated tumours are often insufficient to cure these patients, mainly due to the rapid development of resistance (see section 1.12). Therefore, novel approaches for targeting BRCA deficiency are vital. One intrinsic and important difference between *BRCA*-mutated cancer cells and healthy cells is their HR disability. This opens a window for the development of targeted therapies. Hereof, the DNA repair defect and inability of BRCA-deficient cells to deal with replication stress can be exploited to selectively target BRCA dysfunction. Therefore, the aim of this study was to investigate the roles of BRCA1 and BRCA2 in DNA replication and genome stability.

Firstly, the potential of chemical G4 stabilisation, known to induce replication stress (see section 1.4), was assessed using the small molecule pyridostatin (chapter 3). Treatment with pyridostatin was shown to specifically abrogate BRCA-deficient cell survival (Figure 3.2 and 3.12). This effect was associated with replication defects and DNA damage accumulation in cells lacking BRCA2 (Figure 3.4, 3.5, 3.7 and 3.8). Therefore, we propose a model (Figure 6.1), in which chemically stabilised G4s cause stalled replication forks that cannot be restarted in the absence of BRCA1 or BRCA2 leading to collapse into DSBs. These G4-induced breaks cannot be repaired efficiently without HR, further exacerbating the deleterious effects of G4 stabilisation in the context of BRCA deficiency.

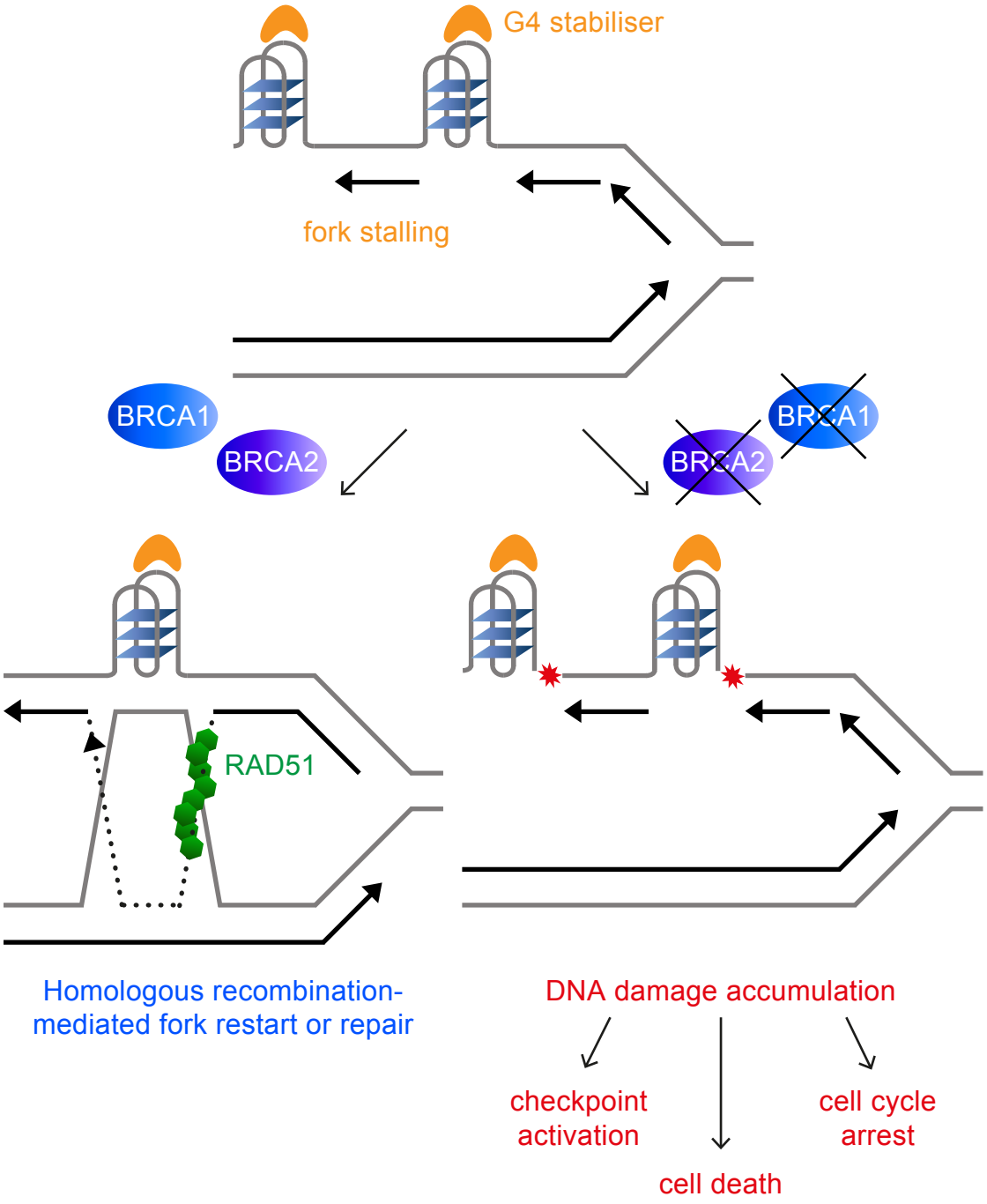


Figure 6.1. Model for G4-induced lethality in the context of BRCA deficiency. Upon chemical stabilisation of G4s, BRCA1 and BRCA2 are required to restart or repair stalled replication forks at persistent G4s. In the absence of BRCA1 or BRCA2, G4 stabilisation leads to DNA damage accumulation, ultimately causing checkpoint activation, cell cycle arrest and cell death. Adapted from Zimmer *et al.* (2016).

Our data suggests that BRCA2 is required to maintain replication fork progression in the presence of persistent G4s and to stabilise pyridostatin-stalled forks (Figure 3.4 and 3.5). RAD51- and RAD52-dependent X-shaped structures have been observed during leading strand synthesis of G4s in yeast (Lopes *et al.*, 2011). This indicates that HR-related pathways may be employed to facilitate replication in the presence of G4s. Importantly, RAD51-deficient cells show similar phenotypes to cells lacking BRCA2 upon treatment with pyridostatin (Zimmer *et al.*, 2016). It would be interesting to test whether restart of stalled forks in the context of G4 stabilisation is dependent on BRCA2 and to elucidate the underlying mechanism. Both, BRCA2 and RAD51 have been implicated in fork restart by template switching and fork reversal (see section 1.6).

Template switching is a key mechanism that repairs DNA nicks behind the replication fork. A block during DNA synthesis can be bypassed through use of the undamaged sister chromatid as a temporary template (see section 1.6). Given the replication stress signatures observed upon pyridostatin treatment in cells lacking BRCA2 (Figure 3.4 and 3.5), it is likely that template switching plays a major role in the bypass of G4s and/or associated lesions. Furthermore, it is possible that cells restart DNA synthesis downstream of a G4 by repriming. In line with this concept, PrimPol has been reported to reprime on the distal end of G4s (Schiavone *et al.*, 2016). The generated DNA gap may subsequently be filled in by translesion synthesis or template switching (see section 1.6). Polη and Polκ have been implicated in translesion synthesis past G4 structures as their depletion results in the formation of DSBs upon treatment with the G4-interacting compound telomestatin (Betous

et al., 2009). However, as stated above, given the drastic sensitivity of BRCA2-deficient cells to pyridostatin (Figure 3.2), template switching may have a more prominent function in promoting replication past stabilised G4 structures. Nonetheless, it may be interesting to assess the role of translesion polymerases in bypassing persistent G4s in BRCA2-deficient cells.

Fork reversal requires reannealing of the nascent DNA strands at a stalled replication fork. This action can be carried out by RAD51 (Zellweger *et al.*, 2015). Furthermore, degradation of reversed forks is blocked by BRCA2 and RAD51, and RAD51 recruits Polα for efficient replication restart at these structures (Kolinjivadi *et al.*, 2017). These functions of BRCA2 and RAD51 could be important to support DNA synthesis in the presence of G4s. In this regard, it would be interesting to visualise and quantify events of fork reversal upon G4 stabilisation using electron microscopy. Additionally, the importance of BRCA2 and RAD51 in this process could be investigated.

In yeast, BIR has been shown to act at secondary DNA structures formed by inverted repeats (Narayanan *et al.*, 2006). Importantly, BIR that restarts collapsed forks in human cells is dependent on RAD52 (Sotiriou *et al.*, 2016). Whilst the involvement of BRCA2 and RAD51 in BIR was not assessed by Sotiriou *et al.* (2016), depletion of either of these factors decreased BIR efficiency in an I-SceI-based reporter assay (Costantino *et al.*, 2014). Therefore, it would be interesting to explore whether collapsed forks are restarted by BIR in the context of G4 stabilisation. The Polδ subunit POLD3 is not essential during conventional DNA replication but is required for BIR (Costantino *et al.*, 2014). Thus, knockdown of POLD3 could be used to examine the effect of BIR abrogation in the presence of persistent G4s.

Cells deficient in BRCA2 recovered from pyridostatin-induced DNA damage by an unknown mechanism (Figure 3.7 and 3.8). One promising candidate for the repair of pyridostatin-associated DNA lesions in the absence of BRCA2 is RAD52. Recently, RAD52 was shown to compensate for the lack of RAD51-dependent HR by mediating SSA (Ochs *et al.*, 2016). Hereof, RAD52 promotes DSB repair by annealing regions of homology after resection (Chang *et al.*, 2017). Given the similarity in substrates required for DSB repair mediated by BRCA2 and RAD52, respectively, pyridostatin-associated lesions may be resolved via the SSA pathway in the absence of BRCA2.

It has previously been reported that loss of 53BP1 restores HR in BRCA1-deficient but not in BRCA2-deficient cells (Bouwman *et al.*, 2010). This was explained by the essential role of BRCA2 in loading the RAD51 recombinase for HR (Moynahan *et al.*, 2001; Yang *et al.*, 2005). BRCA1, on the other hand, has a more upstream function in regulating resection (Bunting *et al.*, 2010; Chapman *et al.*, 2012). Loss of 53BP1 compensates for BRCA1 dysfunction by reactivation of resection and thus RAD51 foci formation indicative of HR (Bunting *et al.*, 2010). This mechanism mediates resistance to PARP inhibitors in BRCA1-, 53BP1-deficient cells (Bunting *et al.*, 2010). Due to the lack of 53BP1, RAD52 is essential for the survival of BRCA1-, 53BP1-deficient cells upon DNA damage induction (Ochs *et al.*, 2016). In line with this, the same study showed that SSA is upregulated in these cells. Whether RAD52 is involved in mediating PARP inhibitor resistance in cells lacking BRCA1 and 53BP1 has not been assessed. Interestingly, BRCA1-, 53BP1-deficient cells fail to induce RAD51 foci upon G4 stabilisation (Zimmer *et al.*, 2016). Whether RAD52 is recruited to sites of DNA damage in this context remains to be

determined. Given the detrimental consequences of G4 stabilisation on BRCA1-, 53BP1-deficient cell survival (Figure 3.12 and Zimmer *et al.* (2016)), it seems unlikely that SSA efficiently repairs pyridostatin-associated breaks. Nonetheless, investigating the involvement of RAD52-mediated SSA in DNA damage repair after pyridostatin treatment could provide important clues regarding another interesting question: Does pyridostatin toxicity in BRCA-deficient cells stem from their replication defects or HR dysfunction, or both?

A recent study proposed that the lethal consequences of PARP inhibition and cisplatin are linked to the replication fork instability of BRCA-deficient cells (Ray Chaudhuri *et al.*, 2016). However, the authors reported that 53BP1 abrogation does not prevent degradation of stalled replication forks in BRCA1-deficient cells. This indicates that PARP inhibitor resistance in these cells is solely due to HR reactivation (Bunting *et al.*, 2010). Strikingly, pyridostatin-sensitive BRCA1-, 53BP1-defective cells fail to reactivate HR upon exposure to pyridostatin (Zimmer *et al.*, 2016). Even though replication fork stability has not been assessed in this system, it is likely that both, lack of HR and replication fork instability, contribute the detrimental consequences of pyridostatin on BRCA1-, 53BP1-deficient cell fate. It would be interesting to address whether loss of PTIP, CHD4 or PARP1 can rescue fork stability in BRCA-deficient cells in the context of pyridostatin-mediated G4 stabilisation as reported for hydroxyurea (Ding *et al.*, 2016; Ray Chaudhuri *et al.*, 2016). If this is the case, these factors may confer pyridostatin resistance in BRCA-deficient cells.

Interestingly, G4 stabilisers have been found to sensitise cells lacking DNA repair mechanisms besides HR, e.g. NHEJ (McLuckie *et al.*, 2013; Xu *et*

al., 2017). In the future, investigating the contribution of various pathways to the repair of G4-induced DNA lesions may provide further insights into the nature of the damage. Moreover, it may identify additional applications for G4-stabilising compounds in the clinic. To gain further understanding of the pathways contributing to pyridostatin toxicity in BRCA-deficient cells, shRNA or CRISPR screens could allow for identification of factors whose dysfunction confer pyridostatin resistance. These factors could provide potential biomarkers to predict patients' response to the compound.

Pyridostatin toxicity has previously been associated with transcriptional deregulation of G4-containing genes (Rodriguez *et al.*, 2012). RNA-seq analyses could be performed to investigate whether and how pyridostatin treatment alters the transcriptional profile in cells lacking BRCA1 or BRCA2. This may elucidate the DNA damage signalling and proliferative pathways altered by pyridostatin in the context of BRCA deficiency. Genes whose transcription is downregulated by pyridostatin could potentially provide novel targets for eliminating BRCA-deficient cells and tumours.

Our finding that chemical G4 stabilisation provides a novel means for targeting BRCA deficiency was underlined by the striking sensitivity of PARP inhibitor-resistant BRCA1-deficient tumour cells to pyridostatin. Therefore, our study provides rationale for exploring the potential of chemical G4 stabilisers therapeutically.

To date, *in vivo* activity of multiple G4-interacting compounds including BRACO-19 (Burger *et al.*, 2005), RHPS4 (Salvati *et al.*, 2007) and telomestatin (Tauchi *et al.*, 2003; Tauchi *et al.*, 2006) has been demonstrated in xenograft models. However, none of the aforementioned compounds

progressed to clinical testing for treatment of human patients likely owing to insufficient drug-like features.

Quarfloxin (also known as CX-3543, Drygin *et al.* (2009)) was the first G4 stabiliser to enter clinical trials providing a proof-of-principle for the therapeutic potential of G4-targeting agents. In addition to quarfloxin, a recent study identified CX-5461 as a G4 stabiliser with activity in BRCA-deficient tumours including those refractory to PARP inhibition (Xu *et al.*, 2017). Consistent with our data, both compounds induce DNA damage and cell death specifically in BRCA-deficient cells. CX-5461 is now in phase I/II clinical trial for patients with *BRCA*-mutated tumours (ClinicalTrials.gov identifier: NCT02719977).

Secondly, given that the key FA component FANCD2 plays essential roles in DNA replication and repair similar to BRCA2 (see sections 1.10 and 1.11), the interaction and dependence between the two proteins were explored (chapter 4). FANCD2 was demonstrated to prevent replication stress and genomic instability in BRCA2-deficient cells (Figure 4.1-4.3). The synthetic lethality between FANCD2 and BRCA2 (Figure 4.8) was linked to the non-epistatic functions of these proteins in protecting stalled replication forks (Figure 4.1). Importantly, FANCD2 was discovered to limit replication fork progression in cells lacking BRCA2 (Figure 4.2). We suggest that, upon loss of FANCD2, excessive replication speed leads to accumulation of DNA damage and chromosome aberrations in BRCA2-deficient cells due to the inability to repair replication-associated damage. Overall, this work provides mechanistic insights into the functional interaction between FANCD2 and BRCA2.

Furthermore, a novel strategy for eliminating BRCA2-deficient cells by inhibiting FANCD2 was discovered.

To elucidate the mechanism that determines the synthetic lethality between FANCD2 and BRCA2, further study of the interaction between the two factors in the maintenance of genomic stability will be required. We hypothesise that FANCD2 limits DNA synthesis in cells lacking BRCA2 by a similar mechanism as reported for hydroxyurea treatment (Lossaint *et al.*, 2013). Here, ATR promotes association of FANCD2 with the MCM complex via phosphorylation of MCM2 on S108. It would be interesting to assess whether ATR-mediated MCM2 phosphorylation is also required to limit replication through a FANCD2-dependent mechanism in BRCA2-deficient cells. In this regard, phosphorylation of MCM2 on S108 could be monitored by immunoblotting and an interaction between FANCD2 and the MCM complex could be detected by immunoprecipitation. Importantly, Lachaud *et al.* (2016) demonstrated that the role of FANCD2 in restricting DNA replication under replication stress conditions depends on the recruitment of FAN1 nuclease. Thus, it would be interesting to assess a potential function of FAN1 in replication dynamics, genome stability and survival of BRCA2-deficient cells.

FANCD2 and BRCA2 protect stalled replication forks in a non-epistatic manner (Figure 4.1). Despite MRE11 being a key factor responsible for degradation of nascent DNA at stalled forks, chemical inhibition of MRE11 nuclease did not fully restore fork stability in FANCD2, BRCA2-deficient cells (Figure 4.1). This suggests that other nucleases may be involved. A prominent candidate for this is DNA2, a nuclease that has been reported to cause fork instability (Higgs *et al.*, 2015). Interestingly, downregulation of DNA2 rescues

sensitivity of FANCD2-deficient cells to crosslinking agents (Karanja *et al.*, 2014). Furthermore, FANCD2 overexpression has been shown to restore fork stability and confer PARP inhibitor resistance in *BRCA1*-mutated cells (Kais *et al.*, 2016). This indicates that fork stability is a key factor for the resistance to chemotherapeutic agents, as proposed recently by Ray Chaudhuri *et al.* (2016). Future experiments could address whether DNA2 degrades forks in the absence of FANCD2 and BRCA2 with detrimental consequences on FANCD2-, BRCA2-deficient cell survival.

Besides fork stability, replication fork restart is crucial for maintaining genome integrity (see section 1.6). While FANCD2 restarts stalled replication forks together with BLM (Chaudhury *et al.*, 2013), the exact mechanism of this restart is not known. BLM has been proposed to resolve D-loops generated during template switching (Liberi *et al.*, 2005; Mankouri *et al.*, 2011), and to mediate fork reversal (Bugreev *et al.*, 2011; Ralf *et al.*, 2006). Furthermore, BRCA2 has been implicated in fork restart by template switching and fork reversal (see section 1.6). We and others have shown that FANCD2 and BRCA2 promote replication fork restart non-epistatically (Kais *et al.*, 2016; Michl *et al.*, 2016a). However, which mechanisms of fork restart are engaged by the two factors remains to be determined.

Interestingly, FANCD2 and BRCA2 both prevent accumulation of endogenous R-loops (RNA-DNA hybrids) and associated DNA damage (Bhatia *et al.*, 2014; Garcia-Rubio *et al.*, 2015). The authors propose that the FA pathway plays an important role in removing R-loops to allow efficient replication. However, the FANCD2- and BRCA2-dependent mechanism that prevents R-loop accumulation has not fully been characterised. In fact, it is not

known whether FANCD2 and BRCA2 indeed resolve R-loop structures via the same mechanism. This would be an important question to address since R-loop accumulation could contribute to the endogenous DNA damage observed in FANCD2-, BRCA2-deficient cells.

A recent study reported that FANCD2 facilitates replication through difficult-to-replicate CFS, a function linked to R-loop formation at these sites (Madireddy *et al.*, 2016). Given the role of BRCA2 in resolving R-loops, combined loss of FANCD2 and BRCA2 may lead to insufficient DNA synthesis at CFS. Recently, it was shown that CFS replication is completed during mitosis under conditions of aphidicolin-induced replication stress (Minocherhomji *et al.*, 2015). Similarly, BRCA2-deficient cells activate replication at CFS in mitosis (Feng *et al.*, 2017; Lai *et al.*, 2017). However, BRCA2-deficient cells exhibit shorter mitotic duration than *wildtype* cells (Choi *et al.*, 2012; Lai *et al.*, 2017). This may be due to a role of BRCA2 in regulating the spindle assembly checkpoint (Choi *et al.*, 2012). Thus, FANCD2-, BRCA2-deficient cells may fail to complete CFS replication and may enter cytokinesis with under-replicated DNA. To test this possibility experimentally, immunofluorescence staining for 53BP1 could be performed. 53BP1 bodies in G1 phase cells are a signature of DNA lesions formed during mitosis due to resolution of incomplete replication intermediates (Harrigan *et al.*, 2011; Lukas *et al.*, 2011). A defect in CFS replication could potentially contribute to the genomic instability in cells lacking FANCD2 and BRCA2.

For clinical application of our findings, it would be important to test potential synthetic lethal interactions between BRCA2 and other FA factors to identify druggable targets. FANCD2 is not an enzyme and may therefore not

be susceptible to chemical inhibition. Nonetheless, targeting E3 ligase components of the FA core complex that mediate ubiquitination of FANCD2 may be a promising strategy. Indeed, abrogating FANCD2 ubiquitination using an ubiquitination mutant or indirectly by depleting FANCA reduces BRCA-deficient cell survival (Kais *et al.*, 2016; Michl *et al.*, 2016a). Alternatively, inhibiting downstream factors of FANCD2 may be an option. A candidate for this is the nuclease FAN1 (discussed above). If FAN1, like FANCD2, confines replication stress and genome instability in cells lacking BRCA function, development of specific chemical inhibitors against FAN1 could prove useful tools for the treatment of BRCA-defective cancers in the future.

Thirdly, inspired by a previous study suggesting a potential lethal interaction between MRE11 nuclease and BRCA2 (Ying *et al.*, 2012), the therapeutic potential of chemical MRE11 nuclease inhibition in the context of BRCA2 deficiency was investigated (chapter 5). This study characterised the novel MRE11 nuclease inhibitor MU147 in comparison to the widely used compound mirin. This is important due to the need for improved chemical inhibitors of MRE11 nuclease to allow detailed studies of its biological functions.

Importantly, MRE11 acts in a complex with RAD50 and NBS1. Both, the endo- and exonuclease activities of MRE11 are stimulated by RAD50 and NBS1 (Stracker *et al.*, 2011). Therefore, it would be important to assess whether MRN complex formation and stability are affected by MU147. Besides MRE11, RAD50 and NBS1 are also required for DNA binding of the MRN complex and subsequent activation of ATM (Cerosaletti *et al.*, 2006; de Jager *et al.*, 2002; Lee *et al.*, 2003). Since MU147 did not impair ATM activation

(Figure 5.5 and 5.6), it seems unlikely that the DNA-binding ability of the MRN complex is affected by MU147. Nonetheless, recruitment of MRN to DNA in the presence of MU147 could be monitored by chromatin fractionation or immunofluorescence.

Furthermore, unravelling the binding mode of MU147 to MRE11 could provide useful clues regarding the mechanism of action of the compound. While human MRE11 failed to crystallise with mirin, information gained from crystallisation of *Thermotoga maritima* MRE11 with bound mirin was used to develop specific MRE11 endo- or exonuclease inhibitors (Shibata *et al.*, 2014). Similar experiments with MU147 could enable the design of potent MRE11 inhibitors in the future.

Additionally, our finding that survival of cells and spheroids lacking BRCA2 is decreased by MU147 or mirin (Figure 5.8 and 5.9) suggests that MRE11 inhibitors could potentially be used to treat BRCA2-deficient tumours in the future. The mechanism underlying the synthetic lethal interaction between MRE11 nuclease and BRCA2 remains to be determined. Ying *et al.* (2012) hypothesised that MRE11 resolves potentially toxic DNA structures at stalled replication forks in BRCA2-deficient cells. Furthermore, they proposed that MRE11 may mediate the restart of stalled forks that frequently occur in cells lacking BRCA2. Studies in *Xenopus* egg extracts support a function of MRE11 in the reassembly of a functional replisome to allow replication restart at stalled forks (Hashimoto *et al.*, 2012). However, a study in mammalian cells showed that MRE11 nuclease threatens fork stability and degrades nascent DNA at stalled forks in the absence of BRCA2 (Schlacher *et al.*, 2011). Furthermore, the embryonic lethality and hypersensitivity of BRCA2-deficient

cells to chemotherapeutic agents has been linked to fork instability caused by MRE11 nuclease activity (Ding *et al.*, 2016; Ray Chaudhuri *et al.*, 2016). Therefore, it seems paradoxical that MRE11 nuclease inhibition is synthetic lethal with BRCA2 deficiency.

One possibility for the observed synthetic lethality is that processing of stalled replication forks or DSBs by MRE11 is required to allow restart and repair by BRCA2-independent mechanisms that required resection, namely A-NHEJ and SSA (Chang *et al.*, 2017). POLQ-mediated repair by A-NHEJ has previous been shown to be essential for BRCA2-deficient cell survival (Ceccaldi *et al.*, 2015). Similarly, RAD52 is required for SSA especially in the absence of HR (Ochs *et al.*, 2016) and its abrogation is synthetic lethal with BRCA2 dysfunction (Feng *et al.*, 2011). The effect of MU147 on the repair efficiency of A-NHEJ and SSA could be assessed using I-SceI-based reporter assays (Gunn *et al.*, 2012). Additionally, future experiments could address whether A-NHEJ/SSA factors and MRE11 nuclease promote survival of cells lacking BRCA2 epistatically.

Recently, MRE11 has been reported to process DNA-protein crosslinks (DPCs) to allow DSB repair mainly by NHEJ (Aparicio *et al.*, 2016; Deshpande *et al.*, 2016; Hoa *et al.*, 2016; Lee *et al.*, 2012). BRCA2 resolves acetaldehyde-induced crosslinks via the FA pathway of ICL repair (Tacconi *et al.*, 2017). Acetaldehyde is known to induce various forms of crosslinks including ICLs and DPCs (Lorenti Garcia *et al.*, 2009). Endogenous DPCs occur when transient DNA-binding proteins become trapped or through endogenous reactive metabolites, such as formaldehydes, that crosslink proteins close to DNA (Stingele *et al.*, 2017). It is possible that both MRE11 and BRCA2 are

required for efficient repair of endogenous DPCs via distinct mechanisms. Simultaneous ablation of both processes by inhibition of MRE11 nuclease in BRCA2-deficient cells may therefore be lethal.

In the future, it would be interesting to test efficacy of MRE11 inhibitors in combination with currently used therapeutic agents such as cisplatin and PARP inhibitors. Work by Ying *et al.* (2012) suggests that MRE11 and PARP inhibition have additive effects on the decrease in proliferation of BRCA2-deficient hamster cells. Their study also reports cross-resistance to mirin and PARP inhibitor olaparib in BRCA2-reverted hamster cells. However, whether BRCA-defective human cells and tumours that have developed resistance to PARP inhibition or platinum drugs can be targeted by MRE11 inhibitors remains to be determined. Furthermore, MRE11 nuclease deficiency is known to cause hypersensitivity to ionising radiation (Buis *et al.*, 2008; Llorente *et al.*, 2004; Westmoreland *et al.*, 2013; Yamaguchi-Iwai *et al.*, 1999). Therefore, MRE11 inhibitors could potentially be used as radiosensitisers in the clinic. It would thus be interesting to investigate the effect of MU147 on radiosensitivity in the future.

Altogether, this study provides mechanistic insights into the essential functions of BRCA1 and BRCA2 during DNA replication and repair. In the future, these findings may be relevant for targeting BRCA-deficient cancers.

7 References

Abdulkareem, I. H. and Zurmi, I. B. 2012. Review of hormonal treatment of breast cancer. *Niger J Clin Pract*. 15:9-14.

Adachi, N., Suzuki, H., Iiizumi, S. and Koyama, H. 2003. Hypersensitivity of nonhomologous DNA end-joining mutants to VP-16 and ICRF-193: implications for the repair of topoisomerase II-mediated DNA damage. *J Biol Chem*. 278:35897-35902.

Ahn, J. Y., Schwarz, J. K., Piwnica-Worms, H. and Canman, C. E. 2000. Threonine 68 phosphorylation by ataxia telangiectasia mutated is required for efficient activation of Chk2 in response to ionizing radiation. *Cancer Res*. 60:5934-5936.

Ahnesorg, P., Smith, P. and Jackson, S. P. 2006. XLF interacts with the XRCC4-DNA ligase IV complex to promote DNA nonhomologous end-joining. *Cell*. 124:301-313.

Alsop, K., Fereday, S., Meldrum, C., deFazio, A., Emmanuel, C., George, J., Dobrovic, A., Birrer, M. J., Webb, P. M., Stewart, C., Friedlander, M., Fox, S., Bowtell, D. and Mitchell, G. 2012. *BRCA* mutation frequency and patterns of treatment response in *BRCA* mutation-positive women with ovarian cancer: a report from the Australian Ovarian Cancer Study Group. *J Clin Oncol*. 30:2654-2663.

Alter, B. P. 1996. Fanconi's anemia and malignancies. *Am J Hematol*. 53:99-110.

Anampa, J., Makower, D. and Sparano, J. A. 2015. Progress in adjuvant chemotherapy for breast cancer: an overview. *BMC Med*. 13:195.

Anders, C. K. and Carey, L. A. 2009. Biology, metastatic patterns, and treatment of patients with triple-negative breast cancer. *Clin Breast Cancer*. 9 Suppl 2:S73-81.

Anderson, B. O., Yip, C. H., Smith, R. A., Shyyan, R., Sener, S. F., Eniu, A., Carlson, R. W., Azavedo, E. and Harford, J. 2008. Guideline implementation for breast healthcare in low-income and middle-income countries: overview of the Breast Health Global Initiative Global Summit 2007. *Cancer*. 113:2221-2243.

Andreassen, P. R., D'Andrea, A. D. and Taniguchi, T. 2004. ATR couples FANCD2 monoubiquitination to the DNA-damage response. *Genes Dev*. 18:1958-1963.

Antoniou, A., Pharoah, P. D., Narod, S., Risch, H. A., Eyfjord, J. E., Hopper, J. L., Loman, N., Olsson, H., Johannsson, O., Borg, A., Pasini, B., Radice, P., Manoukian, S., Eccles, D. M., Tang, N., Olah, E., Anton-Culver, H., Warner, E., Lubinski, J., Gronwald, J., Gorski, B., Tulinius, H., Thorlacius, S., Eerola, H., Nevanlinna, H., Syrjakoski, K., Kallioniemi, O. P., Thompson, D., Evans, C., Peto, J., Lalloo, F., Evans, D. G. and Easton, D. F. 2003. Average risks of breast and ovarian cancer associated with *BRCA1* or *BRCA2* mutations detected in case Series unselected for family history: a combined analysis of 22 studies. *Am J Hum Genet*. 72:1117-1130.

Aparicio, T., Baer, R., Gottesman, M. and Gautier, J. 2016. MRN, CtIP, and BRCA1 mediate repair of topoisomerase II-DNA adducts. *J Cell Biol*. 212:399-408.

Aparicio, T., Guillou, E., Coloma, J., Montoya, G. and Mendez, J. 2009. The human GINS complex associates with Cdc45 and MCM and is essential for DNA replication. *Nucleic Acids Res*. 37:2087-2095.

Arnaudeau, C., Lundin, C. and Helleday, T. 2001. DNA double-strand breaks associated with replication forks are predominantly repaired by homologous recombination involving an exchange mechanism in mammalian cells. *J Mol Biol*. 307:1235-1245.

Artandi, S. E., Chang, S., Lee, S. L., Alson, S., Gottlieb, G. J., Chin, L. and DePinho, R. A. 2000. Telomere dysfunction promotes non-reciprocal translocations and epithelial cancers in mice. *Nature*. 406:641-645.

Ashton, T. M., Mankouri, H. W., Heidenblut, A., McHugh, P. J. and Hickson, I. D. 2011. Pathways for Holliday junction processing during homologous recombination in *Saccharomyces cerevisiae*. *Mol Cell Biol*. 31:1921-1933.

Audebert, M., Salles, B. and Calsou, P. 2004. Involvement of poly(ADP-ribose) polymerase-1 and XRCC1/DNA ligase III in an alternative route for DNA double-strand breaks rejoining. *J Biol Chem*. 279:55117-55126.

Auerbach, A. D., Buchwald, M. and Joenje, H. 2001. The metabolic and molecular bases of inherited disease. McGraw-Hill Medical, New York.

Auerbach, A. D., Rogatko, A. and Schroeder-Kurth, T. M. 1989. International Fanconi Anemia Registry: relation of clinical symptoms to diepoxybutane sensitivity. *Blood*. 73:391-396.

Auerbach, A. D. and Wolman, S. R. 1976. Susceptibility of Fanconi's anaemia fibroblasts to chromosome damage by carcinogens. *Nature*. 261:494-496.

Badie, S., Escandell, J. M., Bouwman, P., Carlos, A. R., Thanasoula, M., Gallardo, M. M., Suram, A., Jaco, I., Benitez, J., Herbig, U., Blasco, M. A., Jonkers, J. and Tarsounas, M. 2010. BRCA2 acts as a RAD51 loader to facilitate telomere replication and capping. *Nat Struct Mol Biol*. 17:1461-1469.

Bakkenist, C. J. and Kastan, M. B. 2003. DNA damage activates ATM through intermolecular autophosphorylation and dimer dissociation. *Nature*. 421:499-506.

Barber, L. J., Sandhu, S., Chen, L., Campbell, J., Kozarewa, I., Fenwick, K., Assiotis, I., Rodrigues, D. N., Reis Filho, J. S., Moreno, V., Mateo, J., Molife, L. R., De Bono, J., Kaye, S., Lord, C. J. and Ashworth, A. 2013. Secondary mutations in *BRCA2* associated with clinical resistance to a PARP inhibitor. *J Pathol*. 229:422-429.

Bartkova, J., Horejsi, Z., Koed, K., Kramer, A., Tort, F., Zieger, K., Guldberg, P., Sehested, M., Nesland, J. M., Lukas, C., Orntoft, T., Lukas, J. and Bartek, J. 2005.

DNA damage response as a candidate anti-cancer barrier in early human tumorigenesis. *Nature*. 434:864-870.

Bartkova, J., Rezaei, N., Liontos, M., Karakaidos, P., Kletsas, D., Issaeva, N., Vassiliou, L. V., Kolettas, E., Niforou, K., Zoumpourlis, V. C., Takaoka, M., Nakagawa, H., Tort, F., Fugger, K., Johansson, F., Sehested, M., Andersen, C. L., Dyrskjot, L., Orntoft, T., Lukas, J., Kittas, C., Helleday, T., Halazonetis, T. D., Bartek, J. and Gorgoulis, V. G. 2006. Oncogene-induced senescence is part of the tumorigenesis barrier imposed by DNA damage checkpoints. *Nature*. 444:633-637.

Bartz, S. R., Zhang, Z., Burchard, J., Imakura, M., Martin, M., Palmieri, A., Needham, R., Guo, J., Gordon, M., Chung, N., Warrener, P., Jackson, A. L., Carleton, M., Oatley, M., Locco, L., Santini, F., Smith, T., Kunapuli, P., Ferrer, M., Strulovici, B., Friend, S. H. and Linsley, P. S. 2006. Small interfering RNA screens reveal enhanced cisplatin cytotoxicity in tumor cells having both BRCA network and TP53 disruptions. *Mol Cell Biol*. 26:9377-9386.

Bass, T. E., Luzwick, J. W., Kavanaugh, G., Carroll, C., Dungrawala, H., Glick, G. G., Feldkamp, M. D., Putney, R., Chazin, W. J. and Cortez, D. 2016. ETAA1 acts at stalled replication forks to maintain genome integrity. *Nat Cell Biol*. 18:1185-1195.

Baumann, P., Benson, F. E. and West, S. C. 1996. Human Rad51 protein promotes ATP-dependent homologous pairing and strand transfer reactions *in vitro*. *Cell*. 87:757-766.

Bedrat, A., Lacroix, L. and Mergny, J. L. 2016. Re-evaluation of G-quadruplex propensity with G4Hunter. *Nucleic Acids Res*. 44:1746-1759.

Bennardo, N., Cheng, A., Huang, N. and Stark, J. M. 2008. Alternative-NHEJ is a mechanistically distinct pathway of mammalian chromosome break repair. *PLoS Genet*. 4:e1000110.

Bennardo, N., Gunn, A., Cheng, A., Hasty, P. and Stark, J. M. 2009. Limiting the persistence of a chromosome break diminishes its mutagenic potential. *PLoS Genet*. 5:e1000683.

Berti, M., Ray Chaudhuri, A., Thangavel, S., Gomathinayagam, S., Kenig, S., Vujanovic, M., Odreman, F., Glatter, T., Graziano, S., Mendoza-Maldonado, R., Marino, F., Lucic, B., Biasin, V., Gstaiger, M., Aebersold, R., Sidorova, J. M., Monnat, R. J., Jr., Lopes, M. and Vindigni, A. 2013. Human RECQ1 promotes restart of replication forks reversed by DNA topoisomerase I inhibition. *Nat Struct Mol Biol*. 20:347-354.

Berti, M. and Vindigni, A. 2016. Replication stress: getting back on track. *Nat Struct Mol Biol*. 23:103-109.

Besnard, E., Babled, A., Lapasset, L., Milhavet, O., Parrinello, H., Dantec, C., Marin, J. M. and Lemaitre, J. M. 2012. Unraveling cell type-specific and reprogrammable human replication origin signatures associated with G-quadruplex consensus motifs. *Nat Struct Mol Biol*. 19:837-844.

Betous, R., Rey, L., Wang, G., Pillaire, M. J., Puget, N., Selves, J., Biard, D. S., Shinya, K., Vasquez, K. M., Cazaux, C. and Hoffmann, J. S. 2009. Role of TLS DNA polymerases eta and kappa in processing naturally occurring structured DNA in human cells. *Mol Carcinog*. 48:369-378.

Bhargava, R., Onyango, D. O. and Stark, J. M. 2016. Regulation of single-strand annealing and its role in genome maintenance. *Trends Genet*. 32:566-575.

Bhatia, V., Barroso, S. I., Garcia-Rubio, M. L., Tumini, E., Herrera-Moyano, E. and Aguilera, A. 2014. BRCA2 prevents R-loop accumulation and associates with TREX-2 mRNA export factor PCID2. *Nature*. 511:362-365.

Bhattacharyya, A., Ear, U. S., Koller, B. H., Weichselbaum, R. R. and Bishop, D. K. 2000. The breast cancer susceptibility gene *BRCA1* is required for subnuclear assembly of Rad51 and survival following treatment with the DNA cross-linking agent cisplatin. *J Biol Chem*. 275:23899-23903.

Bhowmick, R., Minocherhomji, S. and Hickson, I. D. 2016. RAD52 facilitates mitotic DNA synthesis following replication stress. *Mol Cell*. 64:1117-1126.

Bianchi, J., Rudd, S. G., Jozwiakowski, S. K., Bailey, L. J., Soura, V., Taylor, E., Stevanovic, I., Green, A. J., Stracker, T. H., Lindsay, H. D. and Doherty, A. J. 2013. PrimPol bypasses UV photoproducts during eukaryotic chromosomal DNA replication. *Mol Cell*. 52:566-573.

Biffi, G., Tannahill, D., McCafferty, J. and Balasubramanian, S. 2013. Quantitative visualization of DNA G-quadruplex structures in human cells. *Nat Chem*. 5:182-186.

Biffi, G., Tannahill, D., Miller, J., Howat, W. J. and Balasubramanian, S. 2014. Elevated levels of G-quadruplex formation in human stomach and liver cancer tissues. *PloS One*. 9:e102711.

Bishop, D. K., Ear, U., Bhattacharyya, A., Calderone, C., Beckett, M., Weichselbaum, R. R. and Shinohara, A. 1998. Xrcc3 is required for assembly of Rad51 complexes *in vivo*. *J Biol Chem*. 273:21482-21488.

Blackburn, E. H. 2001. Switching and signaling at the telomere. *Cell*. 106:661-673.

Bochman, M. L., Paeschke, K. and Zakian, V. A. 2012. DNA secondary structures: stability and function of G-quadruplex structures. *Nat Rev Genet*. 13:770-780.

Bodnar, A. G., Ouellette, M., Frolkis, M., Holt, S. E., Chiu, C. P., Morin, G. B., Harley, C. B., Shay, J. W., Lichtsteiner, S. and Wright, W. E. 1998. Extension of life-span by introduction of telomerase into normal human cells. *Science*. 279:349-352.

Boersma, V., Moatti, N., Segura-Bayona, S., Peuscher, M. H., van der Torre, J., Wevers, B. A., Orthwein, A., Durocher, D. and Jacobs, J. J. 2015. MAD2L2 controls DNA repair at telomeres and DNA breaks by inhibiting 5' end resection. *Nature*. 521:537-540.

Boos, D., Sanchez-Pulido, L., Rappas, M., Pearl, L. H., Oliver, A. W., Ponting, C. P. and Diffley, J. F. 2011. Regulation of DNA replication through Sld3-Dpb11 interaction is conserved from yeast to humans. *Curr Biol*. 21:1152-1157.

Bothmer, A., Robbiani, D. F., Feldhahn, N., Gazumyan, A., Nussenzweig, A. and Nussenzweig, M. C. 2010. 53BP1 regulates DNA resection and the choice between classical and alternative end joining during class switch recombination. *J Exp Med*. 207:855-865.

Bouwman, P., Aly, A., Escandell, J. M., Pieterse, M., Bartkova, J., van der Gulden, H., Hiddingh, S., Thanasoula, M., Kulkarni, A., Yang, Q., Haffty, B. G., Tommiska, J., Blomqvist, C., Drapkin, R., Adams, D. J., Nevanlinna, H., Bartek, J., Tarsounas, M., Ganesan, S. and Jonkers, J. 2010. 53BP1 loss rescues BRCA1 deficiency and is associated with triple-negative and BRCA-mutated breast cancers. *Nat Struct Mol Biol*. 17:688-695.

Branzei, D., Vanoli, F. and Foiani, M. 2008. SUMOylation regulates Rad18-mediated template switch. *Nature*. 456:915-920.

Bryant, H. E., Petermann, E., Schultz, N., Jemth, A. S., Loseva, O., Issaeva, N., Johansson, F., Fernandez, S., McGlynn, P. and Helleday, T. 2009. PARP is activated at stalled forks to mediate Mre11-dependent replication restart and recombination. *EMBO J*. 28:2601-2615.

Bryant, H. E., Schultz, N., Thomas, H. D., Parker, K. M., Flower, D., Lopez, E., Kyle, S., Meuth, M., Curtin, N. J. and Helleday, T. 2005. Specific killing of BRCA2-deficient tumours with inhibitors of poly(ADP-ribose) polymerase. *Nature*. 434:913-917.

Budzowska, M., Graham, T. G., Sobeck, A., Waga, S. and Walter, J. C. 2015. Regulation of the Rev1-pol zeta complex during bypass of a DNA interstrand cross-link. *EMBO J*. 34:1971-1985.

Bugreev, D. V., Rossi, M. J. and Mazin, A. V. 2011. Cooperation of RAD51 and RAD54 in regression of a model replication fork. *Nucleic Acids Res*. 39:2153-2164.

Buis, J., Wu, Y., Deng, Y., Leddon, J., Westfield, G., Eckersdorff, M., Sekiguchi, J. M., Chang, S. and Ferguson, D. O. 2008. Mre11 nuclease activity has essential roles in DNA repair and genomic stability distinct from ATM activation. *Cell*. 135:85-96.

Bunting, S. F., Callen, E., Kozak, M. L., Kim, J. M., Wong, N., Lopez-Contreras, A. J., Ludwig, T., Baer, R., Faryabi, R. B., Malhowski, A., Chen, H. T., Fernandez-Capetillo, O., D'Andrea, A. and Nussenzweig, A. 2012. BRCA1 functions independently of homologous recombination in DNA interstrand crosslink repair. *Mol Cell*. 46:125-135.

Bunting, S. F., Callen, E., Wong, N., Chen, H. T., Polato, F., Gunn, A., Bothmer, A., Feldhahn, N., Fernandez-Capetillo, O., Cao, L., Xu, X., Deng, C. X., Finkel, T., Nussenzweig, M., Stark, J. M. and Nussenzweig, A. 2010. 53BP1 inhibits homologous recombination in *Brca1*-deficient cells by blocking resection of DNA breaks. *Cell*. 141:243-254.

Burge, S., Parkinson, G. N., Hazel, P., Todd, A. K. and Neidle, S. 2006. Quadruplex DNA: sequence, topology and structure. *Nucleic Acids Res*. 34:5402-5415.

Burger, A. M., Dai, F., Schultes, C. M., Reszka, A. P., Moore, M. J., Double, J. A. and Neidle, S. 2005. The G-quadruplex-interactive molecule BRACO-19 inhibits tumor growth, consistent with telomere targeting and interference with telomerase function. *Cancer Res*. 65:1489-1496.

Burma, S., Chen, B. P., Murphy, M., Kurimasa, A. and Chen, D. J. 2001. ATM phosphorylates histone H2AX in response to DNA double-strand breaks. *J Biol Chem*. 276:42462-42467.

Byrski, T., Huzarski, T., Dent, R., Gronwald, J., Zuziak, D., Cybulski, C., Kladny, J., Gorski, B., Lubinski, J. and Narod, S. A. 2009. Response to neoadjuvant therapy with cisplatin in BRCA1-positive breast cancer patients. *Breast Cancer Res Treat*. 115:359-363.

Byrski, T., Huzarski, T., Dent, R., Marczyk, E., Jasiowka, M., Gronwald, J., Jakubowicz, J., Cybulski, C., Wisniowski, R., Godlewski, D., Lubinski, J. and Narod, S. A. 2014. Pathologic complete response to neoadjuvant cisplatin in BRCA1-positive breast cancer patients. *Breast Cancer Res Treat*. 147:401-405.

Byun, T. S., Pacek, M., Yee, M. C., Walter, J. C. and Cimprich, K. A. 2005. Functional uncoupling of MCM helicase and DNA polymerase activities activates the ATR-dependent checkpoint. *Genes Dev*. 19:1040-1052.

Bzymek, M., Thayer, N. H., Oh, S. D., Kleckner, N. and Hunter, N. 2010. Double Holliday junctions are intermediates of DNA break repair. *Nature*. 464:937-941.

Cahoon, L. A. and Seifert, H. S. 2009. An alternative DNA structure is necessary for pilin antigenic variation in *Neisseria gonorrhoeae*. *Science*. 325:764-767.

Callen, E., Di Virgilio, M., Kruhlak, M. J., Nieto-Soler, M., Wong, N., Chen, H. T., Faryabi, R. B., Polato, F., Santos, M., Starnes, L. M., Wesemann, D. R., Lee, J. E., Tubbs, A., Sleckman, B. P., Daniel, J. A., Ge, K., Alt, F. W., Fernandez-Capetillo, O., Nussenzweig, M. C. and Nussenzweig, A. 2013. 53BP1 mediates productive and mutagenic DNA repair through distinct phosphoprotein interactions. *Cell*. 153:1266-1280.

Cancer Genome Atlas, N. 2012. Comprehensive molecular portraits of human breast tumours. *Nature*. 490:61-70.

Cancer Genome Atlas Research, N. 2011. Integrated genomic analyses of ovarian carcinoma. *Nature*. 474:609-615.

Carlos, A. R., Escandell, J. M., Kotsantis, P., Suwaki, N., Bouwman, P., Badie, S., Folio, C., Benitez, J., Gomez-Lopez, G., Pisano, D. G., Jonkers, J. and Tarsounas, M. 2013. ARF triggers senescence in *Brca2*-deficient cells by altering the spectrum of p53 transcriptional targets. *Nat Commun*. 4:2697.

Castillo Bosch, P., Segura-Bayona, S., Koole, W., van Heteren, J. T., Dewar, J. M., Tijsterman, M. and Knipscheer, P. 2014. FANCJ promotes DNA synthesis through G-quadruplex structures. *EMBO J*. 33:2521-2533.

Cayrou, C., Coulombe, P., Vigneron, A., Stanojcic, S., Ganier, O., Peiffer, I., Rivals, E., Puy, A., Laurent-Chabalier, S., Desprat, R. and Mechali, M. 2011. Genome-scale analysis of metazoan replication origins reveals their organization in specific but flexible sites defined by conserved features. *Genome Res*. 21:1438-1449.

Cayrou, C., Gregoire, D., Coulombe, P., Danis, E. and Mechali, M. 2012. Genome-scale identification of active DNA replication origins. *Methods*. 57:158-164.

Ceccaldi, R., Liu, J. C., Amunugama, R., Hajdu, I., Primack, B., Petalcorin, M. I., O'Connor, K. W., Konstantinopoulos, P. A., Elledge, S. J., Boulton, S. J., Yusufzai, T. and D'Andrea, A. D. 2015. Homologous-recombination-deficient tumours are dependent on Poltheta-mediated repair. *Nature*. 518:258-262.

Cerosaletti, K., Wright, J. and Concannon, P. 2006. Active role for Nibrin in the kinetics of Atm activation. *Mol Cell Biol*. 26:1691-1699.

Chambers, V. S., Marsico, G., Boutell, J. M., Di Antonio, M., Smith, G. P. and Balasubramanian, S. 2015. High-throughput sequencing of DNA G-quadruplex structures in the human genome. *Nat Biotechnol*. 33:877-881.

Chan, S. H., Yu, A. M. and McVey, M. 2010. Dual roles for DNA polymerase theta in alternative end-joining repair of double-strand breaks in *Drosophila*. *PLoS Genet*. 6:e1001005.

Chandramouly, G., Willis, N. A. and Scully, R. 2011. A protective role for BRCA2 at stalled replication forks. *Breast Cancer Res*. 13:314.

Chang, H. H. Y., Pannunzio, N. R., Adachi, N. and Lieber, M. R. 2017. Non-homologous DNA end joining and alternative pathways to double-strand break repair. *Nat Rev Mol Cell Biol*. 18:495-506.

Chapman, J. R., Barral, P., Vannier, J. B., Borel, V., Steger, M., Tomas-Loba, A., Sartori, A. A., Adams, I. R., Batista, F. D. and Boulton, S. J. 2013. RIF1 is essential for 53BP1-dependent nonhomologous end joining and suppression of DNA double-strand break resection. *Mol Cell*. 49:858-871.

Chapman, J. R., Taylor, M. R. and Boulton, S. J. 2012. Playing the end game: DNA double-strand break repair pathway choice. *Mol Cell*. 47:497-510.

Chaudhury, I., Sareen, A., Raghunandan, M. and Sobeck, A. 2013. FANCD2 regulates BLM complex functions independently of FANCI to promote replication fork recovery. *Nucleic Acids Res*. 41:6444-6459.

Chen, H., Lisby, M. and Symington, L. S. 2013. RPA coordinates DNA end resection and prevents formation of DNA hairpins. *Mol Cell*. 50:589-600.

Chen, S. and Parmigiani, G. 2007. Meta-analysis of *BRCA1* and *BRCA2* penetrance. *J Clin Oncol*. 25:1329-1333.

Chen, W. Y., Rosner, B., Hankinson, S. E., Colditz, G. A. and Willett, W. C. 2011. Moderate alcohol consumption during adult life, drinking patterns, and breast cancer risk. *JAMA*. 306:1884-1890.

Chen, Y. H., Jones, M. J., Yin, Y., Crist, S. B., Colnaghi, L., Sims, R. J., 3rd, Rothenberg, E., Jallepalli, P. V. and Huang, T. T. 2015. ATR-mediated phosphorylation of FANCI regulates dormant origin firing in response to replication stress. *Mol Cell*. 58:323-338.

Cheung, I., Schertzer, M., Rose, A. and Lansdorp, P. M. 2002. Disruption of *dog-1* in *Caenorhabditis elegans* triggers deletions upstream of guanine-rich DNA. *Nat Genet*. 31:405-409.

Chilkova, O., Stenlund, P., Isoz, I., Stith, C. M., Grabowski, P., Lundstrom, E. B., Burgers, P. M. and Johansson, E. 2007. The eukaryotic leading and lagging strand DNA polymerases are loaded onto primer-ends via separate mechanisms but have comparable processivity in the presence of PCNA. *Nucleic Acids Res*. 35:6588-6597.

Chini, C. C. and Chen, J. 2003. Human claspin is required for replication checkpoint control. *J Biol Chem*. 278:30057-30062.

Choi, E., Park, P. G., Lee, H. O., Lee, Y. K., Kang, G. H., Lee, J. W., Han, W., Lee, H. C., Noh, D. Y., Lekomtsev, S. and Lee, H. 2012. BRCA2 fine-tunes the spindle assembly checkpoint through reinforcement of BubR1 acetylation. *Dev Cell*. 22:295-308.

Ciccia, A., Bredemeyer, A. L., Sowa, M. E., Terret, M. E., Jallepalli, P. V., Harper, J. W. and Elledge, S. J. 2009. The SIOD disorder protein SMARCAL1 is an RPA-interacting protein involved in replication fork restart. *Genes Dev*. 23:2415-2425.

Ciccia, A., Nimonkar, A. V., Hu, Y., Hajdu, I., Achar, Y. J., Izhar, L., Petit, S. A., Adamson, B., Yoon, J. C., Kowalczykowski, S. C., Livingston, D. M., Haracska, L. and Elledge, S. J. 2012. Polyubiquitinated PCNA recruits the ZRANB3 translocase to maintain genomic integrity after replication stress. *Mol Cell*. 47:396-409.

Clauson, C., Scharer, O. D. and Niedernhofer, L. 2013. Advances in understanding the complex mechanisms of DNA interstrand cross-link repair. *Cold Spring Harb Perspect Biol*. 5:a012732.

Cleaver, J. E. 2005. Cancer in xeroderma pigmentosum and related disorders of DNA repair. *Nat Rev Cancer*. 5:564-573.

Coleman, M. P., Quaresma, M., Berrino, F., Lutz, J. M., De Angelis, R., Capocaccia, R., Baili, P., Rachet, B., Gatta, G., Hakulinen, T., Micheli, A., Sant, M., Weir, H. K., Elwood, J. M., Tsukuma, H., Koifman, S., GA, E. S., Francisci, S., Santaquilani, M., Verdecchia, A., Storm, H. H., Young, J. L. and Group, C. W. 2008. Cancer survival in

five continents: a worldwide population-based study (CONCORD). *Lancet Oncol*. 9:730-756.

Coleman, R. L., Sill, M. W., Bell-McGuinn, K., Aghajanian, C., Gray, H. J., Tewari, K. S., Rubin, S. C., Rutherford, T. J., Chan, J. K., Chen, A. and Swisher, E. M. 2015. A phase II evaluation of the potent, highly selective PARP inhibitor veliparib in the treatment of persistent or recurrent epithelial ovarian, fallopian tube, or primary peritoneal cancer in patients who carry a germline *BRCA1* or *BRCA2* mutation - An NRG Oncology/Gynecologic Oncology Group study. *Gynecol Oncol*. 137:386-391.

Collaborative Group on Hormonal Factors in Breast, C. 2001. Familial breast cancer: collaborative reanalysis of individual data from 52 epidemiological studies including 58,209 women with breast cancer and 101,986 women without the disease. *Lancet*. 358:1389-1399.

Cook, J. G., Chasse, D. A. and Nevins, J. R. 2004. The regulated association of Cdt1 with minichromosome maintenance proteins and Cdc6 in mammalian cells. *J Biol Chem*. 279:9625-9633.

Cortez, D. 2015. Preventing replication fork collapse to maintain genome integrity. *DNA Repair (Amst)*. 32:149-157.

Costa, A., Ilves, I., Tamberg, N., Petojevic, T., Nogales, E., Botchan, M. R. and Berger, J. M. 2011. The structural basis for MCM2-7 helicase activation by GINS and Cdc45. *Nat Struct Mol Biol*. 18:471-477.

Costa, A., Renault, L., Swuec, P., Petojevic, T., Pesavento, J. J., Ilves, I., MacLellan-Gibson, K., Fleck, R. A., Botchan, M. R. and Berger, J. M. 2014. DNA binding polarity, dimerization, and ATPase ring remodeling in the CMG helicase of the eukaryotic replisome. *Elife*. 3:e03273.

Costantino, L., Sotiriou, S. K., Rantala, J. K., Magin, S., Mladenov, E., Helleday, T., Haber, J. E., Iliakis, G., Kallioniemi, O. P. and Halazonetis, T. D. 2014. Break-induced replication repair of damaged forks induces genomic duplications in human cells. *Science*. 343:88-91.

Couch, F. B., Bansbach, C. E., Driscoll, R., Luzwick, J. W., Glick, G. G., Betous, R., Carroll, C. M., Jung, S. Y., Qin, J., Cimprich, K. A. and Cortez, D. 2013. ATR phosphorylates SMARCAL1 to prevent replication fork collapse. *Genes Dev*. 27:1610-1623.

Coverley, D., Pelizon, C., Trewick, S. and Laskey, R. A. 2000. Chromatin-bound Cdc6 persists in S and G2 phases in human cells, while soluble Cdc6 is destroyed in a cyclin A-cdk2 dependent process. *J Cell Sci*. 113:1929-1938.

Crook, T., Brooks, L. A., Crossland, S., Osin, P., Barker, K. T., Waller, J., Philp, E., Smith, P. D., Yulug, I., Peto, J., Parker, G., Allday, M. J., Crompton, M. R. and Gusterson, B. A. 1998. p53 mutation with frequent novel condons but not a mutator phenotype in BRCA1- and BRCA2-associated breast tumours. *Oncogene*. 17:1681-1689.

Crossan, G. P., van der Weyden, L., Rosado, I. V., Langevin, F., Gaillard, P. H., McIntyre, R. E., Sanger Mouse Genetics, P., Gallagher, F., Kettunen, M. I., Lewis, D. Y., Brindle, K., Arends, M. J., Adams, D. J. and Patel, K. J. 2011. Disruption of mouse Slx4, a regulator of structure-specific nucleases, phenocopies Fanconi anemia. *Nat Genet*. 43:147-152.

Cuzick, J., Powles, T., Veronesi, U., Forbes, J., Edwards, R., Ashley, S. and Boyle, P. 2003. Overview of the main outcomes in breast-cancer prevention trials. *Lancet*. 361:296-300.

Czekanska, E. M. 2011. Assessment of cell proliferation with resazurin-based fluorescent dye. *Methods Mol Biol*. 740:27-32.

Danaei, G., Vander Hoorn, S., Lopez, A. D., Murray, C. J., Ezzati, M. and Comparative Risk Assessment collaborating, g. 2005. Causes of cancer in the world: comparative risk assessment of nine behavioural and environmental risk factors. *Lancet*. 366:1784-1793.

Davis, A. P. and Symington, L. S. 2004. RAD51-dependent break-induced replication in yeast. *Mol Cell Biol*. 24:2344-2351.

Davoli, T., Denchi, E. L. and de Lange, T. 2010. Persistent telomere damage induces bypass of mitosis and tetraploidy. *Cell*. 141:81-93.

de Jager, M., van Noort, J., van Gent, D. C., Dekker, C., Kanaar, R. and Wyman, C. 2001. Human Rad50/Mre11 is a flexible complex that can tether DNA ends. *Mol Cell*. 8:1129-1135.

de Jager, M., Wyman, C., van Gent, D. C. and Kanaar, R. 2002. DNA end-binding specificity of human Rad50/Mre11 is influenced by ATP. *Nucleic Acids Res*. 30:4425-4431.

De, S. and Michor, F. 2011. DNA secondary structures and epigenetic determinants of cancer genome evolution. *Nat Struct Mol Biol*. 18:950-955.

Deem, A., Keszthelyi, A., Blackgrove, T., Vayl, A., Coffey, B., Mathur, R., Chabes, A. and Malkova, A. 2011. Break-induced replication is highly inaccurate. *PLoS Biol*. 9:e1000594.

Delmolino, L. M., Saha, P. and Dutta, A. 2001. Multiple mechanisms regulate subcellular localization of human CDC6. *J Biol Chem*. 276:26947-26954.

Dent, R., Hanna, W. M., Trudeau, M., Rawlinson, E., Sun, P. and Narod, S. A. 2009. Pattern of metastatic spread in triple-negative breast cancer. *Breast Cancer Res Treat*. 115:423-428.

Dent, R., Trudeau, M., Pritchard, K. I., Hanna, W. M., Kahn, H. K., Sawka, C. A., Lickley, L. A., Rawlinson, E., Sun, P. and Narod, S. A. 2007. Triple-negative breast cancer: clinical features and patterns of recurrence. *Clin Cancer Res*. 13:4429-4434.

DePamphilis, M. L. 1993. Origins of DNA replication in metazoan chromosomes. *J Biol Chem*. 268:1-4.

Deshpande, R. A., Lee, J. H., Arora, S. and Paull, T. T. 2016. Nbs1 converts the human Mre11/Rad50 nuclease complex into an endo/exonuclease machine specific for protein-DNA adducts. *Mol Cell*. 64:593-606.

Di Micco, R., Fumagalli, M., Cicalese, A., Piccinin, S., Gasparini, P., Luise, C., Schurra, C., Garre, M., Nuciforo, P. G., Bensimon, A., Maestro, R., Pelicci, P. G. and d'Adda di Fagagna, F. 2006. Oncogene-induced senescence is a DNA damage response triggered by DNA hyper-replication. *Nature*. 444:638-642.

Dilley, R. L., Verma, P., Cho, N. W., Winters, H. D., Wondisford, A. R. and Greenberg, R. A. 2016. Break-induced telomere synthesis underlies alternative telomere maintenance. *Nature*. 539:54-58.

Dimri, G. P., Lee, X., Basile, G., Acosta, M., Scott, G., Roskelley, C., Medrano, E. E., Linskens, M., Rubelj, I., Pereira-Smith, O. and et al. 1995. A biomarker that identifies senescent human cells in culture and in aging skin *in vivo*. *Proc Natl Acad Sci U S A*. 92:9363-9367.

Ding, X., Ray Chaudhuri, A., Callen, E., Pang, Y., Biswas, K., Klarmann, K. D., Martin, B. K., Burkett, S., Cleveland, L., Stauffer, S., Sullivan, T., Dewan, A., Marks, H., Tubbs, A. T., Wong, N., Buehler, E., Akagi, K., Martin, S. E., Keller, J. R., Nussenzweig, A. and Sharan, S. K. 2016. Synthetic viability by BRCA2 and PARP1/ARTD1 deficiencies. *Nat Commun*. 7:12425.

Dinkelmann, M., Spehalski, E., Stoneham, T., Buis, J., Wu, Y., Sekiguchi, J. M. and Ferguson, D. O. 2009. Multiple functions of MRN in end-joining pathways during isotype class switching. *Nat Struct Mol Biol*. 16:808-813.

Dobzhansky, T. 1946. Genetics of Natural Populations. Xiii. Recombination and Variability in Populations of *Drosophila Pseudoobscura*. *Genetics*. 31:269-290.

Doil, C., Mailand, N., Bekker-Jensen, S., Menard, P., Larsen, D. H., Pepperkok, R., Ellenberg, J., Panier, S., Durocher, D., Bartek, J., Lukas, J. and Lukas, C. 2009. RNF168 binds and amplifies ubiquitin conjugates on damaged chromosomes to allow accumulation of repair proteins. *Cell*. 136:435-446.

Domchek, S. M., Aghajanian, C., Shapira-Frommer, R., Schmutzler, R. K., Audeh, M. W., Friedlander, M., Balmana, J., Mitchell, G., Fried, G., Stemmer, S. M., Hubert, A., Rosengarten, O., Loman, N., Robertson, J. D., Mann, H. and Kaufman, B. 2016. Efficacy and safety of olaparib monotherapy in germline *BRCA1/2* mutation carriers with advanced ovarian cancer and three or more lines of prior therapy. *Gynecol Oncol*. 140:199-203.

Donnianni, R. A. and Symington, L. S. 2013. Break-induced replication occurs by conservative DNA synthesis. *Proc Natl Acad Sci U S A*. 110:13475-13480.

Downing, B., Morgan, R., VanHulle, K., Deem, A. and Malkova, A. 2008. Large inverted repeats in the vicinity of a single double-strand break strongly affect repair in yeast diploids lacking Rad51. *Mutat Res*. 645:9-18.

Drygin, D., Siddiqui-Jain, A., O'Brien, S., Schwaebe, M., Lin, A., Bliesath, J., Ho, C. B., Proffitt, C., Trent, K., Whitten, J. P., Lim, J. K., Von Hoff, D., Anderes, K. and Rice, W. G. 2009. Anticancer activity of CX-3543: a direct inhibitor of rRNA biogenesis. *Cancer Res*. 69:7653-7661.

Dupre, A., Boyer-Chatenet, L., Sattler, R. M., Modi, A. P., Lee, J. H., Nicolette, M. L., Kopelovich, L., Jasin, M., Baer, R., Paull, T. T. and Gautier, J. 2008. A forward chemical genetic screen reveals an inhibitor of the Mre11-Rad50-Nbs1 complex. *Nat Chem Biol*. 4:119-125.

Durkin, S. G. and Glover, T. W. 2007. Chromosome fragile sites. *Annu Rev Genet*. 41:169-192.

Dynan, W. S. and Yoo, S. 1998. Interaction of Ku protein and DNA-dependent protein kinase catalytic subunit with nucleic acids. *Nucleic Acids Res*. 26:1551-1559.

Eddy, S., Ketkar, A., Zafar, M. K., Maddukuri, L., Choi, J. Y. and Eoff, R. L. 2014. Human Rev1 polymerase disrupts G-quadruplex DNA. *Nucleic Acids Res*. 42:3272-3285.

Edmondson, R., Broglie, J. J., Adcock, A. F. and Yang, L. 2014. Three-dimensional cell culture systems and their applications in drug discovery and cell-based biosensors. *Assay Drug Dev Technol*. 12:207-218.

Edwards, S. L., Brough, R., Lord, C. J., Natrajan, R., Vatcheva, R., Levine, D. A., Boyd, J., Reis-Filho, J. S. and Ashworth, A. 2008. Resistance to therapy caused by intragenic deletion in *BRCA2*. *Nature*. 451:1111-1115.

Elvers, I., Johansson, F., Groth, P., Erixon, K. and Helleday, T. 2011. UV stalled replication forks restart by re-priming in human fibroblasts. *Nucleic Acids Res*. 39:7049-7057.

Escribano-Diaz, C., Orthwein, A., Fradet-Turcotte, A., Xing, M., Young, J. T., Tkac, J., Cook, M. A., Rosebrock, A. P., Munro, M., Canny, M. D., Xu, D. and Durocher, D. 2013. A cell cycle-dependent regulatory circuit composed of 53BP1-RIF1 and BRCA1-CtIP controls DNA repair pathway choice. *Mol Cell*. 49:872-883.

Evers, B., Drost, R., Schut, E., de Bruin, M., van der Burg, E., Derksen, P. W., Holstege, H., Liu, X., van Drunen, E., Beverloo, H. B., Smith, G. C., Martin, N. M., Lau, A., O'Connor, M. J. and Jonkers, J. 2008. Selective inhibition of BRCA2-deficient mammary tumor cell growth by AZD2281 and cisplatin. *Clin Cancer Res*. 14:3916-3925.

Evers, B., Helleday, T. and Jonkers, J. 2010a. Targeting homologous recombination repair defects in cancer. *Trends Pharmacol Sci*. 31:372-380.

Evers, B., Schut, E., van der Burg, E., Braumuller, T. M., Egan, D. A., Holstege, H., Edser, P., Adams, D. J., Wade-Martins, R., Bouwman, P. and Jonkers, J. 2010b. A high-throughput pharmaceutical screen identifies compounds with specific toxicity against BRCA2-deficient tumors. *Clin Cancer Res*. 16:99-108.

Evrin, C., Clarke, P., Zech, J., Lurz, R., Sun, J., Uhle, S., Li, H., Stillman, B. and Speck, C. 2009. A double-hexameric MCM2-7 complex is loaded onto origin DNA during licensing of eukaryotic DNA replication. *Proc Natl Acad Sci U S A*. 106:20240-20245.

Falck, J., Mailand, N., Syljuasen, R. G., Bartek, J. and Lukas, J. 2001. The ATM-Chk2-Cdc25A checkpoint pathway guards against radioresistant DNA synthesis. *Nature*. 410:842-847.

Farmer, H., McCabe, N., Lord, C. J., Tutt, A. N., Johnson, D. A., Richardson, T. B., Santarosa, M., Dillon, K. J., Hickson, I., Knights, C., Martin, N. M., Jackson, S. P., Smith, G. C. and Ashworth, A. 2005. Targeting the DNA repair defect in *BRCA* mutant cells as a therapeutic strategy. *Nature*. 434:917-921.

Fedier, A., Steiner, R. A., Schwarz, V. A., Lenherr, L., Haller, U. and Fink, D. 2003. The effect of loss of *Brca1* on the sensitivity to anticancer agents in p53-deficient cells. *Int J Oncol*. 22:1169-1173.

Feng, S., Zhao, Y., Xu, Y., Ning, S., Huo, W., Hou, M., Gao, G., Ji, J., Guo, R. and Xu, D. 2016. Ewing tumor-associated antigen 1 interacts with replication protein A to promote restart of stalled replication forks. *J Biol Chem*. 291:21956-21962.

Feng, W. and Jasin, M. 2017. BRCA2 suppresses replication stress-induced mitotic and G1 abnormalities through homologous recombination. *Nat Commun*. 8:525.

Feng, Z., Scott, S. P., Bussen, W., Sharma, G. G., Guo, G., Pandita, T. K. and Powell, S. N. 2011. Rad52 inactivation is synthetically lethal with BRCA2 deficiency. *Proc Natl Acad Sci U S A*. 108:686-691.

Fishel, R., Lescoe, M. K., Rao, M. R., Copeland, N. G., Jenkins, N. A., Garber, J., Kane, M. and Kolodner, R. 1993. The human mutator gene homolog MSH2 and its association with hereditary nonpolyposis colon cancer. *Cell*. 75:1027-1038.

Fong, P. C., Boss, D. S., Yap, T. A., Tutt, A., Wu, P., Mergui-Roelvink, M., Mortimer, P., Swaisland, H., Lau, A., O'Connor, M. J., Ashworth, A., Carmichael, J., Kaye, S. B., Schellens, J. H. and de Bono, J. S. 2009. Inhibition of poly(ADP-ribose) polymerase in tumors from *BRCA* mutation carriers. *N Engl J Med*. 361:123-134.

Fong, P. C., Yap, T. A., Boss, D. S., Carden, C. P., Mergui-Roelvink, M., Gourley, C., De Greve, J., Lubinski, J., Shanley, S., Messiou, C., A'Hern, R., Tutt, A., Ashworth, A., Stone, J., Carmichael, J., Schellens, J. H., de Bono, J. S. and Kaye, S. B. 2010. Poly(ADP)-ribose polymerase inhibition: frequent durable responses in *BRCA* carrier ovarian cancer correlating with platinum-free interval. *J Clin Oncol*. 28:2512-2519.

Ford, D., Easton, D. F. and Peto, J. 1995. Estimates of the gene frequency of BRCA1 and its contribution to breast and ovarian cancer incidence. *Am J Hum Genet*. 57:1457-1462.

Fragkos, M., Ganier, O., Coulombe, P. and Mechali, M. 2015. DNA replication origin activation in space and time. *Nat Rev Mol Cell Biol*. 16:360-374.

Francis, L. I., Randell, J. C., Takara, T. J., Uchima, L. and Bell, S. P. 2009. Incorporation into the prereplicative complex activates the Mcm2-7 helicase for Cdc7-Dbf4 phosphorylation. *Genes Dev*. 23:643-654.

Freudenthal, B. D., Gakhar, L., Ramaswamy, S. and Washington, M. T. 2010. Structure of monoubiquitinated PCNA and implications for translesion synthesis and DNA polymerase exchange. *Nat Struct Mol Biol*. 17:479-484.

Fry, M. and Loeb, L. A. 1999. Human werner syndrome DNA helicase unwinds tetrahelical structures of the fragile X syndrome repeat sequence d(CGG)n. *J Biol Chem*. 274:12797-12802.

Fugger, K., Mistrik, M., Neelsen, K. J., Yao, Q., Zellweger, R., Kousholt, A. N., Haahr, P., Chu, W. K., Bartek, J., Lopes, M., Hickson, I. D. and Sorensen, C. S. 2015. FBH1 catalyzes regression of stalled replication forks. *Cell Rep*. 10:1749-1757.

Furukawa, T., Ishibashi, T., Kimura, S., Tanaka, H., Hashimoto, J. and Sakaguchi, K. 2003. Characterization of all the subunits of replication factor C from a higher plant, rice (*Oryza sativa L.*), and their relation to development. *Plant Mol Biol*. 53:15-25.

Gaillard, H., Garcia-Muse, T. and Aguilera, A. 2015. Replication stress and cancer. *Nat Rev Cancer*. 15:276-289.

Galanos, P., Vougas, K., Walter, D., Polyzos, A., Maya-Mendoza, A., Haagensen, E. J., Kokkalis, A., Roumelioti, F. M., Gagos, S., Tzetis, M., Canovas, B., Igea, A., Ahuja, A. K., Zellweger, R., Havaki, S., Kanavakis, E., Kletsas, D., Roninson, I. B., Garbis, S. D., Lopes, M., Nebreda, A., Thanos, D., Blow, J. J., Townsend, P., Sorensen, C. S., Bartek, J. and Gorgoulis, V. G. 2016. Chronic p53-independent p21 expression causes genomic instability by deregulating replication licensing. *Nat Cell Biol*. 18:777-789.

Gambus, A., Khoudoli, G. A., Jones, R. C. and Blow, J. J. 2011. MCM2-7 form double hexamers at licensed origins in *Xenopus* egg extract. *J Biol Chem*. 286:11855-11864.

Gan, W., Guan, Z., Liu, J., Gui, T., Shen, K., Manley, J. L. and Li, X. 2011. R-loop-mediated genomic instability is caused by impairment of replication fork progression. *Genes Dev*. 25:2041-2056.

Gao, Y., Mutter-Rottmayer, E., Zlatanou, A., Vaziri, C. and Yang, Y. 2017. Mechanisms of post-replication DNA repair. *Genes (Basel)*. 8:64.

Garcia-Gomez, S., Reyes, A., Martinez-Jimenez, M. I., Chocron, E. S., Mouron, S., Terrados, G., Powell, C., Salido, E., Mendez, J., Holt, I. J. and Blanco, L. 2013. PrimPol, an archaic primase/polymerase operating in human cells. *Mol Cell*. 52:541-553.

Garcia-Higuera, I., Taniguchi, T., Ganesan, S., Meyn, M. S., Timmers, C., Hejna, J., Grompe, M. and D'Andrea, A. D. 2001. Interaction of the Fanconi anemia proteins and BRCA1 in a common pathway. *Mol Cell*. 7:249-262.

Garcia-Rubio, M. L., Perez-Calero, C., Barroso, S. I., Tumini, E., Herrera-Moyano, E., Rosado, I. V. and Aguilera, A. 2015. The Fanconi anemia pathway protects genome integrity from R-loops. *PLoS Genet*. 11:e1005674.

Gatei, M., Sloper, K., Sorensen, C., Syljuasen, R., Falck, J., Hobson, K., Savage, K., Lukas, J., Zhou, B. B., Bartek, J. and Khanna, K. K. 2003. Ataxia-telangiectasia-mutated (ATM) and NBS1-dependent phosphorylation of Chk1 on Ser-317 in response to ionizing radiation. *J Biol Chem*. 278:14806-14811.

Ge, X. Q., Jackson, D. A. and Blow, J. J. 2007. Dormant origins licensed by excess Mcm2-7 are required for human cells to survive replicative stress. *Genes Dev*. 21:3331-3341.

Gellert, M., Lipsett, M. N. and Davies, D. R. 1962. Helix formation by guanylic acid. *Proc Natl Acad Sci U S A*. 48:2013-2018.

Giannattasio, M., Zwicky, K., Follonier, C., Foiani, M., Lopes, M. and Branzei, D. 2014. Visualization of recombination-mediated damage bypass by template switching. *Nat Struct Mol Biol*. 21:884-892.

Gibbs-Seymour, I., Oka, Y., Rajendra, E., Weinert, B. T., Passmore, L. A., Patel, K. J., Olsen, J. V., Choudhary, C., Bekker-Jensen, S. and Mailand, N. 2015. Ubiquitin-SUMO circuitry controls activated fanconi anemia ID complex dosage in response to DNA damage. *Mol Cell*. 57:150-164.

Gillet, J. P., Varma, S. and Gottesman, M. M. 2013. The clinical relevance of cancer cell lines. *J Natl Cancer Inst*. 105:452-458.

Gilson, E. and Geli, V. 2007. How telomeres are replicated. *Nat Rev Mol Cell Biol*. 8:825-838.

Goggins, M., Hruban, R. H. and Kern, S. E. 2000. BRCA2 is inactivated late in the development of pancreatic intraepithelial neoplasia: evidence and implications. *Am J Pathol*. 156:1767-1771.

Goldfless, S. J., Morag, A. S., Belisle, K. A., Sutera, V. A., Jr. and Lovett, S. T. 2006. DNA repeat rearrangements mediated by DnaK-dependent replication fork repair. *Mol Cell*. 21:595-604.

Gonzalez-Angulo, A. M., Timms, K. M., Liu, S., Chen, H., Litton, J. K., Potter, J., Lanchbury, J. S., Stemke-Hale, K., Hennessy, B. T., Arun, B. K., Hortobagyi, G. N., Do, K. A., Mills, G. B. and Meric-Bernstam, F. 2011. Incidence and outcome of *BRCA* mutations in unselected patients with triple receptor-negative breast cancer. *Clin Cancer Res*. 17:1082-1089.

Goodspeed, A., Heiser, L. M., Gray, J. W. and Costello, J. C. 2016. Tumor-Derived Cell Lines as Molecular Models of Cancer Pharmacogenomics. *Mol Cancer Res*. 14:3-13.

Gorgoulis, V. G., Vassiliou, L. V., Karakaidos, P., Zacharatos, P., Kotsinas, A., Liloglou, T., Venere, M., Ditullio, R. A., Jr., Kastrinakis, N. G., Levy, B., Kletsas, D., Yoneta, A., Herlyn, M., Kittas, C. and Halazonetis, T. D. 2005. Activation of the DNA damage checkpoint and genomic instability in human precancerous lesions. *Nature*. 434:907-913.

Gorodnova, T. V., Sokolenko, A. P., Ivantsov, A. O., Iyevleva, A. G., Suspitsin, E. N., Aleksakhina, S. N., Yanus, G. A., Togo, A. V., Maximov, S. Y. and Imyanitov, E. N. 2015. High response rates to neoadjuvant platinum-based therapy in ovarian cancer patients carrying germ-line *BRCA* mutation. *Cancer Lett*. 369:363-367.

Grawunder, U., Wilm, M., Wu, X., Kulesza, P., Wilson, T. E., Mann, M. and Lieber, M. R. 1997. Activity of DNA ligase IV stimulated by complex formation with XRCC4 protein in mammalian cells. *Nature*. 388:492-495.

Greenblatt, M. S., Chappuis, P. O., Bond, J. P., Hamel, N. and Foulkes, W. D. 2001. *TP53* mutations in breast cancer associated with *BRCA1* or *BRCA2* germ-line mutations: distinctive spectrum and structural distribution. *Cancer Res*. 61:4092-4097.

Greenup, R., Buchanan, A., Lorizio, W., Rhoads, K., Chan, S., Leedom, T., King, R., McLennan, J., Crawford, B., Kelly Marcom, P. and Shelley Hwang, E. 2013. Prevalence of *BRCA* mutations among women with triple-negative breast cancer (TNBC) in a genetic counseling cohort. *Ann Surg Oncol*. 20:3254-3258.

Gretarsdottir, S., Thorlacius, S., Valgardsdottir, R., Gudlaugsdottir, S., Sigurdsson, S., Steinarsdottir, M., Jonasson, J. G., Anamthawat-Jonsson, K. and Eyfjord, J. E. 1998. BRCA2 and p53 mutations in primary breast cancer in relation to genetic instability. *Cancer Res*. 58:859-862.

Gu, J., Lu, H., Tippin, B., Shimazaki, N., Goodman, M. F. and Lieber, M. R. 2007. XRCC4:DNA ligase IV can ligate incompatible DNA ends and can ligate across gaps. *EMBO J*. 26:1010-1023.

Gunn, A. and Stark, J. M. 2012. I-SceI-based assays to examine distinct repair outcomes of mammalian chromosomal double strand breaks. *Methods Mol Biol*. 920:379-391.

Haahr, P., Hoffmann, S., Tollenaere, M. A., Ho, T., Toledo, L. I., Mann, M., Bekker-Jensen, S., Raschle, M. and Mailand, N. 2016. Activation of the ATR kinase by the RPA-binding protein ETAA1. *Nat Cell Biol*. 18:1196-1207.

Hakem, R., de la Pompa, J. L., Sirard, C., Mo, R., Woo, M., Hakem, A., Wakeham, A., Potter, J., Reitmair, A., Billia, F., Firpo, E., Hui, C. C., Roberts, J., Rossant, J. and Mak, T. W. 1996. The tumor suppressor gene *Brca1* is required for embryonic cellular proliferation in the mouse. *Cell*. 85:1009-1023.

Hanada, K., Budzowska, M., Davies, S. L., van Drunen, E., Onizawa, H., Beverloo, H. B., Maas, A., Essers, J., Hickson, I. D. and Kanaar, R. 2007. The structure-specific endonuclease Mus81 contributes to replication restart by generating double-strand DNA breaks. *Nat Struct Mol Biol*. 14:1096-1104.

Hansel-Hertsch, R., Beraldi, D., Lensing, S. V., Marsico, G., Zyner, K., Parry, A., Di Antonio, M., Pike, J., Kimura, H., Narita, M., Tannahill, D. and Balasubramanian, S. 2016. G-quadruplex structures mark human regulatory chromatin. *Nat Genet*. 48:1267-1272.

Haracska, L., Torres-Ramos, C. A., Johnson, R. E., Prakash, S. and Prakash, L. 2004. Opposing effects of ubiquitin conjugation and SUMO modification of PCNA on replicational bypass of DNA lesions in *Saccharomyces cerevisiae*. *Mol Cell Biol*. 24:4267-4274.

Harrigan, J. A., Belotserkovskaya, R., Coates, J., Dimitrova, D. S., Polo, S. E., Bradshaw, C. R., Fraser, P. and Jackson, S. P. 2011. Replication stress induces 53BP1-containing OPT domains in G1 cells. *J Cell Biol*. 193:97-108.

Hashimoto, Y. and Costanzo, V. 2011. Studying DNA replication fork stability in Xenopus egg extract. *Methods Mol Biol*. 745:437-445.

Hashimoto, Y., Puddu, F. and Costanzo, V. 2012. RAD51- and MRE11-dependent reassembly of uncoupled CMG helicase complex at collapsed replication forks. *Nat Struct Mol Biol*. 19:17-24.

Hashimoto, Y. and Takisawa, H. 2003. Xenopus Cut5 is essential for a CDK-dependent process in the initiation of DNA replication. *EMBO J*. 22:2526-2535.

Hastie, N. D., Dempster, M., Dunlop, M. G., Thompson, A. M., Green, D. K. and Allshire, R. C. 1990. Telomere reduction in human colorectal carcinoma and with ageing. *Nature*. 346:866-868.

Hayflick, L. 1965. The limited *in vitro* lifetime of human diploid cell strains. *Exp Cell Res*. 37:614-636.

Hayflick, L. and Moorhead, P. S. 1961. The serial cultivation of human diploid cell strains. *Exp Cell Res*. 25:585-621.

Heller, R. C. and Marians, K. J. 2006. Replication fork reactivation downstream of a blocked nascent leading strand. *Nature*. 439:557-562.

Henderson, A., Wu, Y., Huang, Y. C., Chavez, E. A., Platt, J., Johnson, F. B., Brosh, R. M., Jr., Sen, D. and Lansdorp, P. M. 2014. Detection of G-quadruplex DNA in mammalian cells. *Nucleic Acids Res*. 42:860-869.

Henderson, E., Hardin, C. C., Walk, S. K., Tinoco, I., Jr. and Blackburn, E. H. 1987. Telomeric DNA oligonucleotides form novel intramolecular structures containing guanine-guanine base pairs. *Cell*. 51:899-908.

Heyer, W. D., Ehmsen, K. T. and Liu, J. 2010. Regulation of homologous recombination in eukaryotes. *Annu Rev Genet*. 44:113-139.

Higgs, M. R., Reynolds, J. J., Winczura, A., Blackford, A. N., Borel, V., Miller, E. S., Zlatanou, A., Nieminuszczy, J., Ryan, E. L., Davies, N. J., Stankovic, T., Boulton, S. J., Niedzwiedz, W. and Stewart, G. S. 2015. BOD1L is required to suppress deleterious resection of stressed replication forks. *Mol Cell*. 59:462-477.

Hira, A., Yoshida, K., Sato, K., Okuno, Y., Shiraishi, Y., Chiba, K., Tanaka, H., Miyano, S., Shimamoto, A., Tahara, H., Ito, E., Kojima, S., Kurumizaka, H., Ogawa, S., Takata, M., Yabe, H. and Yabe, M. 2015. Mutations in the gene encoding the E2 conjugating enzyme UBE2T cause Fanconi anemia. *Am J Hum Genet*. 96:1001-1007.

Hoa, N. N., Shimizu, T., Zhou, Z. W., Wang, Z. Q., Deshpande, R. A., Paull, T. T., Akter, S., Tsuda, M., Furuta, R., Tsusui, K., Takeda, S. and Sasanuma, H. 2016. Mre11 is essential for the removal of lethal topoisomerase 2 covalent cleavage complexes. *Mol Cell*. 64:580-592.

Hodskinson, M. R., Silhan, J., Crossan, G. P., Garaycoechea, J. I., Mukherjee, S., Johnson, C. M., Scharer, O. D. and Patel, K. J. 2014. Mouse SLX4 is a tumor suppressor that stimulates the activity of the nuclease XPF-ERCC1 in DNA crosslink repair. *Mol Cell*. 54:472-484.

Hoege, C., Pfander, B., Moldovan, G. L., Pyrowolakis, G. and Jentsch, S. 2002. RAD6-dependent DNA repair is linked to modification of PCNA by ubiquitin and SUMO. *Nature*. 419:135-141.

Howlett, N. G., Taniguchi, T., Olson, S., Cox, B., Waisfisz, Q., De Die-Smulders, C., Persky, N., Grompe, M., Joenje, H., Pals, G., Ikeda, H., Fox, E. A. and D'Andrea, A. D. 2002. Biallelic inactivation of *BRCA2* in Fanconi anemia. *Science*. 297:606-609.

Hu, Y. 2009. BRCA1, hormone, and tissue-specific tumor suppression. *Int J Biol Sci*. 5:20-27.

Huber, M. D., Lee, D. C. and Maizels, N. 2002. G4 DNA unwinding by BLM and Sgs1p: substrate specificity and substrate-specific inhibition. *Nucleic Acids Res*. 30:3954-3961.

Hubscher, U., Nasheuer, H. P. and Syvaoja, J. E. 2000. Eukaryotic DNA polymerases, a growing family. *Trends Biochem Sci*. 25:143-147.

Hucl, T., Rago, C., Gallmeier, E., Brody, J. R., Gorospe, M. and Kern, S. E. 2008. A syngeneic variance library for functional annotation of human variation: application to BRCA2. *Cancer Res*. 68:5023-5030.

Huen, M. S., Grant, R., Manke, I., Minn, K., Yu, X., Yaffe, M. B. and Chen, J. 2007. RNF8 transduces the DNA-damage signal via histone ubiquitylation and checkpoint protein assembly. *Cell*. 131:901-914.

Huertas, P., Cortes-Ledesma, F., Sartori, A. A., Aguilera, A. and Jackson, S. P. 2008. CDK targets Sae2 to control DNA-end resection and homologous recombination. *Nature*. 455:689-692.

Huppert, J. L. 2008. Four-stranded nucleic acids: structure, function and targeting of G-quadruplexes. *Chem Soc Rev*. 37:1375-1384.

Huppert, J. L. and Balasubramanian, S. 2005. Prevalence of quadruplexes in the human genome. *Nucleic Acids Res*. 33:2908-2916.

Husain, A., He, G., Venkatraman, E. S. and Spriggs, D. R. 1998. *BRCA1* up-regulation is associated with repair-mediated resistance to cis-diamminedichloroplatinum(II). *Cancer Res*. 58:1120-1123.

Ibarra, A., Schwob, E. and Mendez, J. 2008. Excess MCM proteins protect human cells from replicative stress by licensing backup origins of replication. *Proc Natl Acad Sci U S A*. 105:8956-8961.

Ilves, I., Petojevic, T., Pesavento, J. J. and Botchan, M. R. 2010. Activation of the MCM2-7 helicase by association with Cdc45 and GINS proteins. *Mol Cell*. 37:247-258.

Ip, S. C., Rass, U., Blanco, M. G., Flynn, H. R., Skehel, J. M. and West, S. C. 2008. Identification of Holliday junction resolvases from humans and yeast. *Nature*. 456:357-361.

Ira, G., Pellicioli, A., Balijja, A., Wang, X., Fiorani, S., Carotenuto, W., Liberi, G., Bressan, D., Wan, L., Hollingsworth, N. M., Haber, J. E. and Foiani, M. 2004. DNA end resection, homologous recombination and DNA damage checkpoint activation require CDK1. *Nature*. 431:1011-1017.

Ishiai, M., Kitao, H., Smogorzewska, A., Tomida, J., Kinomura, A., Uchida, E., Saberi, A., Kinoshita, E., Kinoshita-Kikuta, E., Koike, T., Tashiro, S., Elledge, S. J. and Takata, M. 2008. FANCI phosphorylation functions as a molecular switch to turn on the Fanconi anemia pathway. *Nat Struct Mol Biol*. 15:1138-1146.

Ishida, R. and Buchwald, M. 1982. Susceptibility of Fanconi's anemia lymphoblasts to DNA-cross-linking and alkylating agents. *Cancer Res*. 42:4000-4006.

Issaeva, N., Thomas, H. D., Djureinovic, T., Jaspers, J. E., Stoimenov, I., Kyle, S., Pedley, N., Gottipati, P., Zur, R., Sleeth, K., Chatzakos, V., Mulligan, E. A., Lundin,

C., Gubanova, E., Kersbergen, A., Harris, A. L., Sharma, R. A., Rottenberg, S., Curtin, N. J. and Helleday, T. 2010. 6-thioguanine selectively kills BRCA2-defective tumors and overcomes PARP inhibitor resistance. *Cancer Res*. 70:6268-6276.

Jackson, S. P. and Bartek, J. 2009. The DNA-damage response in human biology and disease. *Nature*. 461:1071-1078.

Jaspers, J. E., Kersbergen, A., Boon, U., Sol, W., van Deemter, L., Zander, S. A., Drost, R., Wientjens, E., Ji, J., Aly, A., Doroshow, J. H., Cranston, A., Martin, N. M., Lau, A., O'Connor, M. J., Ganesan, S., Borst, P., Jonkers, J. and Rottenberg, S. 2013. Loss of 53BP1 causes PARP inhibitor resistance in *Brca1*-mutated mouse mammary tumors. *Cancer Discov*. 3:68-81.

Jeganathan, K., Malureanu, L., Baker, D. J., Abraham, S. C. and van Deursen, J. M. 2007. Bub1 mediates cell death in response to chromosome missegregation and acts to suppress spontaneous tumorigenesis. *J Cell Biol*. 179:255-267.

Joenje, H. and Patel, K. J. 2001. The emerging genetic and molecular basis of Fanconi anaemia. *Nat Rev Genet*. 2:446-457.

Johnson, R. D. and Jasin, M. 2000. Sister chromatid gene conversion is a prominent double-strand break repair pathway in mammalian cells. *EMBO J*. 19:3398-3407.

Johnson, R. D., Liu, N. and Jasin, M. 1999. Mammalian XRCC2 promotes the repair of DNA double-strand breaks by homologous recombination. *Nature*. 401:397-399.

Jones, K. L. and Buzdar, A. U. 2004. A review of adjuvant hormonal therapy in breast cancer. *Endocr Relat Cancer*. 11:391-406.

Jonkers, J., Meuwissen, R., van der Gulden, H., Peterse, H., van der Valk, M. and Berns, A. 2001. Synergistic tumor suppressor activity of BRCA2 and p53 in a conditional mouse model for breast cancer. *Nat Genet*. 29:418-425.

Kais, Z., Rondinelli, B., Holmes, A., O'Leary, C., Kozono, D., D'Andrea, A. D. and Ceccaldi, R. 2016. FANCD2 maintains fork stability in BRCA1/2-deficient tumors and promotes alternative end-joining DNA repair. *Cell Rep*. 15:2488-2499.

Kamimura, Y., Masumoto, H., Sugino, A. and Araki, H. 1998. Sld2, which interacts with Dpb11 in *Saccharomyces cerevisiae*, is required for chromosomal DNA replication. *Mol Cell Biol*. 18:6102-6109.

Kamimura, Y., Tak, Y. S., Sugino, A. and Araki, H. 2001. Sld3, which interacts with Cdc45 (Sld4), functions for chromosomal DNA replication in *Saccharomyces cerevisiae*. *EMBO J*. 20:2097-2107.

Kannouche, P. L., Wing, J. and Lehmann, A. R. 2004. Interaction of human DNA polymerase eta with monoubiquitinated PCNA: a possible mechanism for the polymerase switch in response to DNA damage. *Mol Cell*. 14:491-500.

Karanja, K. K., Lee, E. H., Hendrickson, E. A. and Campbell, J. L. 2014. Preventing over-resection by DNA2 helicase/nuclease suppresses repair defects in Fanconi anemia cells. *Cell Cycle*. 13:1540-1550.

Karras, G. I., Fumasoni, M., Sienski, G., Vanoli, F., Branzei, D. and Jentsch, S. 2013. Noncanonical role of the 9-1-1 clamp in the error-free DNA damage tolerance pathway. *Mol Cell*. 49:536-546.

Karras, G. I. and Jentsch, S. 2010. The RAD6 DNA damage tolerance pathway operates uncoupled from the replication fork and is functional beyond S phase. *Cell*. 141:255-267.

Kast, K., Rhiem, K., Wappenschmidt, B., Hahnen, E., Hauke, J., Bluemcke, B., Zarghooni, V., Herold, N., Ditsch, N., Kiechle, M., Braun, M., Fischer, C., Dikow, N., Schott, S., Rahner, N., Niederacher, D., Fehm, T., Gehrig, A., Mueller-Reible, C., Arnold, N., Maass, N., Borck, G., de Gregorio, N., Scholz, C., Auber, B., Varon-Manteeva, R., Speiser, D., Horvath, J., Lichey, N., Wimberger, P., Stark, S., Faust, U., Weber, B. H., Emons, G., Zachariae, S., Meindl, A., Schmutzler, R. K., Engel, C., German Consortium for Hereditary, B. and Ovarian, C. 2016. Prevalence of *BRCA1/2* germline mutations in 21 401 families with breast and ovarian cancer. *J Med Genet*. 53:465-471.

Kastan, M. B., Zhan, Q., el-Deiry, W. S., Carrier, F., Jacks, T., Walsh, W. V., Plunkett, B. S., Vogelstein, B. and Fornace, A. J., Jr. 1992. A mammalian cell cycle checkpoint pathway utilizing p53 and GADD45 is defective in ataxia-telangiectasia. *Cell*. 71:587-597.

Kaufman, B., Shapira-Frommer, R., Schmutzler, R. K., Audeh, M. W., Friedlander, M., Balmana, J., Mitchell, G., Fried, G., Stemmer, S. M., Hubert, A., Rosengarten, O., Steiner, M., Loman, N., Bowen, K., Fielding, A. and Domchek, S. M. 2015. Olaparib monotherapy in patients with advanced cancer and a germline *BRCA1/2* mutation. *J Clin Oncol*. 33:244-250.

Keeney, S. 2008. Spo11 and the Formation of DNA Double-Strand Breaks in Meiosis. *Genome Dyn Stab*. 2:81-123.

Kent, T., Chandramouly, G., McDevitt, S. M., Ozdemir, A. Y. and Pomerantz, R. T. 2015. Mechanism of microhomology-mediated end-joining promoted by human DNA polymerase theta. *Nat Struct Mol Biol*. 22:230-237.

Kim, Y., Lach, F. P., Desetty, R., Hanenberg, H., Auerbach, A. D. and Smogorzewska, A. 2011. Mutations of the SLX4 gene in Fanconi anemia. *Nat Genet*. 43:142-146.

Kim, Y., Spitz, G. S., Veturi, U., Lach, F. P., Auerbach, A. D. and Smogorzewska, A. 2013. Regulation of multiple DNA repair pathways by the Fanconi anemia protein SLX4. *Blood*. 121:54-63.

King, M.-C., Marks, J. and Mandell, J. 2003. Breast and Ovarian Cancer Risks Due to Inherited Mutations in BRCA1 and BRCA2. *Science*. 302:643-646.

Kinzler, K. W. and Vogelstein, B. 1997. Cancer-susceptibility genes. Gatekeepers and caretakers. *Nature*. 386:761, 763.

Klein Douwel, D., Boonen, R. A., Long, D. T., Szypowska, A. A., Raschle, M., Walter, J. C. and Knipscheer, P. 2014. XPF-ERCC1 acts in unhooking DNA interstrand crosslinks in cooperation with FANCD2 and FANCP/SLX4. *Mol Cell*. 54:460-471.

Knipscheer, P., Raschle, M., Smogorzewska, A., Enoiu, M., Ho, T. V., Scharer, O. D., Elledge, S. J. and Walter, J. C. 2009. The Fanconi anemia pathway promotes replication-dependent DNA interstrand cross-link repair. *Science*. 326:1698-1701.

Kolas, N. K., Chapman, J. R., Nakada, S., Ylanko, J., Chahwan, R., Sweeney, F. D., Panier, S., Mendez, M., Wildenhain, J., Thomson, T. M., Pelletier, L., Jackson, S. P. and Durocher, D. 2007. Orchestration of the DNA-damage response by the RNF8 ubiquitin ligase. *Science*. 318:1637-1640.

Kolinjivadi, A. M., Sannino, V., De Antoni, A., Zadorozhny, K., Kilkenny, M., Techer, H., Baldi, G., Shen, R., Ciccia, A., Pellegrini, L., Krejci, L. and Costanzo, V. 2017. Smarcal1-mediated fork reversal triggers Mre11-dependent degradation of nascent DNA in the absence of Brca2 and stable Rad51 nucleofilaments. *Mol Cell*. 67:867-881 e867.

Koole, W., van Schendel, R., Karambelas, A. E., van Heteren, J. T., Okihara, K. L. and Tijsterman, M. 2014. A polymerase theta-dependent repair pathway suppresses extensive genomic instability at endogenous G4 DNA sites. *Nat Commun*. 5:3216.

Koopman, G., Reutelingsperger, C. P., Kuijten, G. A., Keehnen, R. M., Pals, S. T. and van Oers, M. H. 1994. Annexin V for flow cytometric detection of phosphatidylserine expression on B cells undergoing apoptosis. *Blood*. 84:1415-1420.

Kops, G. J., Weaver, B. A. and Cleveland, D. W. 2005. On the road to cancer: aneuploidy and the mitotic checkpoint. *Nat Rev Cancer*. 5:773-785.

Kruisselbrink, E., Guryev, V., Brouwer, K., Pontier, D. B., Cuppen, E. and Tijsterman, M. 2008. Mutagenic capacity of endogenous G4 DNA underlies genome instability in FANCJ-defective *C. elegans*. *Curr Biol*. 18:900-905.

Kuchenbaecker, K. B., Hopper, J. L., Barnes, D. R., Phillips, K. A., Mooij, T. M., Roos-Blom, M. J., Jervis, S., van Leeuwen, F. E., Milne, R. L., Andrieu, N., Goldgar, D. E., Terry, M. B., Rookus, M. A., Easton, D. F., Antoniou, A. C., Brca, Consortium, B. C., McGuffog, L., Evans, D. G., Barrowdale, D., Frost, D., Adlard, J., Ong, K. R., Izatt, L., Tischkowitz, M., Eeles, R., Davidson, R., Hodgson, S., Ellis, S., Nogues, C., Lasset, C., Stoppa-Lyonnet, D., Fricker, J. P., Faivre, L., Berthet, P., Hooning, M. J., van der Kolk, L. E., Kets, C. M., Adank, M. A., John, E. M., Chung, W. K., Andrulis, I. L., Southey, M., Daly, M. B., Buys, S. S., Osorio, A., Engel, C., Kast, K., Schmutzler, R. K., Caldes, T., Jakubowska, A., Simard, J., Friedlander, M. L., McLachlan, S. A., Machackova, E., Foretova, L., Tan, Y. Y., Singer, C. F., Olah, E., Gerdes, A. M., Arver, B. and Olsson, H. 2017. Risks of breast, ovarian, and contralateral breast cancer for *BRCA1* and *BRCA2* mutation carriers. *JAMA*. 317:2402-2416.

Kumagai, A., Lee, J., Yoo, H. Y. and Dunphy, W. G. 2006. TopBP1 activates the ATR-ATRIP complex. *Cell*. 124:943-955.

Kumagai, A., Shevchenko, A., Shevchenko, A. and Dunphy, W. G. 2010. Treslin collaborates with TopBP1 in triggering the initiation of DNA replication. *Cell*. 140:349-359.

Kumagai, A., Shevchenko, A., Shevchenko, A. and Dunphy, W. G. 2011. Direct regulation of Treslin by cyclin-dependent kinase is essential for the onset of DNA replication. *J Cell Biol*. 193:995-1007.

Kutler, D. I., Auerbach, A. D., Satagopan, J., Giampietro, P. F., Batish, S. D., Huvos, A. G., Goberdhan, A., Shah, J. P. and Singh, B. 2003. High incidence of head and neck squamous cell carcinoma in patients with Fanconi anemia. *Arch Otolaryngol Head Neck Surg*. 129:106-112.

Kuzminov, A. 2001. Single-strand interruptions in replicating chromosomes cause double-strand breaks. *Proc Natl Acad Sci U S A*. 98:8241-8246.

Kuznetsova, A. Y., Seget, K., Moeller, G. K., de Pagter, M. S., de Roos, J. A., Durrbaum, M., Kuffer, C., Muller, S., Zaman, G. J., Kloosterman, W. P. and Storchova, Z. 2015. Chromosomal instability, tolerance of mitotic errors and multidrug resistance are promoted by tetraploidization in human cells. *Cell Cycle*. 14:2810-2820.

Lacey, J. V., Jr., Kreimer, A. R., Buys, S. S., Marcus, P. M., Chang, S. C., Leitzmann, M. F., Hoover, R. N., Prorok, P. C., Berg, C. D., Hartge, P., Prostate, L. C. and Ovarian Cancer Screening Trial Project, T. 2009. Breast cancer epidemiology according to recognized breast cancer risk factors in the prostate, lung, colorectal and ovarian (PLCO) cancer screening trial cohort. *BMC Cancer*. 9:84.

Lachaud, C., Moreno, A., Marchesi, F., Toth, R., Blow, J. J. and Rouse, J. 2016. Ubiquitinated Fancd2 recruits Fan1 to stalled replication forks to prevent genome instability. *Science*. 351:846-849.

Lage, C., de Padula, M., de Alencar, T. A., da Fonseca Goncalves, S. R., da Silva Vidal, L., Cabral-Neto, J. and Leitao, A. C. 2003. New insights on how nucleotide excision repair could remove DNA adducts induced by chemotherapeutic agents and psoralens plus UV-A (PUVA) in *Escherichia coli* cells. *Mutat Res*. 544:143-157.

Lai, X., Broderick, R., Bergoglio, V., Zimmer, J., Badie, S., Niedzwiedz, W., Hoffmann, J. S. and Tarsounas, M. 2017. MUS81 nuclease activity is essential for replication stress tolerance and chromosome segregation in BRCA2-deficient cells. *Nat Commun*. 8:15983.

Lam, E. Y., Beraldi, D., Tannahill, D. and Balasubramanian, S. 2013. G-quadruplex structures are stable and detectable in human genomic DNA. *Nat Commun*. 4:1796.

Leach, F. S., Nicolaides, N. C., Papadopoulos, N., Liu, B., Jen, J., Parsons, R., Peltomaki, P., Sistonen, P., Aaltonen, L. A., Nystrom-Lahti, M. and et al. 1993.

Mutations of a mutS homolog in hereditary nonpolyposis colorectal cancer. *Cell*. 75:1215-1225.

Lee, J. H., Ghirlando, R., Bhaskara, V., Hoffmeyer, M. R., Gu, J. and Paull, T. T. 2003. Regulation of Mre11/Rad50 by Nbs1: effects on nucleotide-dependent DNA binding and association with ataxia-telangiectasia-like disorder mutant complexes. *J Biol Chem*. 278:45171-45181.

Lee, J. H. and Paull, T. T. 2004a. Direct activation of the ATM protein kinase by the Mre11/Rad50/Nbs1 complex. *Science*. 304:93-96.

Lee, J. H. and Paull, T. T. 2005. ATM activation by DNA double-strand breaks through the Mre11-Rad50-Nbs1 complex. *Science*. 308:551-554.

Lee, J. K., Choi, Y. L., Kwon, M. and Park, P. J. 2016a. Mechanisms and consequences of cancer genome instability: lessons from genome sequencing studies. *Annu Rev Pathol*. 11:283-312.

Lee, K. C., Padget, K., Curtis, H., Cowell, I. G., Moiani, D., Sondka, Z., Morris, N. J., Jackson, G. H., Cockell, S. J., Tainer, J. A. and Austin, C. A. 2012. MRE11 facilitates the removal of human topoisomerase II complexes from genomic DNA. *Biol Open*. 1:863-873.

Lee, K. M., Choi, K. H. and Ouellette, M. M. 2004b. Use of exogenous hTERT to immortalize primary human cells. *Cytotechnology*. 45:33-38.

Lee, Y. C., Zhou, Q., Chen, J. and Yuan, J. 2016b. RPA-binding protein ETAA1 is an ATR activator involved in DNA replication stress response. *Curr Biol*. 26:3257-3268.

Leman, A. R. and Noguchi, E. 2013. The replication fork: understanding the eukaryotic replication machinery and the challenges to genome duplication. *Genes (Basel)*. 4:1-32.

Li, X., Zhao, Q., Liao, R., Sun, P. and Wu, X. 2003. The SCF(Skp2) ubiquitin ligase complex interacts with the human replication licensing factor Cdt1 and regulates Cdt1 degradation. *J Biol Chem*. 278:30854-30858.

Liang, L., Deng, L., Nguyen, S. C., Zhao, X., Maulion, C. D., Shao, C. and Tischfield, J. A. 2008. Human DNA ligases I and III, but not ligase IV, are required for microhomology-mediated end joining of DNA double-strand breaks. *Nucleic Acids Res*. 36:3297-3310.

Liberi, G., Maffioletti, G., Lucca, C., Chiolo, I., Baryshnikova, A., Cotta-Ramusino, C., Lopes, M., Pellicioli, A., Haber, J. E. and Foiani, M. 2005. Rad51-dependent DNA structures accumulate at damaged replication forks in sgs1 mutants defective in the yeast ortholog of BLM RecQ helicase. *Genes Dev*. 19:339-350.

Lieber, M. R. 2010. The mechanism of double-strand DNA break repair by the nonhomologous DNA end-joining pathway. *Annu Rev Biochem*. 79:181-211.

Liedtke, C., Mazouni, C., Hess, K. R., Andre, F., Tordai, A., Mejia, J. A., Symmans, W. F., Gonzalez-Angulo, A. M., Hennessy, B., Green, M., Cristofanilli, M., Hortobagyi, G. N. and Pusztai, L. 2008. Response to neoadjuvant therapy and long-term survival in patients with triple-negative breast cancer. *J Clin Oncol*. 26:1275-1281.

Liu, S., Bekker-Jensen, S., Mailand, N., Lukas, C., Bartek, J. and Lukas, J. 2006. Claspin operates downstream of TopBP1 to direct ATR signaling towards Chk1 activation. *Mol Cell Biol*. 26:6056-6064.

Llorente, B., Smith, C. E. and Symington, L. S. 2008. Break-induced replication: what is it and what is it for? *Cell Cycle*. 7:859-864.

Llorente, B. and Symington, L. S. 2004. The Mre11 nuclease is not required for 5' to 3' resection at multiple HO-induced double-strand breaks. *Mol Cell Biol*. 24:9682-9694.

Loeb, L. A. 1991. Mutator phenotype may be required for multistage carcinogenesis. *Cancer Res*. 51:3075-3079.

Loeb, L. A., Springgate, C. F. and Battula, N. 1974. Errors in DNA replication as a basis of malignant changes. *Cancer Res*. 34:2311-2321.

Lomax, M. E., Folkes, L. K. and O'Neill, P. 2013. Biological consequences of radiation-induced DNA damage: relevance to radiotherapy. *Clin Oncol (R Coll Radiol)*. 25:578-585.

London, T. B., Barber, L. J., Mosedale, G., Kelly, G. P., Balasubramanian, S., Hickson, I. D., Boulton, S. J. and Hiom, K. 2008. FANCJ is a structure-specific DNA helicase associated with the maintenance of genomic G/C tracts. *J Biol Chem*. 283:36132-36139.

Long, D. T., Joukov, V., Budzowska, M. and Walter, J. C. 2014. BRCA1 promotes unloading of the CMG helicase from a stalled DNA replication fork. *Mol Cell*. 56:174-185.

Lopes, J., Piazza, A., Bermejo, R., Kriegsman, B., Colosio, A., Teulade-Fichou, M. P., Foiani, M. and Nicolas, A. 2011. G-quadruplex-induced instability during leading-strand replication. *EMBO J*. 30:4033-4046.

Lopes, M., Foiani, M. and Sogo, J. M. 2006. Multiple mechanisms control chromosome integrity after replication fork uncoupling and restart at irreparable UV lesions. *Mol Cell*. 21:15-27.

Lorenti Garcia, C., Mechilli, M., Proietti De Santis, L., Schinoppi, A., Kobos, K. and Palitti, F. 2009. Relationship between DNA lesions, DNA repair and chromosomal damage induced by acetaldehyde. *Mutat Res*. 662:3-9.

Lossaint, G., Larroque, M., Ribeyre, C., Bec, N., Larroque, C., Decaillet, C., Gari, K. and Constantinou, A. 2013. FANCD2 binds MCM proteins and controls replisome function upon activation of S phase checkpoint signaling. *Mol Cell*. 51:678-690.

Ludwig, T., Chapman, D. L., Papaioannou, V. E. and Efstratiadis, A. 1997. Targeted mutations of breast cancer susceptibility gene homologs in mice: lethal phenotypes of *Brca1*, *Brca2*, *Brca1/Brca2*, *Brca1/p53*, and *Brca2/p53* nullizygous embryos. *Genes Dev*. 11:1226-1241.

Luebben, S. W., Shima, N. and Kawabata, T. 2014. Methods for the detection of genome instability derived from replication stress in primary mouse embryonic fibroblasts. *Methods Mol Biol*. 1194:341-352.

Lukas, C., Savic, V., Bekker-Jensen, S., Doil, C., Neumann, B., Pedersen, R. S., Grofte, M., Chan, K. L., Hickson, I. D., Bartek, J. and Lukas, J. 2011. 53BP1 nuclear bodies form around DNA lesions generated by mitotic transmission of chromosomes under replication stress. *Nat Cell Biol*. 13:243-253.

Lukas, J., Lukas, C. and Bartek, J. 2004. Mammalian cell cycle checkpoints: signalling pathways and their organization in space and time. *DNA Repair (Amst)*. 3:997-1007.

Ly, D., Forman, D., Ferlay, J., Brinton, L. A. and Cook, M. B. 2013. An international comparison of male and female breast cancer incidence rates. *Int J Cancer*. 132:1918-1926.

Lydeard, J. R., Jain, S., Yamaguchi, M. and Haber, J. E. 2007. Break-induced replication and telomerase-independent telomere maintenance require Pol32. *Nature*. 448:820-823.

Lydeard, J. R., Lipkin-Moore, Z., Sheu, Y. J., Stillman, B., Burgers, P. M. and Haber, J. E. 2010. Break-induced replication requires all essential DNA replication factors except those specific for pre-RC assembly. *Genes Dev*. 24:1133-1144.

Ma, Y., Pannicke, U., Schwarz, K. and Lieber, M. R. 2002. Hairpin opening and overhang processing by an Artemis/DNA-dependent protein kinase complex in nonhomologous end joining and V(D)J recombination. *Cell*. 108:781-794.

MacDougall, C. A., Byun, T. S., Van, C., Yee, M. C. and Cimprich, K. A. 2007. The structural determinants of checkpoint activation. *Genes Dev*. 21:898-903.

Madireddy, A., Kosiyatrakul, S. T., Boisvert, R. A., Herrera-Moyano, E., Garcia-Rubio, M. L., Gerhardt, J., Vuono, E. A., Owen, N., Yan, Z., Olson, S., Aguilera, A., Howlett, N. G. and Schildkraut, C. L. 2016. FANCD2 facilitates replication through common fragile sites. *Mol Cell*. 64:388-404.

Mailand, N., Bekker-Jensen, S., Faustrup, H., Melander, F., Bartek, J., Lukas, C. and Lukas, J. 2007. RNF8 ubiquitylates histones at DNA double-strand breaks and promotes assembly of repair proteins. *Cell*. 131:887-900.

Majka, J. and Burgers, P. M. 2004. The PCNA-RFC families of DNA clamps and clamp loaders. *Prog Nucleic Acid Res Mol Biol*. 78:227-260.

Makiniemi, M., Hillukkala, T., Tuusa, J., Reini, K., Vaara, M., Huang, D., Pospiech, H., Majuri, I., Westerling, T., Makela, T. P. and Syvaoja, J. E. 2001. BRCT domain-containing protein TopBP1 functions in DNA replication and damage response. *J Biol Chem*. 276:30399-30406.

Malkova, A., Naylor, M. L., Yamaguchi, M., Ira, G. and Haber, J. E. 2005. RAD51-dependent break-induced replication differs in kinetics and checkpoint responses from RAD51-mediated gene conversion. *Mol Cell Biol*. 25:933-944.

Mankouri, H. W., Ashton, T. M. and Hickson, I. D. 2011. Holliday junction-containing DNA structures persist in cells lacking Sgs1 or Top3 following exposure to DNA damage. *Proc Natl Acad Sci U S A*. 108:4944-4949.

Mansour, W. Y., Rhein, T. and Dahm-Daphi, J. 2010. The alternative end-joining pathway for repair of DNA double-strand breaks requires PARP1 but is not dependent upon microhomologies. *Nucleic Acids Res*. 38:6065-6077.

Mardin, B. R., Drainas, A. P., Waszak, S. M., Weischenfeldt, J., Isokane, M., Stutz, A. M., Raeder, B., Efthymiopoulos, T., Buccitelli, C., Segura-Wang, M., Northcott, P., Pfister, S. M., Lichter, P., Ellenberg, J. and Korbel, J. O. 2015. A cell-based model system links chromothripsis with hyperploidy. *Mol Syst Biol*. 11:828.

Mari, P. O., Florea, B. I., Persengiev, S. P., Verkaik, N. S., Bruggenwirth, H. T., Modesti, M., Giglia-Mari, G., Bezstarosti, K., Demmers, J. A., Luider, T. M., Houtsmuller, A. B. and van Gent, D. C. 2006. Dynamic assembly of end-joining complexes requires interaction between Ku70/80 and XRCC4. *Proc Natl Acad Sci U S A*. 103:18597-18602.

Masumoto, H., Muramatsu, S., Kamimura, Y. and Araki, H. 2002. S-Cdk-dependent phosphorylation of Sld2 essential for chromosomal DNA replication in budding yeast. *Nature*. 415:651-655.

Mateos-Gomez, P. A., Gong, F., Nair, N., Miller, K. M., Lazzerini-Denchi, E. and Sfeir, A. 2015. Mammalian polymerase theta promotes alternative NHEJ and suppresses recombination. *Nature*. 518:254-257.

Matsuno, K., Kumano, M., Kubota, Y., Hashimoto, Y. and Takisawa, H. 2006. The N-terminal noncatalytic region of Xenopus RecQ4 is required for chromatin binding of DNA polymerase alpha in the initiation of DNA replication. *Mol Cell Biol*. 26:4843-4852.

Matsuoka, S., Huang, M. and Elledge, S. J. 1998. Linkage of ATM to cell cycle regulation by the Chk2 protein kinase. *Science*. 282:1893-1897.

Matsuoka, S., Rotman, G., Ogawa, A., Shiloh, Y., Tamai, K. and Elledge, S. J. 2000. Ataxia telangiectasia-mutated phosphorylates Chk2 *in vivo* and *in vitro*. *Proc Natl Acad Sci U S A*. 97:10389-10394.

Matsuzaki, K., Borel, V., Adelman, C. A., Schindler, D. and Boulton, S. J. 2015. FANCJ suppresses microsatellite instability and lymphomagenesis independent of the Fanconi anemia pathway. *Genes Dev*. 29:2532-2546.

Matulonis, U. A., Penson, R. T., Domchek, S. M., Kaufman, B., Shapira-Frommer, R., Audeh, M. W., Kaye, S., Molife, L. R., Gelmon, K. A., Robertson, J. D., Mann, H., Ho, T. W. and Coleman, R. L. 2016. Olaparib monotherapy in patients with advanced relapsed ovarian cancer and a germline *BRCA1/2* mutation: a multistudy analysis of response rates and safety. *Ann Oncol*. 27:1013-1019.

Mayle, R., Campbell, I. M., Beck, C. R., Yu, Y., Wilson, M., Shaw, C. A., Bjergbaek, L., Lupski, J. R. and Ira, G. 2015. DNA REPAIR. Mus81 and converging forks limit the mutagenicity of replication fork breakage. *Science*. 349:742-747.

Mazloum, N. and Holloman, W. K. 2009. Brh2 promotes a template-switching reaction enabling recombinational bypass of lesions during DNA synthesis. *Mol Cell*. 36:620-630.

McCabe, N., Turner, N. C., Lord, C. J., Kluzek, K., Bialkowska, A., Swift, S., Giavara, S., O'Connor, M. J., Tutt, A. N., Zdzienicka, M. Z., Smith, G. C. and Ashworth, A. 2006. Deficiency in the repair of DNA damage by homologous recombination and sensitivity to poly(ADP-ribose) polymerase inhibition. *Cancer Res*. 66:8109-8115.

McClintock, B. 1941. The stability of broken ends of chromosomes in *Zea Mays*. *Genetics*. 26:234-282.

McLuckie, K. I., Di Antonio, M., Zecchini, H., Xian, J., Caldas, C., Krippendorff, B. F., Tannahill, D., Lowe, C. and Balasubramanian, S. 2013. G-quadruplex DNA as a molecular target for induced synthetic lethality in cancer cells. *J Am Chem Soc*. 135:9640-9643.

Mechali, M. 2010. Eukaryotic DNA replication origins: many choices for appropriate answers. *Nat Rev Mol Cell Biol*. 11:728-738.

Mehta, G., Hsiao, A. Y., Ingram, M., Luker, G. D. and Takayama, S. 2012. Opportunities and challenges for use of tumor spheroids as models to test drug delivery and efficacy. *J Control Release*. 164:192-204.

Melchionna, R., Chen, X. B., Blasina, A. and McGowan, C. H. 2000. Threonine 68 is required for radiation-induced phosphorylation and activation of Cds1. *Nat Cell Biol*. 2:762-765.

Mendez, J., Zou-Yang, X. H., Kim, S. Y., Hidaka, M., Tansey, W. P. and Stillman, B. 2002. Human origin recognition complex large subunit is degraded by ubiquitin-mediated proteolysis after initiation of DNA replication. *Mol Cell*. 9:481-491.

Mergny, J. L., De Cian, A., Ghelab, A., Sacca, B. and Lacroix, L. 2005. Kinetics of tetramolecular quadruplexes. *Nucleic Acids Res*. 33:81-94.

Meselson, M. and Stahl, F. W. 1958. The replication of DNA in *Escherichia coli*. *Proc Natl Acad Sci U S A*. 44:671-682.

Michel, L. S., Liberal, V., Chatterjee, A., Kirchwegger, R., Pasche, B., Gerald, W., Dobles, M., Sorger, P. K., Murty, V. V. and Benezra, R. 2001. MAD2 haplo-insufficiency causes premature anaphase and chromosome instability in mammalian cells. *Nature*. 409:355-359.

Michl, J., Zimmer, J., Buffa, F. M., McDermott, U. and Tarsounas, M. 2016a. FANCD2 limits replication stress and genome instability in cells lacking BRCA2. *Nat Struct Mol Biol*. 23:755-757.

Michl, J., Zimmer, J. and Tarsounas, M. 2016b. Interplay between Fanconi anemia and homologous recombination pathways in genome integrity. *EMBO J*. 35:909-923.

Miki, Y., Swensen, J., Shattuck-Eidens, D., Futreal, P. A., Harshman, K., Tavtigian, S., Liu, Q., Cochran, C., Bennett, L. M., Ding, W. and et al. 1994. A strong candidate for the breast and ovarian cancer susceptibility gene *BRCA1*. *Science*. 266:66-71.

Miles, J. A., Frost, M. G., Carroll, E., Rowe, M. L., Howard, M. J., Sidhu, A., Chaugule, V. K., Alpi, A. F. and Walden, H. 2015. The Fanconi anemia DNA repair pathway is regulated by an interaction between ubiquitin and the E2-like fold domain of FANCL. *J Biol Chem*. 290:20995-21006.

Minocherhomji, S., Ying, S., Bjerregaard, V. A., Bursomanno, S., Aleliunaite, A., Wu, W., Mankouri, H. W., Shen, H., Liu, Y. and Hickson, I. D. 2015. Replication stress activates DNA repair synthesis in mitosis. *Nature*. 528:286-290.

Mohaghegh, P., Karow, J. K., Brosh, R. M., Jr., Bohr, V. A. and Hickson, I. D. 2001. The Bloom's and Werner's syndrome proteins are DNA structure-specific helicases. *Nucleic Acids Res*. 29:2843-2849.

Motegi, A., Liaw, H. J., Lee, K. Y., Roest, H. P., Maas, A., Wu, X., Moinova, H., Markowitz, S. D., Ding, H., Hoeijmakers, J. H. and Myung, K. 2008. Polyubiquitination of proliferating cell nuclear antigen by HLTF and SHPRH prevents genomic instability from stalled replication forks. *Proc Natl Acad Sci U S A*. 105:12411-12416.

Motegi, A., Sood, R., Moinova, H., Markowitz, S. D., Liu, P. P. and Myung, K. 2006. Human SHPRH suppresses genomic instability through proliferating cell nuclear antigen polyubiquitination. *J Cell Biol*. 175:703-708.

Motycka, T. A., Bessho, T., Post, S. M., Sung, P. and Tomkinson, A. E. 2004. Physical and functional interaction between the XPF/ERCC1 endonuclease and hRad52. *J Biol Chem*. 279:13634-13639.

Mouron, S., Rodriguez-Acebes, S., Martinez-Jimenez, M. I., Garcia-Gomez, S., Chocron, S., Blanco, L. and Mendez, J. 2013. Repriming of DNA synthesis at stalled replication forks by human PrimPol. *Nat Struct Mol Biol*. 20:1383-1389.

Moyer, S. E., Lewis, P. W. and Botchan, M. R. 2006. Isolation of the Cdc45/Mcm2-7/GINS (CMG) complex, a candidate for the eukaryotic DNA replication fork helicase. *Proc Natl Acad Sci U S A*. 103:10236-10241.

Moynahan, M. E., Pierce, A. J. and Jasin, M. 2001. BRCA2 is required for homology-directed repair of chromosomal breaks. *Mol Cell*. 7:263-272.

Muller, S., Kumari, S., Rodriguez, R. and Balasubramanian, S. 2010. Small-molecule-mediated G-quadruplex isolation from human cells. *Nat Chem*. 2:1095-1098.

Narayanan, V., Mieczkowski, P. A., Kim, H. M., Petes, T. D. and Lobachev, K. S. 2006. The pattern of gene amplification is determined by the chromosomal location of hairpin-capped breaks. *Cell*. 125:1283-1296.

Nazarali, S. A. and Narod, S. A. 2014. Tamoxifen for women at high risk of breast cancer. *Breast Cancer (Dove Med Press)*. 6:29-36.

Neelsen, K. J. and Lopes, M. 2015. Replication fork reversal in eukaryotes: from dead end to dynamic response. *Nat Rev Mol Cell Biol*. 16:207-220.

Neelsen, K. J., Zanini, I. M., Mijic, S., Herrador, R., Zellweger, R., Ray Chaudhuri, A., Creavin, K. D., Blow, J. J. and Lopes, M. 2013. Deregulated origin licensing leads to chromosomal breaks by rereplication of a gapped DNA template. *Genes Dev*. 27:2537-2542.

Negrini, S., Gorgoulis, V. G. and Halazonetis, T. D. 2010. Genomic instability--an evolving hallmark of cancer. *Nat Rev Mol Cell Biol*. 11:220-228.

Newman, B., Millikan, R. C. and King, M. C. 1997. Genetic epidemiology of breast and ovarian cancers. *Epidemiol Rev*. 19:69-79.

Nguyen, V. Q., Co, C., Irie, K. and Li, J. J. 2000. Clb/Cdc28 kinases promote nuclear export of the replication initiator proteins Mcm2-7. *Curr Biol*. 10:195-205.

Nick McElhinny, S. A., Gordenin, D. A., Stith, C. M., Burgers, P. M. and Kunkel, T. A. 2008. Division of labor at the eukaryotic replication fork. *Mol Cell*. 30:137-144.

Nicum, S., Roberts, C., Boyle, L., Kopijasz, S., Gourley, C., Hall, M., Montes, A., Poole, C., Collins, L., Schuh, A., Dutton, S. J. and Group, M. P. C. 2014. A phase II clinical trial of 6-mercaptopurine (6MP) and methotrexate in patients with BRCA defective tumours: a study protocol. *BMC Cancer*. 14:983.

Nielsen, F. C., van Overeem Hansen, T. and Sorensen, C. S. 2016. Hereditary breast and ovarian cancer: new genes in confined pathways. *Nat Rev Cancer*. 16:599-612.

Nimonkar, A. V., Genschel, J., Kinoshita, E., Polaczek, P., Campbell, J. L., Wyman, C., Modrich, P. and Kowalczykowski, S. C. 2011. BLM-DNA2-RPA-MRN and EXO1-BLM-RPA-MRN constitute two DNA end resection machineries for human DNA break repair. *Genes Dev*. 25:350-362.

Nimonkar, A. V., Ozsoy, A. Z., Genschel, J., Modrich, P. and Kowalczykowski, S. C. 2008. Human exonuclease 1 and BLM helicase interact to resect DNA and initiate DNA repair. *Proc Natl Acad Sci U S A*. 105:16906-16911.

Nishitani, H., Sugimoto, N., Roukos, V., Nakanishi, Y., Saijo, M., Obuse, C., Tsurimoto, T., Nakayama, K. I., Nakayama, K., Fujita, M., Lygerou, Z. and Nishimoto, T. 2006. Two E3 ubiquitin ligases, SCF-Skp2 and DDB1-Cul4, target human Cdt1 for proteolysis. *EMBO J*. 25:1126-1136.

Norquist, B., Wurz, K. A., Pennil, C. C., Garcia, R., Gross, J., Sakai, W., Karlan, B. Y., Taniguchi, T. and Swisher, E. M. 2011. Secondary somatic mutations restoring *BRCA1/2* predict chemotherapy resistance in hereditary ovarian carcinomas. *J Clin Oncol*. 29:3008-3015.

Nowell, P. C. 1976. The clonal evolution of tumor cell populations. *Science*. 194:23-28.

O'Sullivan, J. N., Bronner, M. P., Brentnall, T. A., Finley, J. C., Shen, W. T., Emerson, S., Emond, M. J., Gollahon, K. A., Moskovitz, A. H., Crispin, D. A., Potter, J. D. and Rabinovitch, P. S. 2002. Chromosomal instability in ulcerative colitis is related to telomere shortening. *Nat Genet*. 32:280-284.

Ochs, F., Somyajit, K., Altmeyer, M., Rask, M. B., Lukas, J. and Lukas, C. 2016. 53BP1 fosters fidelity of homology-directed DNA repair. *Nat Struct Mol Biol*. 23:714-721.

Okazaki, R., Okazaki, T., Sakabe, K., Sugimoto, K., Kainuma, R., Sugino, A. and Iwatsuki, N. 1968. *In vivo* mechanism of DNA chain growth. *Cold Spring Harb Symp Quant Biol*. 33:129-143.

Osher, D. J., Kushner, Y. B., Arseneau, J. and Foulkes, W. D. 2011. Melphalan as a treatment for *BRCA*-related ovarian carcinoma: can you teach an old drug new tricks? *J Clin Pathol*. 64:924-926.

Pabla, N., Huang, S., Mi, Q. S., Daniel, R. and Dong, Z. 2008. ATR-Chk2 signaling in p53 activation and DNA damage response during cisplatin-induced apoptosis. *J Biol Chem*. 283:6572-6583.

Pacek, M. and Walter, J. C. 2004. A requirement for MCM7 and Cdc45 in chromosome unwinding during eukaryotic DNA replication. *EMBO J*. 23:3667-3676.

Paeschke, K., Bochman, M. L., Garcia, P. D., Cejka, P., Friedman, K. L., Kowalczykowski, S. C. and Zakian, V. A. 2013. Pif1 family helicases suppress genome instability at G-quadruplex motifs. *Nature*. 497:458-462.

Paeschke, K., Capra, J. A. and Zakian, V. A. 2011. DNA replication through G-quadruplex motifs is promoted by the *Saccharomyces cerevisiae* Pif1 DNA helicase. *Cell*. 145:678-691.

Pagano, G., d'Ischia, M. and Pallardo, F. V. 2015. Fanconi anemia (FA) and crosslinker sensitivity: Re-appraising the origins of FA definition. *Pediatr Blood Cancer*. 62:1137-1143.

Palm, W. and de Lange, T. 2008. How shelterin protects mammalian telomeres. *Annu Rev Genet*. 42:301-334.

Palumbo, M. O., Kavan, P., Miller, W. H., Jr., Panasci, L., Assouline, S., Johnson, N., Cohen, V., Patenaude, F., Pollak, M., Jagoe, R. T. and Batist, G. 2013. Systemic cancer therapy: achievements and challenges that lie ahead. *Front Pharmacol*. 4:57.

Paques, F. and Haber, J. E. 1999. Multiple pathways of recombination induced by double-strand breaks in *Saccharomyces cerevisiae*. *Microbiol Mol Biol Rev*. 63:349-404.

Parkinson, G. N., Lee, M. P. and Neidle, S. 2002. Crystal structure of parallel quadruplexes from human telomeric DNA. *Nature*. 417:876-880.

Parsons, J. L., Tait, P. S., Finch, D., Dianova, II, Edelmann, M. J., Khoronenkova, S. V., Kessler, B. M., Sharma, R. A., McKenna, W. G. and Dianov, G. L. 2009. Ubiquitin ligase ARF-BP1/Mule modulates base excision repair. *EMBO J*. 28:3207-3215.

Patch, A. M., Christie, E. L., Etemadmoghadam, D., Garsed, D. W., George, J., Fereday, S., Nones, K., Cowin, P., Alsop, K., Bailey, P. J., Kassahn, K. S., Newell, F., Quinn, M. C., Kazakoff, S., Quek, K., Wilhelm-Benartzi, C., Curry, E., Leong, H. S., Australian Ovarian Cancer Study, G., Hamilton, A., Mileshkin, L., Au-Yeung, G., Kennedy, C., Hung, J., Chiew, Y. E., Harnett, P., Friedlander, M., Quinn, M., Pyman, J., Cordner, S., O'Brien, P., Leditschke, J., Young, G., Strachan, K., Waring, P., Azar, W., Mitchell, C., Traficante, N., Hendley, J., Thorne, H., Shackleton, M., Miller, D. K., Arnau, G. M., Tothill, R. W., Holloway, T. P., Semple, T., Harliwong, I., Nourse, C., Nourbakhsh, E., Manning, S., Idrisoglu, S., Bruxner, T. J., Christ, A. N., Poudel, B., Holmes, O., Anderson, M., Leonard, C., Lonie, A., Hall, N., Wood, S., Taylor, D. F., Xu, Q., Fink, J. L., Waddell, N., Drapkin, R., Stronach, E., Gabra, H., Brown, R., Jewell, A., Nagaraj, S. H., Markham, E., Wilson, P. J., Ellul, J., McNally, O., Doyle, M. A., Vedururu, R., Stewart, C., Lengyel, E., Pearson, J. V., Waddell, N., deFazio, A., Grimmond, S. M. and Bowtell, D. D. 2015. Whole-genome characterization of chemoresistant ovarian cancer. *Nature*. 521:489-494.

Patel, D. J., Phan, A. T. and Kuryavyi, V. 2007. Human telomere, oncogenic promoter and 5'-UTR G-quadruplexes: diverse higher order DNA and RNA targets for cancer therapeutics. *Nucleic Acids Res*. 35:7429-7455.

Patel, K. J., Yu, V. P., Lee, H., Corcoran, A., Thistlethwaite, F. C., Evans, M. J., Colledge, W. H., Friedman, L. S., Ponder, B. A. and Venkitaraman, A. R. 1998. Involvement of Brca2 in DNA repair. *Mol Cell*. 1:347-357.

Paul, K., Wang, M., Mladenov, E., Bencsik-Theilen, A., Bednar, T., Wu, W., Arakawa, H. and Iliakis, G. 2013. DNA ligases I and III cooperate in alternative non-homologous end-joining in vertebrates. *PloS One*. 8:e59505.

Paull, T. T. and Gellert, M. 1998. The 3' to 5' exonuclease activity of Mre 11 facilitates repair of DNA double-strand breaks. *Mol Cell*. 1:969-979.

Peng, C. Y., Graves, P. R., Thoma, R. S., Wu, Z., Shaw, A. S. and Piwnica-Worms, H. 1997. Mitotic and G2 checkpoint control: regulation of 14-3-3 protein binding by phosphorylation of Cdc25C on serine-216. *Science*. 277:1501-1505.

Petermann, E. and Helleday, T. 2010a. Pathways of mammalian replication fork restart. *Nat Rev Mol Cell Biol*. 11:683-687.

Petermann, E., Orta, M. L., Issaeva, N., Schultz, N. and Helleday, T. 2010b. Hydroxyurea-stalled replication forks become progressively inactivated and require two different RAD51-mediated pathways for restart and repair. *Mol Cell*. 37:492-502.

Petersen, B. O., Lukas, J., Sorensen, C. S., Bartek, J. and Helin, K. 1999. Phosphorylation of mammalian CDC6 by cyclin A/CDK2 regulates its subcellular localization. *EMBO J*. 18:396-410.

Peto, J., Collins, N., Barfoot, R., Seal, S., Warren, W., Rahman, N., Easton, D. F., Evans, C., Deacon, J. and Stratton, M. R. 1999. Prevalence of *BRCA1* and *BRCA2* gene mutations in patients with early-onset breast cancer. *J Natl Cancer Inst*. 91:943-949.

Phillips, D. H. 1996. DNA adducts in human tissues: biomarkers of exposure to carcinogens in tobacco smoke. *Environ Health Perspect*. 104 Suppl 3:453-458.

Phillips, K. A., Nichol, K., Ozcelik, H., Knight, J., Done, S. J., Goodwin, P. J. and Andrulis, I. L. 1999. Frequency of *p53* mutations in breast carcinomas from Ashkenazi Jewish carriers of *BRCA1* mutations. *J Natl Cancer Inst*. 91:469-473.

Phuah, S. Y., Looi, L. M., Hassan, N., Rhodes, A., Dean, S., Taib, N. A., Yip, C. H. and Teo, S. H. 2012. Triple-negative breast cancer and PTEN (phosphatase and tensin homologue) loss are predictors of *BRCA1* germline mutations in women with early-onset and familial breast cancer, but not in women with isolated late-onset breast cancer. *Breast Cancer Res*. 14:R142.

Piazza, A., Boule, J. B., Lopes, J., Mingo, K., Largy, E., Teulade-Fichou, M. P. and Nicolas, A. 2010. Genetic instability triggered by G-quadruplex interacting Phen-DC compounds in *Saccharomyces cerevisiae*. *Nucleic Acids Res*. 38:4337-4348.

Pizot, C., Boniol, M., Mullie, P., Koechlin, A., Boniol, M., Boyle, P. and Autier, P. 2016. Physical activity, hormone replacement therapy and breast cancer risk: A meta-analysis of prospective studies. *Eur J Cancer*. 52:138-154.

Pizzolato, J., Mukherjee, S., Scharer, O. D. and Jiricny, J. 2015. FANCD2-associated nuclease 1, but not exonuclease 1 or flap endonuclease 1, is able to unhook DNA interstrand cross-links *in vitro*. *J Biol Chem*. 290:22602-22611.

Povirk, L. F., Zhou, T., Zhou, R., Cowan, M. J. and Yannone, S. M. 2007. Processing of 3'-phosphoglycolate-terminated DNA double strand breaks by Artemis nuclease. *J Biol Chem*. 282:3547-3558.

Prasanth, S. G., Prasanth, K. V. and Stillman, B. 2002. Orc6 involved in DNA replication, chromosome segregation, and cytokinesis. *Science*. 297:1026-1031.

Pursell, Z. F., Isoz, I., Lundstrom, E. B., Johansson, E. and Kunkel, T. A. 2007. Yeast DNA polymerase epsilon participates in leading-strand DNA replication. *Science*. 317:127-130.

Raghunandan, M., Chaudhury, I., Kelich, S. L., Hanenberg, H. and Sobeck, A. 2015. FANCD2, FANCJ and BRCA2 cooperate to promote replication fork recovery independently of the Fanconi Anemia core complex. *Cell Cycle*. 14:342-353.

Ralf, C., Hickson, I. D. and Wu, L. 2006. The Bloom's syndrome helicase can promote the regression of a model replication fork. *J Biol Chem*. 281:22839-22846.

Ramus, S. J., Bobrow, L. G., Pharoah, P. D., Finnigan, D. S., Fishman, A., Altaras, M., Harrington, P. A., Gayther, S. A., Ponder, B. A. and Friedman, L. S. 1999. Increased frequency of *TP53* mutations in *BRCA1* and *BRCA2* ovarian tumours. *Genes Chromosomes Cancer*. 25:91-96.

Rao, C. V., Yang, Y. M., Swamy, M. V., Liu, T., Fang, Y., Mahmood, R., Jhanwar-Uniyal, M. and Dai, W. 2005. Colonic tumorigenesis in *BubR1+/-ApcMin/+* compound mutant mice is linked to premature separation of sister chromatids and enhanced genomic instability. *Proc Natl Acad Sci U S A*. 102:4365-4370.

Rass, E., Grabarz, A., Plo, I., Gautier, J., Bertrand, P. and Lopez, B. S. 2009. Role of Mre11 in chromosomal nonhomologous end joining in mammalian cells. *Nat Struct Mol Biol*. 16:819-824.

Rass, U., Compton, S. A., Matos, J., Singleton, M. R., Ip, S. C., Blanco, M. G., Griffith, J. D. and West, S. C. 2010. Mechanism of Holliday junction resolution by the human GEN1 protein. *Genes Dev*. 24:1559-1569.

Ray Chaudhuri, A., Callen, E., Ding, X., Gogola, E., Duarte, A. A., Lee, J. E., Wong, N., Lafarga, V., Calvo, J. A., Panzarino, N. J., John, S., Day, A., Crespo, A. V., Shen, B., Starnes, L. M., de Ruiter, J. R., Daniel, J. A., Konstantinopoulos, P. A., Cortez, D., Cantor, S. B., Fernandez-Capetillo, O., Ge, K., Jonkers, J., Rottenberg, S., Sharan, S. K. and Nussenzweig, A. 2016. Replication fork stability confers chemoresistance in BRCA-deficient cells. *Nature*. 535:382-387.

Ray Chaudhuri, A., Hashimoto, Y., Herrador, R., Neelsen, K. J., Fachinetti, D., Bermejo, R., Cocito, A., Costanzo, V. and Lopes, M. 2012. Topoisomerase I poisoning results in PARP-mediated replication fork reversal. *Nat Struct Mol Biol*. 19:417-423.

Remus, D., Beuron, F., Tolun, G., Griffith, J. D., Morris, E. P. and Diffley, J. F. 2009. Concerted loading of Mcm2-7 double hexamers around DNA during DNA replication origin licensing. *Cell*. 139:719-730.

Ribeyre, C., Lopes, J., Boule, J. B., Piazza, A., Guedin, A., Zakian, V. A., Mergny, J. L. and Nicolas, A. 2009. The yeast Pif1 helicase prevents genomic instability caused by G-quadruplex-forming CEB1 sequences *in vivo*. *PLoS Genet*. 5:e1000475.

Rice, J. A., Crothers, D. M., Pinto, A. L. and Lippard, S. J. 1988. The major adduct of the antitumor drug cis-diamminedichloroplatinum(II) with DNA bends the duplex by approximately equal to 40 degrees toward the major groove. *Proc Natl Acad Sci U S A*. 85:4158-4161.

Rickman, K. A., Lach, F. P., Abhyankar, A., Donovan, F. X., Sanborn, E. M., Kennedy, J. A., Sougnez, C., Gabriel, S. B., Elemento, O., Chandrasekharappa, S. C., Schindler, D., Auerbach, A. D. and Smogorzewska, A. 2015. Deficiency of UBE2T, the E2 ubiquitin ligase necessary for FANCD2 and FANCI ubiquitination, causes FA-T subtype of Fanconi anemia. *Cell Rep*. 12:35-41.

Rigakos, G. and Razis, E. 2012. BRCAness: finding the Achilles heel in ovarian cancer. *Oncologist*. 17:956-962.

Risitano, A. and Fox, K. R. 2004. Influence of loop size on the stability of intramolecular DNA quadruplexes. *Nucleic Acids Res*. 32:2598-2606.

Ritte, R., Lukanova, A., Berrino, F., Dossus, L., Tjonneland, A., Olsen, A., Overvad, T. F., Overvad, K., Clavel-Chapelon, F., Fournier, A., Fagherazzi, G., Rohrmann, S., Teucher, B., Boeing, H., Aleksandrova, K., Trichopoulou, A., Lagiou, P., Trichopoulos, D., Palli, D., Sieri, S., Panico, S., Tumino, R., Vineis, P., Quiros, J. R., Buckland, G., Sanchez, M. J., Amiano, P., Chirlaque, M. D., Ardanaz, E., Sund, M., Lenner, P., Bueno-de-Mesquita, B., van Gils, C. H., Peeters, P. H., Krum-Hansen, S., Gram, I. T., Lund, E., Khaw, K. T., Wareham, N., Allen, N. E., Key, T. J., Romieu, I., Rinaldi, S., Siddiq, A., Cox, D., Riboli, E. and Kaaks, R. 2012. Adiposity, hormone replacement therapy use and breast cancer risk by age and hormone receptor status: a large prospective cohort study. *Breast Cancer Res*. 14:R76.

Rodriguez, R., Miller, K. M., Forment, J. V., Bradshaw, C. R., Nikan, M., Britton, S., Oelschlaegel, T., Xhemalce, B., Balasubramanian, S. and Jackson, S. P. 2012. Small-molecule-induced DNA damage identifies alternative DNA structures in human genes. *Nat Chem Biol*. 8:301-310.

Rodriguez, R., Muller, S., Yeoman, J. A., Trentesaux, C., Riou, J. F. and Balasubramanian, S. 2008. A novel small molecule that alters shelterin integrity and triggers a DNA-damage response at telomeres. *J Am Chem Soc*. 130:15758-15759.

Roerink, S. F., van Schendel, R. and Tijsterman, M. 2014. Polymerase theta-mediated end joining of replication-associated DNA breaks in *C. elegans*. *Genome Res*. 24:954-962.

Rogakou, E. P., Boon, C., Redon, C. and Bonner, W. M. 1999. Megabase chromatin domains involved in DNA double-strand breaks *in vivo*. *J Cell Biol*. 146:905-916.

Rogakou, E. P., Pilch, D. R., Orr, A. H., Ivanova, V. S. and Bonner, W. M. 1998. DNA double-stranded breaks induce histone H2AX phosphorylation on serine 139. *J Biol Chem*. 273:5858-5868.

Rosenberg, P. S., Greene, M. H. and Alter, B. P. 2003. Cancer incidence in persons with Fanconi anemia. *Blood*. 101:822-826.

Rothenberg, E., Grimme, J. M., Spies, M. and Ha, T. 2008. Human Rad52-mediated homology search and annealing occurs by continuous interactions between overlapping nucleoprotein complexes. *Proc Natl Acad Sci U S A*. 105:20274-20279.

Rottenberg, S., Jaspers, J. E., Kersbergen, A., van der Burg, E., Nygren, A. O., Zander, S. A., Derksen, P. W., de Bruin, M., Zevenhoven, J., Lau, A., Boulter, R., Cranston, A., O'Connor, M. J., Martin, N. M., Borst, P. and Jonkers, J. 2008. High sensitivity of BRCA1-deficient mammary tumors to the PARP inhibitor AZD2281 alone and in combination with platinum drugs. *Proc Natl Acad Sci U S A*. 105:17079-17084.

Roumelioti, F. M., Sotiriou, S. K., Katsini, V., Chiourea, M., Halazonetis, T. D. and Gagos, S. 2016. Alternative lengthening of human telomeres is a conservative DNA replication process with features of break-induced replication. *EMBO Rep*. 17:1731-1737.

Roy, R., Chun, J. and Powell, S. N. 2012. BRCA1 and BRCA2: different roles in a common pathway of genome protection. *Nat Rev Cancer*. 12:68-78.

Rudd, G. N., Hartley, J. A. and Souhami, R. L. 1995. Persistence of cisplatin-induced DNA interstrand crosslinking in peripheral blood mononuclear cells from elderly and young individuals. *Cancer Chemother Pharmacol*. 35:323-326.

Rudolph, K. L., Millard, M., Bosenberg, M. W. and DePinho, R. A. 2001. Telomere dysfunction and evolution of intestinal carcinoma in mice and humans. *Nat Genet*. 28:155-159.

Saini, N., Ramakrishnan, S., Elango, R., Ayyar, S., Zhang, Y., Deem, A., Ira, G., Haber, J. E., Lobachev, K. S. and Malkova, A. 2013. Migrating bubble during break-induced replication drives conservative DNA synthesis. *Nature*. 502:389-392.

Sakai, W., Swisher, E. M., Jacquemont, C., Chandramohan, K. V., Couch, F. J., Langdon, S. P., Wurz, K., Higgins, J., Villegas, E. and Taniguchi, T. 2009. Functional restoration of BRCA2 protein by secondary *BRCA2* mutations in *BRCA2*-mutated ovarian carcinoma. *Cancer Res*. 69:6381-6386.

Sakai, W., Swisher, E. M., Karlan, B. Y., Agarwal, M. K., Higgins, J., Friedman, C., Villegas, E., Jacquemont, C., Farrugia, D. J., Couch, F. J., Urban, N. and Taniguchi, T. 2008. Secondary mutations as a mechanism of cisplatin resistance in *BRCA2*-mutated cancers. *Nature*. 451:1116-1120.

Sakofsky, C. J., Roberts, S. A., Malc, E., Mieczkowski, P. A., Resnick, M. A., Gordenin, D. A. and Malkova, A. 2014. Break-induced replication is a source of mutation clusters underlying kataegis. *Cell Rep*. 7:1640-1648.

Saleh-Gohari, N., Bryant, H. E., Schultz, N., Parker, K. M., Cassel, T. N. and Helleday, T. 2005. Spontaneous homologous recombination is induced by collapsed replication forks that are caused by endogenous DNA single-strand breaks. *Mol Cell Biol*. 25:7158-7169.

Salvati, E., Leonetti, C., Rizzo, A., Scarsella, M., Mottolese, M., Galati, R., Sperduti, I., Stevens, M. F., D'Incalci, M., Blasco, M., Chiorino, G., Bauwens, S., Horard, B., Gilson, E., Stoppacciaro, A., Zupi, G. and Biroccio, A. 2007. Telomere damage induced by the G-quadruplex ligand RHPS4 has an antitumor effect. *J Clin Invest*. 117:3236-3247.

Sanchez, Y., Wong, C., Thoma, R. S., Richman, R., Wu, Z., Piwnica-Worms, H. and Elledge, S. J. 1997. Conservation of the Chk1 checkpoint pathway in mammals: linkage of DNA damage to Cdk regulation through Cdc25. *Science*. 277:1497-1501.

Sanders, C. M. 2010. Human Pif1 helicase is a G-quadruplex DNA-binding protein with G-quadruplex DNA-unwinding activity. *Biochem J*. 430:119-128.

Sareen, A., Chaudhury, I., Adams, N. and Sobeck, A. 2012. Fanconi anemia proteins FANCD2 and FANCI exhibit different DNA damage responses during S-phase. *Nucleic Acids Res*. 40:8425-8439.

Sarkar, S., Davies, A. A., Ulrich, H. D. and McHugh, P. J. 2006. DNA interstrand crosslink repair during G1 involves nucleotide excision repair and DNA polymerase zeta. *EMBO J*. 25:1285-1294.

Sarkies, P., Murat, P., Phillips, L. G., Patel, K. J., Balasubramanian, S. and Sale, J. E. 2012. FANCJ coordinates two pathways that maintain epigenetic stability at G-quadruplex DNA. *Nucleic Acids Res*. 40:1485-1498.

Sarkies, P., Reams, C., Simpson, L. J. and Sale, J. E. 2010. Epigenetic instability due to defective replication of structured DNA. *Mol Cell*. 40:703-713.

Sartori, A. A., Lukas, C., Coates, J., Mistrik, M., Fu, S., Bartek, J., Baer, R., Lukas, J. and Jackson, S. P. 2007. Human CtIP promotes DNA end resection. *Nature*. 450:509-514.

Sasaki, M. S. and Tonomura, A. 1973. A high susceptibility of Fanconi's anemia to chromosome breakage by DNA cross-linking agents. *Cancer Res*. 33:1829-1836.

Satoh, M. S. and Lindahl, T. 1992. Role of poly(ADP-ribose) formation in DNA repair. *Nature*. 356:356-358.

Sawyer, S. L., Tian, L., Kahkonen, M., Schwartzentruber, J., Kircher, M., University of Washington Centre for Mendelian, G., Consortium, F. C., Majewski, J., Dyment, D. A.,

Innes, A. M., Boycott, K. M., Moreau, L. A., Moilanen, J. S. and Greenberg, R. A. 2015. Biallelic mutations in *BRCA1* cause a new Fanconi anemia subtype. *Cancer Discov*. 5:135-142.

Schaffitzel, C., Berger, I., Postberg, J., Hanes, J., Lipps, H. J. and Pluckthun, A. 2001. *In vitro* generated antibodies specific for telomeric guanine-quadruplex DNA react with *Stylonychia lemnae* macronuclei. *Proc Natl Acad Sci U S A*. 98:8572-8577.

Schiavone, D., Jozwiakowski, S. K., Romanello, M., Guilbaud, G., Guilliam, T. A., Bailey, L. J., Sale, J. E. and Doherty, A. J. 2016. PrimPol is required for replicative tolerance of G quadruplexes in vertebrate cells. *Mol Cell*. 61:161-169.

Schlacher, K., Christ, N., Siaud, N., Egashira, A., Wu, H. and Jasin, M. 2011. Double-strand break repair-independent role for BRCA2 in blocking stalled replication fork degradation by MRE11. *Cell*. 145:529-542.

Schlacher, K., Wu, H. and Jasin, M. 2012. A distinct replication fork protection pathway connects Fanconi anemia tumor suppressors to RAD51-BRCA1/2. *Cancer Cell*. 22:106-116.

Schneider, B. P., Winer, E. P., Foulkes, W. D., Garber, J., Perou, C. M., Richardson, A., Sledge, G. W. and Carey, L. A. 2008. Triple-negative breast cancer: risk factors to potential targets. *Clin Cancer Res*. 14:8010-8018.

Scully, R. and Livingston, D. M. 2000. In search of the tumour-suppressor functions of BRCA1 and BRCA2. *Nature*. 408:429-432.

Sen, D. and Gilbert, W. 1988. Formation of parallel four-stranded complexes by guanine-rich motifs in DNA and its implications for meiosis. *Nature*. 334:364-366.

Shah, R., Rosso, K. and Nathanson, S. D. 2014. Pathogenesis, prevention, diagnosis and treatment of breast cancer. *World J Clin Oncol*. 5:283-298.

Sharan, S. K., Morimatsu, M., Albrecht, U., Lim, D. S., Regel, E., Dinh, C., Sands, A., Eichele, G., Hasty, P. and Bradley, A. 1997. Embryonic lethality and radiation hypersensitivity mediated by Rad51 in mice lacking *Brca2*. *Nature*. 386:804-810.

Sheu, Y. J. and Stillman, B. 2006. Cdc7-Dbf4 phosphorylates MCM proteins via a docking site-mediated mechanism to promote S phase progression. *Mol Cell*. 24:101-113.

Sheu, Y. J. and Stillman, B. 2010. The Dbf4-Cdc7 kinase promotes S phase by alleviating an inhibitory activity in Mcm4. *Nature*. 463:113-117.

Shibata, A., Conrad, S., Birraux, J., Geuting, V., Barton, O., Ismail, A., Kakarougkas, A., Meek, K., Taucher-Scholz, G., Lobrich, M. and Jeggo, P. A. 2011. Factors determining DNA double-strand break repair pathway choice in G2 phase. *EMBO J*. 30:1079-1092.

Shibata, A., Moiani, D., Arvai, A. S., Perry, J., Harding, S. M., Genois, M. M., Maity, R., van Rossum-Fikkert, S., Kertokalio, A., Romoli, F., Ismail, A., Ismalaj, E., Petricci, E., Neale, M. J., Bristow, R. G., Masson, J. Y., Wyman, C., Jeggo, P. A. and Tainer, J. A. 2014. DNA double-strand break repair pathway choice is directed by distinct MRE11 nuclease activities. *Mol Cell*. 53:7-18.

Siddiqui, K. and Stillman, B. 2007. ATP-dependent assembly of the human origin recognition complex. *J Biol Chem*. 282:32370-32383.

Siddiqui-Jain, A., Grand, C. L., Bearss, D. J. and Hurley, L. H. 2002. Direct evidence for a G-quadruplex in a promoter region and its targeting with a small molecule to repress *c-MYC* transcription. *Proc Natl Acad Sci U S A*. 99:11593-11598.

Siegel, R. L., Miller, K. D. and Jemal, A. 2016. Cancer statistics, 2016. *CA Cancer J Clin*. 66:7-30.

Simsek, D. and Jasin, M. 2010. Alternative end-joining is suppressed by the canonical NHEJ component Xrcc4-ligase IV during chromosomal translocation formation. *Nat Struct Mol Biol*. 17:410-416.

Skoulidis, F., Cassidy, L. D., Pisupati, V., Jonasson, J. G., Bjarnason, H., Eyfjord, J. E., Karreth, F. A., Lim, M., Barber, L. M., Clatworthy, S. A., Davies, S. E., Olive, K. P., Tuveson, D. A. and Venkitaraman, A. R. 2010. Germline *Brca2* heterozygosity promotes *Kras(G12D)*-driven carcinogenesis in a murine model of familial pancreatic cancer. *Cancer Cell*. 18:499-509.

Smith, C. E., Lam, A. F. and Symington, L. S. 2009. Aberrant double-strand break repair resulting in half crossovers in mutants defective for Rad51 or the DNA polymerase delta complex. *Mol Cell Biol*. 29:1432-1441.

Smith, C. E., Llorente, B. and Symington, L. S. 2007. Template switching during break-induced replication. *Nature*. 447:102-105.

Sorensen, C. S., Syljuasen, R. G., Falck, J., Schroeder, T., Ronnstrand, L., Khanna, K. K., Zhou, B. B., Bartek, J. and Lukas, J. 2003. Chk1 regulates the S phase checkpoint by coupling the physiological turnover and ionizing radiation-induced accelerated proteolysis of Cdc25A. *Cancer Cell*. 3:247-258.

Sorlie, T., Perou, C. M., Tibshirani, R., Aas, T., Geisler, S., Johnsen, H., Hastie, T., Eisen, M. B., van de Rijn, M., Jeffrey, S. S., Thorsen, T., Quist, H., Matese, J. C., Brown, P. O., Botstein, D., Lonning, P. E. and Borresen-Dale, A. L. 2001. Gene expression patterns of breast carcinomas distinguish tumor subclasses with clinical implications. *Proc Natl Acad Sci U S A*. 98:10869-10874.

Sotiriou, S. K., Kamileri, I., Lugli, N., Evangelou, K., Da-Re, C., Huber, F., Padayachy, L., Tardy, S., Nicati, N. L., Barriot, S., Ochs, F., Lukas, C., Lukas, J., Gorgoulis, V. G., Scapozza, L. and Halazonetis, T. D. 2016. Mammalian RAD52 functions in break-induced replication repair of collapsed DNA replication forks. *Mol Cell*. 64:1127-1134.

Stelter, P. and Ulrich, H. D. 2003. Control of spontaneous and damage-induced mutagenesis by SUMO and ubiquitin conjugation. *Nature*. 425:188-191.

Stewart, G. S., Panier, S., Townsend, K., Al-Hakim, A. K., Kolas, N. K., Miller, E. S., Nakada, S., Ylanko, J., Olivarius, S., Mendez, M., Oldreive, C., Wildenhain, J., Tagliaferro, A., Pelletier, L., Taubenheim, N., Durandy, A., Byrd, P. J., Stankovic, T., Taylor, A. M. and Durocher, D. 2009. The RIDDLE syndrome protein mediates a ubiquitin-dependent signaling cascade at sites of DNA damage. *Cell*. 136:420-434.

Stiff, T., O'Driscoll, M., Rief, N., Iwabuchi, K., Lobrich, M. and Jeggo, P. A. 2004. ATM and DNA-PK function redundantly to phosphorylate H2AX after exposure to ionizing radiation. *Cancer Res*. 64:2390-2396.

Stingele, J., Bellelli, R. and Boulton, S. J. 2017. Mechanisms of DNA-protein crosslink repair. *Nat Rev Mol Cell Biol*. 18:563-573.

Stone, M. P., Cho, Y. J., Huang, H., Kim, H. Y., Kozekov, I. D., Kozekova, A., Wang, H., Minko, I. G., Lloyd, R. S., Harris, T. M. and Rizzo, C. J. 2008. Interstrand DNA cross-links induced by alpha,beta-unsaturated aldehydes derived from lipid peroxidation and environmental sources. *Acc Chem Res*. 41:793-804.

Stracker, T. H. and Petrini, J. H. 2011. The MRE11 complex: starting from the ends. *Nat Rev Mol Cell Biol*. 12:90-103.

Stucki, M., Clapperton, J. A., Mohammad, D., Yaffe, M. B., Smerdon, S. J. and Jackson, S. P. 2005. MDC1 directly binds phosphorylated histone H2AX to regulate cellular responses to DNA double-strand breaks. *Cell*. 123:1213-1226.

Sugawara, N., Paques, F., Colaiacovo, M. and Haber, J. E. 1997. Role of *Saccharomyces cerevisiae* Msh2 and Msh3 repair proteins in double-strand break-induced recombination. *Proc Natl Acad Sci U S A*. 94:9214-9219.

Sullivan, A., Yuille, M., Repellin, C., Reddy, A., Reelfs, O., Bell, A., Dunne, B., Gusterson, B. A., Osin, P., Farrell, P. J., Yulug, I., Evans, A., Ozcelik, T., Gasco, M. and Crook, T. 2002. Concomitant inactivation of p53 and Chk2 in breast cancer. *Oncogene*. 21:1316-1324.

Sun, H., Karow, J. K., Hickson, I. D. and Maizels, N. 1998. The Bloom's syndrome helicase unwinds G4 DNA. *J Biol Chem*. 273:27587-27592.

Sun, J., Fernandez-Cid, A., Riera, A., Tognetti, S., Yuan, Z., Stillman, B., Speck, C. and Li, H. 2014. Structural and mechanistic insights into Mcm2-7 double-hexamer assembly and function. *Genes Dev*. 28:2291-2303.

Sundquist, W. I. and Klug, A. 1989. Telomeric DNA dimerizes by formation of guanine tetrads between hairpin loops. *Nature*. 342:825-829.

Sung, P. 1994. Catalysis of ATP-dependent homologous DNA pairing and strand exchange by yeast RAD51 protein. *Science*. 265:1241-1243.

Sung, P. and Robberson, D. L. 1995. DNA strand exchange mediated by a RAD51-ssDNA nucleoprotein filament with polarity opposite to that of RecA. *Cell*. 82:453-461.

Suzuki, A., de la Pompa, J. L., Hakem, R., Elia, A., Yoshida, R., Mo, R., Nishina, H., Chuang, T., Wakeham, A., Itie, A., Koo, W., Billia, P., Ho, A., Fukumoto, M., Hui, C. C. and Mak, T. W. 1997. *Brca2* is required for embryonic cellular proliferation in the mouse. *Genes Dev*. 11:1242-1252.

Swisher, E. M., Sakai, W., Karlan, B. Y., Wurz, K., Urban, N. and Taniguchi, T. 2008. Secondary *BRCA1* mutations in *BRCA1*-mutated ovarian carcinomas with platinum resistance. *Cancer Res*. 68:2581-2586.

Tacconi, E. M., Lai, X., Folio, C., Porru, M., Zonderland, G., Badie, S., Michl, J., Sechi, I., Rogier, M., Matia Garcia, V., Batra, A. S., Rueda, O. M., Bouwman, P., Jonkers, J., Ryan, A., Reina-San-Martin, B., Hui, J., Tang, N., Bruna, A., Biroccio, A. and Tarsounas, M. 2017. BRCA1 and BRCA2 tumor suppressors protect against endogenous acetaldehyde toxicity. *EMBO Mol Med*.

Tada, S., Li, A., Maiorano, D., Mechali, M. and Blow, J. J. 2001. Repression of origin assembly in metaphase depends on inhibition of RLF-B/Cdt1 by geminin. *Nat Cell Biol*. 3:107-113.

Takahara, P. M., Rosenzweig, A. C., Frederick, C. A. and Lippard, S. J. 1995. Crystal structure of double-stranded DNA containing the major adduct of the anticancer drug cisplatin. *Nature*. 377:649-652.

Takeda, D. Y., Parvin, J. D. and Dutta, A. 2005. Degradation of Cdt1 during S phase is Skp2-independent and is required for efficient progression of mammalian cells through S phase. *J Biol Chem*. 280:23416-23423.

Tanaka, S., Umemori, T., Hirai, K., Muramatsu, S., Kamimura, Y. and Araki, H. 2007. CDK-dependent phosphorylation of Sld2 and Sld3 initiates DNA replication in budding yeast. *Nature*. 445:328-332.

Tanaka, T., Umemori, T., Endo, S., Muramatsu, S., Kanemaki, M., Kamimura, Y., Obuse, C. and Araki, H. 2011. Sld7, an Sld3-associated protein required for efficient chromosomal DNA replication in budding yeast. *EMBO J*. 30:2019-2030.

Tarsounas, M., Davies, A. A. and West, S. C. 2004. RAD51 localization and activation following DNA damage. *Philos Trans R Soc Lond B Biol Sci*. 359:87-93.

Tauchi, T., Shin-Ya, K., Sashida, G., Sumi, M., Nakajima, A., Shimamoto, T., Ohyashiki, J. H. and Ohyashiki, K. 2003. Activity of a novel G-quadruplex-interactive telomerase inhibitor, telomestatin (SOT-095), against human leukemia cells: involvement of ATM-dependent DNA damage response pathways. *Oncogene*. 22:5338-5347.

Tauchi, T., Shin-ya, K., Sashida, G., Sumi, M., Okabe, S., Ohyashiki, J. H. and Ohyashiki, K. 2006. Telomerase inhibition with a novel G-quadruplex-interactive

agent, telomestatin: *in vitro* and *in vivo* studies in acute leukemia. *Oncogene*. 25:5719-5725.

Taylor, J. H. 1977. Increase in DNA replication sites in cells held at the beginning of S phase. *Chromosoma*. 62:291-300.

Techer, H., Koundrioukoff, S., Nicolas, A. and Debatisse, M. 2017. The impact of replication stress on replication dynamics and DNA damage in vertebrate cells. *Nat Rev Genet*. 18:535-550.

Tercero, J. A. and Diffley, J. F. 2001. Regulation of DNA replication fork progression through damaged DNA by the Mec1/Rad53 checkpoint. *Nature*. 412:553-557.

Thangavel, S., Berti, M., Levikova, M., Pinto, C., Gomathinayagam, S., Vujanovic, M., Zellweger, R., Moore, H., Lee, E. H., Hendrickson, E. A., Cejka, P., Stewart, S., Lopes, M. and Vindigni, A. 2015. DNA2 drives processing and restart of reversed replication forks in human cells. *J Cell Biol*. 208:545-562.

Thomae, A. W., Baltin, J., Pich, D., Deutsch, M. J., Ravasz, M., Zeller, K., Gossen, M., Hammerschmidt, W. and Schepers, A. 2011. Different roles of the human Orc6 protein in the replication initiation process. *Cell Mol Life Sci*. 68:3741-3756.

Thompson, S. L. and Compton, D. A. 2008. Examining the link between chromosomal instability and aneuploidy in human cells. *J Cell Biol*. 180:665-672.

Tirkkonen, M., Johannsson, O., Agnarsson, B. A., Olsson, H., Ingvarsson, S., Karhu, R., Tanner, M., Isola, J., Barkardottir, R. B., Borg, A. and Kallioniemi, O. P. 1997. Distinct somatic genetic changes associated with tumor progression in carriers of *BRCA1* and *BRCA2* germ-line mutations. *Cancer Res*. 57:1222-1227.

Todd, A. K., Johnston, M. and Neidle, S. 2005. Highly prevalent putative quadruplex sequence motifs in human DNA. *Nucleic Acids Res*. 33:2901-2907.

Tomasz, M. and Palom, Y. 1997. The mitomycin bioreductive antitumor agents: cross-linking and alkylation of DNA as the molecular basis of their activity. *Pharmacol Ther*. 76:73-87.

Tommiska, J., Bartkova, J., Heinonen, M., Hautala, L., Kilpivaara, O., Eerola, H., Aittomaki, K., Hofstetter, B., Lukas, J., von Smitten, K., Blomqvist, C., Ristimaki, A., Heikkila, P., Bartek, J. and Nevanlinna, H. 2008. The DNA damage signalling kinase ATM is aberrantly reduced or lost in BRCA1/BRCA2-deficient and ER/PR/ERBB2-triple-negative breast cancer. *Oncogene*. 27:2501-2506.

Torres-Ramos, C. A., Prakash, S. and Prakash, L. 1997. Requirement of yeast DNA polymerase delta in post-replicational repair of UV-damaged DNA. *J Biol Chem*. 272:25445-25448.

Trenz, K., Smith, E., Smith, S. and Costanzo, V. 2006. ATM and ATR promote Mre11 dependent restart of collapsed replication forks and prevent accumulation of DNA breaks. *EMBO J*. 25:1764-1774.

Tsantoulis, P. K., Kotsinas, A., Sfikakis, P. P., Evangelou, K., Sideridou, M., Levy, B., Mo, L., Kittas, C., Wu, X. R., Papavassiliou, A. G. and Gorgoulis, V. G. 2008. Oncogene-induced replication stress preferentially targets common fragile sites in preneoplastic lesions. A genome-wide study. *Oncogene*. 27:3256-3264.

Tsouroula, K., Furst, A., Rogier, M., Heyer, V., Maglott-Roth, A., Ferrand, A., Reina-San-Martin, B. and Soutoglou, E. 2016. Temporal and spatial uncoupling of DNA double strand break repair pathways within mammalian heterochromatin. *Mol Cell*. 63:293-305.

Tsubouchi, H. and Ogawa, H. 1998. A novel *mre11* mutation impairs processing of double-strand breaks of DNA during both mitosis and meiosis. *Mol Cell Biol*. 18:260-268.

Tsurimoto, T. and Stillman, B. 1990. Functions of replication factor C and proliferating-cell nuclear antigen: functional similarity of DNA polymerase accessory proteins from human cells and bacteriophage T4. *Proc Natl Acad Sci U S A*. 87:1023-1027.

Turner, N. C. and Jones, A. L. 2008a. Management of breast cancer--Part I. *BMJ*. 337:a421.

Turner, N. C. and Jones, A. L. 2008b. Management of breast cancer--Part II. *BMJ*. 337:a540.

Tutt, A., Bertwistle, D., Valentine, J., Gabriel, A., Swift, S., Ross, G., Griffin, C., Thacker, J. and Ashworth, A. 2001. Mutation in *Brca2* stimulates error-prone homology-directed repair of DNA double-strand breaks occurring between repeated sequences. *EMBO J*. 20:4704-4716.

Tutt, A., Robson, M., Garber, J. E., Domchek, S. M., Audeh, M. W., Weitzel, J. N., Friedlander, M., Arun, B., Loman, N., Schmutzler, R. K., Wardley, A., Mitchell, G., Earl, H., Wickens, M. and Carmichael, J. 2010. Oral poly(ADP-ribose) polymerase inhibitor olaparib in patients with *BRCA1* or *BRCA2* mutations and advanced breast cancer: a proof-of-concept trial. *Lancet*. 376:235-244.

Uematsu, N., Weterings, E., Yano, K., Morotomi-Yano, K., Jakob, B., Taucher-Scholz, G., Mari, P. O., van Gent, D. C., Chen, B. P. and Chen, D. J. 2007. Autophosphorylation of DNA-PKCS regulates its dynamics at DNA double-strand breaks. *J Cell Biol*. 177:219-229.

Ulrich, H. D. and Jentsch, S. 2000. Two RING finger proteins mediate cooperation between ubiquitin-conjugating enzymes in DNA repair. *EMBO J*. 19:3388-3397.

Unk, I., Hajdu, I., Fatyol, K., Hurwitz, J., Yoon, J. H., Prakash, L., Prakash, S. and Haracska, L. 2008. Human HLTF functions as a ubiquitin ligase for proliferating cell nuclear antigen polyubiquitination. *Proc Natl Acad Sci U S A*. 105:3768-3773.

Unk, I., Hajdu, I., Fatyol, K., Szakal, B., Blastyak, A., Bermudez, V., Hurwitz, J., Prakash, L., Prakash, S. and Haracska, L. 2006. Human SHPRH is a ubiquitin ligase for Mms2-Ubc13-dependent polyubiquitylation of proliferating cell nuclear antigen. *Proc Natl Acad Sci U S A*. 103:18107-18112.

Valton, A. L., Hassan-Zadeh, V., Lema, I., Boggetto, N., Alberti, P., Saintome, C., Riou, J. F. and Prioleau, M. N. 2014. G4 motifs affect origin positioning and efficiency in two vertebrate replicators. *EMBO J*. 33:732-746.

van der Noll, R., Marchetti, S., Steeghs, N., Beijnen, J. H., Mergui-Roelvink, M. W., Harms, E., Rehorst, H., Sonke, G. S. and Schellens, J. H. 2015. Long-term safety and anti-tumour activity of olaparib monotherapy after combination with carboplatin and paclitaxel in patients with advanced breast, ovarian or fallopian tube cancer. *Br J Cancer*. 113:396-402.

van Engeland, M., Nieland, L. J., Ramaekers, F. C., Schutte, B. and Reutelingsperger, C. P. 1998. Annexin V-affinity assay: a review on an apoptosis detection system based on phosphatidylserine exposure. *Cytometry*. 31:1-9.

van Gent, D. C., Hoeijmakers, J. H. and Kanaar, R. 2001. Chromosomal stability and the DNA double-stranded break connection. *Nat Rev Genet*. 2:196-206.

van Hatten, R. A., Tutter, A. V., Holway, A. H., Khederian, A. M., Walter, J. C. and Michael, W. M. 2002. The *Xenopus* Xmus101 protein is required for the recruitment of Cdc45 to origins of DNA replication. *J Cell Biol*. 159:541-547.

Vannier, J. B., Pavicic-Kaltenbrunner, V., Petalcorin, M. I., Ding, H. and Boulton, S. J. 2012. RTEL1 dismantles T loops and counteracts telomeric G4-DNA to maintain telomere integrity. *Cell*. 149:795-806.

Vanoli, F., Fumasoni, M., Szakal, B., Maloisel, L. and Branzei, D. 2010. Replication and recombination factors contributing to recombination-dependent bypass of DNA lesions by template switch. *PLoS Genet*. 6:e1001205.

Vashee, S., Cvetic, C., Lu, W., Simancek, P., Kelly, T. J. and Walter, J. C. 2003. Sequence-independent DNA binding and replication initiation by the human origin recognition complex. *Genes Dev*. 17:1894-1908.

Vencken, P. M., Kriege, M., Hoogwerf, D., Beugelink, S., van der Burg, M. E., Hooning, M. J., Berns, E. M., Jager, A., Collee, M., Burger, C. W. and Seynaeve, C. 2011. Chemosensitivity and outcome of *BRCA1*- and *BRCA2*-associated ovarian cancer patients after first-line chemotherapy compared with sporadic ovarian cancer patients. *Ann Oncol*. 22:1346-1352.

Venkitaraman, A. R. 2000. The breast cancer susceptibility gene, *BRCA2*: at the crossroads between DNA replication and recombination? *Philos Trans R Soc Lond B Biol Sci*. 355:191-198.

Venkitaraman, A. R. 2009. Linking the cellular functions of *BRCA* genes to cancer pathogenesis and treatment. *Annu Rev Pathol*. 4:461-487.

Verkaik, N. S., Esveldt-van Lange, R. E., van Heemst, D., Bruggenwirth, H. T., Hoeijmakers, J. H., Zdzienicka, M. Z. and van Gent, D. C. 2002. Different types of V(D)J recombination and end-joining defects in DNA double-strand break repair mutant mammalian cells. *Eur J Immunol*. 32:701-709.

Verlander, P. C., Kaporis, A., Liu, Q., Zhang, Q., Seligsohn, U. and Auerbach, A. D. 1995. Carrier frequency of the IVS4 + 4 A-->T mutation of the Fanconi anemia gene FAC in the Ashkenazi Jewish population. *Blood*. 86:4034-4038.

Virts, E. L., Jankowska, A., Mackay, C., Glaas, M. F., Wiek, C., Kelich, S. L., Lottmann, N., Kennedy, F. M., Marchal, C., Lehnert, E., Scharf, R. E., Dufour, C., Lanciotti, M., Farruggia, P., Santoro, A., Savasan, S., Scheckenbach, K., Schipper, J., Wagenmann, M., Lewis, T., Leffak, M., Farlow, J. L., Foroud, T. M., Honisch, E., Niederacher, D., Chakraborty, S. C., Vance, G. H., Pruss, D., Timms, K. M., Lanchbury, J. S., Alpi, A. F. and Hanenberg, H. 2015. AluY-mediated germline deletion, duplication and somatic stem cell reversion in UBE2T defines a new subtype of Fanconi anemia. *Hum Mol Genet*. 24:5093-5108.

Vorlickova, M., Chladkova, J., Kejnovska, I., Fialova, M. and Kypr, J. 2005. Guanine tetraplex topology of human telomere DNA is governed by the number of (TTAGGG) repeats. *Nucleic Acids Res*. 33:5851-5860.

Vujanovic, M., Krietsch, J., Raso, M. C., Terraneo, N., Zellweger, R., Schmid, J. A., Taglialatela, A., Huang, J. W., Holland, C. L., Zwicky, K., Herrador, R., Jacobs, H., Cortez, D., Ciccia, A., Penengo, L. and Lopes, M. 2017. Replication fork slowing and reversal upon DNA damage require PCNA polyubiquitination and ZRANB3 DNA translocase activity. *Mol Cell*. 67:882-890 e885.

Wahba, H. A. and El-Hadaad, H. A. 2015. Current approaches in treatment of triple-negative breast cancer. *Cancer Biol Med*. 12:106-116.

Wajnrajch, M. P., Gertner, J. M., Huma, Z., Popovic, J., Lin, K., Verlander, P. C., Batish, S. D., Giampietro, P. F., Davis, J. G., New, M. I. and Auerbach, A. D. 2001. Evaluation of growth and hormonal status in patients referred to the International Fanconi Anemia Registry. *Pediatrics*. 107:744-754.

Wang, H., Perrault, A. R., Takeda, Y., Qin, W., Wang, H. and Iliakis, G. 2003. Biochemical evidence for Ku-independent backup pathways of NHEJ. *Nucleic Acids Res*. 31:5377-5388.

Wang, H., Rosidi, B., Perrault, R., Wang, M., Zhang, L., Windhofer, F. and Iliakis, G. 2005. DNA ligase III as a candidate component of backup pathways of nonhomologous end joining. *Cancer Res*. 65:4020-4030.

Wang, J., Aroumougame, A., Lobrich, M., Li, Y., Chen, D., Chen, J. and Gong, Z. 2014. PTIP associates with Artemis to dictate DNA repair pathway choice. *Genes Dev*. 28:2693-2698.

Wang, J. C. 1996. DNA topoisomerases. *Annu Rev Biochem*. 65:635-692.

Wang, Y., Cortez, D., Yazdi, P., Neff, N., Elledge, S. J. and Qin, J. 2000. BASC, a super complex of BRCA1-associated proteins involved in the recognition and repair of aberrant DNA structures. *Genes Dev*. 14:927-939.

Wang, Y. and Patel, D. J. 1993. Solution structure of the human telomeric repeat d[AG3(T2AG3)3] G-tetraplex. *Structure*. 1:263-282.

Ward, I. M. and Chen, J. 2001. Histone H2AX is phosphorylated in an ATR-dependent manner in response to replicational stress. *J Biol Chem*. 276:47759-47762.

Ward, J. D., Barber, L. J., Petalcorin, M. I., Yanowitz, J. and Boulton, S. J. 2007. Replication blocking lesions present a unique substrate for homologous recombination. *EMBO J*. 26:3384-3396.

Watanabe, K., Tateishi, S., Kawasuji, M., Tsurimoto, T., Inoue, H. and Yamaizumi, M. 2004. Rad18 guides poleta to replication stalling sites through physical interaction and PCNA monoubiquitination. *EMBO J*. 23:3886-3896.

Waters, L. S., Minesinger, B. K., Wiltrout, M. E., D'Souza, S., Woodruff, R. V. and Walker, G. C. 2009. Eukaryotic translesion polymerases and their roles and regulation in DNA damage tolerance. *Microbiol Mol Biol Rev*. 73:134-154.

Watkins, J. A., Irshad, S., Grigoriadis, A. and Tutt, A. N. 2014. Genomic scars as biomarkers of homologous recombination deficiency and drug response in breast and ovarian cancers. *Breast Cancer Res*. 16:211.

Weksberg, R., Buchwald, M., Sargent, P., Thompson, M. W. and Siminovitch, L. 1979. Specific cellular defects in patients with Fanconi anemia. *J Cell Physiol*. 101:311-323.

Westmoreland, J. W. and Resnick, M. A. 2013. Coincident resection at both ends of random, gamma-induced double-strand breaks requires MRX (MRN), Sae2 (Ctp1), and Mre11-nuclease. *PLoS Genet*. 9:e1003420.

Wiederschain, D., Wee, S., Chen, L., Loo, A., Yang, G., Huang, A., Chen, Y., Caponigro, G., Yao, Y. M., Lengauer, C., Sellers, W. R. and Benson, J. D. 2009. Single-vector inducible lentiviral RNAi system for oncology target validation. *Cell Cycle*. 8:498-504.

Williams, R. S., Moncalian, G., Williams, J. S., Yamada, Y., Limbo, O., Shin, D. S., Groocock, L. M., Cahill, D., Hitomi, C., Guenther, G., Moiani, D., Carney, J. P.,

Russell, P. and Tainer, J. A. 2008. Mre11 dimers coordinate DNA end bridging and nuclease processing in double-strand-break repair. *Cell*. 135:97-109.

Wilson, M. A., Kwon, Y., Xu, Y., Chung, W. H., Chi, P., Niu, H., Mayle, R., Chen, X., Malkova, A., Sung, P. and Ira, G. 2013. Pif1 helicase and Poldelta promote recombination-coupled DNA synthesis via bubble migration. *Nature*. 502:393-396.

Wohlschlegel, J. A., Dwyer, B. T., Dhar, S. K., Cvetic, C., Walter, J. C. and Dutta, A. 2000. Inhibition of eukaryotic DNA replication by geminin binding to Cdt1. *Science*. 290:2309-2312.

Woodward, A. M., Gohler, T., Luciani, M. G., Oehlmann, M., Ge, X., Gartner, A., Jackson, D. A. and Blow, J. J. 2006. Excess Mcm2-7 license dormant origins of replication that can be used under conditions of replicative stress. *J Cell Biol*. 173:673-683.

Wooster, R., Bignell, G., Lancaster, J., Swift, S., Seal, S., Mangion, J., Collins, N., Gregory, S., Gumbs, C. and Micklem, G. 1995. Identification of the breast cancer susceptibility gene *BRCA2*. *Nature*. 378:789-792.

Wooster, R. and Weber, B. L. 2003. Breast and ovarian cancer. *N Engl J Med*. 348:2339-2347.

Wu, L. and Hickson, I. D. 2003. The Bloom's syndrome helicase suppresses crossing over during homologous recombination. *Nature*. 426:870-874.

Wu, Y., Shin-ya, K. and Brosh, R. M., Jr. 2008. FANCJ helicase defective in Fanconia anemia and breast cancer unwinds G-quadruplex DNA to defend genomic stability. *Mol Cell Biol*. 28:4116-4128.

Wyatt, H. D., Sarbajna, S., Matos, J. and West, S. C. 2013. Coordinated actions of SLX1-SLX4 and MUS81-EME1 for Holliday junction resolution in human cells. *Mol Cell*. 52:234-247.

Xia, F., Taghian, D. G., DeFrank, J. S., Zeng, Z. C., Willers, H., Iliakis, G. and Powell, S. N. 2001. Deficiency of human BRCA2 leads to impaired homologous recombination but maintains normal nonhomologous end joining. *Proc Natl Acad Sci U S A*. 98:8644-8649.

Xie, A., Kwok, A. and Scully, R. 2009. Role of mammalian Mre11 in classical and alternative nonhomologous end joining. *Nat Struct Mol Biol*. 16:814-818.

Xu, G., Chapman, J. R., Brandsma, I., Yuan, J., Mistrik, M., Bouwman, P., Bartkova, J., Gogola, E., Warmerdam, D., Barazas, M., Jaspers, J. E., Watanabe, K., Pieterse, M., Kersbergen, A., Sol, W., Celie, P. H., Schouten, P. C., van den Broek, B., Salman, A., Nieuwland, M., de Rink, I., de Ronde, J., Jalink, K., Boulton, S. J., Chen, J., van Gent, D. C., Bartek, J., Jonkers, J., Borst, P. and Rottenberg, S. 2015. REV7 counteracts DNA double-strand break resection and affects PARP inhibition. *Nature*. 521:541-544.

Xu, H., Di Antonio, M., McKinney, S., Mathew, V., Ho, B., O'Neil, N. J., Santos, N. D., Silvester, J., Wei, V., Garcia, J., Kabeer, F., Lai, D., Soriano, P., Banath, J., Chiu, D. S., Yap, D., Le, D. D., Ye, F. B., Zhang, A., Thu, K., Soong, J., Lin, S. C., Tsai, A. H., Osako, T., Algara, T., Saunders, D. N., Wong, J., Xian, J., Bally, M. B., Brenton, J. D., Brown, G. W., Shah, S. P., Cescon, D., Mak, T. W., Caldas, C., Stirling, P. C., Hieter, P., Balasubramanian, S. and Aparicio, S. 2017. CX-5461 is a DNA G-quadruplex stabilizer with selective lethality in BRCA1/2 deficient tumours. *Nat Commun*. 8:14432.

Xu, X., Wagner, K. U., Larson, D., Weaver, Z., Li, C., Ried, T., Hennighausen, L., Wynshaw-Boris, A. and Deng, C. X. 1999a. Conditional mutation of *Brca1* in mammary epithelial cells results in blunted ductal morphogenesis and tumour formation. *Nat Genet*. 22:37-43.

Xu, X., Weaver, Z., Linke, S. P., Li, C., Gotay, J., Wang, X. W., Harris, C. C., Ried, T. and Deng, C. X. 1999b. Centrosome amplification and a defective G2-M cell cycle checkpoint induce genetic instability in BRCA1 exon 11 isoform-deficient cells. *Mol Cell*. 3:389-395.

Yamaguchi-Iwai, Y., Sonoda, E., Sasaki, M. S., Morrison, C., Haraguchi, T., Hiraoka, Y., Yamashita, Y. M., Yagi, T., Takata, M., Price, C., Kakazu, N. and Takeda, S. 1999. Mre11 is essential for the maintenance of chromosomal DNA in vertebrate cells. *EMBO J*. 18:6619-6629.

Yamamoto, K. N., Kobayashi, S., Tsuda, M., Kurumizaka, H., Takata, M., Kono, K., Jiricny, J., Takeda, S. and Hirota, K. 2011. Involvement of SLX4 in interstrand cross-link repair is regulated by the Fanconi anemia pathway. *Proc Natl Acad Sci U S A*. 108:6492-6496.

Yan, C. T., Boboila, C., Souza, E. K., Franco, S., Hickernell, T. R., Murphy, M., Gumaste, S., Geyer, M., Zarrin, A. A., Manis, J. P., Rajewsky, K. and Alt, F. W. 2007. IgH class switching and translocations use a robust non-classical end-joining pathway. *Nature*. 449:478-482.

Yang, H., Ganguly, A. and Cabral, F. 2010. Inhibition of cell migration and cell division correlates with distinct effects of microtubule inhibiting drugs. *J Biol Chem*. 285:32242-32250.

Yang, H., Li, Q., Fan, J., Holloman, W. K. and Pavletich, N. P. 2005. The BRCA2 homologue Brh2 nucleates RAD51 filament formation at a dsDNA-ssDNA junction. *Nature*. 433:653-657.

Yeeles, J. T. and Marians, K. J. 2011. The *Escherichia coli* replisome is inherently DNA damage tolerant. *Science*. 334:235-238.

Yeo, B., Turner, N. C. and Jones, A. 2014. An update on the medical management of breast cancer. *BMJ*. 348:g3608.

Ying, S., Hamdy, F. C. and Helleday, T. 2012. Mre11-dependent degradation of stalled DNA replication forks is prevented by BRCA2 and PARP1. *Cancer Res*. 72:2814-2821.

Youds, J. L., O'Neil, N. J. and Rose, A. M. 2006. Homologous recombination is required for genome stability in the absence of DOG-1 in *Caenorhabditis elegans*. *Genetics*. 173:697-708.

Yu, V. P., Koehler, M., Steinlein, C., Schmid, M., Hanakahi, L. A., van Gool, A. J., West, S. C. and Venkitaraman, A. R. 2000. Gross chromosomal rearrangements and genetic exchange between nonhomologous chromosomes following BRCA2 inactivation. *Genes Dev*. 14:1400-1406.

Zamborszky, J., Szikriszt, B., Gervai, J. Z., Pipek, O., Poti, A., Krzystanek, M., Ribli, D., Szalai-Gindl, J. M., Csabai, I., Szallasi, Z., Swanton, C., Richardson, A. L. and Szuts, D. 2017. Loss of BRCA1 or BRCA2 markedly increases the rate of base substitution mutagenesis and has distinct effects on genomic deletions. *Oncogene*. 36:746-755.

Zegerman, P. and Diffley, J. F. 2007. Phosphorylation of Sld2 and Sld3 by cyclin-dependent kinases promotes DNA replication in budding yeast. *Nature*. 445:281-285.

Zellweger, R., Dalcher, D., Mutreja, K., Berti, M., Schmid, J. A., Herrador, R., Vindigni, A. and Lopes, M. 2015. Rad51-mediated replication fork reversal is a global response to genotoxic treatments in human cells. *J Cell Biol*. 208:563-579.

Zeman, M. K. and Cimprich, K. A. 2014. Causes and consequences of replication stress. *Nat Cell Biol*. 16:2-9.

Zhang, H. and Lawrence, C. W. 2005. The error-free component of the RAD6/RAD18 DNA damage tolerance pathway of budding yeast employs sister-strand recombination. *Proc Natl Acad Sci U S A*. 102:15954-15959.

Zhang, J., Dewar, J. M., Budzowska, M., Motnenko, A., Cohn, M. A. and Walter, J. C. 2015. DNA interstrand cross-link repair requires replication-fork convergence. *Nat Struct Mol Biol*. 22:242-247.

Zhang, Y. and Jasin, M. 2011. An essential role for CtIP in chromosomal translocation formation through an alternative end-joining pathway. *Nat Struct Mol Biol*. 18:80-84.

Zhou, B. B., Chaturvedi, P., Spring, K., Scott, S. P., Johanson, R. A., Mishra, R., Mattern, M. R., Winkler, J. D. and Khanna, K. K. 2000. Caffeine abolishes the mammalian G(2)/M DNA damage checkpoint by inhibiting ataxia-telangiectasia-mutated kinase activity. *J Biol Chem*. 275:10342-10348.

Zimmer, J., Tacconi, E. M., Folio, C., Badie, S., Porru, M., Klare, K., Tumiati, M., Markkanen, E., Halder, S., Ryan, A., Jackson, S. P., Ramadan, K., Kuznetsov, S. G., Biroccio, A., Sale, J. E. and Tarsounas, M. 2016. Targeting BRCA1 and BRCA2 deficiencies with G-quadruplex-interacting compounds. *Mol Cell*. 61:449-460.

Zimmermann, M., Lottersberger, F., Buonomo, S. B., Sfeir, A. and de Lange, T. 2013. 53BP1 regulates DSB repair using Rif1 to control 5' end resection. *Science*. 339:700-704.

Zou, L. and Elledge, S. J. 2003a. Sensing DNA damage through ATRIP recognition of RPA-ssDNA complexes. *Science*. 300:1542-1548.

Zou, L., Liu, D. and Elledge, S. J. 2003b. Replication protein A-mediated recruitment and activation of Rad17 complexes. *Proc Natl Acad Sci U S A*. 100:13827-13832.

Zou, L. and Stillman, B. 1998. Formation of a preinitiation complex by S-phase cyclin CDK-dependent loading of Cdc45p onto chromatin. *Science*. 280:593-596.

8 Appendices

8.1 Conference proceedings

Department of Oncology internal seminar, CRUK/MRC Oxford Institute for Radiation Oncology, University of Oxford, 18th January 2017, Targeting BRCA2 deficiency (oral presentation)

13th Genome Stability Network Meeting, West Road Concert Hall, Cambridge, 6th January 2017

CNRS Meeting: Transcription-replication crosstalk and genome instability, Roscoff, France, 14th - 18th November 2016, Characterisation of a novel MRE11 inhibitor with activity on cell models for BRCA2 deficiency (oral presentation)

Annual Oncology Student Symposium, St Hilda's College, University of Oxford, 23rd June 2016, Targeting BRCA1 and BRCA2 deficiencies with G-quadruplex-interacting compounds (oral presentation)

12th Genome Stability Network Meeting, Robinson College, University of Cambridge, 8th January 2015

3rd Symposium CRUK/MRC Oxford Institute for Radiation Oncology, Oxford, 10th - 11th September 2015, Targeting BRCA1 and BRCA2 deficiencies with G-quadruplex-interacting compounds (poster)

CSHL Meeting: Eukaryotic DNA Replication & Genome Maintenance, Cold Spring Harbor, USA, 1st - 5th September 2015, Targeting BRCA1 and BRCA2 deficiencies with G-quadruplex-interacting compounds (oral presentation)

Annual Oncology Student Symposium, St Hilda's College, University of Oxford, 3rd July 2015, Targeting BRCA1 and BRCA2 deficiencies with G-quadruplex-interacting compounds (poster)

Cell Press LabLinks Ubiquitous Ubiquitin: Structure, Specificity and Function, MRC Laboratory of Molecular Biology, Cambridge, 18th March 2015

11th Genome Stability Network Meeting, Robinson College, University of Cambridge, 9th January 2015, BRCA2 prevents G-quadruplex-induced replication stress and chromosomal breakage (oral presentation)

8.2 Publications arising from this work

Michl, J.*, **Zimmer, J.***, Buffa, F. M., McDermott, U. and Tarsounas, M. 2016. FANCD2 limits replication stress and genome instability in cells lacking BRCA2. *Nat Struct Mol Biol*. 23:755-757. *These authors contributed equally to this work.

Michl, J., **Zimmer, J.** and Tarsounas, M. 2016. Interplay between Fanconi anemia and homologous recombination pathways in genome integrity. *The EMBO J*. 35:909-923.

Zimmer, J., Tacconi, E. M., Folio, C., Badie, S., Porru, M., Klare, K., Tumiati, M., Markkanen, E., Halder, S., Ryan, A., Jackson, S. P., Ramadan, K., Kuznetsov, S. G., Biroccio, A., Sale, J. E. and Tarsounas, M. 2016. Targeting BRCA1 and BRCA2 deficiencies with G-quadruplex-interacting compounds. *Mol Cell*. 61:449-460.

FANCD2 limits replication stress and genome instability in cells lacking BRCA2

Johanna Michl[1,3], Jutta Zimmer[1,3], Francesca M Buffa[1], Ultan McDermott[2] & Madalena Tarsounas[1]

The tumor suppressor BRCA2 plays a key role in genome integrity by promoting replication-fork stability and homologous recombination (HR) DNA repair. Here we report that human cancer cells lacking BRCA2 rely on the Fanconi anemia protein FANCD2 to limit replication-fork progression and genomic instability. Our results identify a new role of FANCD2 in limiting constitutive replication stress in BRCA2-deficient cells, thereby affecting cell survival and treatment responses.

© 2016 Nature America, Inc. All rights reserved.

Mutations in breast cancer susceptibility gene 2 (*BRCA2*) predispose individuals to breast and ovarian cancer. As a result of compromised HR repair, *BRCA2*-mutated tumor cells differ from normal cells in their responses to exogenous DNA damage and to endogenous challenges that arise during DNA replication (for example, at telomeres)[1,2]. These differences are due to the essential function of BRCA2 in protecting stalled replication forks against nucleolytic degradation[3,4]. A similar role in DNA replication has been ascribed to the Fanconi anemia group D2 protein (FANCD2)[5]. FANCD2 is a central component of the Fanconi anemia pathway for DNA cross-link repair, and its inactivation is associated with progressive bone-marrow failure and cancer predisposition.

Recent work has demonstrated that FANCD2 regulates responses to replication stress induced by mitomycin C and hydroxyurea (HU)[5–7]. BRCA2 abrogation likewise triggers replication stress, a hallmark of BRCA2-deficient cancer cells that drives the associated pathologies[8]. Hence, we sought to investigate whether FANCD2 mediates replication-stress responses in cells lacking BRCA2 and how this mediation might contribute to the genome integrity and survival of these cells.

FANCD2 and BRCA2 are both required to prevent MRE11-dependent degradation of nascent DNA at stalled replication forks[3,5]. However, whether the two factors functionally interact with each other during this process has not been addressed. To investigate fork protection in cells lacking both FANCD2 and BRCA2, we transfected short interfering RNA (siRNA) against FANCD2 into H1299 cells stably expressing doxycycline (Dox)-inducible short hairpin RNA (shRNA) against BRCA2 (**Fig. 1a**). We monitored replication-fork degradation after prolonged HU treatment by using DNA fiber analyses (**Fig. 1b**). Consistently with the previously described roles of FANCD2 and BRCA2 in the protection of replication forks[3,5], DNA tracks were significantly shorter in FANCD2- or BRCA2-depleted cells. Importantly, concomitant depletion of FANCD2 and BRCA2 resulted in increased levels of fork degradation, thus indicating that the two proteins mediated the protection of stalled forks by distinct mechanisms. Inhibition of MRE11 nuclease activity with mirin partially rescued the degradation of nascent DNA in cells lacking FANCD2 and BRCA2, thus implicating MRE11 as one of the nucleases required for fork resection in this context.

Replication at stalled forks can be restarted by multiple mechanisms[9]. However, the roles of FANCD2 and BRCA2 in replication-fork restart remain controversial[3,5,10]. In cells lacking FANCD2 or BRCA2, we observed impaired replication restart after HU treatment (**Fig. 1c**). This defect was more pronounced in cells deficient in both proteins, thus suggesting that FANCD2 and BRCA2 play independent roles in restarting HU-arrested replication forks.

FANCD2 restricts DNA synthesis after HU-induced replication stress, thus preventing the accumulation of deleterious single-stranded-DNA gaps[7]. BRCA2-deficient cells exhibit high levels of endogenous replication stress[11] resembling that induced by HU treatment. To determine whether FANCD2 limits DNA synthesis under replication-stress conditions associated with BRCA2 inactivation, we measured replication rates in two BRCA2-deficient human cell lines treated with FANCD2 siRNA or control siRNA. In both cell lines, FANCD2 depletion increased the track length (**Fig. 1d–f** and **Supplementary Fig. 1a**), thus indicating that FANCD2 inhibits replication-fork progression in the absence of BRCA2. Additionally, we observed an increase in origin firing in BRCA2-deficient cells lacking FANCD2 (**Supplementary Fig. 1b**), thus suggesting that FANCD2 suppresses the activation of origins and thereby prevents uncontrolled replication in the context of BRCA2 deficiency, similarly to HU[12]. Uncontrolled replication leads to accumulation of DNA damage[9]. Hence, in cells lacking FANCD2 and BRCA2, we observed enhanced levels of chromosomal aberrations (relative to single depletion, **Fig. 1g**,**h**), as well as elevated levels of phosphorylated histone H2AX (γ-H2AX) foci (**Fig. 1i**), which mark DNA-damage sites. Thus, FANCD2 is required to prevent genomic instability in BRCA2-deficient cells.

DNA-damage accumulation triggers DNA-damage responses, ultimately leading to senescence and apoptosis[13]. To determine whether the genomic instability observed in cells lacking FANCD2 and BRCA2 affects cell fate, we assessed apoptosis and senescence by using Annexin V and β-galactosidase staining, respectively. We observed a significant increase in apoptotic, Annexin V–binding cells after concomitant abrogation of FANCD2 and BRCA2 expression in H1299

[1]CR-UK/MRC Oxford Institute for Radiation Oncology, Department of Oncology, University of Oxford, Oxford, UK. [2]Cancer Genome Project, Wellcome Trust Sanger Institute, Hinxton, UK. [3]These authors contributed equally to this work. Correspondence should be addressed to M.T. (madalena.tarsounas@oncology.ox.ac.uk).

Received 11 April; accepted 7 June; published online 20 June 2016; doi:10.1038/nsmb.3252

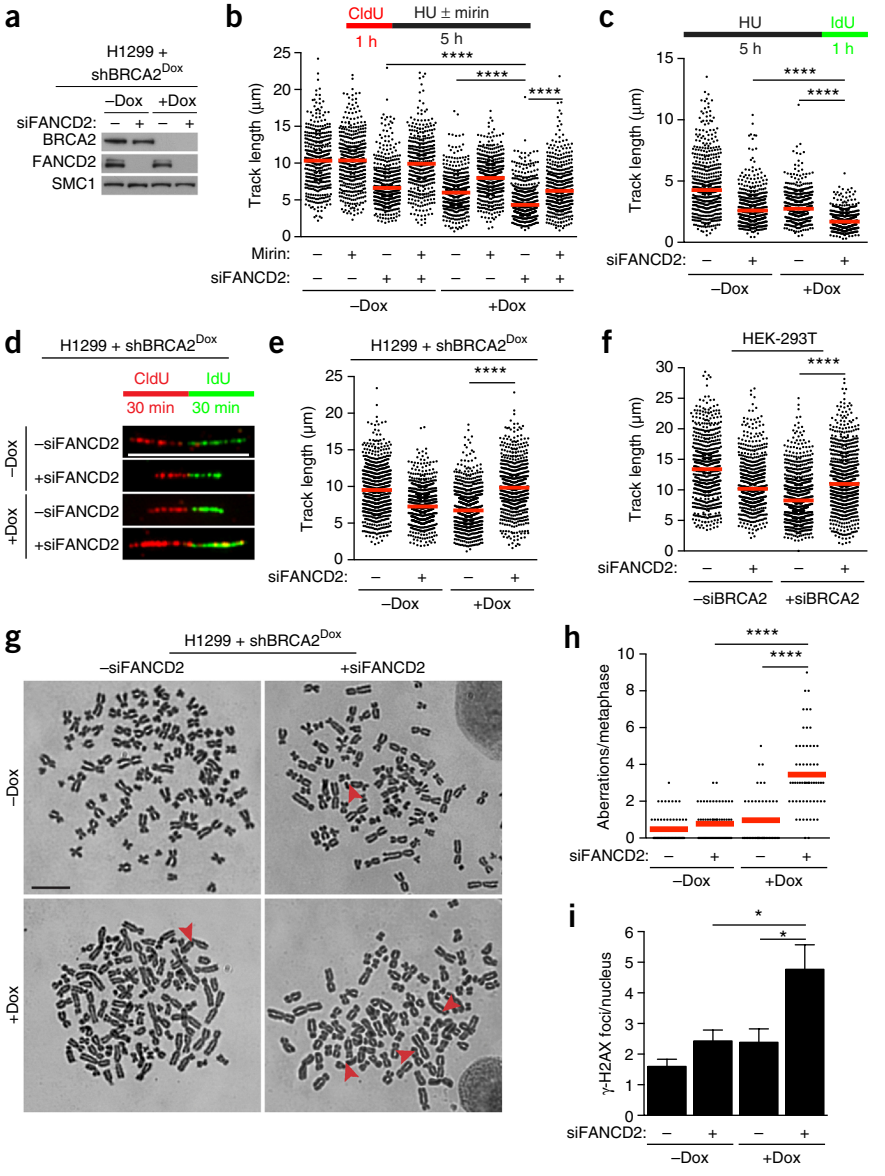


Figure 1 FANCD2 restricts replication and prevents accumulation of DNA damage in BRCA2-deficient cells. (**a**) Western blot showing FANCD2 siRNA (siFANCD2)-mediated depletion and BRCA2 knockdown by Dox-inducible shRNA (shBRCA2^{Dox}) in H1299 cells. Uncropped blots are shown in **Supplementary Data Set 1**. (**b**,**c**) Quantification of fiber track length of H1299 cells treated as indicated. CldU, 5-chloro-2′-deoxyuridine; IdU, 5-iodo-2′-deoxyuridine. Each dot represents one fiber, red bars are medians. Numbers of fibers quantified from two independent experiments are listed in **Supplementary Tables 3** and **4**. $^{****}P < 0.0001$ (two-tailed Mann–Whitney test). (**d**–**f**) Representative images (**d**) and quantification of fiber track length of H1299 (**e**) and HEK-293T (**f**) cells treated as indicated. Each dot represents one fiber, red bars are medians. Numbers of fibers quantified from three independent experiments are listed in **Supplementary Tables 5** and **6**; $^{****}P < 0.0001$ (two-tailed Mann–Whitney test). Scale bar, 10 μm. (**g**,**h**) Representative images (**g**) and quantification of chromosomal aberrations per metaphase (**h**) in H1299 cells. In **g**, arrowheads point to aberrations; scale bar, 10 μm. In **h**, each dot represents one metaphase; red bars are means. 60 metaphases from two independent experiments were quantified. $^{****}P < 0.0001$ (two-tailed Mann–Whitney test). (**i**) Quantification of γ-H2AX foci per nucleus in H1299 cells. $n = 4$ independent experiments; error bars, s.e.m.; $^{*}P < 0.05$ (unpaired two-tailed t test).

cells, as compared with inhibition of each factor alone (**Fig. 2a**). Likewise, FANCD2- and BRCA2-depleted primary MRC-5 human cells entered senescence at a higher rate than did cells lacking either FANCD2 or BRCA2 (**Supplementary Fig. 2**), as measured through β-galactosidase staining.

Next, we investigated a potential synthetic lethality between FANCD2 and BRCA2. FANCD2 inhibition through two different siRNAs significantly decreased survival of H1299, DLD1 and MDA-MB-231 cells lacking BRCA2 expression in clonogenic assays (**Fig. 2b–d** and **Supplementary Fig. 3a–d**). Consistently with this observation, survival of DLD1 cells, in which FANCD2 expression was abrogated through the CRISPR–Cas9 technique, was significantly decreased by siRNA-mediated depletion of BRCA2 (**Fig. 2e** and **Supplementary Fig. 3e**). This result indicated that FANCD2 is required for survival of BRCA2-deficient cells and suggests a synthetic lethal interaction between the two genes[14]. Depletion of the Fanconi anemia core-complex component FANCA led to significantly impaired survival of BRCA2-deficient cells (**Supplementary Fig. 3f**), thus indicating that ubiquitination of FANCD2 is required in cells lacking BRCA2.

Interestingly, cell lines and tumors carrying *BRCA2* mutations exhibited higher *FANCD2* mRNA expression levels than cell lines and tumors with wild-type *BRCA2* (**Fig. 2f**, **Supplementary Fig. 4** and **Supplementary Tables 1** and **2**). Thus far, no functional assays have been carried out to establish whether these mutations result in loss of BRCA2 function. However, our findings raise the possibility that upregulated *FANCD2* transcription promotes the survival of BRCA2-deficient cells and tumors.

BRCA2 deficiency is commonly targeted by chemical inhibition of poly(ADP-ribose) polymerase 1 (PARP1), whereas Fanconi anemia patient cell lines are generally not sensitive to PARP inhibitors[15]. To address whether FANCD2 modulates the response to PARP inhibition, we treated H1299 cells lacking FANCD2, BRCA2 or both with low doses of olaparib (**Fig. 2g**). Consistently with previous results[15], this treatment was not toxic in the context of FANCD2 loss. However, we observed that FANCD2 abrogation enhanced the sensitivity of BRCA2-deficient cells to olaparib, thus suggesting that FANCD2 mediates mechanisms of resistance to this drug.

In summary, we demonstrated that FANCD2 is essential for cell survival in the absence of BRCA2. FANCD2 promotes DNA synthesis and replication-fork protection and restart in BRCA2-deficient cells. This role of FANCD2 is analogous to that previously reported in response to exogenously induced replication stress (for example, HU). FANCD2 provides a protection mechanism against genomic instability in cells lacking BRCA2, and its abrogation is lethal to these cells. Elevated apoptosis and decreased survival of BRCA2-compromised cells after FANCD2 abrogation could be exploited therapeutically by treating BRCA2-deficient tumors with FANCD2 inhibitors.

© 2016 Nature America, Inc. All rights reserved.

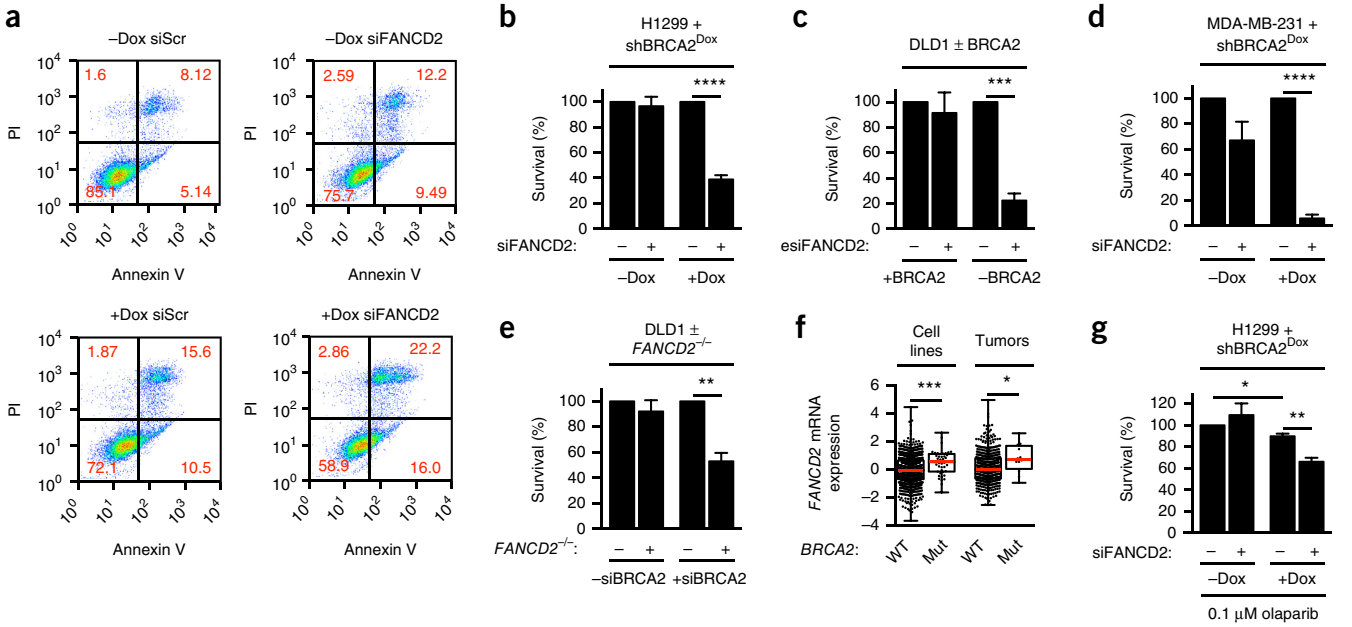


Figure 2 FANCD2 is required for BRCA2-deficient cell survival and alters olaparib sensitivity. (**a**) Analysis of apoptosis by Annexin V staining in H1299 cells. Graphs show results from one experiment, representative of four independent experiments. siScr, scrambled control siRNA; PI, propidium iodide. (**b**–**d**) Clonogenic survival assays in H1299 (**b**), DLD1 (**c**) and MDA-MB-231 (**d**) cells lacking BRCA2. $n = 3$ independent experiments; error bars, s.e.m.; $^{***}P < 0.001$; $^{****}P < 0.0001$ (unpaired two-tailed t test). esiFANCD2, endoribonuclease-prepared FANCD2 siRNA. (**e**) Clonogenic survival assays in FANCD2-deficient DLD1 cells. $n = 3$ independent experiments; error bars, s.e.m.; $^{**}P < 0.01$ (unpaired two-tailed t test). (**f**) *FANCD2* mRNA expression in cell lines ($n = 976$ for wild type (WT); $n = 43$ for mutant (Mut)) and tumors ($n = 497$ for WT; $n = 12$ for Mut). Dots in graphs represent individual cell lines and tumors. Middle line, median; box limits, 25th and 75th percentiles; whiskers, minimum and maximum values. $^{*}P < 0.05$; $^{***}P < 0.001$ (two-tailed Mann–Whitney test). siBRCA2, BRCA2 siRNA. (**g**) Clonogenic survival assay in olaparib-treated H1299 cells. $n = 3$ independent experiments; error bars, s.e.m.; $^{*}P < 0.05$; $^{**}P < 0.01$ (unpaired two-tailed t test).

METHODS

Methods and any associated references are available in the online version of the paper.

Note: Any Supplementary Information and Source Data files are available in the online version of the paper.

ACKNOWLEDGMENTS

We thank S. Bertrand for assistance with the senescence assays. We are grateful to G. Brown and M. Woodcock for assistance with microscopy and FACS analyses, respectively. J.Z. is supported by a Cancer Research UK PhD Studentship. The laboratory of M.T. is funded by Cancer Research UK A17201, the Medical Research Council, the University of Oxford and the EMBO Young Investigator Programme.

AUTHOR CONTRIBUTIONS

M.T., J.M. and J.Z. designed the study and the experiments. J.Z. and M.T. wrote the paper. J.M. and J.Z. performed the experiments. U.M. and F.M.B. analyzed *FANCD2* expression levels in cell lines and tumors, respectively.

COMPETING FINANCIAL INTERESTS

The authors declare no competing financial interests.

Reprints and permissions information is available online at http://www.nature.com/reprints/index.html.

1. Zimmer, J. *et al. Mol. Cell* **61**, 449–460 (2016).
2. Badie, S. *et al. Nat. Struct. Mol. Biol.* **17**, 1461–1469 (2010).
3. Schlacher, K. *et al. Cell* **145**, 529–542 (2011).
4. Lomonosov, M., Anand, S., Sangrithi, M., Davies, R. & Venkitaraman, A.R. *Genes Dev.* **17**, 3017–3022 (2003).
5. Schlacher, K., Wu, H. & Jasin, M. *Cancer Cell* **22**, 106–116 (2012).
6. Lachaud, C. *et al. Science* **351**, 846–849 (2016).
7. Lossaint, G. *et al. Mol. Cell* **51**, 678–690 (2013).
8. Michl, J., Zimmer, J. & Tarsounas, M. *EMBO J.* **35**, 909–923 (2016).
9. Zeman, M.K. & Cimprich, K.A. *Nat. Cell Biol.* **16**, 2–9 (2014).
10. Chaudhury, I., Sareen, A., Raghunandan, M. & Sobeck, A. *Nucleic Acids Res.* **41**, 6444–6459 (2013).
11. Carlos, A.R. *et al. Nat. Commun.* **4**, 2697 (2013).
12. Chen, Y.H. *et al. Mol. Cell* **58**, 323–338 (2015).
13. Jackson, S.P. & Bartek, J. *Nature* **461**, 1071–1078 (2009).
14. Nijman, S.M. *FEBS Lett.* **585**, 1–6 (2011).
15. Kim, Y. *et al. Blood* **121**, 54–63 (2013).

© 2016 Nature America, Inc. All rights reserved.

ONLINE METHODS

Cell lines and culture conditions. Human non-small cell lung carcinoma H1299 cells, human embryonic kidney HEK-293T cells, human mammary gland MDA-MB-231 cells, primary human fibroblast MRC-5 cells (all from American Type Culture Collection) and colorectal adenocarcinoma DLD1 cells (parental and *BRCA2* mutated, Horizon Discovery) were cultivated in monolayers in DMEM (Sigma-Aldrich) supplemented with 10% FBS (Life Technologies), 1% penicillin and streptomycin (Sigma-Aldrich). H1299 and MDA-MB-231 cells expressing Dox-inducible BRCA2 shRNA were established as previously described[1]. Cell lines were routinely tested for mycoplasma contamination. H1299 and DLD1 cell lines were authenticated in February 2016.

Generation of *FANCD2*$^{-/-}$ cells by CRISPR–Cas9. FANCD2 double nickase plasmid (sc-400445-NIC) and FANCD2 homology-directed repair (HDR) plasmid (sc-400445-HDR) were purchased from Santa Cruz. DLD1 cells were transfected with 1 μg of each construct by using Lipofectamine 2000 (Thermo Fisher Scientific). The medium was replaced with antibiotic-free medium 24 h after transfection. After 24 h, puromycin (2 μg/ml) was added for 72 h to select cells expressing Cas9 nickase. Cells were left to recover for 6 d before being seeded for single-cell cloning. Clones showing loss of all detectable FANCD2 by immunoblotting were selected for subsequent analysis.

RNA interference. Cells were transfected with siRNA by reverse transfection with DharmaFECT 1 (Dharmacon). FANCD2 and BRCA2 siGENOME SMARTpool (used at 40 nM) were obtained from Dharmacon, FANCA and FANCD2 esiRNA (used at 20 nM) were obtained from Sigma-Aldrich, and AllStars negative-control siRNA was obtained from Qiagen.

Clonogenic survival assays. Cells were plated in triplicate at densities between 200 and 1,000 cells per well in six-well plates, and drug treatment was initiated after cells had adhered. After 24-h incubation with the drug, fresh medium without the drug was added, and cells continued to grow for 10–14 d. Colonies were stained with 0.5% crystal violet (Sigma Aldrich) in 50% methanol and 20% ethanol in dH_2O. Cell survival was expressed relative to untreated cells of the same cell line.

β-galactosidase assay. Cells were fixed with 2% formaldehyde and 0.2% glutaraldehyde for 10–15 min at room temperature and stained by incubation with freshly prepared staining solution (1 mg/ml X-Gal, 5 mM potassium ferrocyanide, 5 mM potassium ferricyanide, 150 mM NaCl, 2 mM $MgCl_2$ and 40 mM citric acid, pH 6.0) at 37 °C under atmospheric CO_2 levels. Staining was stopped after 6 h. Cells were examined through light microscopy. The numbers of cells analyzed per sample from three independent experiments were: −Dox, −FANCD2, $n = 2{,}342$; −Dox, +FANCD2, $n = 1{,}971$; +Dox, −siFANCD2, $n = 1{,}926$; and +Dox, +siFANCD2, $n = 2{,}330$.

Annexin V assay. Apoptotic and dead cells were labeled with a FITC Annexin V/Dead Cell Apoptosis Kit (Thermo Fisher Scientific) according to the manufacturer's instructions. Stained cells were immediately analyzed by flow cytometry (FACSCalibur, BD Biosciences). Early apoptotic cells bound Annexin V–FITC but excluded propidium iodide (PI). Cells in necrotic or late apoptotic stages were labeled with both Annexin V-FITC and PI. 20,000 events were analyzed per condition and experiment with FlowJo software.

Immunofluorescence. Cells were washed in PBS, swollen in hypotonic solution (85.5 mM NaCl and 5 mM $MgCl_2$) for 5 min, fixed with 4% paraformaldehyde for 10 min at room temperature and permeabilized by addition of 0.03% SDS to the fixative. After blocking with blocking buffer (1% goat serum, 0.3% BSA and 0.005% Triton X-100 in PBS), cells were incubated with primary antibody diluted in blocking buffer overnight at room temperature. Then they were washed again and incubated with fluorochrome-conjugated secondary antibody for 1 h at room temperature (1:300, anti-mouse Alexa 546, A-11003, Molecular Probes). Dried coverslips were mounted on microscope slides with ProLong Gold Antifade Mountant with DAPI (Thermo Fisher Scientific). Specimens were imaged with an LSM780 (Carl Zeiss Microscopy) confocal microscope, and nuclei were analyzed with ImageJ software (NIH). The numbers of nuclei analyzed per sample from four independent experiments were: −Dox, −siFANCD2, $n = 767$; −Dox, +siFANCD2, $n = 668$; +Dox, −siFANCD2, $n = 737$; and +Dox, +siFANCD2, $n = 650$.

Preparation of metaphase spreads. Mitotic cells were collected by mitotic shake-off and swollen in hypotonic buffer (0.03 M sodium acetate) at 37 °C for 25 min, then fixed in a freshly prepared 3:1 mix of methanol/glacial acetic acid. Nuclear preparations were deposited onto slides presoaked in 45% acetic acid and stained with Giemsa. Metaphases were viewed with a Leica DMI6000B inverted microscope equipped with an HCX PL APO 100×/1.4–0.7 oil objective. Images were acquired with a Leica DFC350 FX R2 digital camera and LAS-AF software (Leica). Brightness levels and contrast adjustments were applied with Photoshop CS3 (Adobe). 60 metaphases from two independent experiments were quantified per condition.

DNA fiber assay. DNA was labeled with 25 μM CldU and 250 μM IdU, as outlined in the figures. HU was used at 2 mM, and mirin was used at 50 μM. The reaction was terminated by addition of ice-cold PBS. After cell lysis, DNA was spread on glass slides, fixed in methanol/acetic acid, denatured with HCl, blocked with 2% BSA and stained with anti-rat anti-CldU (1:500, ab6326, Abcam, validated in Zimmer, *et al.*[1]) and mouse anti-IdU (1:100, clone B44, 347580, Beckton Dickinson, validated in Zimmer, *et al.*[1]) antibodies. Anti-rat Cy3 (1:300, 712-116-153, Jackson ImmunoResearch) and anti-mouse Alexa 488 (1:300, A-11001, Molecular Probes) were used as secondary antibodies. Images were acquired as described for metaphases, and at least 200 tracks per condition from at least two independent experiments were analyzed with ImageJ software (NIH). Newly fired origins were defined as IdU track only. Exact numbers of tracks analyzed can be found in **Supplementary Tables 3–7**.

Immunoblotting. Cells were harvested by trypsinization, washed with cold PBS, resuspended in SDS–PAGE loading buffer, sonicated and boiled at 70 °C for 10 min to prepare cell extracts. Equal amounts of protein (80–100 μg) were analyzed by gel electrophoresis and subsequent western blotting. NuPAGE-Novex 3–8% Tris-acetate gels (Life Technologies) were run according to the manufacturer's instructions. Original uncropped images of gels used in this study can be found in **Supplementary Data Set 1**.

Antibodies. The following antibodies were used for immunoblotting: rabbit polyclonal antisera raised against FANCD2 (NB100-182, Novus Biologicals, validated in Lossaint, *et al.*[7]) and SMC1 (A300-055A, Bethyl Laboratories, validated in Zimmer, *et al.*[1]), and a mouse monoclonal antibody raised against BRCA2 (OP95, Merck Millipore, validated in Zimmer, *et al.*[1]). The following secondary antibodies were used: polyclonal goat anti-rabbit immunoglobulins/HRP (P0448, Dako) and polyclonal goat anti-mouse immunoglobulin/HRP (P0447, Dako). A mouse monoclonal antibody raised against phosphorylated histone H2AX S139 (05-636, clone JBW301, Merck Millipore, validated in Zimmer, *et al.*[1]) was used for immunofluorescence detection.

Genomic and transcriptional analysis in cell lines. Genomic data for a panel of 1,025 human cell lines were assembled from the COSMIC database[16]. Cell-line pellets collected during exponential growth in RPMI or DMEM/F12 were used to generate microarray data with the Human Genome U219 array (Affymetrix). The robust multiarray analysis algorithm[17] was used to establish intensity values for each of 18,562 loci (BrainArray v.10 (ref. 18)). The normalized data were then normalized gene-wise. Subsequently, the expression of each gene was centered across each tissue (0 mean and unitary s.d.). Raw data were from ArrayExpress E-MTAB-3610. Driver mutations in *BRCA2* were defined as those that were truncating and therefore likely to result in a shortened translation product (frameshift, nonsense and essential splice mutations) or homozygous deletions at the copy-number level. These mutations were then correlated with *FANCD2* gene expression.

***FANCD2* mRNA expression levels in tumors.** Data of 971 human breast cancer and normal matched samples were considered from The Cancer Genome Atlas[19]. Expression of *FANCD2* mRNA was considered in samples with and without *BRCA2* somatic mutations. The equality of expression distribution was tested with a Kruskal–Wallis rank-sum test (Kruskal–Wallis chi-squared = 10.043, df = 2, $P = 0.006596$).

16. Forbes, S.A. *et al. Nucleic Acids Res.* **43**, D805–D811 (2015).
17. Irizarry, R.A. *et al. Biostatistics* **4**, 249–264 (2003).
18. Dai, M. *et al. Nucleic Acids Res.* **33**, e175 (2005).
19. Ciriello, G. *et al. Cell* **163**, 506–519 (2015).

© 2016 Nature America, Inc. All rights reserved.
npg

doi:10.1038/3252

Published online: April 1, 2016

Review

OPEN ACCESS

THE EMBO JOURNAL

Interplay between Fanconi anemia and homologous recombination pathways in genome integrity

Johanna Michl, Jutta Zimmer & Madalena Tarsounas*

Abstract

The Fanconi anemia (FA) pathway plays a central role in the repair of DNA interstrand crosslinks (ICLs) and regulates cellular responses to replication stress. Homologous recombination (HR), the error-free pathway for double-strand break (DSB) repair, is required during physiological cell cycle progression for the repair of replication-associated DNA damage and protection of stalled replication forks. Substantial crosstalk between the two pathways has recently been unravelled, in that key HR proteins such as the RAD51 recombinase and the tumour suppressors BRCA1 and BRCA2 also play important roles in ICL repair. Consistent with this, rare patient mutations in these HR genes cause FA pathologies and have been assigned FA complementation groups. Here, we focus on the clinical and mechanistic implications of the connection between these two cancer susceptibility syndromes and on how these two molecular pathways of DNA replication and repair interact functionally to prevent genomic instability.

Keywords Fanconi anemia; homologous recombination; DNA repair; replication stress; DNA damage response; genome stability

DOI 10.15252/embj.201693860 | Received 12 January 2016 | Revised 2 March 2016 | Accepted 8 March 2016 | Published online 1 April 2016

The EMBO Journal (2016) 35: 909–923

Introduction

The Fanconi anemia (FA) family includes 19 distinct functional complementation groups (A, B, C, D1, D2, E, F, G, I, J, L, M, N, O, P, Q, R, S, T) whose gene products suppress interstrand crosslink (ICL) sensitivity. Roles in the repair of other types of DNA damage and in the regulation of replication stress responses have been additionally ascribed. One FA gene subset encodes nine proteins of the FA core complex (FANCA/B/C/E/F/G/L/M/T), which activates the FANCI–FANCD2 heterodimer through monoubiquitination. The remaining eight FA proteins (FANCD1/J/N/O/P/Q/R/S) mediate recombinational and nucleolytic reactions to complete repair (Zhang & Walter, 2014).

Mutations in most FA genes lead to a chromosomal instability disorder characterised by multiple developmental abnormalities, progressive bone marrow failure and cancer predisposition (Kim & D'Andrea, 2012). In many cases, assignment of a gene to the FA family is based on the identification of a small number of patients displaying partial FA pathologies (Table 1). A subset of FA proteins includes the well-characterised RAD51 recombinase, as well as the tumour suppressors BRCA1 and BRCA2, which are directly involved in the homologous recombination (HR) pathway of double-strand break (DSB) repair (Venkitaraman, 2009). In this review, we highlight the clinical features of patients carrying mutations in FA and HR genes. We furthermore discuss the roles of FA and HR pathways in the cellular response to exogenous and endogenous sources of DNA damage, and how they impact on telomere and genome integrity.

Pathologies associated with FA and HR gene mutations

FA is a predominantly autosomal recessive disease with an incidence of 1–5 per 1,000,000 births (Auerbach *et al*, 2001). FA patients harbour biallelic mutations in a particular FA gene, with notable exceptions of *FANCB*, which is X-linked and therefore susceptible to X-chromosome inactivation, and *FANCR/RAD51* (Table 1), in which all identified mutations are dominant negative. FA clinical characteristics include bone marrow failure, developmental abnormalities and an increased risk to develop malignancies. FA diagnosis is confirmed when, in addition to this clinical constellation, ICL hypersensitivity is detected at the cellular level.

Interstrand crosslinks can be induced by a variety of agents, most notably diepoxybutane (DEB), which continues to be used in the clinic as a major FA diagnostic tool (Auerbach & Wolman, 1976), and DNA crosslinking agents used in cancer treatment such as mitomycin C (MMC) and cisplatin. In cells lacking a functional FA pathway, ICLs elicit complex DNA lesions, illegitimately repaired to produce radial chromosomes, which represent the cellular FA signature. These chromosomal aberrations underlie the extreme toxicity of ICL-inducing treatments to FA cells (Auerbach *et al*, 1989).

At least 20% of FA patients develop cancers (Kutler *et al*, 2003), in particular acute myelogenous leukaemia (AML). However, other

Genome Stability and Tumourigenesis Group, Department of Oncology, The CRUK-MRC Oxford Institute for Radiation Oncology, University of Oxford, Oxford, UK
*Corresponding author. Tel.: +44 1865 617319; E-mail: madalena.tarsounas@oncology.ox.ac.uk

© 2016 The Authors. Published under the terms of the CC BY 4.0 license

Table 1. FA genes, proteins and pathologies associated with their inactivation.

Gene	Synonym	Main protein functions	Gene frequency within FA patient population (%)	Symptoms	References
FANCA		Component of FA core complex; interacts with BRCA1	66	FA pathologies	Apostolou *et al* (1996)
FANCB		Component of FA core complex	2	FA pathologies	Meetei *et al* (2004)
FANCC		Component of FA core complex	10	FA pathologies	Strathdee *et al* (1992)
FANCD1	*BRCA2*	HR repair; loads RAD51 onto DNA; interacts with FANCD2 and FANCN; stalled replication fork protection	Rare	FA pathologies; not all patients display bone marrow failure; mutation carriers have higher risk of breast and ovarian tumours and lower onset age	Alter (2006), Howlett *et al* (2002), Wagner *et al* (2004)
FANCD2		Ubiquitinated after DNA damage; MCM interaction; stalled replication fork protection	2	FA pathologies	Timmers *et al* (2001)
FANCE		Component of FA core complex; interacts with FANCD2	2	FA pathologies	de Winter *et al* (2000)
FANCF		Component of FA core complex	2	FA pathologies	de Winter *et al* (2000)
FANCG	*XRCC9*	Component of FA core complex	9	FA pathologies	de Winter *et al* (2000)
FANCI		Ubiquitinated after DNA damage; activates dormant origins	< 2	FA pathologies	Dorsman *et al* (2007), Sims *et al* (2007), Smogorzewska *et al* (2007)
FANCJ	*BACH, BRIP1*	FA repair; HR repair; 3′ to 5′ helicase; interacts with BRCA1; checkpoint activation	< 2	FA pathologies	Levitus *et al* (2005), Levran *et al* (2005), Litman *et al* (2005)
FANCL		E3 ubiquitin ligase; component of FA core complex	Rare	FA pathologies; no cancers reported	Meetei *et al* (2003)
FANCM		DNA helicase/translocase; localises the core complex to DNA; required for FANCI–FANCD2 ubiquitination; checkpoint activation	Rare	Phenotype unknown because the only patient described in the literature also has a FANCA mutation	Meetei *et al* (2005)
FANCN	*PALB2*	HR repair; promotes BRCA2 function; interacts with BRCA1 and BRCA2	< 2	FA pathologies; mutation carriers have higher risk of breast cancer	Reid *et al* (2007), Xia *et al* (2006a)
FANCO (provisional)	*RAD51C*	HR repair; promotes RAD51 nucleoprotein filament stability; ICL repair	Rare	FA-like syndrome; patients do not thus far display bone marrow failure or cancer	Meindl *et al* (2010), Vaz *et al* (2010)
FANCP	*SLX4*	Coordinates XPF–ERCC1, MUS81–EME1 and SLX1 nucleases; resolves Holliday junctions	Rare	FA pathologies	Kim *et al* (2011), Schuster *et al* (2013), Stoepker *et al* (2011)
FANCQ	*ERCC4, XPF*	Endonuclease; binds to ERCC1; crosslink unhooking	Rare	FA pathologies; one patient also displayed Cockayne syndrome and xeroderma pigmentosum	Bogliolo *et al* (2013), Kashiyama *et al* (2013)
FANCR	*RAD51*	HR repair; ICL repair; protection of nascent strands from DNA2- and WRN-mediated resection; stalled replication fork protection	Rare	FA-like syndrome; patients do not thus far display bone marrow failure or cancer	Ameziane *et al* (2015), Wang *et al* (2015)
FANCS	*BRCA1*	HR repair; promotes RAD51 loading; ICL repair; chromatin dissociation of replicative helicase; stalled replication fork protection; interacts with FANCD2 and FANCN	Rare	FA-like syndrome; patients do not display bone marrow failure; mutation carriers have higher risk of breast and ovarian tumours and lower onset age	Sawyer *et al* (2015)
FANCT	*UBE2T*	E2 ubiquitin-conjugating enzyme for FANCI–FANCD2 complex; interacts with FANCL	Rare	FA pathologies	Hira *et al* (2015), Machida *et al* (2006), Rickman *et al* (2015), Virts *et al* (2015)

© 2016 The Authors

tumours including head and neck squamous cell carcinoma, gynaecological squamous cell carcinoma, oesophageal carcinoma, and liver, brain, skin and renal tumours are also associated with FA gene mutations (Alter, 1996; Joenje & Patel, 2001).

It is noteworthy that breast and ovarian tumours rarely occur in FA patients carrying mutations in the core FA genes (Alter, 1996). This may be due to the fact that many FA patients are sterile and probably oestrogen-depleted. Carriers of monoallelic *FANCC* mutations have only a modest increase in breast cancer risk (Berwick *et al*, 2007). Likewise, *FANCJ* monoallelic mutations rarely predispose carriers to breast and ovarian cancer (Cantor *et al*, 2001; Rutter *et al*, 2003; Seal *et al*, 2006; Rafnar *et al*, 2011). One recent study reported a nonsense variant in *FANCM* (c.5101C>T) associated with a twofold increase in breast cancer susceptibility in the Finnish population (Kiiski *et al*, 2014). A second study reported that the *FANCM* non-sense mutation c.5791C>T, leading to exon 22 deletion and loss of DNA repair function, also confers a small increase in the familial breast cancer risk (Peterlongo *et al*, 2015). In contrast, mutations in HR genes that have also been assigned to the FA pathway carry a clear risk of breast and ovarian tumour development (discussed below).

Breast and ovarian tumours associated with mutations in BRCA genes

Monoallelic germline mutations in the tumour suppressor genes *BRCA1* and *BRCA2* predispose women to breast and ovarian cancer (Peto *et al*, 1999). Heterozygous carriers of *BRCA1* or *BRCA2* mutations have a 82% lifetime risk of breast cancer, as well as 54 and 23% risks of ovarian cancer, respectively (King *et al*, 2003). *BRCA1* and *BRCA2* mutations account for approximately 16% of the familial risk of breast cancer (Anglian Breast Cancer Study Group, 2000) and are also associated with increased risk of pancreatic, stomach, laryngeal, fallopian tube and prostate cancer (Venkitaraman, 2009; Roy *et al*, 2012).

Genomic instability caused by defects in DNA replication and repair is the key molecular mechanism underlying cancer predisposition in *BRCA* mutation carriers. *BRCA1/2* heterozygosity is not associated with the overwhelming chromosome instability characteristic of cells with biallelic mutations. Loss of heterozygosity in the affected *BRCA* gene leads to chromosome rearrangements. Subsequent oncogenic events, such as inactivation of tumour suppressors (e.g. *p53*) and/or oncogene induction (e.g. *KRAS*), provide tolerance to chromosomal instability and sustain proliferation under genotoxic stress.

The breast cancer susceptibility associated with *BRCA1/2* deficiencies has been recapitulated in mouse models carrying the respective gene deletions (Evers & Jonkers, 2006). Null mutations in either *Brca* gene are embryonic lethal in mice, with only a mild rescuing effect conferred by concomitant *p53* abrogation. However, studies using a combination of *p53* deletion and conditional *Brca1* or *Brca2* inactivation in skin and mammary gland epithelium (Xu *et al*, 1999; Jonkers *et al*, 2001) have demonstrated prevalent development of mammary tumours. Tumour induction mechanisms other than *p53* deletion are known to potentiate the loss of tumour suppressor functions of *BRCA* genes. For example, a recent study has demonstrated that *Brca2* germline heterozygous mutations are sufficient to promote tumourigenesis in a $Kras^{G12D}$ mouse model for pancreatic ductal adenocarcinoma, independently of p53 status (Skoulidis *et al*, 2010).

Classification of BRCA1 and BRCA2 as FA proteins

Patients with homozygous *BRCA1* or *BRCA2* germline mutations are rare, consistent with these genes being essential for viability. Conceivably, the human mutations reported so far are hypomorphic, with the residual gene expression sustaining survival in the presence of diminished cellular functions. Nevertheless, *BRCA1* and *BRCA2* genes have been assigned FA gene denominations, as *FANCS* and *FANCD1*, respectively (Table 1; Howlett *et al*, 2002; Sawyer *et al*, 2015). The fundamental problem here is the very low number of patients with *BRCA1/2* homozygous germline mutations, who do not live long enough and do not show sufficiently penetrating FA phenotypes to justify this inclusion. For example, the haematological defects or bone marrow failure characteristic of FA are clearly absent in the two patients with homozygous *BRCA1* mutations reported so far (Domchek *et al*, 2013; Sawyer *et al*, 2015).

The first *BRCA1* mutant patient displayed congenital abnormalities, inherited ovarian cancer and carboplatin hypersensitivity, but normal blood count (Domchek *et al*, 2013). Patient death prevented further critical analyses, such as radial chromosome induction by DEB treatment that would have substantiated a *bona fide* FA phenotype. The second patient was a woman diagnosed with multiple congenital anomalies (growth failure, microcephaly and dysmorphic face) indicative of Dubowitz syndrome, who developed breast cancer at age 23 (Sawyer *et al*, 2015). Whole-exome sequencing revealed distinct *BRCA1* mutations in the two alleles, one of which (c.5095C>T) generates a 35-amino acids internal deletion and the other a one-amino acid substitution previously reported to underlie breast cancer susceptibility. Full-length BRCA1 reconstitution was not performed, although an N-terminal BRCA1 truncation (BRCA1Δ512-1283) suppressed DNA damage sensitivity in skin fibroblasts from this patient. Thus, FA pathologies in both cases seem inconclusive and a FA-like syndrome designation may be more suitable for *BRCA1* mutations (Wang & Smogorzewska, 2015).

The data supporting *BRCA2* classification as a FA gene appear more convincing. The first study that assigned *BRCA2* to the FA complementation group D1 (Table 1) was based on two *BRCA2* homozygous patients with classical FA pathologies, including congenital abnormalities, abnormal skin pigmentation and cellular sensitivity to MMC (Howlett *et al*, 2002). Bone marrow failure or haematological tumours were not detected. However, two more recent studies performed in larger patient cohorts reported that homozygous *BRCA2* mutations are associated with high risk of acute leukaemia during early childhood: 6 out of 7 patients (Wagner *et al*, 2004) and 13 out of 27 patients (Alter, 2006) developed the disease. In *BRCA2* patients, leukaemia was largely refractory to chemotherapy (Wagner *et al*, 2004), suggesting accumulation of additional mutations that obstruct clinical intervention.

Furthermore, haematological defects detected in mouse models for *Brca2* gene inactivation support the latter clinical data. Mice homozygous for a constitutive *Brca2* exon 11 deletion, which abrogates approximately 45% of the *Brca2* transcript, succumb to thymic lymphomas (Friedman *et al*, 1998). A robust hematopoietic defect, albeit without lymphoma development, was reported in mice carrying a homozygous *Brca2* exon 27 deletion ($Brca2^{D27/D27}$) (Navarro *et al*, 2006). In addition to spontaneous chromosomal instability in bone marrow cells, these mice show a prominent proliferation defect in hematopoietic progenitors and self-renewing hematopoietic stem cells.

© 2016 The Authors

Other HR proteins included in the FA pathway

In addition to *BRCA1* and *BRCA2*, other HR genes have been assigned to FA complementation groups (Table 1). Biallelic mutations in PALB2 (partner and localiser of BRCA2, also designated *FANCN)* have been associated with FA clinical features (Levitus *et al*, 2005; Levran *et al*, 2005; Litman *et al*, 2005; Xia *et al*, 2006a; Reid *et al*, 2007). At the molecular level, PALB2 protein bridges the interaction between BRCA1 and BRCA2 in DSB repair (Xia *et al*, 2006b). The PALB2–BRCA1 interaction is regulated by ubiquitination to suppress homologous recombination repair in G1 (Orthwein *et al*, 2015). Importantly, monoallelic mutations in *PALB2* increase the risk of breast cancer (Roy *et al*, 2012).

The *RAD51C* gene, encoding a member of the RAD51 paralog family of HR repair proteins and component of the BRCA2 interactome (Suwaki *et al*, 2011; Reuter *et al*, 2015), has also been implicated in FA. A carrier of a homozygous mutation (c.773G>A) in *RAD51C* leading to a single amino acid substitution was reported to exhibit congenital anomalies characteristic of FA (Vaz *et al*, 2010). However, no bone marrow failure was detected; therefore, *RAD51C* has been provisionally assigned the FA complementation group O (Table 1) and the associated pathology termed an FA-like syndrome (Kottemann & Smogorzewska, 2013). Moreover, six *RAD51C* monoallelic mutations, which predisposed to breast and ovarian cancer, were identified in German families (Meindl *et al*, 2010). However, the susceptibility of *RAD51C* heterozygous mutation carriers to breast and ovarian cancer has been a topic of debate (Akbari *et al*, 2010; Zheng *et al*, 2010).

One of the newest members of the FA gene family is *RAD51*, which has been assigned the FA complementation group R (Ameziane *et al*, 2015; Wang *et al*, 2015). The first patient identified with a *RAD51* heterozygous mutation featured developmental abnormalities and ICL sensitivity, measured by increased levels of diepoxybutane- and MMC-induced radial chromosomes in peripheral blood lymphoblasts and skin fibroblasts (Wang *et al*, 2015). Lack of bone marrow defects led to classification of the associated disease as an FA-like syndrome. This *de novo RAD51* heterozygous mutation (c.391A>C) results in a single amino acid substitution, which specifically abrogated ICL repair, whilst recombinational repair remained intact. Mechanistically, the mutant protein acts in co-dominant-negative manner (with the wild-type protein still expressed), triggering extensive DNA2/WRN-dependent resection (see below) and hyper-phosphorylation of Replication Protein A (RPA). Characterisation of this FA patient is a remarkable illustration of an entirely novel concept, namely that naturally occurring separation-of-function mutants enable distinction between ICL versus DSB repair roles of factors previously believed to exclusively play roles in HR. More recently, a second patient carrying a distinct dominant-negative heterozygous mutation in *RAD51* (c.877G>A) has been identified (Ameziane *et al*, 2015). This patient's clinical pathologies included primarily aberrant neurological functions. Sensitivity to crosslinking agents could be detected at the cellular level; however, HR repair capacity has not been investigated.

The FA and HR pathways of DNA repair

The current model of ICL repair

The FA repair pathway is required for genome protection against ICLs. This specific type of DNA damage, considered to be amongst the most deleterious DNA lesions, obstructs both replication and transcription (Kee & D'Andrea, 2010). ICLs can be induced by chemotherapeutic agents (e.g. cisplatin, MMC), which are used as non-specific DNA damage inducing agents in the clinic. Additionally, acetaldehyde and formaldehyde—aldehyde by-products of cellular metabolism—have been identified as endogenous ICL sources that require FA proteins for repair (Langevin *et al*, 2011; Pontel *et al*, 2015). Thus, disruption of FA genes in normal cells leads to accumulation of ICL-induced replication-associated damage, mutations and chromosomal aberrations, which underlie the pathologies associated with FA.

The most recent model for ICL repair (Fig 1A) (Zhang & Walter, 2014) suggests that two convergent replication forks collide at an ICL site. This implies that the DNA surrounding the lesion is already replicated when the block is encountered and replication restart is not required. According to this widely accepted model, ICL repair is elicited when the replisome is partially dismantled by eviction of MCM replicative helicase subunits from the chromatin, thereby enabling ICL recognition by FANCM and its interacting partners FAAP24 and MHF1/2 (Ciccia *et al*, 2007; Collis *et al*, 2008). FANCM binding adjacent to ICLs leads to recruitment of the core FA complex and ATR-dependent checkpoint activation, which stalls the replisome. The binding of the FA core complex to the lesion triggers monoubiquitination of the FANCI–FANCD2 complex, as the central event in the FA pathway. Monoubiquitinated FANCI–FANCD2 is recruited to the chromatin and orchestrates downstream reactions including endonucleolytic incision, translesion synthesis and DSB repair. Additionally, FANCI–FANCD2 SUMOylation has recently been reported to occur in response to DNA damage in ATR- and FA core-dependent manner (Gibbs-Seymour *et al*, 2015). This important posttranslational modification is known to coordinate various

Figure 1. Interstrand crosslink (ICL) and double strand break (DSB) repair pathways.
(A) The Fanconi anemia (FA) pathway of ICL repair. Upon fork stalling at ICL sites, BRCA1 acts to dismantle the replisome (not shown) and RAD51 binds to the single-stranded DNA to protect the fork. Subsequent FANCM–FAAP24–MHF1/2 complex binding activates ATR signalling and promotes recruitment of the FA core complex. The core complex in turn ubiquitinates the FANCI–FANCD2 heterodimer, which acts via SLX4 as a platform to recruit multiple nucleases (ERCC1-XPF, SLX1 and MUS81-EME). Nucleolytic incisions unhook the ICL and facilitate translesion synthesis-dependent lesion bypass, mediated by REV1 or Polζ polymerases. The thus-generated DSB is repaired by HR. (B) The HR pathway of DSB repair. DNA ends at a break site are resected to generate single-stranded DNA tails. Resection is initiated by the MRN complex, stimulated though CtIP interaction and further extended though the activities of EXO1, BLM, WRN and DNA2. The resulting single-stranded DNA is a substrate for RAD51 monomer loading in BRCA2- and RAD51 paralog-dependent manner. The nucleoprotein filament thus generated invades a homologous double-stranded DNA and, following second-end capture, a double Holliday junction structure is generated. Branch migration facilitates cleavage of Holliday junctions by GEN1 or SLX4-MUS81-EME1-SLX1 resolvases, or their dissolution dependent on the BLM–TOPIIIα–RMI1 complex. Crossover or non-crossover molecules are the final products of the DNA repair reaction. Blue, FA proteins; red, HR proteins annotated as FA complementation groups; grey, other proteins associated with each pathway.

 © 2016 The Authors

aspects of the DNA damage response, in concert with ubiquitination (Jackson & Durocher, 2013). In the case of FANCI–FANCD2 complex, SUMOylation regulates its eviction from chromatin to limit incision at the ICL site.

Six different endonucleases have been implicated in ICL repair: MUS81-EME1, SLX1-SLX4, XPF-ERCC1 (FANCQ), Fanconi-associated nuclease 1 (FAN1), SNM1A and SNM1B. Whether the last two function in FA-dependent manner is unclear (Zhang &

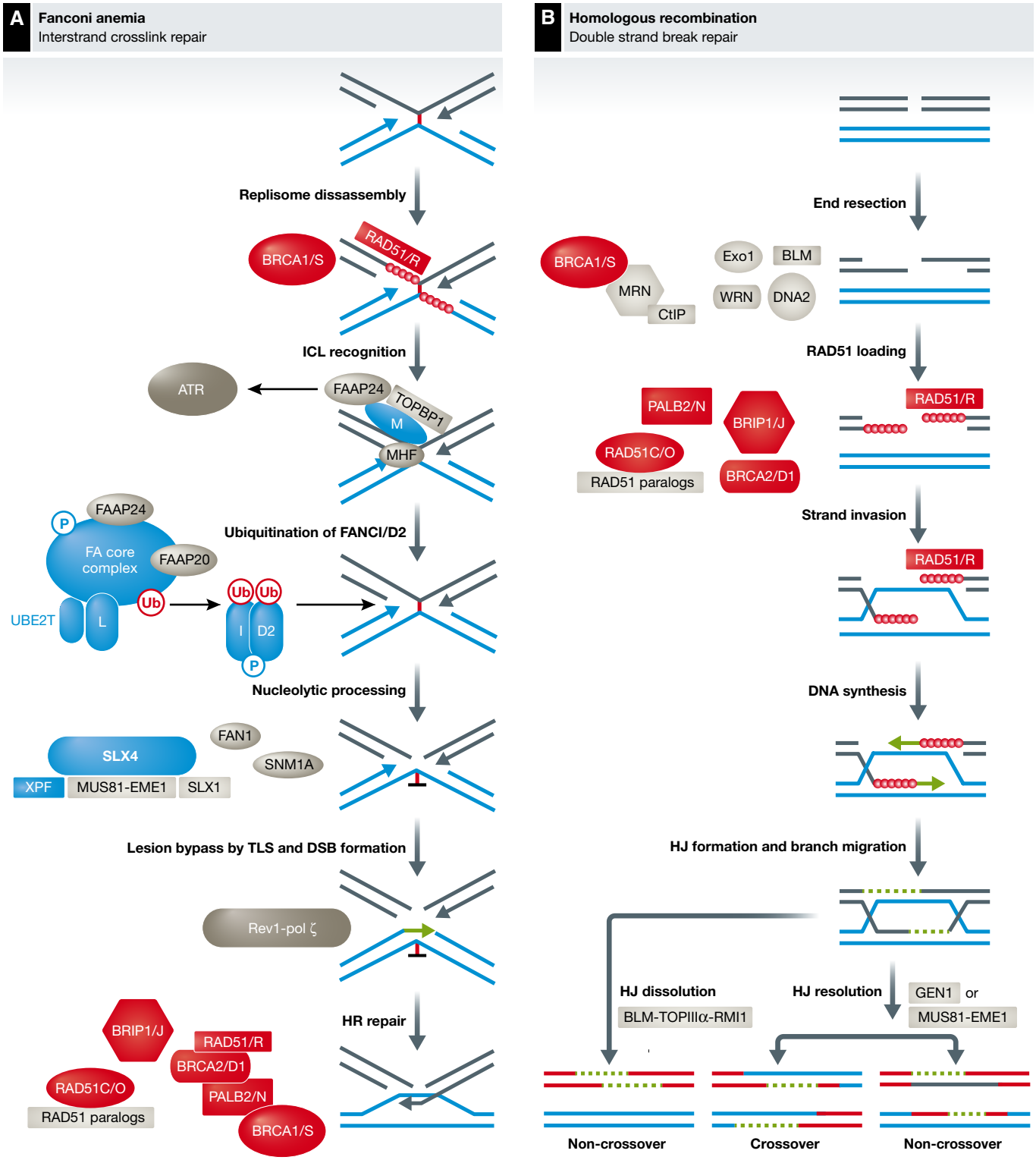


Figure 1.

© 2016 The Authors

Walter, 2014). SLX4 functions as the scaffold protein for incision nucleases and may be recruited by monoubiquitinated FANCI–FANCD2 (Fig 1A; Kim *et al*, 2011). However, subsequent work has shown that SLX4 recruitment to ICLs precedes FA core complex binding and FANCI–FANCD2 ubiquitination (Raschle *et al*, 2015). The main function of SLX4 is to recruit XPF-ERCC1, the key nuclease for the direct incision that unhooks the crosslink (Klein Douwel *et al*, 2014). In addition to XPF-ERCC1, the nucleases SLX1, MUS81-EME1 and FAN1 have redundant functions in introducing incisions, and their interaction with SLX4 is required to various degrees for ICL repair (Kim *et al*, 2013). The resulting lesion on one sister chromatid is bypassed by translesion DNA synthesis, dependent on REV1 and DNA polymerase ζ (Budzowska *et al*, 2015), concomitantly with removal of the unhooked adduct by nucleotide excision repair. The DSB generated on the second sister chromatid is most commonly repaired by HR, although other repair pathways can also be engaged (see below).

Studies using *Xenopus* egg extracts have established important roles for HR factors during early stages of ICL processing, prior to DSB formation. Fork stalling in the proximity of ICLs triggers dissociation of the replicative helicase to enable lesion processing (Fu *et al*, 2011). The single-stranded DNA generated in this way must be "primed" for subsequent HR repair reactions (Long *et al*, 2011). Consistent with this notion, RPA and RAD51 bind in proximity of ICLs before DSB formation, and act there to prevent fork breakage or degradation and to promote regulated incisions. Human RAD51 also acts to protect ICL-stalled forks against nucleolytic degradation (Wang *et al*, 2015). Whether BRCA2 mediates loading of RAD51 at these sites, as it does at DSBs, has not yet been determined.

In addition to RAD51, BRCA1 also functions early in ICL repair, before the incision stage (Long *et al*, 2014). In hydroxyurea (HU)-treated mammalian cells, BRCA1 plays fork protection roles, a function shared by RAD51, BRCA2 and FANCD2 (Schlacher *et al*, 2011, 2012; Hashimoto *et al*, 2012). In *Xenopus* egg extracts, BRCA1 is additionally required to unload the replicative GMC (GINS, CDC45, MCM2-7) helicase (Ilves *et al*, 2010), rendering the surrounding chromatin conducive for ICL repair reactions (Long *et al*, 2014). However, complementation of the BRCA1-depleted extracts by BRCA1–BARD1 does not restore unloading, suggesting that additional factors/modifications are necessary.

The HR pathway of DSB repair

DSBs represent key intermediates in ICL repair. It is therefore anticipated that one of the two major DSB repair pathways, HR or non-homologous end joining (NHEJ), is involved in the final steps of ICL repair. NHEJ provides an error-prone mechanism for the repair of DSBs, which is active throughout the cell cycle, whilst HR reactions occur primarily in S and G2 when a sister chromatid is available for use as repair template. The complex interplay between NHEJ and FA factors, as well as the contribution of NHEJ to ICL repair in cells lacking a functional FA pathway, has been discussed in detail elsewhere (Kottemann & Smogorzewska, 2013). In this review, we focus on HR, known to provide the major mechanism for repair of replication-associated DNA damage, including crosslink repair (Tsang & Carr, 2008; Aze *et al*, 2013). Moreover, HR factors assemble at ICL sites during early stages of damage processing. Therefore, it is likely that most DSB intermediates in ICL repair are channelled into the HR pathway.

The HR repair reaction involves three major steps (Fig 1B; Tacconi & Tarsounas, 2015): DSB end resection, strand invasion and Holliday junction resolution. Resection is initiated by the MRE11–RAD50–NBS1 (MRN) complex, together with the interacting partner CtIP, and is further extended through concerted activities of exonuclease 1 (Exo1), Bloom's syndrome RecQ helicase-like protein (BLM), Werner syndrome ATP-dependent helicase (WRN) and DNA replication ATP-dependent helicase/nuclease 2 (DNA2) (Mimitou & Symington, 2011; Nimonkar *et al*, 2011). The 3′ overhang thus generated is stabilised by RPA binding. BRCA2 recruitment facilitates active removal of RPA, concomitant with RAD51 loading onto the single-stranded DNA overhangs. The RAD51 paralog family also plays a role at this stage, possibly by stabilising the RAD51 nucleoprotein filaments and/or promoting their invasion into a homologous, intact double-stranded DNA. Following second-end capture and DNA synthesis, a double Holliday junction structure is formed. Branch migration promotes Holliday junction cleavage by GEN1 or SLX4-MUS81-EME1-SLX1 resolvases, or junction dissolution mediated by the BLM–TOPIIIα–RMI1 complex.

The roles of FA and HR in the replication stress response

While it is clear that FA and HR pathways are strongly linked to each other genetically, the precise molecular mechanisms underlying the functional interactions between HR and the FA proteins in normal cell physiology remain to be elucidated. During unchallenged cell cycle progression, FA and HR proteins fulfil repair-independent functions, regulating the cellular responses to endogenous replication stress. Failure of these functions leads to mutations, chromosome rearrangements, which drive FA pathologies and HR-loss-induced tumorigenesis.

In order to achieve high-fidelity duplication of the genome, the replisome must overcome barriers arising not only at sites of DNA crosslinks introduced by endogenous aldehydes, but also at DNA secondary structures such as G-quadruplexes (G4s), RNA–DNA hybrids (R-loops) or stable protein–DNA complexes. Replication forks frequently stall at these sites, leading to aberrant replication fork structures which accumulate single-stranded DNA and elicit replication stress responses (Zeman & Cimprich, 2014). To study replication stress *in vivo*, replication is perturbed using replication-stalling agents, for example HU (Fig 2). FA and HR proteins share several protective functions against replication failure, including regulation of origin firing and replication fork restart, stabilisation and protection of stalled replication forks against nucleolytic degradation. These, together with additional functions specific to FA (e.g. replication fork remodelling, unwinding of G4 DNA) or HR factors (e.g. repair of DSBs arising at sites of stalled replication), are discussed below.

BRCA1 and BRCA2

A role for BRCA2 in stabilising stalled forks was first reported by Venkitaraman and colleagues in 2003 (Lomonosov *et al*, 2003). This study reported that Y-shaped DNA junctions that identify stalled replication forks detected in 2D gel electrophoresis disappear during

 © 2016 The Authors

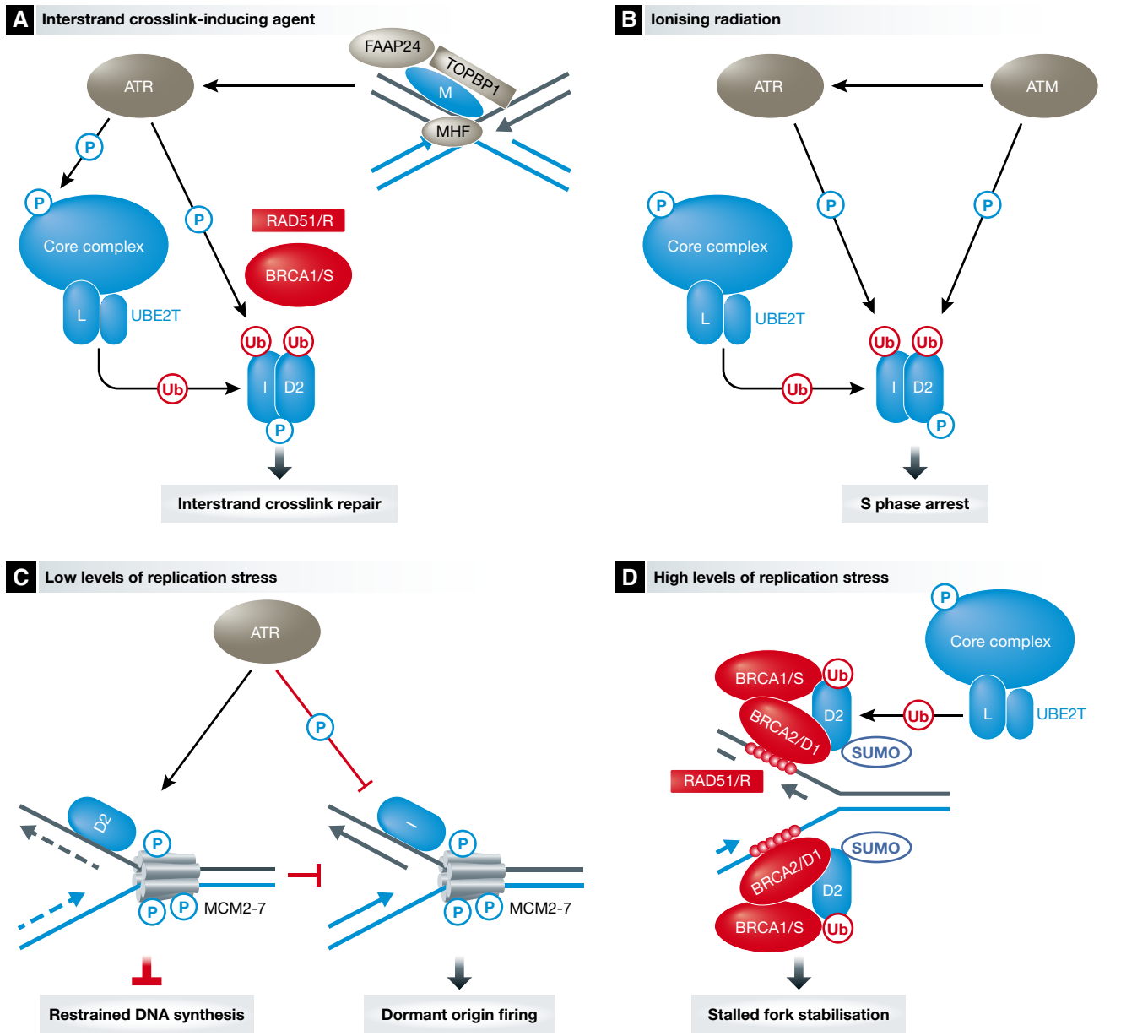


Figure 2. Fanconi anemia (FA) pathway activation in response to DNA damage and replication stress.
(A) ICL-induced fork stalling recruits the FANCM–FAAP24–MHF1/2 complex, which, in turn, activates ATR signalling. ATR phosphorylates components of the FA core complex (FANCA and FANCE) and FANCI–FANCD2. FA core complex recruitment to damage site leads to FANCI–FANCD2 monoubiquitination and chromatin binding to initiate repair. (B) IR-induced DNA damage elicits ATM and ATR activation leading to phosphorylation of FANCD2. ATR is required for the efficient monoubiquitination of FANCD2 by the core complex, which triggers cell cycle arrest. (C) Low-dose (e.g. 0.5 mM) HU treatment elicits ATR activation and FANCD2 binding to MCM2-7, which limits DNA synthesis. Concomitantly, FANCI also binds the MCM complex to promote dormant origin firing. ATR-dependent FANCI phosphorylation inhibits dormant origin firing and initiates DNA repair/replication fork restart. FANCD2 also inhibits FANCI-mediated dormant origin firing, independently of its monoubiquitination status. (D) High-dose (2–5 mM) HU treatment elicits activation of the classical FA pathway. BRCA1, BRCA2 and monoubiquitinated FANCD2 are recruited to stalled replication forks to protect them from degradation by stabilising RAD51 filaments on single-stranded DNA.

HU-induced replication arrest in BRCA2-deficient mouse cells. The explanation for this puzzling observation came from a later study (Schlacher *et al*, 2011), which used DNA fibre analyses to demonstrate that in the absence of BRCA2 stalled forks are degraded in MRE11-dependent manner. Mutational analysis revealed that the conserved BRCA2 C-terminus, required to stabilise RAD51 filaments, but not to load RAD51 onto DNA, was essential for the protection of stalled forks. A subsequent study also implicated FANCD2 and BRCA1 in this fork protection mechanism (Schlacher *et al*, 2012).

BRCA1 and BRCA2 are also known to preserve genome integrity by repairing R-loop-associated DNA damage. R-loops are three-stranded structures, consisting of a RNA:DNA hybrid plus the DNA coding strand, known to identify replication fork barriers.

© 2016 The Authors

BRCA2-depleted cells accumulate R-loops, suggesting a role for BRCA2 in their processing (Bhatia *et al*, 2014). A similar function for BRCA1 was recently reported (Hatchi *et al*, 2015). Genome-wide analyses revealed BRCA1 enrichment at R-loop-rich termination regions of actively transcribed genes, where it facilitates senataxin recruitment to provide a mechanism for repair of R-loop-induced DNA damage.

G-quadruplexes or G4-DNA are DNA secondary structures that obstruct replication fork progression and pose a threat to genome integrity. BRCA1- and BRCA2-compromised cells are hypersensitive to G4 accumulation, highlighting the role for HR in the repair of G4-associated DNA damage (Zimmer *et al*, 2016). G4 stabilisation with chemical ligands (e.g. pyridostatin) triggers excessive levels of replication stress, particularly toxic in the context of BRCA1/2 deficiency. This provides means for selective targeting of *BRCA1/2*-mutated cells and tumours.

FANCI and FANCD2: coordinated and independent functions

FANCI and FANCD2, central components of the FA pathway, play key roles in the cellular response to replication stress (Fig 2C and D). A replication function for FANCD2 was first proposed in 2005, based on the observation that FANCD2 monoubiquitination in response to HU or aphidicolin treatment blocks processive DNA synthesis (Howlett *et al*, 2005). FANCD2 is required for protection of replication forks stalled in the presence of HU (Schlacher *et al*, 2012), further substantiating a FANCD2 function in replication stress responses.

Using isolation of proteins on nascent DNA (iPOND) combined with mass spectrometry, FANCD2 and FANCI were identified as replisome-associated factors in HU-arrested cells, specifically bound to the nascent DNA (Lossaint *et al*, 2013; Sirbu *et al*, 2013). FANCD2 interacts directly with MCM helicase subunits to limit DNA synthesis in the presence of reduced nucleotide pools (Lossaint *et al*, 2013). FANCI also interacts with MCMs, but promotes dormant origin firing under low replication stress conditions (Fig 2C; Chen *et al*, 2015b). In addition to HU-induced replication arrest, FANCI and FANCD2 are required for common chromosomal fragile site stability in response to aphidicolin treatment (Howlett *et al*, 2005; Chan *et al*, 2009). Importantly, the two proteins co-localise to damaged chromosomal fragile sites on mitotic chromosomes in response to replication stress, suggesting that chromatin recruitment is essential for their function (Chan *et al*, 2009; Naim & Rosselli, 2009).

Recent studies identified R-loops as an endogenous substrate for activation of the FA pathway under physiological conditions. FANCD2 and FANCA abrogations (García-Rubio *et al*, 2015; Schwab *et al*, 2015) lead to R-loop accumulation. Inhibition of transcription or enzymatic degradation of R-loops through RNaseH1 overexpression rescued replication fork arrest and DNA damage accumulation in FA-compromised cells (Schwab *et al*, 2015), establishing R-loops as an important source of replication stress in these cells.

Most of the studies outlined above focused on FANCD2-deficient cells. It is not clear, however, whether these phenotypes can be extended to cells lacking FANCI. According to current models (Fig 1A), the FANCI–FANCD2 complex binds to DNA upon ICL induction and becomes monoubiquitinated by the FA core complex via the E3 activity of FANCL. A recent study identified a module of FANCL, FANCB and FAAP100 as the minimal sub-complex required for FANCI–FANCD2 ubiquitination *in vitro* (Rajendra *et al*, 2014). Moreover, ubiquitination of either FANCI or FANCD2 is essential for the maintenance of ubiquitin on the other (Smogorzewska *et al*, 2007). FANCD2 ubiquitination is required to prevent R-loop accumulation (Schwab *et al*, 2015) and nucleolytic degradation of stalled forks (Schlacher *et al*, 2012). It is therefore conceivable, although not yet demonstrated, that FANCI plays a similar role in these processes. However, a variety of recent studies demonstrated that FANCI and FANCD2 fulfil several of their functions independently of each other and of monoubiquitination by the FA core complex (discussed below).

FANCD2-independent functions of FANCI

Although both FANCD2 and FANCI have by iPOND been found to associated with replisomes after HU treatment, only FANCI was detected at active replication forks already prior to fork stalling (Sirbu *et al*, 2013). This suggested the possibility that FANCI plays FANCD2-independent roles in the replication stress response. For example, FANCI promotes dormant origin firing in response to low levels of replication stress, whilst FANCD2 suppresses it (Chen *et al*, 2015b). Interestingly, this function of FANCI is inhibited by ATR-dependent phosphorylation and is independent of the canonical FA pathway (Fig 2C). Likewise, FANCI function in ICL repair is independent of its monoubiquitination by the FA core complex, because complementation of FA-I patient cells with the FANCI K523R ubiquitination mutant rescued the MMC sensitivity of these cells (Smogorzewska *et al*, 2007).

Whilst the roles of FANCI in replication seem to be FA core-independent, FANCI itself is critically required for FA pathway activation in response to replication stress. FANCI, but not its partner FANCD2, acts to recruit the FA core complex to sites of DNA damage (Castella *et al*, 2015). FA core complex recruitment does not require monoubiquitination or ATR-dependent phosphorylation of FANCI, but is dependent on USP1-mediated FANCI deubiquitination. Collectively, these results support the view that FANCI activation and its cellular roles are far more complex than originally anticipated.

FANCI-independent functions of FANCD2

HU-induced FANCD2 interaction with the MCM2-MCM7 replicative helicase is critical for FANCD2-dependent replisome surveillance and does not require FANCD2 ubiquitination (Lossaint *et al*, 2013). This is therefore a FANCD2 function independent of FANCI and the FA core complex. Moreover, FANCD2 K561R ubiquitination-defective mutant can suppress origin firing during low-dose HU treatments (Fig 2C) at similar levels to its wild-type counterpart (Chen *et al*, 2015b). In contrast, high-dose HU elicits FA- and FANCD2-dependent monoubiquitination of FANCI to promote replication fork protection and/or restart of stalled forks, suggesting a concerted action of FANCI and FANCD2 under severe replication stress conditions (Fig 2D).

FANCD2, but not FANCI, is a key regulator and interacting partner of the BLM helicase (Chaudhury *et al*, 2013). Consistent with a FA pathway- and FANCI-independent function, non-ubiquitinated FANCD2 recruits BLM and its interacting partners RMI1, TOP3a and RPA1-3 to chromatin to restart stalled forks and suppress new origin firing. Upon HU exposure, FANCD2 forms a complex with RAD51 and RAD18, the E3 ubiquitin ligase responsible for PCNA sliding clamp monoubiquitination and translesion synthesis activation,

 © 2016 The Authors

again independent of FANCD2 monoubiquitination (Chen *et al*, 2015a).

FANCM

The *FANCM* gene encodes a DNA helicase/translocase, proposed to scan the DNA for ICLs and to recruit the FA core complex for ICL repair (Fig 1A). Consistent with this, FANCM is required for FANCD2 phosphorylation and ubiquitination, a downstream event in the FA pathway (Meetei *et al*, 2005; Mosedale *et al*, 2005). Additionally, FANCM can also function independently of the FA core complex to activate ATR signalling in response to replication stress. This role requires the ATPase domain, but not the translocase domain of FANCM (Collis *et al*, 2008; Huang *et al*, 2010). Further substantiating this unique role of FANCM, the FA core components are not required for ICL-induced RPA recruitment to the chromatin, a critical step for checkpoint activation (Huang *et al*, 2010). The FANCM stress-induced checkpoint function is mediated by FANCM-dependent chromatin recruitment of TOPBP1, an essential ATR co-factor (Schwab *et al*, 2010). Failure to retain TOPBP1 on the chromatin leads to a defect in phosphorylation of downstream ATR targets, including CHK1 and SMC1. Interestingly, CHK1 and FANCM protect each other from proteasomal degradation during DNA replication stress (Luke-Glaser *et al*, 2010), probably mediated by a direct interaction between FANCM and the checkpoint kinase.

In the presence of replication inhibitors that cause low levels of DNA damage (e.g. aphidicolin), FANCM counteracts fork movement, possibly by remodelling fork structures (Luke-Glaser *et al*, 2010). In contrast, at sites of damage, FANCM promotes replication fork restart (Luke-Glaser *et al*, 2010; Schwab *et al*, 2010). In cells lacking FANCM, the progression of replication forks is accelerated, suggesting that FANCM controls DNA chain elongation in the absence of exogenous sources of DNA replication stress. These data have led to the proposal that FANCM constitutively binds to DNA, acting as a DNA lesion sensor and activating the S-phase checkpoint to recruit the FA core complex. This, in turn, enables repair of damage and restart of stalled replication (Luke-Glaser *et al*, 2010; Schwab *et al*, 2010). In addition, FANCM effectively dismantles R-loops, transcription intermediates known to interfere with DNA replication (Schwab *et al*, 2015). This is mediated by the robust DNA translocase activity intrinsic to FANCM, with high affinity for a variety of branched DNA molecules including those whose single-stranded DNA is bound by RPA (Gari *et al*, 2008).

FANCJ

FANCJ, a RECQ-like helicase with 5′ to 3′ directionality, was initially identified as BACH1 (BRCA1-associated C-terminal helicase; also known as BRIP1; Cantor *et al*, 2001) required for HR repair of IR- or HU-induced DSBs (Litman *et al*, 2005). FANCJ is required for FANCD2 loading onto the chromatin and FANCD2 foci formation in response to MMC (Zhang *et al*, 2010; Chen *et al*, 2014), but paradoxically, it is not implicated in FANCD2 monoubiquitination (Litman *et al*, 2005). Additional studies are required to clarify whether FANCJ functions downstream of this critical step in FA repair.

Similarly to FANCI and FANCD2, FANCJ acts at the interface between DNA damage repair and replication stress. FANCJ foci assemble spontaneously during S-phase progression; upon HU-induced replication stress, they co-localise with PCNA (Zhang *et al*, 2010). The recruitment of FANCJ to RPA-containing replication foci is dependent on its helicase activity and its ability to interact with BRCA1 (Gupta *et al*, 2007). *In vitro*, RPA stimulates the helicase activity of FANCJ. Importantly, FANCJ also interacts with TOPBP1, a factor required for ATR checkpoint activation. Both TOPBP1 interaction and FANCJ helicase activity are required for RPA chromatin accumulation and checkpoint activation (Gong *et al*, 2010). Taken together, these results suggest that FANCJ promotes checkpoint signalling in response to replication stress, possibly through unwinding and exposing single-stranded DNA at stalled replication forks.

Characterisation of Dog-1, the *C. elegans* ortholog of mammalian FANCJ, provided the first evidence that FANCJ can act to resolve G4 DNA structures (Cheung *et al*, 2002; Youds *et al*, 2007). During normal development, *dog-1* mutant worms evict extensive guanine-rich tracts from their genome, which were subsequently shown to contain the G4 signature (Kruisselbrink *et al*, 2008). Consistent with a role in G4 resolution, human FANCJ, a structure-specific 5′–3′ DNA helicase, can unwind G4 DNA *in vitro* (London *et al*, 2008; Wu *et al*, 2008). Importantly, FA-J patient cells accumulate large genomic deletions in the proximity of sequences with high G4-forming potential, reminiscent of the worm phenotype. *In vitro*, the mutant protein form of FANCJ expressed in these patient cells was also unable to resolve G4s (London *et al*, 2008).

The function of FANCJ in G4 stability was strengthened by subsequent studies in DT40 chicken cells, where FANCJ plays a dual role: it mediates epigenetic stability in the proximity of G4s by coordinating the action of REV1 translesion polymerase with BLM/WRN helicases (Sarkies *et al*, 2012) and it promotes processive DNA synthesis and maintenance of chromatin structure at G4 sites (Schwab *et al*, 2013). Recently, the role of FANCJ in resolving G4s during eukaryotic DNA replication was reconstituted in *Xenopus* egg extracts (Castillo Bosch *et al*, 2014).

Telomeres have well-established G4-forming potential due to their G-rich repetitive sequence. It is therefore surprising that FANCJ does not appear to have telomeric functions. In *C. elegans*, telomere length is unaffected in *dog-1* mutants. This could be due to the low G4-forming potential of telomeric DNA sequence in worms, which consist of TTAGGC repeats (Cheung *et al*, 2002). In human cells, treatment with the G4-stabilising compound telomestatin, known to cause telomere dysfunction, induces apoptosis in FANCJ-depleted cells (Wu *et al*, 2008). However, the contribution of telomere dysfunction to this compound toxicity has not been evaluated. Surprisingly, a recent study reported that *Fancj*$^{-/-}$ mouse cells lack sensitivity to G4-stabilising compounds (Matsuzaki *et al*, 2015), which seems to contradict biochemical and *in vivo* data supporting a role for FANCJ in G4 resolution.

Crosstalk between FA and HR in DNA repair

The integrated action of FA and HR pathways in the maintenance of genome integrity was initially established through co-immunoprecipitation and co-localisation studies, although follow-up data to strengthen such findings are still missing for several of these cases (see below). Upon exposure to ionising radiation, HU or MMC, monoubiquitinated FANCD2 is targeted to nuclear foci containing BRCA1, BRCA2 and RAD51 (Garcia-Higuera *et al*, 2001; Taniguchi *et al*, 2002; Hussain *et al*, 2004; Wang *et al*, 2004; Nakanishi *et al*,

© 2016 The Authors

2005). One study reported that FANCD2 and BRCA2 co-immunoprecipitate from MMC-treated human and hamster cells, but this observation requires further validation (Hussain *et al*, 2004). Likewise, the IR-induced FANCD2 interactions with BRCA1 (Garcia-Higuera *et al*, 2001) or the MRN subunit NBS1 (Nakanishi *et al*, 2002) represent potentially important preliminary observations, which, however, are yet to be confirmed by independent studies. Whilst recombinational repair of IR-induced DNA damage is well documented, whether the FA pathway proper plays a role in the IR response remains unclear. Consistent with this notion, FA cells are only mildly sensitive to IR (Kalb *et al*, 2004), probably because the HR machinery remains intact.

Conversely, however, it is well established that ICL-inducing treatments are toxic to HR-deficient cells. In particular, BRCA1- and BRCA2-deficient cells are highly sensitive to cisplatin and MMC (Patel *et al*, 1998; Moynahan *et al*, 2001; Rottenberg *et al*, 2007). This sensitivity is exploited in the clinic through selective targeting of *BRCA1*/2-deficient tumours with ICL-inducing agents, including MMC and cisplatin (Powell *et al*, 2002). The major drawback of such therapies is that acquired secondary mutations restore the wild-type BRCA1/2 reading frame or enable other mechanisms of resistance to platinum-based chemotherapy (Sakai *et al*, 2008; Bouwman & Jonkers, 2012). MMC and cisplatin treatments are likewise toxic to RAD51- and RAD51 paralog-deficient cells (Godthelp *et al*, 2002; Ohashi *et al*, 2005; Meindl *et al*, 2010; Jensen *et al*, 2013; Wang *et al*, 2015).

The hypersensitivity of HR-compromised cells to ICL-inducing treatments may stem from loss of recombinational repair of DSBs arising during ICL processing. Alternatively, HR deficiency may interfere with other key steps of the FA pathway. For example, BRCA1 inactivation in *Xenopus* egg extracts prevents removal of the replicative helicase and subsequent loading of ubiquitinated FANCD2 in the vicinity of ICLs (Fig 2A; Long *et al*, 2014). Consistent with this, FANCD2 foci formation is impaired in mouse $Brca1^{D11/D11}$ cells after exposure to DNA crosslinking agents (Bunting *et al*, 2012). Thus, toxic ICL accumulation resulting from inadequate FANCD2 recruitment underlies the hypersensitivity of BRCA1-deficient cells to crosslinking agents. Whether the same is true for BRCA2 deficiency remains to be determined. It is conceivable that BRCA2 promotes RAD51 loading onto ICL sites during early steps of ICL processing (Long *et al*, 2011; Wang *et al*, 2015). Although not yet formally demonstrated, an early role for BRCA2 in ICL repair would be consistent with the ICL sensitivity of BRCA2-deficient cells and tumours.

It is noteworthy that FA patients cells are generally not sensitive to poly(ADP-ribose) polymerase (PARP) inhibitors (Kim *et al*, 2013), although a broader spectrum of toxicity against FA cell lines had initially been suggested (Gaymes *et al*, 2008). Only mutations in genes with basic HR roles (*FANCD1/BRCA2*, *FANCN/PALB2*, *FANCR/RAD51* and *FANCS/BRCA1*) are notably hypersensitive to PARP inhibitors (Kim *et al*, 2013).

The role of FA and HR pathways at telomeres

Telomeres are specialised structures that cap the ends of chromosomes, thereby preventing their recognition as DSBs. Telomere dysfunction triggered by telomere shortening and fusions between short or uncapped telomeres can lead to genomic instability. Whether telomere dysfunction can contribute significantly to the genomic instability, characteristic of FA cells, has not yet been established. Moreover, unaltered telomeres were reported in human and mouse FANCG-deficient cells (Franco *et al*, 2004) and in *Fancj*-deleted mouse cells (Matsuzaki *et al*, 2015). Likewise, no effect of *Fancc* deletion was detected in mouse cells with normal telomerase activity (Rhee *et al*, 2010). Only when *Fancc* was abrogated in a mouse model lacking telomerase activity, short telomeres showed higher levels of recombination, suggesting that FANCC may suppress such events when telomerase is abrogated.

Surprisingly, FA patient cells show some telomere shortening. The comparison is most frequently to non-isogenic normal controls and therefore not entirely reliable. It is generally accepted, however, that telomere shortening in FA is due to stem cell failure and increased cell proliferation, but not to an intrinsic telomere maintenance defect. This is contrary to dyskeratosis congenita, another bone marrow failure syndrome, where the telomere shortening is far more profound and emanates directly from severely damaged telomeres (Alter *et al*, 2015).

Consistent with a role in telomerase-independent telomere maintenance, the FA pathway is involved in telomere length maintenance through the alternative lengthening of telomeres (ALT), a mechanism known to act in cells in which telomerase activity is compromised. FANCD2 co-localised with telomeres in ALT cells, but not in non-ALT cells, in manner dependent on FANCL and FANCA (Fan *et al*, 2009), factors that also sustain FANCD2 monoubiquitination.

In contrast to FA, HR factors including RAD51, RAD51 paralogs and BRCA2 are required for telomere replication and capping (Tacconi & Tarsounas, 2015) and thus the genomic instability characteristic of HR-deficient cells and tumours may have a telomere dysfunction component. Cells lacking the HR factors RAD51C, BRCA2 and RAD51 have short telomeres, as a result of unrepaired DSBs and loss of telomeric DNA. Telomere breakage is thought to emanate from telomere replication defects, as telomeres constitute intrinsic barriers to replication fork progression due to their heterochromatic structure and G4-forming potential. Consistent with this notion, HR-deficient cells display elevated levels of fragile telomeres (Badie *et al*, 2010). More recently, fragility of telomeric G-rich strand with G4-forming potential was detected in HR-deficient cells, supporting the HR role in facilitating replication of telomeric G4 structures (Zimmer *et al*, 2016).

Similarly to HR factors BRCA1 and BRCA2, FANCD2 acts to protect stalled replication forks genome-wide (Schlacher *et al*, 2011). It is therefore conceivable that FA and HR proteins could act together at telomeres to prevent replication-induced telomere damage. Thus, the pathologies characteristic of FA- and HR-compromised cells are likely caused in part by a telomere replication defect.

Future perspectives

The interplay between FA and HR pathways in DNA repair and replication is crucial for the maintenance of genome integrity. A better understanding of the fine mechanistic details of their interactions will enable not only a better understanding of DNA repair in general, but will also open new opportunities for clinical applications. In particular, this may be relevant to ICL-inducing

 © 2016 The Authors

platinum-based chemotherapies routinely used in breast and ovarian cancer treatment, including *BRCA*-deficient cancers. The major problem with these drugs is that most patients become resistant to them, which leads to tumour relapse. Reactivation of the FA pathway in these tumours may be one of the resistance mechanisms. If this proves to be the case, current approaches to target FA deficiency can be redeployed to the chemotherapy-resistant *BRCA1/2*-mutated patient subset.

Importantly, cancer treatments for FA patients are limited, as all cells of FA patients are as sensitive to DNA-damaging agents as the cancer cells. Thus, most of the currently used treatments specific to BRCA1/2-deficient tumours are likely to be very toxic to FA patients, which creates an enormous problem. Genetic alterations specific to the cancer cells need to be identified in order to allow specific targeting of tumours, without highly toxic/potentially lethal side effects for the patient.

The physiological functions of FA and HR pathways are not completely understood. Recent research provided a glimpse into how both pathways facilitate replication through cell-intrinsic obstacles, including ICLs, fragile sites, G4s and R-loops. Unravelling the full range of sources of endogenous damage that activate the two pathways represents a challenge for the future. With new technologies advancing fast, it becomes possible to identify genomic locations where damage is likely to arise upon specific loss of FA or HR factors. These, in turn, may be informative on the source of damage and enable better management of the associated pathologies.

Acknowledgements

We thank Dr. Angelos Constantinou (Institute of Human Genetics, Montpellier, France) and members of the Tarsounas laboratory for their comments on the manuscript. Work in the M.T. laboratory is supported by Cancer Research UK, Medical Research Council and EMBO Young Investigator Programme.

Conflict of interest

The authors declare that they have no conflict of interest.

References

Akbari MR, Tonin P, Foulkes WD, Ghadirian P, Tischkowitz M, Narod SA (2010) RAD51C germline mutations in breast and ovarian cancer patients. *Breast Cancer Res* 12: 404

Alter BP (1996) Fanconi's anemia and malignancies. *Am J Hematol* 53: 99 – 110

Alter BP (2006) The association between FANCD1/BRCA2 mutations and leukaemia. *Br J Haematol* 133: 446 – 448

Alter BP, Giri N, Savage SA, Rosenberg PS (2015) Telomere length in inherited bone marrow failure syndromes. *Haematologica* 100: 49 – 54

Ameziane N, May P, Haitjema A, van de Vrugt HJ, van Rossum-Fikkert SE, Ristic D, Williams GJ, Balk J, Rockx D, Li H, Rooimans MA, Oostra AB, Velleuer E, Dietrich R, Bleijerveld OB, Maarten Altelaar AF, Meijers-Heijboer H, Joenje H, Glusman G, Roach J *et al* (2015) A novel Fanconi anaemia subtype associated with a dominant-negative mutation in RAD51. *Nat Commun* 6: 8829

Anglian Breast Cancer Study Group (2000) Prevalence and penetrance of BRCA1 and BRCA2 mutations in a population-based series of breast cancer cases. *Br J Cancer* 83: 1301 – 1308

Apostolou S, Whitmore SA, Crawford J, Lennon G, Sutherland GR, Callen DF, lanzano L, Savino M, D'Apolito M, Notarangeio A, Memeo E, Piemontese MR, Zelante L, Savoia A, Gibson RA, Tipping AJ, Morgan NV, Hassock S, Jansen S, de Ravel TJ *et al* (1996) Positional cloning of the Fanconi anaemia group A gene. *Nat Genet* 14: 324 – 328

Auerbach AD, Buchwald M, Joenje H (2001) Fanconi Anemia. In *Metabolic and Molecular Bases of Inherited Disease*, Scriver C, Beaudet AL, Sly WS, Valle D, Vogelstein B, Childs B (eds), pp 753 – 768. New York: McGraw-Hill Medical

Auerbach AD, Rogatko A, Schroeder-Kurth TM (1989) International Fanconi anemia registry: relation of clinical symptoms to diepoxybutane sensitivity. *Blood* 73: 391 – 396

Auerbach AD, Wolman SR (1976) Susceptibility of Fanconi's anaemia fibroblasts to chromosome damage by carcinogens. *Nature* 261: 494 – 496

Aze A, Zhou JC, Costa A, Costanzo V (2013) DNA replication and homologous recombination factors: acting together to maintain genome stability. *Chromosoma* 122: 401 – 413

Badie S, Escandell JM, Bouwman P, Carlos AR, Thanasoula M, Gallardo MM, Suram A, Jaco I, Benitez J, Herbig U, Blasco MA, Jonkers J, Tarsounas M (2010) BRCA2 acts as a RAD51 loader to facilitate telomere replication and capping. *Nat Struct Mol Biol* 17: 1461 – 1469

Berwick M, Satagopan JM, Ben-Porat L, Carlson A, Mah K, Henry R, Diotti R, Milton K, Pujara K, Landers T, Dev Batish S, Morales J, Schindler D, Hanenberg H, Hromas R, Levran O, Auerbach AD (2007) Genetic heterogeneity among Fanconi anemia heterozygotes and risk of cancer. *Cancer Res* 67: 9591 – 9596

Bhatia V, Barroso SI, Garcia-Rubio ML, Tumini E, Herrera-Moyano E, Aguilera A (2014) BRCA2 prevents R-loop accumulation and associates with TREX-2 mRNA export factor PCID2. *Nature* 511: 362 – 365

Bogliolo M, Schuster B, Stoepker C, Derkunt B, Su Y, Raams A, Trujillo Juan P, Minguillón J, Ramírez María J, Pujol R, Casado José A, Baños R, Rio P, Knies K, Zúñiga S, Benítez J, Bueren Juan A, Jaspers Nicolaas GJ, Schärer Orlando D, de Winter Johan P *et al* (2013) Mutations in ERCC4, encoding the DNA-repair endonuclease XPF, cause Fanconi anemia. *Am J Hum Genet* 92: 800 – 806

Bouwman P, Jonkers J (2012) The effects of deregulated DNA damage signalling on cancer chemotherapy response and resistance. *Nat Rev Cancer* 12: 587 – 598

Budzowska M, Graham TG, Sobeck A, Waga S, Walter JC (2015) Regulation of the Rev1-pol zeta complex during bypass of a DNA interstrand cross-link. *EMBO J* 34: 1971 – 1985

Bunting SF, Callen E, Kozak ML, Kim JM, Wong N, Lopez-Contreras AJ, Ludwig T, Baer R, Faryabi RB, Malhowski A, Chen HT, Fernandez-Capetillo O, D'Andrea A, Nussenzweig A (2012) BRCA1 functions independently of homologous recombination in DNA interstrand crosslink repair. *Mol Cell* 46: 125 – 135

Cantor SB, Bell DW, Ganesan S, Kass EM, Drapkin R, Grossman S, Wahrer DC, Sgroi DC, Lane WS, Haber DA, Livingston DM (2001) BACH1, a novel helicase-like protein, interacts directly with BRCA1 and contributes to its DNA repair function. *Cell* 105: 149 – 160

Castella M, Jacquemont C, Thompson EL, Yeo JE, Cheung RS, Huang J-W, Sobeck A, Hendrickson EA, Taniguchi T (2015) FANCI regulates recruitment of the FA core complex at sites of DNA damage independently of FANCD2. *PLoS Genet* 11: e1005563

Castillo Bosch P, Segura-Bayona S, Koole W, van Heteren JT, Dewar JM, Tijsterman M, Knipscheer P (2014) FANCJ promotes DNA synthesis through G-quadruplex structures. *EMBO J* 33: 2521 – 2533

Chan KL, Palmai-Pallag T, Ying S, Hickson ID (2009) Replication stress induces sister-chromatid bridging at fragile site loci in mitosis. *Nat Cell Biol* 11: 753 – 760

© 2016 The Authors

Chaudhury I, Sareen A, Raghunandan M, Sobeck A (2013) FANCD2 regulates BLM complex functions independently of FANCI to promote replication fork recovery. *Nucleic Acids Res* 41: 6444 – 6459

Chen X, Bosques L, Sung P, Kupfer GM (2015a) A novel role for non-ubiquitinated FANCD2 in response to hydroxyurea-induced DNA damage. *Oncogene* 35: 22 – 34

Chen X, Wilson JB, McChesney P, Williams SA, Kwon Y, Longerich S, Marriott AS, Sung P, Jones NJ, Kupfer GM (2014) The Fanconi anemia proteins FANCD2 and FANCJ interact and regulate each other's chromatin localization. *J Biol Chem* 289: 25774 – 25782

Chen YH, Jones MJ, Yin Y, Crist SB, Colnaghi L, Sims RJ 3rd, Rothenberg E, Jallepalli PV, Huang TT (2015b) ATR-mediated phosphorylation of FANCI regulates dormant origin firing in response to replication stress. *Mol Cell* 58: 323 – 338

Cheung I, Schertzer M, Rose A, Lansdorp PM (2002) Disruption of dog-1 in *Caenorhabditis elegans* triggers deletions upstream of guanine-rich DNA. *Nat Genet* 31: 405 – 409

Ciccia A, Ling C, Coulthard R, Yan ZJ, Xue YT, Meetei AR, Laghmani EH, Joenje H, McDonald N, de Winter JP, Wang WD, West SC (2007) Identification of FAAP24, a Fanconi anemia core complex protein that interacts with FANCM. *Mol Cell* 25: 331 – 343

Collis SJ, Ciccia A, Deans AJ, Horejsi Z, Martin JS, Maslen SL, Skehel JM, Elledge SJ, West SC, Boulton SJ (2008) FANCM and FAAP24 function in ATR-mediated checkpoint signaling independently of the Fanconi anemia core complex. *Mol Cell* 32: 313 – 324

Domchek SM, Tang J, Stopfer J, Lilli DR, Hamel N, Tischkowitz M, Monteiro AN, Messick TE, Powers J, Yonker A, Couch FJ, Goldgar DE, Davidson HR, Nathanson KL, Foulkes WD, Greenberg RA (2013) Biallelic deleterious BRCA1 mutations in a woman with early-onset ovarian cancer. *Cancer Discov* 3: 399 – 405

Dorsman JC, Levitus M, Rockx D, Rooimans MA, Oostra AB, Haitjema A, Bakker ST, Steltenpool J, Schuler D, Mohan S, Schindler D, Arwert F, Pals G, Mathew CG, Waisfisz Q, de Winter JP, Joenje H (2007) Identification of the Fanconi anemia complementation group I gene, FANCI. *Cell Oncol* 29: 211 – 218

Evers B, Jonkers J (2006) Mouse models of BRCA1 and BRCA2 deficiency: past lessons, current understanding and future prospects. *Oncogene* 25: 5885 – 5897

Fan Q, Zhang F, Barrett B, Ren K, Andreassen PR (2009) A role for monoubiquitinated FANCD2 at telomeres in ALT cells. *Nucleic Acids Res* 37: 1740 – 1754

Franco S, van de Vrugt HJ, Fernandez P, Aracil M, Arwert F, Blasco MA (2004) Telomere dynamics in Fancg-deficient mouse and human cells. *Blood* 104: 3927 – 3935

Friedman LS, Thistlethwaite FC, Patel KJ, Yu VP, Lee H, Venkitaraman AR, Abel KJ, Carlton MB, Hunter SM, Colledge WH, Evans MJ, Ponder BA (1998) Thymic lymphomas in mice with a truncating mutation in Brca2. *Cancer Res* 58: 1338 – 1343

Fu YV, Yardimci H, Long DT, Ho TV, Guainazzi A, Bermudez VP, Hurwitz J, van Oijen A, Scharer OD, Walter JC (2011) Selective bypass of a lagging strand roadblock by the eukaryotic replicative DNA helicase. *Cell* 146: 931 – 941

Garcia-Higuera I, Taniguchi T, Ganesan S, Meyn MS, Timmers C, Hejna J, Grompe M, D'Andrea AD (2001) Interaction of the Fanconi anemia proteins and BRCA1 in a common pathway. *Mol Cell* 7: 249 – 262

García-Rubio ML, Pérez-Calero C, Barroso SI, Tumini E, Herrera-Moyano E, Rosado IV, Aguilera A (2015) The Fanconi anemia pathway protects genome integrity from R-loops. *PLoS Genet* 11: e1005674

Gari K, Decaillet C, Delannoy M, Wu L, Constantinou A (2008) Remodeling of DNA replication structures by the branch point translocase FANCM. *Proc Natl Acad Sci USA* 105: 16107 – 16112

Gaymes TJ, Shall S, Farzaneh F, Mufti GJ (2008) Chromosomal instability syndromes are sensitive to poly ADP-ribose polymerase inhibitors. *Haematologica* 93: 1886 – 1889

Gibbs-Seymour I, Oka Y, Rajendra E, Weinert BT, Passmore LA, Patel KJ, Olsen JV, Choudhary C, Bekker-Jensen S, Mailand N (2015) Ubiquitin-SUMO circuitry controls activated fanconi anemia ID complex dosage in response to DNA damage. *Mol Cell* 57: 150 – 164

Godthelp BC, Wiegant WW, van Duijn-Goedhart A, Schärer OD, van Buul PPW, Kanaar R, Zdzienicka MZ (2002) Mammalian Rad51C contributes to DNA cross-link resistance, sister chromatid cohesion and genomic stability. *Nucleic Acids Res* 30: 2172 – 2182

Gong Z, Kim JE, Leung CC, Glover JN, Chen J (2010) BACH1/FANCJ acts with TopBP1 and participates early in DNA replication checkpoint control. *Mol Cell* 37: 438 – 446

Gupta R, Sharma S, Sommers JA, Kenny MK, Cantor SB, Brosh RM Jr (2007) FANCJ (BACH1) helicase forms DNA damage inducible foci with replication protein A and interacts physically and functionally with the single-stranded DNA-binding protein. *Blood* 110: 2390 – 2398

Hashimoto Y, Puddu F, Costanzo V (2012) RAD51- and MRE11-dependent reassembly of uncoupled CMG helicase complex at collapsed replication forks. *Nat Struct Mol Biol* 19: 17 – 24

Hatchi E, Skourti-Stathaki K, Ventz S, Pinello L, Yen A, Kamieniarz-Gdula K, Dimitrov S, Pathania S, McKinney Kristine M, Eaton Matthew L, Kellis M, Hill Sarah J, Parmigiani G, Proudfoot Nicholas J, Livingston David M (2015) BRCA1 recruitment to transcriptional pause sites is required for R-loop-driven DNA damage repair. *Mol Cell* 57: 636 – 647

Hira A, Yoshida K, Sato K, Okuno Y, Shiraishi Y, Chiba K, Tanaka H, Miyano S, Shimamoto A, Tahara H, Ito E, Kojima S, Kurumizaka H, Ogawa S, Takata M, Yabe H, Yabe M (2015) Mutations in the gene encoding the E2 conjugating enzyme UBE2T cause Fanconi anemia. *Am J Hum Genet* 96: 1001 – 1007

Howlett NG, Taniguchi T, Durkin SG, D'Andrea AD, Glover TW (2005) The Fanconi anemia pathway is required for the DNA replication stress response and for the regulation of common fragile site stability. *Hum Mol Genet* 14: 693 – 701

Howlett NG, Taniguchi T, Olson S, Cox B, Waisfisz Q, De Die-Smulders C, Persky N, Grompe M, Joenje H, Pals G, Ikeda H, Fox EA, D'Andrea AD (2002) Biallelic inactivation of BRCA2 in Fanconi anemia. *Science* 297: 606 – 609

Huang M, Kim JM, Shiotani B, Yang K, Zou L, D'Andrea AD (2010) The FANCM/FAAP24 complex is required for the DNA interstrand crosslink-induced checkpoint response. *Mol Cell* 39: 259 – 268

Hussain S, Wilson JB, Medhurst AL, Hejna J, Witt E, Ananth S, Davies A, Masson JY, Moses R, West SC, de Winter JP, Ashworth A, Jones NJ, Mathew CG (2004) Direct interaction of FANCD2 with BRCA2 in DNA damage response pathways. *Hum Mol Genet* 13: 1241 – 1248

Ilves I, Petojevic T, Pesavento JJ, Botchan MR (2010) Activation of the MCM2-7 helicase by association with Cdc45 and GINS proteins. *Mol Cell* 37: 247 – 258

Jackson SP, Durocher D (2013) Regulation of DNA damage responses by ubiquitin and SUMO. *Mol Cell* 49: 795 – 807

Jensen RB, Ozes A, Kim T, Estep A, Kowalczykowski SC (2013) BRCA2 is epistatic to the RAD51 paralogs in response to DNA damage. *DNA Repair* 12: 306 – 311

 © 2016 The Authors

Joenje H, Patel KJ (2001) The emerging genetic and molecular basis of Fanconi anaemia. *Nat Rev Genet* 2: 446 – 459

Jonkers J, Meuwissen R, van der Gulden H, Peterse H, van der Valk M, Berns A (2001) Synergistic tumor suppressor activity of BRCA2 and p53 in a conditional mouse model for breast cancer. *Nat Genet* 29: 418 – 425

Kalb R, Duerr M, Wagner M, Herterich S, Gross M, Digweed M, Joenje H, Hoehn H, Schindler D (2004) Lack of sensitivity of primary Fanconi's anemia fibroblasts to UV and ionizing radiation. *Radiat Res* 161: 318 – 325

Kashiyama K, Nakazawa Y, Pilz DT, Guo C, Shimada M, Sasaki K, Fawcett H, Wing JF, Lewin SO, Carr L, Li T-S, Yoshiura K, Utani A, Hirano A, Yamashita S, Greenblatt D, Nardo T, Stefanini M, McGibbon D, Sarkany R *et al* (2013) Malfunction of nuclease ERCC1-XPF results in diverse clinical manifestations and causes cockayne syndrome, Xeroderma pigmentosum, and Fanconi anemia. *Am J Hum Genet* 92: 807 – 819

Kee Y, D'Andrea AD (2010) Expanded roles of the Fanconi anemia pathway in preserving genomic stability. *Genes Dev* 24: 1680 – 1694

Kiiski JI, Pelttari LM, Khan S, Freysteinsdottir ES, Reynisdottir I, Hart SN, Shimelis H, Vilske S, Kallioniemi A, Schleutker J, Leminen A, Bützow R, Blomqvist C, Barkardottir RB, Couch FJ, Aittomäki K, Nevanlinna H (2014) Exome sequencing identifies FANCM as a susceptibility gene for triple-negative breast cancer. *Proc Natl Acad Sci USA* 111: 15172 – 15177

Kim H, D'Andrea AD (2012) Regulation of DNA cross-link repair by the Fanconi anemia/BRCA pathway. *Genes Dev* 26: 1393 – 1408

Kim Y, Lach FP, Desetty R, Hanenberg H, Auerbach AD, Smogorzewska A (2011) Mutations of the SLX4 gene in Fanconi anemia. *Nat Genet* 43: 142 – 146

Kim Y, Spitz GS, Veturi U, Lach FP, Auerbach AD, Smogorzewska A (2013) Regulation of multiple DNA repair pathways by the Fanconi anemia protein SLX4. *Blood* 121: 54 – 63

King M-C, Marks J, Mandell J (2003) Breast and ovarian cancer risks due to inherited mutations in BRCA1 and BRCA2. *Science* 302: 643 – 646

Klein Douwel D, Boonen RA, Long DT, Szypowska AA, Raschle M, Walter JC, Knipscheer P (2014) XPF-ERCC1 acts in Unhooking DNA interstrand crosslinks in cooperation with FANCD2 and FANCP/SLX4. *Mol Cell* 54: 460 – 471

Kottemann MC, Smogorzewska A (2013) Fanconi anaemia and the repair of Watson and Crick DNA crosslinks. *Nature* 493: 356 – 363

Kruisselbrink E, Guryev V, Brouwer K, Pontier DB, Cuppen E, Tijsterman M (2008) Mutagenic capacity of endogenous G4 DNA underlies genome instability in FANCJ-defective *C. elegans*. *Curr Biol* 18: 900 – 905

Kutler DI, Singh B, Satagopan J, Batish SD, Berwick M, Giampietro PF, Hanenberg H, Auerbach AD (2003) A 20-year perspective on the International Fanconi Anemia Registry (IFAR). *Blood* 101: 1249 – 1256

Langevin F, Crossan GP, Rosado IV, Arends MJ, Patel KJ (2011) Fancd2 counteracts the toxic effects of naturally produced aldehydes in mice. *Nature* 475: 53 – 58

Levitus M, Waisfisz Q, Godthelp BC, de Vries Y, Hussain S, Wiegant WW, Elghalbzouri-Maghrani E, Steltenpool J, Rooimans MA, Pals G, Arwert F, Mathew CG, Zdzienicka MZ, Hiom K, De Winter JP, Joenje H (2005) The DNA helicase BRIP1 is defective in Fanconi anemia complementation group. *J Nat Genet* 37: 934 – 935

Levran O, Attwooll C, Henry RT, Milton KL, Neveling K, Rio P, Batish SD, Kalb R, Velleuer E, Barral S, Ott J, Petrini J, Schindler D, Hanenberg H, Auerbach AD (2005) The BRCA1-interacting helicase BRIP1 is deficient in Fanconi anemia. *Nat Genet* 37: 931 – 933

Litman R, Peng M, Jin Z, Zhang F, Zhang J, Powell S, Andreassen PR, Cantor SB (2005) BACH1 is critical for homologous recombination and appears to be the Fanconi anemia gene product FANCJ. *Cancer Cell* 8: 255 – 265

Lomonosov M, Anand S, Sangrithi M, Davies R, Venkitaraman AR (2003) Stabilization of stalled DNA replication forks by the BRCA2 breast cancer susceptibility protein. *Genes Dev* 17: 3017 – 3022

London TB, Barber LJ, Mosedale G, Kelly GP, Balasubramanian S, Hickson ID, Boulton SJ, Hiom K (2008) FANCJ is a structure-specific DNA helicase associated with the maintenance of genomic G/C tracts. *J Biol Chem* 283: 36132 – 36139

Long DT, Joukov V, Budzowska M, Walter JC (2014) BRCA1 promotes unloading of the CMG helicase from a stalled DNA replication fork. *Mol Cell* 56: 174 – 185

Long DT, Raschle M, Joukov V, Walter JC (2011) Mechanism of RAD51-dependent DNA interstrand cross-link repair. *Science* 333: 84 – 87

Lossaint G, Larroque M, Ribeyre C, Bec N, Larroque C, Decaillet C, Gari K, Constantinou A (2013) FANCD2 binds MCM proteins and controls replisome function upon activation of s phase checkpoint signaling. *Mol Cell* 51: 678 – 690

Luke-Glaser S, Luke B, Grossi S, Constantinou A (2010) FANCM regulates DNA chain elongation and is stabilized by S-phase checkpoint signalling. *EMBO J* 29: 795 – 805

Machida YJ, Machida Y, Chen Y, Gurtan AM, Kupfer GM, D'Andrea AD, Dutta A (2006) UBE2T is the E2 in the *Fanconi anemia* pathway and undergoes negative autoregulation. *Mol Cell* 23: 589 – 596

Matsuzaki K, Borel V, Adelman CA, Schindler D, Boulton SJ (2015) FANCJ suppresses microsatellite instability and lymphomagenesis independent of the Fanconi anemia pathway. *Genes Dev* 29: 2532 – 2546

Meetei AR, de Winter JP, Medhurst AL, Wallisch M, Waisfisz Q, van de Vrugt HJ, Oostra AB, Yan Z, Ling C, Bishop CE, Hoatlin ME, Joenje H, Wang W (2003) A novel ubiquitin ligase is deficient in Fanconi anemia. *Nat Genet* 35: 165 – 170

Meetei AR, Levitus M, Xue Y, Medhurst AL, Zwaan M, Ling C, Rooimans MA, Bier P, Hoatlin M, Pals G, de Winter JP, Wang W, Joenje H (2004) X-linked inheritance of *Fanconi anemia* complementation group B. *Nat Genet* 36: 1219 – 1224

Meetei AR, Medhurst AL, Ling C, Xue Y, Singh TR, Bier P, Steltenpool J, Stone S, Dokal I, Mathew CG, Hoatlin M, Joenje H, de Winter JP, Wang W (2005) A human ortholog of archaeal DNA repair protein Hef is defective in Fanconi anemia complementation group M. *Nat Genet* 37: 958 – 963

Meindl A, Hellebrand H, Wiek C, Erven V, Wappenschmidt B, Niederacher D, Freund M, Lichtner P, Hartmann L, Schaal H, Ramser J, Honisch E, Kubisch C, Wichmann HE, Kast K, Deissler H, Engel C, Muller-Myhsok B, Neveling K, Kiechle M *et al* (2010) Germline mutations in breast and ovarian cancer pedigrees establish RAD51C as a human cancer susceptibility gene. *Nat Genet* 42: 410 – 414

Mimitou EP, Symington LS (2011) DNA end resection–unraveling the tail. *DNA Repair* 10: 344 – 348

Mosedale G, Niedzwiedz W, Alpi A, Perrina F, Pereira-Leal JB, Johnson M, Langevin F, Pace P, Patel KJ (2005) The vertebrate Hef ortholog is a component of the Fanconi anemia tumor-suppressor pathway. *Nat Struct Mol Biol* 12: 763 – 771

Moynahan ME, Pierce AJ, Jasin M (2001) BRCA2 is required for homology-directed repair of chromosomal breaks. *Mol Cell* 7: 263 – 272

Naim V, Rosselli F (2009) The FANC pathway and BLM collaborate during mitosis to prevent micro-nucleation and chromosome abnormalities. *Nat Cell Biol* 11: 761 – 768

Nakanishi K, Taniguchi T, Ranganathan V, New HV, Moreau LA, Stotsky M, Mathew CG, Kastan MB, Weaver DT, D'Andrea AD (2002) Interaction of FANCD2 and NBS1 in the DNA damage response. *Nat Cell Biol* 4: 913 – 920

© 2016 The Authors

Nakanishi K, Yang YG, Pierce AJ, Taniguchi T, Digweed M, D'Andrea AD, Wang ZQ, Jasin M (2005) Human Fanconi anemia monoubiquitination pathway promotes homologous DNA repair. *Proc Natl Acad Sci USA* 102: 1110 – 1115

Navarro S, Meza NW, Quintana-Bustamante O, Casado JA, Jacome A, McAllister K, Puerto S, Surralles J, Segovia JC, Bueren JA (2006) Hematopoietic dysfunction in a mouse model for Fanconi anemia group D1. *Mol Ther* 14: 525 – 535

Nimonkar AV, Genschel J, Kinoshita E, Polaczek P, Campbell JL, Wyman C, Modrich P, Kowalczykowski SC (2011) BLM-DNA2-RPA-MRN and EXO1-BLM-RPA-MRN constitute two DNA end resection machineries for human DNA break repair. *Genes Dev* 25: 350 – 362

Ohashi A, Zdzienicka MZ, Chen J, Couch FJ (2005) Fanconi anemia complementation group D2 (FANCD2) functions independently of BRCA2- and RAD51-associated homologous recombination in response to DNA damage. *J Biol Chem* 280: 14877 – 14883

Orthwein A, Noordermeer SM, Wilson MD, Landry S, Enchev RI, Sherker A, Munro M, Pinder J, Salsman J, Dellaire G, Xia B, Peter M, Durocher D (2015) A mechanism for the suppression of homologous recombination in G1 cells. *Nature* 528: 422 – 426

Patel KJ, Yu VP, Lee H, Corcoran A, Thistlethwaite FC, Evans MJ, Colledge WH, Friedman LS, Ponder BA, Venkitaraman AR (1998) Involvement of Brca2 in DNA repair. *Mol Cell* 1: 347 – 357

Peterlongo P, Catucci I, Colombo M, Caleca L, Mucaki E, Bogliolo M, Marin M, Damiola F, Bernard L, Pensotti V, Volorio S, Dall'Olio V, Meindl A, Bartram C, Sutter C, Surowy H, Sornin V, Dondon MG, Eon-Marchais S, Stoppa-Lyonnet D *et al* (2015) FANCM c.5791C>T nonsense mutation (rs144567652) induces exon skipping, affects DNA repair activity and is a familial breast cancer risk factor. *Hum Mol Genet* 24: 5345 – 5355

Peto J, Collins N, Barfoot R, Seal S, Warren W, Rahman N, Easton DF, Evans C, Deacon J, Stratton MR (1999) Prevalence of BRCA1 and BRCA2 gene mutations in patients with early-onset breast cancer. *J Natl Cancer Inst* 91: 943 – 949

Pontel LB, Rosado IV, Burgos-Barragan G, Garaycoechea JI, Yu R, Arends MJ, Chandrasekaran G, Broecker V, Wei W, Liu L, Swenberg JA, Crossan GP, Patel KJ (2015) Endogenous formaldehyde is a hematopoietic stem cell genotoxin and metabolic carcinogen. *Mol Cell* 60: 177 – 188

Powell SN, Xia F, Zhang J, Feng Z (2002) Breast cancer cells with deficiencies in BRCA1/BRCA2 show hypersensitivity to mitomycin C. *Int J Radiat Oncol* 54: 52

Rafnar T, Gudbjartsson DF, Sulem P, Jonasdottir A, Sigurdsson A, Besenbacher S, Lundin P, Stacey SN, Gudmundsson J, Magnusson OT, le Roux L, Orlygsdottir G, Helgadottir HT, Johannsdottir H, Gylfason A, Tryggvadottir L, Jonasson JG, de Juan A, Ortega E, Ramon-Cajal JM *et al* (2011) Mutations in BRIP1 confer high risk of ovarian cancer. *Nat Genet* 43: 1104 – 1107

Rajendra E, Oestergaard Vibe H, Langevin F, Wang M, Dornan Gillian L, Patel Ketan J, Passmore Lori A (2014) The genetic and biochemical basis of FANCD2 monoubiquitination. *Mol Cell* 54: 858 – 869

Raschle M, Smeenk G, Hansen RK, Temu T, Oka Y, Hein MY, Nagaraj N, Long DT, Walter JC, Hofmann K, Storchova Z, Cox J, Bekker-Jensen S, Mailand N, Mann M (2015) DNA repair. Proteomics reveals dynamic assembly of repair complexes during bypass of DNA cross-links. *Science* 348: 1253671

Reid S, Schindler D, Hanenberg H, Barker K, Hanks S, Kalb R, Neveling K, Kelly P, Seal S, Freund M, Wurm M, Batish SD, Lach FP, Yetgin S, Neitzel H, Ariffin H, Tischkowitz M, Mathew CG, Auerbach AD, Rahman N (2007) Biallelic mutations in PALB2 cause Fanconi anemia subtype FA-N and predispose to childhood cancer. *Nat Genet* 39: 162 – 164

Reuter M, Zelensky A, Smal I, Meijering E, van Cappellen WA, de Gruiter HM, van Belle GJ, van Royen ME, Houtsmuller AB, Essers J, Kanaar R, Wyman C (2015) BRCA2 diffuses as oligomeric clusters with RAD51 and changes mobility after DNA damage in live cells. *J Cell Biol* 207: 599 – 613

Rhee DB, Wang Y, Mizesko M, Zhou F, Haneline L, Liu Y (2010) FANCC suppresses short telomere-initiated telomere sister chromatid exchange. *Hum Mol Genet* 19: 879 – 887

Rickman KA, Lach FP, Abhyankar A, Donovan FX, Sanborn EM, Kennedy JA, Sougnez C, Gabriel SB, Elemento O, Chandrasekharappa SC, Schindler D, Auerbach AD, Smogorzewska A (2015) Deficiency of UBE2T, the E2 ubiquitin ligase necessary for FANCD2 and FANCI ubiquitination, causes FA-T subtype of Fanconi anemia. *Cell Rep* 12: 35 – 41

Rottenberg S, Nygren AOH, Pajic M, van Leeuwen FWB, van der Heijden I, van de Wetering K, Liu X, de Visser KE, Gilhuijs KG, van Tellingen O, Schouten JP, Jonkers J, Borst P (2007) Selective induction of chemotherapy resistance of mammary tumors in a conditional mouse model for hereditary breast cancer. *Proc Natl Acad Sci USA* 104: 12117 – 12122

Roy R, Chun J, Powell SN (2012) BRCA1 and BRCA2: different roles in a common pathway of genome protection. *Nat Rev Cancer* 12: 68 – 78

Rutter JL, Smith AM, Davila MR, Sigurdson AJ, Giusti RM, Pineda MA, Doody MM, Tucker MA, Greene MH, Zhang J, Struewing JP (2003) Mutational analysis of the BRCA1-interacting genes ZNF350/ZBRK1 and BRIP1/BACH1 among BRCA1 and BRCA2-negative probands from breast-ovarian cancer families and among early-onset breast cancer cases and reference individuals. *Hum Mutat* 22: 121 – 128

Sakai W, Swisher EM, Karlan BY, Agarwal MK, Higgins J, Friedman C, Villegas E, Jacquemont C, Farrugia DJ, Couch FJ, Urban N, Taniguchi T (2008) Secondary mutations as a mechanism of cisplatin resistance in BRCA2-mutated cancers. *Nature* 451: 1116 – 1120

Sarkies P, Murat P, Phillips LG, Patel KJ, Balasubramanian S, Sale JE (2012) FANCJ coordinates two pathways that maintain epigenetic stability at G-quadruplex DNA. *Nucleic Acids Res* 40: 1485 – 1498

Sawyer SL, Tian L, Kahkonen M, Schwartzentruber J, Kircher M, Majewski J, Dyment DA, Innes AM, Boycott KM, Moreau LA, Moilanen JS, Greenberg RA (2015) Biallelic mutations in BRCA1 cause a new Fanconi anemia subtype. *Cancer Discov* 5: 135 – 142

Schlacher K, Christ N, Siaud N, Egashira A, Wu H, Jasin M (2011) Double-strand break repair-independent role for BRCA2 in blocking stalled replication fork degradation by MRE11. *Cell* 145: 529 – 542

Schlacher K, Wu H, Jasin M (2012) A distinct replication fork protection pathway connects Fanconi anemia tumor suppressors to RAD51-BRCA1/2. *Cancer Cell* 22: 106 – 116

Schwab RA, Blackford AN, Niedzwiedz W (2010) ATR activation and replication fork restart are defective in FANCM-deficient cells. *EMBO J* 29: 806 – 818

Schuster B, Knies K, Stoepker C, Velleuer E, Friedl R, Gottwald-Mühlhauser B, de Winter JP, Schindler D (2013) Whole exome sequencing reveals uncommon mutations in the recently identified *Fanconi anemia* gene SLX4/FANCP. *Hum Mutat* 34: 93 – 96

Schwab RA, Nieminuszczy J, Shah F, Langton J, Lopez Martinez D, Liang C-C, Cohn Martin A, Gibbons Richard J, Deans Andrew J, Niedzwiedz W (2015) The Fanconi anemia pathway maintains genome stability by coordinating replication and transcription. *Mol Cell* 60: 351 – 361

Schwab RA, Nieminuszczy J, Shin-ya K, Niedzwiedz W (2013) FANCJ couples replication past natural fork barriers with maintenance of chromatin structure. *J Cell Biol* 201: 33 – 48

 © 2016 The Authors

Seal S, Thompson D, Renwick A, Elliott A, Kelly P, Barfoot R, Chagtai T, Jayatilake H, Ahmed M, Spanova K, North B, McGuffog L, Evans DG, Eccles D, Easton DF, Stratton MR, Rahman N (2006) Truncating mutations in the Fanconi anemia J gene BRIP1 are low-penetrance breast cancer susceptibility alleles. *Nat Genet* 38: 1239 – 1241

Sims AE, Spiteri E, Sims RJ 3rd, Arita AG, Lach FP, Landers T, Wurm M, Freund M, Neveling K, Hanenberg H, Auerbach AD, Huang TT (2007) FANCI is a second monoubiquitinated member of the *Fanconi anemia* pathway. *Nat Struct Mol Biol* 14: 564 – 567

Sirbu BM, McDonald WH, Dungrawala H, Badu-Nkansah A, Kavanaugh GM, Chen Y, Tabb DL, Cortez D (2013) Identification of proteins at active, stalled, and collapsed replication forks using isolation of proteins on nascent DNA (iPOND) coupled with mass spectrometry. *J Biol Chem* 288: 31458 – 31467

Skoulidis F, Cassidy LD, Pisupati V, Jonasson JG, Bjarnason H, Eyfjord JE, Karreth FA, Lim M, Barber LM, Clatworthy SA, Davies SE, Olive KP, Tuveson DA, Venkitaraman AR (2010) Germline Brca2 heterozygosity promotes KrasG12D - driven carcinogenesis in a murine model of familial pancreatic cancer. *Cancer Cell* 18: 499 – 509

Smogorzewska A, Matsuoka S, Vinciguerra P, McDonald ER 3rd, Hurov KE, Luo J, Ballif BA, Gygi SP, Hofmann K, D'Andrea AD, Elledge SJ (2007) Identification of the FANCI protein, a monoubiquitinated FANCD2 paralog required for DNA repair. *Cell* 129: 289 – 301

Strathdee CA, Gavish H, Shannon WR, Buchwald M (1992) Cloning of cDNAs for Fanconi's anaemia by functional complementation. *Nature* 356: 763 – 767

Stoepker C, Hain K, Schuster B, Hilhorst-Hofstee Y, Rooimans MA, Steltenpool J, Oostra AB, Eirich K, Korthof ET, Nieuwint AW, Jaspers NG, Bettecken T, Joenje H, Schindler D, Rouse J, de Winter JP (2011) SLX4, a coordinator of structure-specific endonucleases, is mutated in a new Fanconi anemia subtype. *Nat Genet* 43: 138 – 141

Suwaki N, Klare K, Tarsounas M (2011) RAD51 paralogs: roles in DNA damage signalling, recombinational repair and tumorigenesis. *Semin Cell Dev Biol* 22: 898 – 905

Tacconi EM, Tarsounas M (2015) How homologous recombination maintains telomere integrity. *Chromosoma* 124: 119 – 130

Taniguchi T, Garcia-Higuera I, Andreassen PR, Gregory RC, Grompe M, Andrea AD (2002) S-phase–specific interaction of the Fanconi anemia protein, FANCD2, with BRCA1 and RAD51. *Blood* 100: 2414 – 2420

Timmers C, Taniguchi T, Hejna J, Reifsteck C, Lucas L, Bruun D, Thayer M, Cox B, Olson S, D'Andrea AD, Moses R, Grompe M (2001) Positional cloning of a novel *Fanconi anemia* gene, FANCD2. *Mol Cell* 7: 241 – 248

Tsang E, Carr AM (2008) Replication fork arrest, recombination and the maintenance of ribosomal DNA stability. *DNA Repair (Amst)* 7: 1613 – 1623

Vaz F, Hanenberg H, Schuster B, Barker K, Wiek C, Erven V, Neveling K, Endt D, Kesterton I, Autore F, Fraternali F, Freund M, Hartmann L, Grimwade D, Roberts RG, Schaal H, Mohammed S, Rahman N, Schindler D, Mathew CG (2010) Mutation of the RAD51C gene in a Fanconi anemia-like disorder. *Nat Genet* 42: 406 – 409

Venkitaraman AR (2009) Linking the cellular functions of BRCA genes to cancer pathogenesis and treatment. *Annu Rev Pathol* 4: 461 – 487

Virts EL, Jankowska A, Mackay C, Glaas MF, Wiek C, Kelich SL, Lottmann N, Kennedy FM, Marchal C, Lehnert E, Scharf RE, Dufour C, Lanciotti M, Farruggia P, Santoro A, Savasan S, Scheckenbach K, Schipper J, Wagenmann M, Lewis T *et al* (2015) AluY-mediated germline deletion, duplication and somatic stem cell reversion in UBE2T defines a new subtype of *Fanconi anemia*. *Hum Mol Genet* 24: 5093 – 5108

Wagner JE, Tolar J, Levran O, Scholl T, Deffenbaugh A, Satagopan J, Ben-Porat L, Mah K, Batish SD, Kutler DI, MacMillan ML, Hanenberg H, Auerbach AD (2004) Germline mutations in BRCA2: shared genetic susceptibility to breast cancer, early onset leukemia, and Fanconi anemia. *Blood* 103: 3226 – 3229

Wang X, Andreassen PR, D'Andrea AD (2004) Functional interaction of monoubiquitinated FANCD2 and BRCA2/FANCD1 in chromatin. *Mol Cell Biol* 24: 5850 – 5862

Wang AT, Kim T, Wagner JE, Conti BA, Lach FP, Huang AL, Molina H, Sanborn EM, Zierhut H, Cornes BK, Abhyankar A, Sougnez C, Gabriel SB, Auerbach AD, Kowalczykowski SC, Smogorzewska A (2015) A dominant mutation in human RAD51 reveals its function in DNA interstrand crosslink repair independent of homologous recombination. *Mol Cell* 59: 478 – 490

Wang AT, Smogorzewska A (2015) SnapShot: Fanconi anemia and associated proteins. *Cell* 160: 354-354.e1

de Winter JP, Rooimans MA, van Der Weel L, van Berkel CG, Alon N, Bosnoyan-Collins L, de Groot J, Zhi Y, Waisfisz Q, Pronk JC, Arwert F, Mathew CG, Scheper RJ, Hoatlin ME, Buchwald M, Joenje H (2000) The *Fanconi anaemia* gene FANCF encodes a novel protein with homology to ROM. *Nat Genet* 24: 15 – 16

Wu Y, Shin-ya K, Brosh RM Jr (2008) FANCJ helicase defective in Fanconia anemia and breast cancer unwinds G-quadruplex DNA to defend genomic stability. *Mol Cell Biol* 28: 4116 – 4128

Xia B, Dorsman JC, Ameziane N, de Vries Y, Rooimans MA, Sheng Q, Pals G, Errami A, Gluckman E, Llera J, Wang W, Livingston DM, Joenje H, de Winter JP (2006a) Fanconi anemia is associated with a defect in the BRCA2 partner PALB2. *Nat Genet* 39: 159 – 161

Xia B, Sheng Q, Nakanishi K, Ohashi A, Wu J, Christ N, Liu X, Jasin M, Couch FJ, Livingston DM (2006b) Control of BRCA2 cellular and clinical functions by a nuclear partner, PALB2. *Mol Cell* 22: 719 – 729

Xu X, Wagner K-U, Larson D, Weaver Z, Li C, Ried T, Hennighausen L, Wynshaw-Boris A, Deng C-X (1999) Conditional mutation of Brca1 in mammary epithelial cells results in blunted ductal morphogenesis and tumour formation. *Nat Genet* 22: 37 – 43

Youds JL, Barber LJ, Ward JD, Collis SJ, O'Neil NJ, Boulton SJ, Rose AM (2007) DOG-1 is the *Caenorhabditis elegans* BRIP1/FANCJ homologue and functions in interstrand cross-link repair. *Mol Cell Biol* 28: 1470 – 1479

Zeman MK, Cimprich KA (2014) Causes and consequences of replication stress. *Nat Cell Biol* 16: 2 – 9

Zhang F, Fan Q, Ren K, Auerbach AD, Andreassen PR (2010) FANCJ/BRIP1 recruitment and regulation of FANCD2 in DNA damage responses. *Chromosoma* 119: 637 – 649

Zhang J, Walter JC (2014) Mechanism and regulation of incisions during DNA interstrand cross-link repair. *DNA Repair* 19: 135 – 142

Zheng Y, Zhang J, Hope K, Niu Q, Huo D, Olopade O (2010) Screening RAD51C nucleotide alterations in patients with a family history of breast and ovarian cancer. *Breast Cancer Res Treat* 124: 857 – 861

Zimmer J, Tacconi EM, Folio C, Badie S, Porru M, Klare K, Tumiati M, Markkanen E, Halder S, Ryan A, Jackson SP, Ramadan K, Kuznetsov SG, Biroccio A, Sale JE, Tarsounas M (2016) Targeting BRCA1 and BRCA2 deficiencies with G-quadruplex-interacting compounds. *Mol Cell* 61: 449 – 460

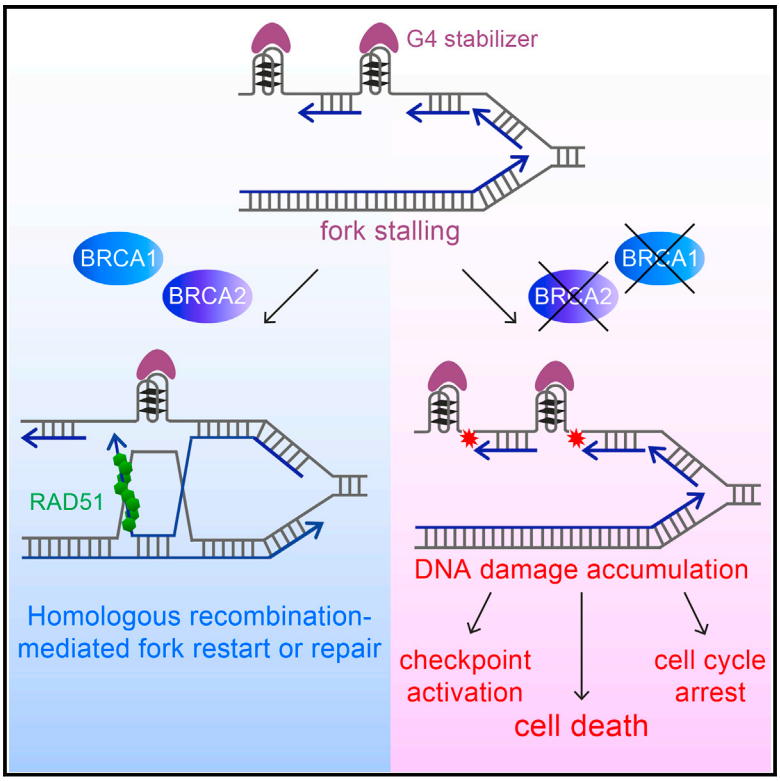
License: This is an open access article under the terms of the Creative Commons Attribution 4.0 License, which permits use, distribution and reproduction in any medium, provided the original work is properly cited.

Article

Molecular Cell

Targeting BRCA1 and BRCA2 Deficiencies with G-Quadruplex-Interacting Compounds

Graphical Abstract



Highlights

- G4 formation on the G-rich strand drives telomere fragility in HR-deficient cells
- G4-stabilizing compounds reduce viability of cells lacking BRCA1, BRCA2, or RAD51
- G4 toxicity stems from excessive replication stress and DNA damage accumulation
- Olaparib-resistant, BRCA-defective cells are sensitive to G4-stabilizing compounds

Authors

Jutta Zimmer, Eliana M.C. Tacconi, Cecilia Folio, ..., Annamaria Biroccio, Julian E. Sale, Madalena Tarsounas

Correspondence

madalena.tarsounas@oncology.ox.ac.uk

In Brief

Zimmer et al. discovered that homologous recombination activities of BRCA1 and BRCA2 facilitate replication of genomic regions with G-quadruplex-forming potential, including telomeres, and suppress genomic instability stemming from inefficient replication of these sites. G4-stabilizing compounds are toxic to BRCA1- and BRCA2-deficient cells, highlighting their therapeutic potential in targeting BRCA deficiency.

Zimmer et al., 2016, Molecular Cell *61*, 449–460
February 4, 2016 ©2016 The Authors
http://dx.doi.org/10.1016/j.molcel.2015.12.004

Molecular Cell
Article

Targeting BRCA1 and BRCA2 Deficiencies with G-Quadruplex-Interacting Compounds

Jutta Zimmer,[1] Eliana M.C. Tacconi,[1] Cecilia Folio,[1] Sophie Badie,[1] Manuela Porru,[2] Kerstin Klare,[1,10] Manuela Tumiati,[3] Enni Markkanen,[4,11] Swagata Halder,[5] Anderson Ryan,[6] Stephen P. Jackson,[7,8] Kristijan Ramadan,[5] Sergey G. Kuznetsov,[3] Annamaria Biroccio,[2] Julian E. Sale,[9] and Madalena Tarsounas[1,*]

[1]Genome Stability and Tumourigenesis Group, CRUK/MRC Oxford Institute for Radiation Oncology, Department of Oncology, University of Oxford, Old Road Campus Research Building, Oxford OX3 7DQ, UK
[2]Area of Translational Research, Regina Elena National Cancer Institute, 00144 Rome, Italy
[3]Institute for Molecular Medicine Finland (FIMM), University of Helsinki, P.O. Box 20, FIN-00014 Helsinki, Finland
[4]Biochemistry and Regulation of DNA Repair Group, CRUK/MRC Oxford Institute for Radiation Oncology, Department of Oncology, University of Oxford, Old Road Campus Research Building, Oxford OX3 7DQ, UK
[5]DNA Damage and Repair Group, CRUK/MRC Oxford Institute for Radiation Oncology, Department of Oncology, University of Oxford, Old Road Campus Research Building, Oxford OX3 7DQ, UK
[6]Lung Cancer Translational Science Research Group, CRUK/MRC Oxford Institute for Radiation Oncology, Department of Oncology, University of Oxford, Old Road Campus Research Building, Oxford OX3 7DQ, UK
[7]The Gurdon Institute, CRUK Laboratories, University of Cambridge, Tennis Court Road, Cambridge CB2 1QN, UK
[8]The Sanger Institute, Hinxton, Cambridge CB10 1SA, UK
[9]Medical Research Council Laboratory of Molecular Biology, Francis Crick Avenue, Cambridge CB2 0QH, UK
[10]Present address: Department of Mechanistic Cell Biology, Max Planck Institute of Molecular Physiology, 44227 Dortmund, Germany
[11]Present address: Institute of Pharmacology and Toxicology, Vetsuisse Faculty, University of Zürich, 8006 Zürich, Switzerland
*Correspondence: madalena.tarsounas@oncology.ox.ac.uk
http://dx.doi.org/10.1016/j.molcel.2015.12.004
This is an open access article under the CC BY license (http://creativecommons.org/licenses/by/4.0/).

SUMMARY

G-quadruplex (G4)-forming genomic sequences, including telomeres, represent natural replication fork barriers. Stalled replication forks can be stabilized and restarted by homologous recombination (HR), which also repairs DNA double-strand breaks (DSBs) arising at collapsed forks. We have previously shown that HR facilitates telomere replication. Here, we demonstrate that the replication efficiency of guanine-rich (G-rich) telomeric repeats is decreased significantly in cells lacking HR. Treatment with the G4-stabilizing compound pyridostatin (PDS) increases telomere fragility in BRCA2-deficient cells, suggesting that G4 formation drives telomere instability. Remarkably, PDS reduces proliferation of HR-defective cells by inducing DSB accumulation, checkpoint activation, and deregulated G2/M progression and by enhancing the replication defect intrinsic to HR deficiency. PDS toxicity extends to HR-defective cells that have acquired olaparib resistance through loss of 53BP1 or REV7. Altogether, these results highlight the therapeutic potential of G4-stabilizing drugs to selectively eliminate HR-compromised cells and tumors, including those resistant to PARP inhibition.

INTRODUCTION

Genomic instability is a hallmark of cancer caused by failure of normal DNA replication and/or repair mechanisms (Halazonetis et al., 2008; Negrini et al., 2010). During replication, the enzymatic activities of DNA polymerases, helicases, and nucleases act in concert to assemble the active replication fork and to achieve high-fidelity duplication of the genome. Damaged DNA, secondary DNA structures, and DNA-protein complexes obstruct progression of replication forks, leading to fork stalling or, in more severe cases, to irreversible fork collapse and DNA breakage. Several mechanisms have evolved to overcome barriers to replication-fork movement, one of which exploits the HR DNA repair machinery. HR factors act to stabilize stalled replication forks by preventing their nucleolytic degradation (Hashimoto et al., 2010; Schlacher et al., 2011) to restart arrested forks (Lambert et al., 2010) and to repair double-strand breaks (DSBs) arising from disintegrated forks (Aze et al., 2013).

The tumor suppressor BRCA2 is a key component of the HR pathway of DSB repair. BRCA2 promotes recombination reactions by loading the RAD51 recombinase onto single-stranded DNA (ssDNA) in concert with the family of proteins known as the RAD51 paralogs, of which RAD51C is a member (Suwaki et al., 2011). RAD51-coated ssDNA invades an intact, homologous duplex DNA molecule, most commonly a sister chromatid, which becomes the template for accurate DSB repair.

In vitro, G-rich ssDNA can adopt secondary structures known as G4s under physiological-like conditions (Lipps and Rhodes, 2009). G4s consist of stacks of two or more G-quartets formed by four guanines via Hoogsteen base pairing stabilized by a monovalent cation. While in silico analyses have identified more than 300,000 sites with G4-forming potential in the human genome (Huppert and Balasubramanian, 2005), more recent G4-seq approaches enabled detection of more than 700,000 G4 structures genome-wide (Chambers et al., 2015). The first in vitro visualization of a G4 structure was based on diffraction

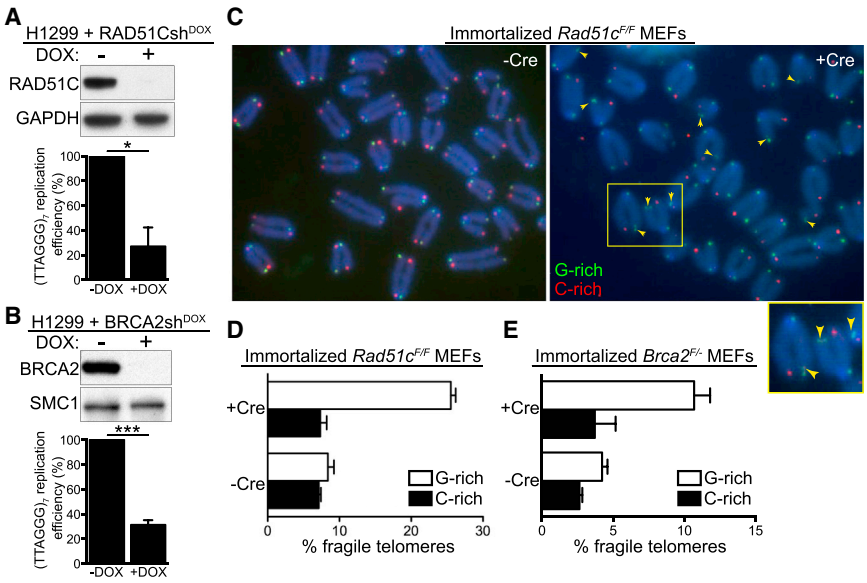


Figure 1. RAD51C and BRCA2 Prevent Lagging-Strand Telomere Fragility

(A and B) Replication efficiency of a plasmid containing $(TTAGGG)_7$ in H1299 cells expressing doxycycline (DOX)-inducible RAD51C (A) or BRCA2 (B) shRNAs is shown relative to the replication efficiency of the empty vector (n = 3 for $RAD51Csh^{DOX}$; n = 4 for $BRCA2sh^{DOX}$; error bars, SEM). p values were calculated using a one-sample t test (*$p \leq 0.05$ and ***$p \leq 0.001$). Cell extracts prepared at the time of plasmid transfection were immunoblotted as indicated. GAPDH and SMC1 were used as loading controls.

(C) CO-FISH detection of lagging (G-rich, green) and leading (C-rich, red) telomeric strands in immortalized $Rad51c^{F/F}$ MEFs treated with Cre (+Cre) and control (−Cre) retroviruses. Enlarged inset shows the area marked with the yellow rectangle. Arrows mark lagging-strand fragile telomeres.

(D and E) Quantification of fragile telomeres in immortalized $Rad51c^{F/F}$ (D) and $Brca2^{F/-}$ (E) MEFs. Approximately 1,000 telomeres were scored per condition per replica (n = 2; error bars, SD). See also Figure S1.

patterns of a guanylic acid solution (Gellert et al., 1962), while evidence that G4s assemble in vivo initially came from immunostaining of *Stylonychia* macronuclei with antibodies raised against G4 structures with telomere sequences (Schaffitzel et al., 2001). This study demonstrated that telomeres adopt a G4 configuration in vivo. G4 structures have been subsequently detected with several other structure-specific antibodies (Biffi et al., 2013; Henderson et al., 2014; Schaffitzel et al., 2001) and interacting small molecules (Lam et al., 2013; Müller et al., 2010; Rodriguez et al., 2012). Importantly, telomeric G-rich DNA sequences have a high propensity to adopt G4 configurations (Parkinson et al., 2002). Telomeres, repetitive DNA sequences bound by the protein complex shelterin, protect chromosome ends from degradation and fusion. Telomeric G4s can interfere with telomere replication, leading to fragile, shorter telomeres. Supporting this concept, treatment with G4-stabilizing compounds induces telomere dysfunction (Gomez et al., 2006; Rodriguez et al., 2008; Salvati et al., 2007; Tahara et al., 2006).

During DNA replication, G4s are thought to assemble spontaneously on G-rich ssDNA displaced during fork movement. Due to their thermodynamic stability, G4s cause uncoupling of replisome components and fork stalling, which have the potential to trigger genomic instability. Helicases such as FANCJ, PIF1, RECQ, BLM, and WRN, the chromatin remodeler ATRX, and the REV1 translesion polymerase act to dismantle G4s in vitro. Several lines of evidence support a similar function in vivo for these factors, essential to preserve genome stability during DNA replication (Murat and Balasubramanian, 2014). Conversely, G4 configurations can be stabilized by specific ligands that exhibit higher binding specificity for G4s over duplex DNA, with the G4-interacting compound PDS being one example (Chambers et al., 2015). In mammalian cells, G4 stabilization by PDS results in dissociation of shelterin components from telomeres (Rodriguez et al., 2008). More recently, PDS was demonstrated to trigger replication- and transcription-associated DNA damage at genomic sites with predicted G4-forming potential (Lam et al., 2013; Rodriguez et al., 2012). These findings highlight the deleterious consequences of persistent G4s for telomere and genome integrity.

HR factors, including BRCA2 and RAD51, are required to facilitate telomere replication and to prevent telomere shortening (Badie et al., 2010). It remained unclear, however, whether assembly of telomeric G4s could contribute to the telomere replication defect of HR-deficient cells. In this work, we demonstrate that telomere fragility in cells lacking HR repair is enhanced by PDS treatment. Importantly, G4-stabilizing compounds, including PDS, decrease the viability of BRCA1-, BRCA2-, or RAD51-deficient cells, which is associated with elevated levels of DNA damage and replication stress. We suggest that in the context of HR deficiency, persistent G4 structures exacerbate the cell-intrinsic challenges that arise during replication of regions with G4-forming potential, thus eliciting checkpoint activation, G2/M cell-cycle arrest, and cell death. This work is therefore highly relevant to the search for treatments that selectively kill tumor cells whose capacity for HR-mediated repair has been compromised.

RESULTS

BRCA2 and RAD51C Are Required for G-Rich Strand Telomere Replication

Abrogation of key HR activities elicits telomere fragility (Badie et al., 2010) suggestive of a role for HR in telomere replication. To further investigate this concept, we used a plasmid-based replication assay (Szüts et al., 2008) in H1299 cells harboring inducible small hairpin RNA (shRNA) against RAD51C or BRCA2. Doxycycline addition induced efficient depletion of both proteins, as determined by western blotting (Figures 1A and 1B). The replication efficiency of a plasmid containing an array of seven telomeric repeats $(TTAGGG)_7$ was significantly lower in RAD51C- or BRCA2-deficient cells compared to control

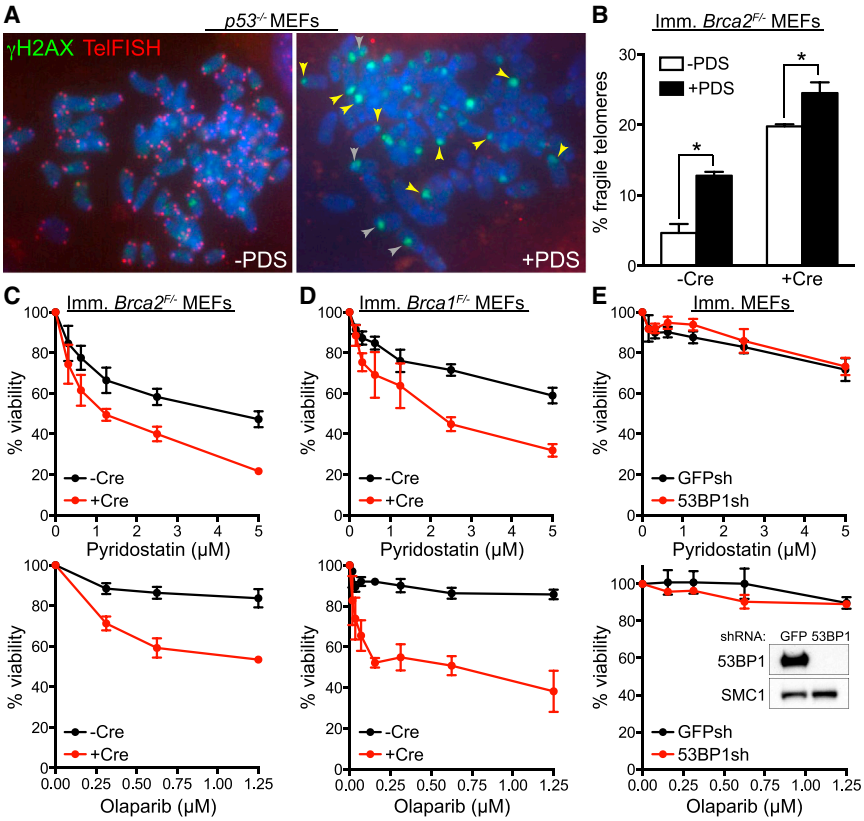


Figure 2. Effect of the G4-Interacting Compound PDS on Telomere Fragility and Viability of *Brca*-Deficient MEFs

(A) Mitotic chromosome spreads of $p53^{-/-}$ MEFs grown in the presence (+PDS) or absence (−PDS) of 5 μM PDS for 48 hr. Preparations were fixed and stained with anti-γH2AX monoclonal antibody (green). Telomeres were visualized with a Cy3-conjugated $(CCCTAA)_6$-PNA probe (red), using identical exposure conditions for untreated and PDS-treated cells. DNA was counterstained with DAPI (blue).

(B) Quantification of fragile telomeres visualized by FISH on metaphase chromosomes from $Brca2^{F/-}$ MEFs treated with Cre (+Cre) and control (−Cre) retroviruses incubated with 5 μM PDS for 40 hr (n = 2; > 1,500 long-arm telomeres were scored per condition per replica; error bars, SD). p values were calculated using an unpaired two-tailed t test (*$p \leq 0.05$).

(C) Dose-dependent viability assays of $Brca2^{F/-}$ MEFs treated with Cre (+Cre) and control (−Cre) retroviruses exposed to PDS or olaparib at the indicated concentrations.

(D) Dose-dependent viability assays of $Brca1^{F/-}$ MEFs treated as in (C).

(E) Dose-dependent viability assays of immortalized (imm.) MEFs treated as in (C) with retroviruses encoding shRNA against GFP or 53BP1 (Bouwman et al., 2010). Cell extracts were immunoblotted as indicated. SMC1 was used as a loading control. See also Figures S1 and S2. Graphs shown are representative of at least two independent experiments, each performed in triplicate. Error bars represent SD of triplicate values obtained from a single experiment.

cells (Figures 1A and 1B). RAD51C inhibition did not affect cell proliferation rate (Figure S1A, available online). Full-length human RAD51C rescued the telomere replication defect completely, indicating specificity of the shRNA for its target (Figure S1B). Importantly, replication of a plasmid containing a $(TTACGC)_7$ sequence, with two G-to-C substitutions in the telomere repeat, which abrogate the G4-forming potential of the sequence, was not affected by loss of RAD51C expression (Figure S1C). Collectively, these data suggest that assembly of G4 secondary structures on the telomere-containing plasmid underlines its inefficient replication in BRCA2- or RAD51C-depleted cells.

We previously reported that *Brca2* or *Rad51c* deletion in mouse embryonic fibroblasts (MEFs) leads to increased levels of multiple telomeric fluorescence in situ hybridization (FISH) signals (Badie et al., 2010), indicative of telomere fragility. To examine the specificity of the fragile telomere phenotype to the leading or lagging-strand template, chromosome orientation FISH (CO-FISH) assays were performed in immortalized $Brca2^{F/-}$ or $Rad51c^{F/F}$ MEFs, in which gene deletion was induced with "hit-and-run" Cre recombinase. The telomeric G-rich strand showed a clear propensity for FISH signal fragmentation (Figure 1C, green). Quantification of fragmented telomeric CO-FISH signals further demonstrated the bias toward fragility of the G-rich telomeric strand in Cre-treated $Brca2^{F/-}$ and $Rad51c^{F/F}$ MEFs (Figures 1D and 1E) as well as in a $Brca2^{-/-}$ mouse mammary tumor-derived cell line (Evers et al., 2010; Figure S1D).

G4 Structure Stabilization Exacerbates the Telomere Fragility in *Brca2*-Deleted MEFs

Telomere fragility indicates a telomere replication defect (Martínez et al., 2009; Sfeir et al., 2009), which is thought to stem from the potential of telomere DNA sequences to adopt G4 secondary structures known to obstruct replication fork progression. To test whether telomere fragility in HR-deficient cells was linked to G4 formation, we used the G4 ligand PDS (Rodriguez et al., 2008, 2012) to treat $p53^{-/-}$ MEFs, which are known to proliferate in the presence of DNA damage, followed by immunofluorescence combined with telomere FISH (IF-FISH) detection. Exposure to PDS led to accumulation of nuclear foci of the Ser139-phosphorylated form of histone H2AX (γH2AX, Figure 2A), a well-established DSB marker. A subset of these foci colocalized with chromosome ends (Figure 2A, yellow arrowheads), while others localized intrachromosomally (Figure 2A, gray arrowheads). A similar PDS effect has been reported in human cells (Rodriguez et al., 2012). In addition, PDS triggered a dramatic reduction in the intensity of telomere FISH signals corresponding to the G-rich telomere strand (Figures 2A and S1E). In these images, the same exposure time was used for image

acquisition of untreated and PDS-treated cells, to enable comparison of the telomeric signal intensity between the two samples. In contrast, in Figure 2B the exposure time was increased when acquiring images of PDS-treated samples (but not in untreated controls) in order to compensate for the reduced telomeric FISH signal and to enable quantification of fragile telomeres. G4 stabilization significantly enhanced the telomere fragility characteristic of *Brca2*-deleted MEFs (Figure 2B), suggesting that persistent G4 structures contribute to the telomere replication defect intrinsic to cells lacking BRCA2.

We next monitored the viability of *Brca2*-deleted MEFs grown in the presence of PDS or poly (ADP-ribose) polymerase 1 (PARP1) inhibitor olaparib. Even though PDS was moderately toxic to BRCA2-proficient MEFs, we detected a more prominent dose-dependent reduction in the viability of Cre-treated $Brca2^{F/-}$ MEFs exposed to this compound or olaparib (Figure 2C). The same specific elimination by PDS was observed for BRCA2-deficient V-C8 hamster cells (Kraakman-van der Zwet et al., 2002; Figure S2A) and $Brca2^{-/-}$ mouse mammary tumor-derived cells (Figure S2B).

The tumor suppressor BRCA1 plays a key role in HR by promoting end resection, which enables loading of the RAD51 recombinase and initiation of HR-mediated repair. This activity of BRCA1 is antagonized by 53BP1, which protects broken DNA ends and channels their repair into non-homologous end joining (NHEJ) (Bouwman et al., 2010; Bunting et al., 2010). To address whether NHEJ deficiency also sensitizes cells to G4 stabilizing agents, similarly to HR ablation, we tested whether *Brca1* or 53BP1 loss confers sensitivity to PDS. Only viability of *Brca1*-deleted cells was affected by exposure to PDS (Figures 2D and 2E), suggesting that G4 stabilization is specifically toxic to HR-, but not to NHEJ-compromised cells. A similar HR-specific effect was observed in response to olaparib (Figures 2D and 2E).

G4-Interacting Compounds Specifically Kill HR-Deficient Human Cells

To investigate whether PDS-induced G4 stabilization affects viability of human cells lacking BRCA2, we used a matched pair of BRCA2-proficient and deficient DLD1 colorectal adenocarcinoma cell lines (Hucl et al., 2008). Exposure of BRCA2-deficient DLD1 cells to PDS led to a marked decrease in viability compared to BRCA2-proficient cells within 3 days (Figure S2C), which became more pronounced after six days of treatment (Figure 3A). The PARP1 inhibitor olaparib was used as a control in these experiments based on its ability to preferentially kill BRCA2-deficient cells (Figure 3B). Importantly, PDS toxicity to cells lacking BRCA2 was recapitulated in clonogenic assays in which cells were exposed to the drug for only 24 hr (Figure S2D).

BRCA2 plays a central role in HR repair by recruiting RAD51 to the sites of DSBs ssDNA present at stalled replication forks to initiate strand-invasion reactions. We therefore investigated whether RAD51 deficiency sensitized cells to G4-interacting compounds, similarly to loss of BRCA2. Indeed, exposure to PDS caused a substantial drop in cell viability of HEK293T cells lacking RAD51 compared to control cells (Figures 3C and S2C). Olaparib reduced the viability of RAD51-depleted cells; however,

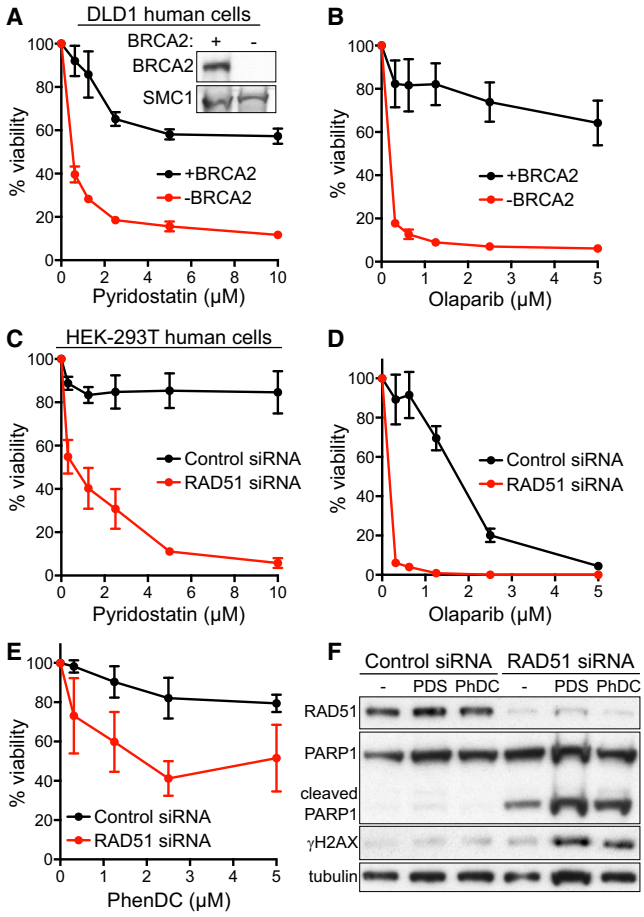


Figure 3. Effect of PDS on BRCA2- or RAD51-Deficient Human Cell Viability

(A and B) Dose-dependent viability assays of DLD1 cells, BRCA2 proficient (+BRCA2) or deficient (−BRCA2), treated with indicated concentrations of PDS (A) or olaparib (B).

(C–E) Dose-dependent viability assays of HEK293T cells transfected with control or RAD51 siRNA treated with indicated concentrations of PDS (C), olaparib (D), or PhenDC (E). Graphs shown are representative of at least two independent experiments, each performed in triplicate. Error bars represent SD of triplicate values obtained from a single experiment.

(F) Whole-cell extracts prepared after 4 days of treatment with 2 μM PDS or PhenDC (PhDC) were immunoblotted as indicated. Tubulin was used as a loading control. See also Figure S2.

it also exhibited toxicity against control cells (Figure 3D). Moreover, RAD51 depletion sensitized HEK293T cells to the G4 ligand PhenDC (Figure 3E; Piazza et al., 2010). In western blot analyses (Figure 3F), PDS and PhenDC both induced apoptosis specifically in RAD51-deficient cells, detected by cleaved PARP1 and γH2AX expression, a well-established marker for DNA damage that is also induced by apoptosis (Rogakou et al., 2000). Thus, treatment with G4-interacting agents elicits DNA damage leading to specific killing of cells lacking BRCA2 or RAD51. While PhenDC drastically reduced viability of $Brca1^{-/-}$ mouse tumor-derived cells (Figure S2E), its toxicity against BRCA2-deficient V-C8 cells was rather modest (Figure S2A).

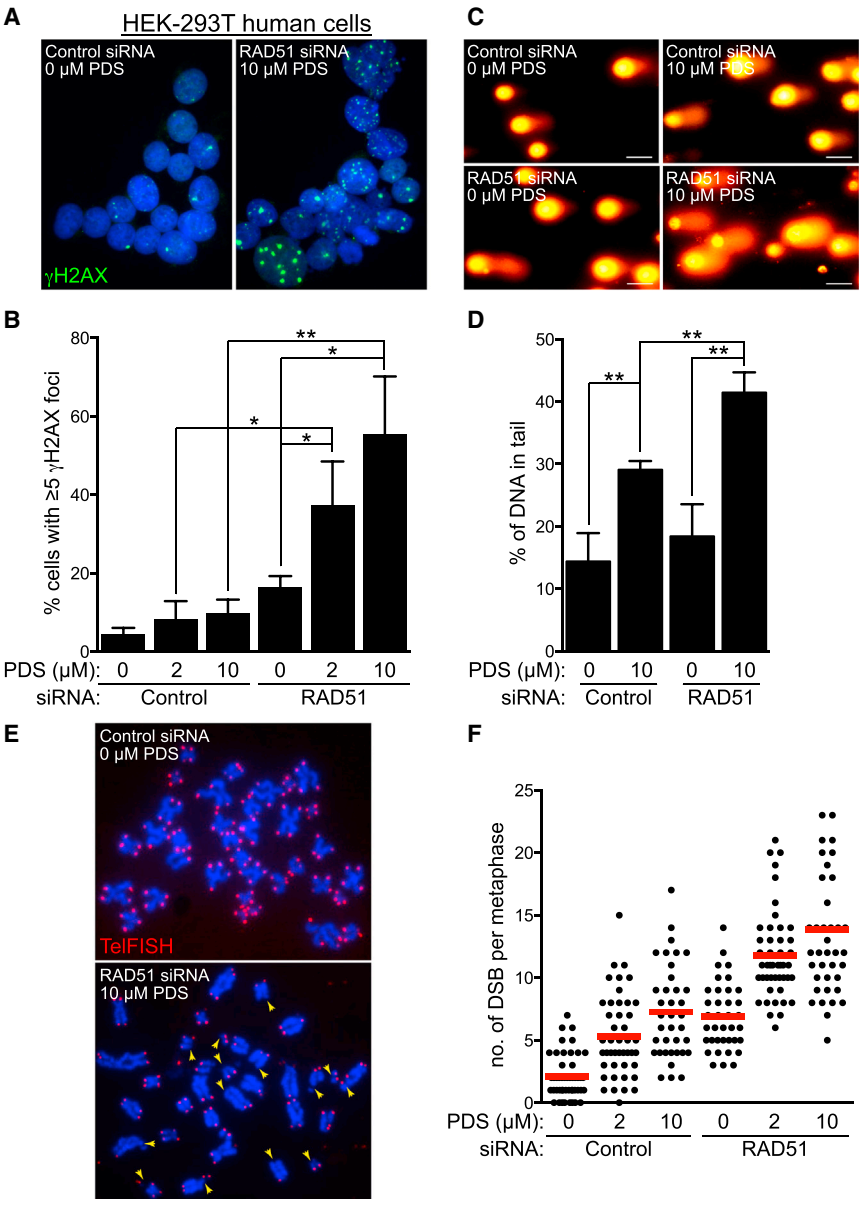


Figure 4. Elevated Levels of DNA Damage in RAD51-Deficient Human Cells Treated with PDS

(A) Representative images of HEK293T cells transfected with control or RAD51 siRNA and treated with PDS for 4 days before processing for immunofluorescence staining with anti-γH2AX antibody (green). DNA was counterstained with DAPI (blue).

(B) Quantification of the frequency of cells with ≥5 γH2AX foci treated as in (A); n = 3; error bars, SD. p values were calculated using an unpaired two-tailed t test (*$p \leq 0.05$; **$p \leq 0.01$).

(C) Representative images of cells treated as in (A) processed for comet assays. Scale bar, 50 μm.

(D) Quantification of tail moment using comet assays of cells treated as in (A); n = 3; error bars, SD. p values were calculated using an unpaired two-tailed t test (*$p \leq 0.05$).

(E) Representative images of FISH analysis of metaphase chromosome spreads of cells treated as in (A) with a Cy3-conjugated telomeric probe (red). DNA was counterstained with DAPI (blue). Arrowheads point to chromatid/chromosome breaks.

(F) Quantification of mean DSB frequencies (red bars) in cells treated as in (A). Approximately 40 metaphases were analyzed for each sample. See also Figure S3.

PDS Enhances DNA Damage Levels in HR-Compromised Cells

We next focused on understanding the mechanism underlying the impaired viability of RAD51-deficient cells in the presence of PDS. Quantification of γH2AX foci as detected by immunofluorescence staining (Figures 4A and S3A) revealed a significant increase in the frequency of HR-deficient cells containing γH2AX foci in response to PDS (Figure 4B). On average, 16.5% of untreated RAD51-depleted cells exhibited five or more γH2AX foci, which escalated to 37.3% and 55.4% following treatment with 2 or 10 μM PDS, respectively. In control cells, the focal γH2AX accumulation upon PDS treatment was not statistically significant (from 4.5% to 8.2% and 9.7%). Alkaline comet assays, in which the percentage of tail DNA relative to total DNA was indicative of the levels of DNA damage present in an individual cell (Figure 4C), confirmed that PDS-triggered DNA damage was significantly augmented in HR-deficient compared to HR-proficient cells (Figure 4D). In agreement with this, PDS elicited increased numbers of DBSs per metaphase in control cells, and RAD51 depletion further enhanced this effect (Figures 4E, 4F, and S3B). In these images we used telomeric FISH probes that helped define individual chromosomes. Given the reduced intensity of the FISH signal for the telomeric G-rich strand in PDS-treated samples, we increased acquisition time for these images, as described for Figure 2B. The average number of breaks detected in this assay reflects break accumulation in mitosis, while cells with higher levels of DNA damage most likely arrest during G2/M transition. Consistently, PDS treatment and RAD51 depletion caused a decrease in the mitotic index (Figure S3C). Taken together, these data supported the concept that G4 stabilization triggers DNA damage, with lethal consequences in cells with compromised capacity for HR-mediated repair.

Acute Replication Stress Induced by PDS in Cells Lacking RAD51 or BRCA2

PDS has been proposed to induce replication-dependent DNA damage (Rodriguez et al., 2012). This prompted us to monitor the assembly of replication protein A (RPA) subnuclear foci

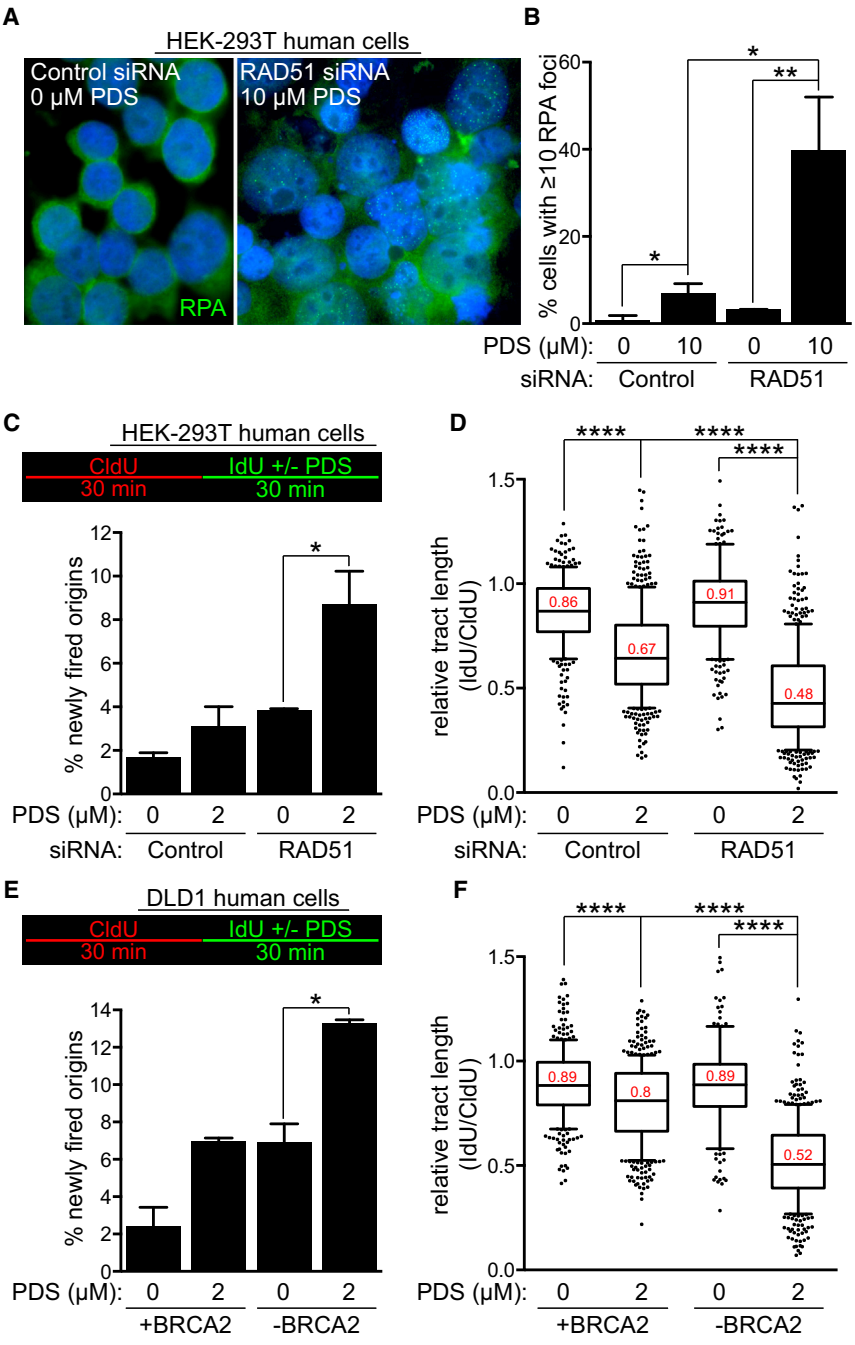


Figure 5. PDS Exacerbates the Replication Defect of RAD51- and BRCA2-Deficient Human Cells.

(A) Representative images of HEK293T cells transfected with control or RAD51 siRNA and treated with PDS for 4 days before processing for immunofluorescence staining with anti-RPA antibody (green). DNA was counterstained with DAPI (blue).

(B) Quantification of the frequency of cells with ≥10 RPA foci treated as in (A); n = 3; error bars, SD. p values were calculated using an unpaired two-tailed t test (*$p \leq 0.05$; **$p \leq 0.01$).

(C) HEK293T cells transfected with control or RAD51 esiRNA were processed for DNA fiber analysis as outlined in the inset, followed by quantification of the frequency of newly fired origins (n = 2; error bars, SD). p values were calculated using an unpaired two-tailed t test (*$p \leq 0.05$).

(D) Quantification of the relative replication tract length (IdU/CldU) in cells treated as in (C). Middle line represents median, and the box extends from the 25th to 75th percentiles. The whiskers mark the 10th and 90th percentiles. p values were calculated using a Mann-Whitney test (n = 2; ****$p < 0.0001$).

(E) DLD1 cells, BRCA2 proficient (+BRCA2) or deficient (−BRCA2), were processed for DNA fiber analysis as outlined in the inset, followed by quantification of the frequency of newly fired origins (n = 2; error bars, SD). p values were calculated using an unpaired two-tailed t test (*$p \leq 0.05$).

(F) Quantification of the relative replication tract length (IdU/CldU) in cells treated as in (E). Middle line represents median, and the box extends from the 25th to 75th percentiles. The whiskers mark the 10th and 90th percentiles. p values were calculated using a Mann-Whitney test (n = 2; ****$p < 0.0001$). See also Figure S4.

(Figures 5A and S4A) as a readout for genome-wide ssDNA accumulation. PDS induced an approximately 6-fold increase in the levels of RPA foci in control cells and approximately 12-fold increase in RAD51-deficient cells (Figure 5B). RPA accumulation on the chromatin, together with elevated frequency of origin firing and reduced replication rates, represents signatures of replicative stress (Zeman and Cimprich, 2014). To define the nature of this replication defect, we performed DNA fiber analyses in which replication tracks were labeled with consecutive 30 min pulses of CldU and IdU. Addition of PDS during the second pulse enabled us to evaluate the immediate effect of G4 stabilization on replication. Relative tract length was decreased significantly in PDS-treated cells compared to untreated cells, an effect that was more prominent in cells lacking RAD51 or BRCA2 expression (Figures 5D, 5F, S4B, and S4C). PDS may induce persistent G4s that reduce replication rate or cause DNA breakage that obstructs replication fork progression. Possibly as a compensatory mechanism, PDS treatment significantly increased the number of newly fired origins, detected as green tract only, specifically in RAD51- (Figure 5C) or BRCA2-deficient cells (Figure 5E). Notably, elevated origin firing was also detected in untreated HR-deficient cells. Thus, the replication stress endogenous to HR-compromised cells may be potentiated by chemical G4 stabilization to levels that become lethal. To test this possibility, we used aphidicolin as an alternative means to elicit replication stress (Figure S4D). Treatment with a nontoxic

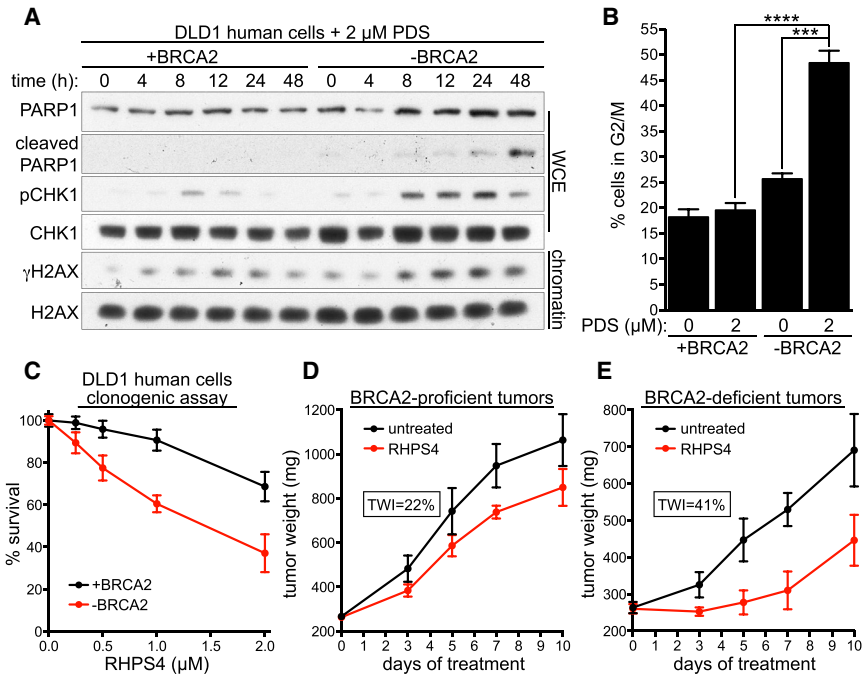


Figure 6. Effect of PDS on Viability of BRCA2-Deficient Cells and Tumors

(A) DLD1 cells, BRCA2 proficient (+BRCA2) or deficient (−BRCA2), were incubated with 2 μM PDS. Whole-cell extracts (WCE) or chromatin fractions prepared at indicated time points were immunoblotted as shown.

(B) Cells treated as in (A) were processed for FACS analyses of DNA content after 48 hr. Quantification of the percentage of cells in G2/M is shown (n = 3; error bars, SD). p values were calculated using an unpaired two-tailed t test (***$p \leq 0.001$; ****$p \leq 0.0001$).

(C) Clonogenic survival assays of DLD1 cells, BRCA2 proficient (+BRCA2) or deficient (−BRCA2), exposed to the indicated concentrations of RHPS4 for 24 hr. Error bars represent SD of triplicate values obtained from a single experiment.

(D and E) Mean tumor weights in untreated and RHPS4-treated mice injected with BRCA2-proficient (+BRCA2; D) or deficient (−BRCA2; E) DLD1 cells (n = 8; error bars, SD). Tumor weight inhibition (TWI) was calculated at the time point of maximum effect. See also Figures S5 and S6.

dose of aphidicolin led to sensitization of BRCA2-proficient cells to PDS. The synergy between the two compounds was not observed in BRCA2-deficient cells. This suggested that BRCA2 abrogation and aphidicolin treatment cause equivalent levels of replication stress and DNA damage, leading to comparable outcomes in the context of G4 stabilization by PDS.

PDS Triggers Checkpoint Activation and G2/M Arrest in HR-Defective Cells

Given the profound antiproliferative effect of PDS in BRCA2- or RAD51-deficient cells, we examined its impact on the DNA damage response (DDR). In cells lacking BRCA2 or RAD51 expression, continuous PDS treatment for 4 days elicited a robust phosphorylation of KAP1 (Ser824), CHK1 (Ser314/345), and RPA (Ser4/8), indicative of ATM/ATR checkpoint activation, as well as PARP1 cleavage, a marker for apoptosis (Figures S5A and S5B). To establish whether DDR preceded apoptosis onset, we monitored the response to PDS over a 48 hr interval. In BRCA2-deficient cells, PDS triggered H2AX and CHK1 phosphorylation after 8 hr of treatment, whereas PARP1 cleavage was initiated between 24 hr and 48 hr (Figure 6A). RAD51-depleted HEK293T cells similarly exhibited γH2AX activation prior to PARP1 cleavage (Figure S5C). These results indicate that PDS-induced DDRs are provoked prior to apoptosis in cells lacking BRCA2 or RAD51. Accordingly, BRCA2- and RAD51-deficient cells accumulated in G2/M after PDS treatment (Figures 6B and S6A). A decrease in S-phase cells further reflected the effect of PDS on cell-cycle progression and checkpoint activation specifically in HR-deficient cells (Figures S6A and S6B). PDS induces replication-associated DSBs, although transcription-related DNA damage may accumulate in stages of the cell cycle other than S phase (Rodriguez et al., 2012). To address whether PDS causes damage in noncycling cells, G0/G1 arrest was induced by serum starvation in the presence or absence of PDS. Arrested cells lacked the ability to incorporate the thymidine analog EdU, in contrast to cells released into the cell cycle by serum addition to the media (Figure S6C). Quantification of γH2AX-positive cells demonstrated that PDS treatment for 48 hr did not induce DNA damage in noncycling cells, while a marked increase in the percentage of cells expressing γH2AX was detected in the subset of cycling cells treated with PDS (Figure S6C).

In Vivo Responses of BRCA2-Deficient Tumors to G4 Ligands

Regardless of the effective suppression of HR-deficient cell viability and survival by PDS-mediated G4 stabilization (Figures 3A and S2D), the efficacy of PDS could not be established in vivo due to its toxicity predicted by in vitro studies (Rodriguez et al., 2012). Instead, we tested in our cellular models a previously reported G4-stabilizing drug, RHPS4 (Gavathiotis et al., 2003; Gowan et al., 2001; Heald et al., 2002), with well-characterized pharmacological features (Leonetti et al., 2008; Salvati et al., 2007). RHPS4 markedly diminished survival of BRCA2-deficient DLD1 cells relative to BRCA2-proficient cells (Figure 6C). To test its efficacy in vivo, DLD1 cells were injected into mice and allowed to form palpable tumors. In line with previous publications reporting the antitumor effect of RHPS4 (Leonetti et al., 2008; Salvati et al., 2007), this drug repressed growth of BRCA2-proficient tumors as assessed by tumor weight inhibition (TWI) (22%, Figure 6D). Importantly, the growth inhibitory effect of RHPS4 was almost twice as pronounced in BRCA2-deficient tumors (TWI = 41%, Figure 6E). RHPS4 treatment elicited a marked delay in tumor regrowth (approximately 7 days in BRCA2-deficient compared to 4 days in BRCA2-proficient tumors). Thus, our conclusions based on cellular models can be translated

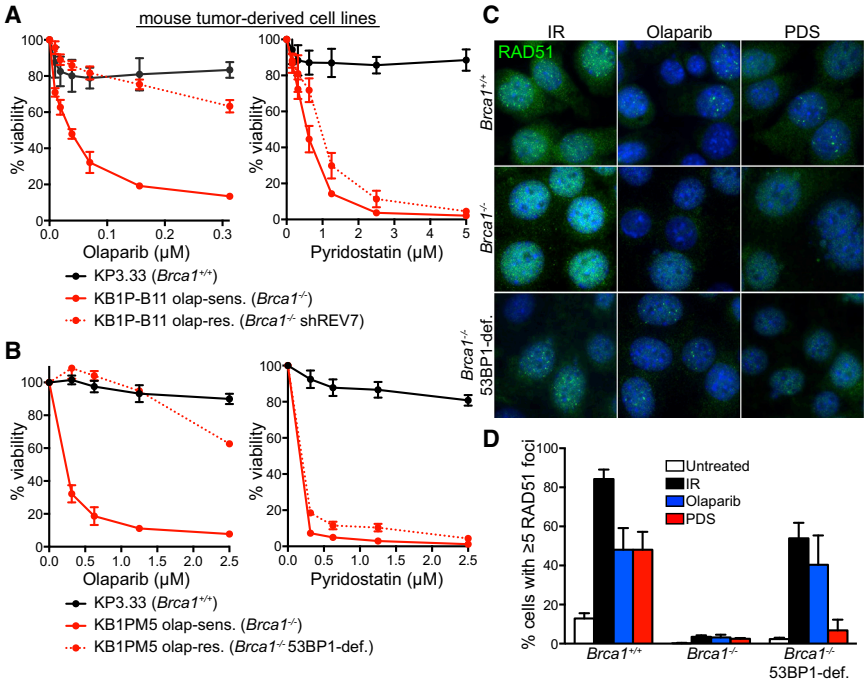


Figure 7. Olaparib-Resistant *Brca1*-Deleted Tumor Cells Exhibit PDS Sensitivity

(A and B) Dose-dependent viability assays of mouse mammary tumor-derived cell lines deficient in REV7 (A) or 53BP1 (B) treated with indicated concentrations of PDS or olaparib. Graphs shown are representative of at least two independent experiments, each performed in triplicate. Error bars represent SD of triplicate values obtained from a single experiment.

(C) Representative images of cells described in (A) incubated with 0.5 μM olaparib (OLAP), PDS for 40 hr, or irradiated with 10 Gy of IR followed by 1 hr recovery and processed for immunofluorescence staining with anti-RAD51 antibody (green). DNA was counterstained with DAPI (blue).

(D) Quantification of the frequency of cells with ≥5 RAD51 foci in cells treated as in (C); n = 2; error bars, SD; >200 nuclei were analyzed for each condition per replica. See also Figure S7.

in vivo and support the concept that G4-stabilizing compounds identify a class of drugs, which may facilitate future development of novel therapeutic strategies for targeting BRCA2-deficient tumors.

PDS Kills Olaparib-Resistant Tumor-Derived Cells

Treatment of BRCA-deficient tumors poses a major challenge in the clinic due to the rapid emergence of drug resistance. To test the potential of PDS to eliminate *Brca1*-deficient mouse tumor-derived cells refractory to olaparib, we used two *Brca1*$^{-/-}$ cellular mouse models, in which olaparib resistance was mediated by concomitant loss of REV7 (Figure 7A; Xu et al., 2015) or 53BP1 (Figure 7B; Jaspers et al., 2013). Cells carrying intact *Brca1* (*Brca1*$^{+/+}$) showed no sensitivity to PDS or olaparib, while cells established from a *Brca1*$^{-/-}$ tumor were sensitive to both drugs, as determined in viability and clonogenic assays (Figures 7A, 7B, S7A, and S7B). Strikingly, olaparib-resistant *Brca1*-deficient cells lacking REV7 or 53BP1 expression (*Brca1*$^{-/-}$ shREV7; *Brca1*$^{-/-}$ 53BP1-deficient) were hypersensitive to PDS (Figures 7A, 7B, S7A, and S7B). These effects were recapitulated in human cells, in which 53BP1 and BRCA1 were depleted using siRNA (Figure S7C). Our results, therefore, strongly suggest that BRCA1-deficient cells, including those resistant to PARP inhibitors, can be targeted by treatment with G4-stabilizing compounds.

HR restoration in *Brca1*-deleted cells and tumors is driven by 53BP1 loss, which enables survival (Bouwman et al., 2010; Bunting et al., 2010). Moreover, ionizing radiation (IR)-induced RAD51 foci assemble in olaparib-resistant *Brca1*$^{-/-}$, 53BP1-deficient cells (albeit not at the same level as in *Brca1*$^{+/+}$ cells), but not in olaparib-sensitive *Brca1*$^{-/-}$ tumor-derived cells (Jaspers et al., 2013). Our data (Figures 7C and 7D) demonstrate that olaparib treatment itself triggers RAD51 foci in wild-type and olaparib-resistant, but not olaparib-sensitive, cells, thereby providing a direct correlation between olaparib-induced HR reactivation and its impact on cell survival. PDS treatment induced RAD51 foci in *Brca1*$^{+/+}$ cells, similarly to olaparib (Figures 7C and 7D). However, RAD51 foci were absent in both olaparib-sensitive and olaparib-resistant cells upon treatment with PDS (Figures 7C and 7D), suggesting that failure to reactivate HR repair contributes to the toxicity of this compound in *Brca1*$^{-/-}$, 53BP1-deficient cells. To gain further insight into the mechanism of RAD51 foci suppression, we evaluated the levels of chromatin-associated RPA, indicative of end resection activity. In the chromatin fraction of PDS-treated cells, less RPA was detected than in cells exposed to olaparib or IR (Figure S7D). Thus, impaired HR reactivation upon PDS treatment in a *Brca1*$^{-/-}$, 53BP1-deficient background is likely caused by defects in end resection.

DISCUSSION

The ability of G-rich DNA to adopt G4 secondary structures in vitro was reported over 50 years ago (Gellert et al., 1962). Although G4s are thought to positively regulate key cellular processes, they can also obstruct replication-fork progression, leading to genomic instability (Tarsounas and Tijsterman, 2013). In this study, we establish that effective replication of G4 structures requires HR activities. G4s represent potent replication barriers, and HR provides a well-characterized mechanism for replication-fork restart and repair of replication-associated DSBs. Yet, the potential requirement for HR in G4 stability has not been investigated, with the notable exception of *Saccharomyces cerevisiae pif1* mutants, in which attempts to restart forks stalled in the vicinity of G4 structures generated recombination intermediates. This suggested a role for HR in fork restart when Pif1 activity is abrogated (Ribeyre et al., 2009).

HR Is Required for Effective Replication of Genomic Regions with G4-Forming Potential

HR factors have previously been implicated in telomere maintenance (Tacconi and Tarsounas, 2015). In the present work, we used a plasmid-based replication assay in human cells to show that replication of telomeric repeats is ineffective when key HR activities are abrogated. Two lines of evidence established the HR requirement for replication of the G-rich telomeric strand. First, telomere fragility triggered by HR gene deletion was specific to the G-rich telomeric strand, which possesses G4-forming potential. Second, disruption of the G4-forming telomeric repeats through G-to-C substitutions rescued its replication defect in HR-deficient cells.

We propose that HR promotes replication in the presence of obstructive G4 structures by restarting stalled forks and/or by repairing replication-associated DSBs within telomeres, rather than contributing to telomeric G4 dissolution per se. The latter process is likely mediated by the shelterin component TRF1, which recruits BLM helicase to telomeres to unwind G4 structures (Zimmermann et al., 2014). The concept that HR and shelterin provide distinct mechanisms for telomere replication is supported by the synthetic lethality observed between *Brca2* and *Trf1* gene deletions in immortalized MEFs, accompanied by additive levels of telomere fragility (Badie et al., 2010). Inhibition of BLM expression with shRNA in *Brca2*-deleted cells similarly induced cell-cycle arrest (J.Z. and M.T., unpublished data), further arguing that independent mechanisms act during telomere replication to dismantle G4s and to repair the DNA damage induced by persistent G4 structures.

Importantly, G4 stabilization by PDS reduced viability of mouse, human, and hamster cells lacking BRCA1, BRCA2, or RAD51. It exacerbated telomere fragility and DNA damage levels in HR-deficient cells. Conceivably, unresolved G4s presenting intrachromosomally or within telomeres are converted to DSBs, eliciting in turn checkpoint activation, cell-cycle arrest, and/or specific elimination of HR-compromised cells by apoptotic mechanisms.

The efficacy of PDS in cell killing was previously attributed to its genome-wide toxicity, suggested by the accumulation of DNA damage marker γH2AX at genomic sites with computationally inferred G4-forming sequences (Rodriguez et al., 2012). It is conceivable that the same sites may be prone to breakage in HR-deficient cells treated with PDS. Our mitotic DSB quantification illustrates the additive effect of PDS on the levels of DNA damage triggered by HR abrogation itself. A conundrum posed by this quantification was that PDS induced approximately fifteen DSBs per metaphase in cells lacking RAD51, yet in silico predictions suggested that more than 300,000 genomic sites can adopt G4 configurations (Huppert and Balasubramanian, 2005). This discrepancy could be explained by the multitude of mechanisms known to maintain genome integrity by dismantling G4s formed during genome replication (Tarsounas and Tijsterman, 2013). While most genomic G4s are dissolved by alternative mechanisms, our data suggest that a subset triggers fork stalling and DSBs, which are particularly toxic in HR-deficient cells lacking a key pathway of fork restart and break repair. G4-induced DNA damage may be repaired by error-prone mechanisms in the absence of HR, which seems insufficient for the survival of these cells. Moreover, checkpoint activation prevented entry of cells with elevated DSB levels into mitosis, which further justifies the lower number of mitotic DSBs detected in our assay.

Implications for Cancer Therapies

The work presented here demonstrates that the G4-stabilizing drug RHPS4 limits the growth of BRCA2-deficient tumors grafted in mice. The well-characterized ability of RHPS4 to trigger telomere dysfunction may contribute to its toxicity to BRCA2-deficient cells (Salvati et al., 2007). Therefore, we propose that the anticancer potential of the G4-stabilizing drug RHPS4 can be exploited in the clinic for specific targeting of BRCA2-deficient tumors. This tumor subset is likely to benefit most from this novel class of anticancer drugs. Furthermore, these results open a favorable prospective for future clinical development of PDS into a drug-like compound, with a more robust anticipated antitumor activity than RHPS4 in models for BRCA2 inactivation.

Mutations in HR genes such as *BRCA1*, *BRCA2*, or *RAD51C* predispose individuals to breast and ovarian cancers. Tumors carrying HR gene deletions are vulnerable to drugs that either introduce replication-associated DNA damage (e.g., platinum drugs) or inhibit DNA repair pathways other than HR (e.g., PARP1 inhibitors, such as olaparib). In both cases, excessive DNA-damage accumulation triggers cell death. Here, we propose that G4-binding compounds identify a novel class of molecules that can be used to target BRCA deficiency. They act by stabilizing secondary structures in genomic regions with high G-rich content, thus reducing replication fork speed and inducing RPA foci indicative of ssDNA accumulation. *BRCA* gene abrogation is associated with the same responses (Carlos et al., 2013). In the absence of HR, G4-interacting compounds are likely to elevate the endogenous replication stress to levels that become lethal due to excessive DNA-damage accumulation.

One well-documented caveat of targeted drug treatments, such as olaparib, is that tumors rapidly acquire resistance through mechanisms that include activation of P-glycoprotein drug efflux transporter, genetic *Brca1/2* re-activation, and loss of 53BP1/REV7 (Bouwman and Jonkers, 2014; Jaspers et al., 2013; Xu et al., 2015). In this work, we establish that G4-stabilizing compounds are profoundly toxic to BRCA-defective cells, including those resistant to PARP inhibitors. In particular, the striking cytotoxicity of PDS is due to the combined replication failure induced by this drug and the DNA repair defect associated with HR abrogation. Therefore, pharmacological G4 stabilization could be exploited in future therapeutic modalities targeting this difficult to treat tumor subset. Olaparib-resistant cells fail to reactivate HR in response to PDS, which may account for the lethality induced by this G4-stabilizing compound. We therefore anticipate that further clinical development of G4-stabilizing compounds will enhance their ability to selectively eliminate HR-compromised tumors, including those that have acquired resistance to existing therapies.

EXPERIMENTAL PROCEDURES

For detailed descriptions of these and additional procedures, see Supplemental Experimental Procedures.

Cell Lines, Culture Conditions, and In Vivo Experiments

HEK293T, H1299, and DLD1 cells were cultured under conventional growth conditions. In vivo experiments were performed as previously described (Salvati et al., 2007). All animal procedures were in compliance with the national and international directives (D.L. March 4, 2014, no. 26; directive 2010/63/EU of the European Parliament and of the council; Guide for the Care and Use of Laboratory Animals, United States National Research Council, 2011).

Plasmid-Based Replication Assay

Plasmid-based replication assays were performed as previously described (Sarkies et al., 2010; Szüts et al., 2008) with modifications listed in Supplemental Experimental Procedures.

RNAi

DLD1 and HEK293T cells were transfected with 40 nM siRNA using Dharmafect 1 (Dharmacon) according to manufacturer's instructions.

Cell Viability Assays

Cell viability was determined by incubation with 10 μg/ml of resazurin for 2 hr. Fluorescence was measured at 590 nm using a plate reader (POLARstar, Omega one). Cell viability was expressed relative to untreated cells of the same cell line, thus accounting for any differences in viability caused by HR deficiency. Graphs shown are representative of at least two independent experiments, each performed in triplicate. Error bars represent SD of triplicate values obtained from a single experiment.

FACS Analysis

Cells were harvested by trypsinization, washed in cold PBS, and fixed in ice-cold 70% ethanol overnight at 4°C. Following two washes in PBS, cells were incubated with 20 μg/ml propidium iodide and 10 μg/ml RNase A (Sigma) in PBS. At least 10,000 cells were analyzed by flow cytometry (Becton Dickinson). Data were processed using CellQuest (Becton Dickinson) and ModFit LT software.

Alkaline Single-Cell Gel Electrophoresis Comet Assay

The comet assay was performed as previously described (Singh et al., 1988). Tail measurement was performed using the Komet 5.5 image analysis software.

Immunofluorescence

Cells were subjected to immunofluorescence staining as described (Tarsounas et al., 2004).

Preparation of Metaphase Spreads and Telomere FISH

Metaphase spread preparation and telomeric FISH were performed as previously described (Badie et al., 2015).

Chromosome Orientation FISH and IF-FISH

For CO-FISH, cells were plated at 50%–60% confluency and treated with 10 μM bromodeoxyuridine (BrdU) for 20 hr. Colcemid (0.2 μg/ml) was added to the cells 4–6 hr before metaphases were processed for CO-FISH as previously described (Bailey et al., 2001).

For IF-FISH, metaphases were spun onto coverslips using a cytospin apparatus (Cytospin 4, Fisher) and subjected to immunofluorescence staining as described (Tarsounas et al., 2004). Samples were fixed again in 4% paraformaldehyde in PBS, and FISH was performed as described (Tarsounas et al., 2004) using 15 μg/ml Cy3-conjugated $(CCCTAA)_6$-PNA telomeric probe (Applied Biosystems).

DNA Fiber Assay

DNA fiber assays were performed as described previously (Jackson and Pombo, 1998).

Immunoblotting

SDS-PAGE and immunoblotting were performed as previously described (Badie et al., 2015). See Supplemental Experimental Procedures for antibodies used in this study.

SUPPLEMENTAL INFORMATION

Supplemental Information includes Supplemental Experimental Procedures and seven figures and can be found with this article online at http://dx.doi.org/10.1016/j.molcel.2015.12.004.

ACKNOWLEDGMENTS

E.M.C.T. and C.F. contributed equally to this work. We are grateful to Peter Bouwman and Alexandra Duarte (NKI, Amsterdam), Sven Rottenberg (Vetsuisse, University of Bern), Marie-Paule Teulade-Fichou (Curie Institute, Paris), Steve West (CRUK Clare Hall Laboratories), Hyunsook Lee (Seoul National University), and Carmen D'Angelo (Regina Elena Cancer Institute, Italy) for valuable reagents and/or technical suggestions. Research in the S.P.J. lab is funded by Cancer Research UK program grant C6/A11224, the European Research Council, and the European Community Seventh Framework Program grant agreement number HEALTH-F2-2010-259893 (DDResponse). Core infrastructure funding was provided by Cancer Research UK grant C6946/A14492 and Wellcome Trust grant WT092096. S.P.J. receives salary from the University of Cambridge, supplemented by Cancer Research UK. Research in the K.R. lab is supported by Medical Research Council (MC_PC_12001/1), University of Oxford, and Swiss National Science Foundation (31003A_141197). Work in the A.B. lab is supported by Italian Association for Cancer Research (AIRC # #11567). Work in the J.E.S. lab is supported by a central grant to the Laboratory of Molecular Biology, Cambridge from the Medical Research Council (U105178808). J.Z. is supported by a Cancer Research UK D.Phil. Studentship and E.M.C.T. by a Medical Research Council D.Phil. Studentship. Work in the M.T. lab is supported by Cancer Research UK, Medical Research Council, University of Oxford, and EMBO Young Investigator Program.

Received: March 27, 2015
Revised: September 17, 2015
Accepted: November 2, 2015
Published: December 31, 2015

REFERENCES

Aze, A., Zhou, J.C., Costa, A., and Costanzo, V. (2013). DNA replication and homologous recombination factors: acting together to maintain genome stability. Chromosoma *122*, 401–413.

Badie, S., Escandell, J.M., Bouwman, P., Carlos, A.R., Thanasoula, M., Gallardo, M.M., Suram, A., Jaco, I., Benitez, J., Herbig, U., et al. (2010). BRCA2 acts as a RAD51 loader to facilitate telomere replication and capping. Nat. Struct. Mol. Biol. *17*, 1461–1469.

Badie, S., Carlos, A.R., Folio, C., Okamoto, K., Bouwman, P., Jonkers, J., and Tarsounas, M. (2015). BRCA1 and CtIP promote alternative non-homologous end-joining at uncapped telomeres. EMBO J. *34*, 828.

Bailey, S.M., Cornforth, M.N., Kurimasa, A., Chen, D.J., and Goodwin, E.H. (2001). Strand-specific postreplicative processing of mammalian telomeres. Science *293*, 2462–2465.

Biffi, G., Tannahill, D., McCafferty, J., and Balasubramanian, S. (2013). Quantitative visualization of DNA G-quadruplex structures in human cells. Nat. Chem. *5*, 182–186.

Bouwman, P., and Jonkers, J. (2014). Molecular pathways: how can BRCA-mutated tumors become resistant to PARP inhibitors? Clin. Cancer Res. *20*, 540–547.

Bouwman, P., Aly, A., Escandell, J.M., Pieterse, M., Bartkova, J., van der Gulden, H., Hiddingh, S., Thanasoula, M., Kulkarni, A., Yang, Q., et al. (2010). 53BP1 loss rescues BRCA1 deficiency and is associated with triple-negative and BRCA-mutated breast cancers. Nat. Struct. Mol. Biol. *17*, 688–695.

Bunting, S.F., Callén, E., Wong, N., Chen, H.T., Polato, F., Gunn, A., Bothmer, A., Feldhahn, N., Fernandez-Capetillo, O., Cao, L., et al. (2010). 53BP1 inhibits

homologous recombination in Brca1-deficient cells by blocking resection of DNA breaks. Cell *141*, 243–254.

Carlos, A.R., Escandell, J.M., Kotsantis, P., Suwaki, N., Bouwman, P., Badie, S., Folio, C., Benitez, J., Gomez-Lopez, G., Pisano, D.G., et al. (2013). ARF triggers senescence in Brca2-deficient cells by altering the spectrum of p53 transcriptional targets. Nat. Commun. *4*, 2697.

Chambers, V.S., Marsico, G., Boutell, J.M., Di Antonio, M., Smith, G.P., and Balasubramanian, S. (2015). High-throughput sequencing of DNA G-quadruplex structures in the human genome. Nat. Biotechnol. *33*, 877–881.

Evers, B., Schut, E., van der Burg, E., Braumuller, T.M., Egan, D.A., Holstege, H., Edser, P., Adams, D.J., Wade-Martins, R., Bouwman, P., and Jonkers, J. (2010). A high-throughput pharmaceutical screen identifies compounds with specific toxicity against BRCA2-deficient tumors. Clin. Cancer Res. *16*, 99–108.

Gavathiotis, E., Heald, R.A., Stevens, M.F., and Searle, M.S. (2003). Drug recognition and stabilisation of the parallel-stranded DNA quadruplex d(TTAGGGT)4 containing the human telomeric repeat. J. Mol. Biol. *334*, 25–36.

Gellert, M., Lipsett, M.N., and Davies, D.R. (1962). Helix formation by guanylic acid. Proc. Natl. Acad. Sci. USA *48*, 2013–2018.

Gomez, D., Wenner, T., Brassart, B., Douarre, C., O'Donohue, M.F., El Khoury, V., Shin-Ya, K., Morjani, H., Trentesaux, C., and Riou, J.F. (2006). Telomestatin-induced telomere uncapping is modulated by POT1 through G-overhang extension in HT1080 human tumor cells. J. Biol. Chem. *281*, 38721–38729.

Gowan, S.M., Heald, R., Stevens, M.F., and Kelland, L.R. (2001). Potent inhibition of telomerase by small-molecule pentacyclic acridines capable of interacting with G-quadruplexes. Mol. Pharmacol. *60*, 981–988.

Halazonetis, T.D., Gorgoulis, V.G., and Bartek, J. (2008). An oncogene-induced DNA damage model for cancer development. Science *319*, 1352–1355.

Hashimoto, Y., Ray Chaudhuri, A., Lopes, M., and Costanzo, V. (2010). Rad51 protects nascent DNA from Mre11-dependent degradation and promotes continuous DNA synthesis. Nat. Struct. Mol. Biol. *17*, 1305–1311.

Heald, R.A., Modi, C., Cookson, J.C., Hutchinson, I., Laughton, C.A., Gowan, S.M., Kelland, L.R., and Stevens, M.F. (2002). Antitumor polycyclic acridines. 8.(1) Synthesis and telomerase-inhibitory activity of methylated pentacyclic acridinium salts. J. Med. Chem. *45*, 590–597.

Henderson, A., Wu, Y., Huang, Y.C., Chavez, E.A., Platt, J., Johnson, F.B., Brosh, R.M.J., Jr., Sen, D., and Lansdorp, P.M. (2014). Detection of G-quadruplex DNA in mammalian cells. Nucleic Acids Res. *42*, 860–869.

Hucl, T., Rago, C., Gallmeier, E., Brody, J.R., Gorospe, M., and Kern, S.E. (2008). A syngeneic variance library for functional annotation of human variation: application to BRCA2. Cancer Res. *68*, 5023–5030.

Huppert, J.L., and Balasubramanian, S. (2005). Prevalence of quadruplexes in the human genome. Nucleic Acids Res. *33*, 2908–2916.

Jackson, D.A., and Pombo, A. (1998). Replicon clusters are stable units of chromosome structure: evidence that nuclear organization contributes to the efficient activation and propagation of S phase in human cells. J. Cell Biol. *140*, 1285–1295.

Jaspers, J.E., Kersbergen, A., Boon, U., Sol, W., van Deemter, L., Zander, S.A., Drost, R., Wientjens, E., Ji, J., Aly, A., et al. (2013). Loss of 53BP1 causes PARP inhibitor resistance in Brca1-mutated mouse mammary tumors. Cancer Discov. *3*, 68–81.

Kraakman-van der Zwet, M., Overkamp, W.J.I., van Lange, R.E.E., Essers, J., van Duijn-Goedhart, A., Wiggers, I., Swaminathan, S., van Buul, P.P.W., Errami, A., Tan, R.T.L., et al. (2002). Brca2 (XRCC11) deficiency results in radioresistant DNA synthesis and a higher frequency of spontaneous deletions. Mol. Cell. Biol. *22*, 669–679.

Lam, E.Y., Beraldi, D., Tannahill, D., and Balasubramanian, S. (2013). G-quadruplex structures are stable and detectable in human genomic DNA. Nat. Commun. *4*, 1796.

Lambert, S., Mizuno, K., Blaisonneau, J., Martineau, S., Chanet, R., Fréon, K., Murray, J.M., Carr, A.M., and Baldacci, G. (2010). Homologous recombination restarts blocked replication forks at the expense of genome rearrangements by template exchange. Mol. Cell *39*, 346–359.

Leonetti, C., Scarsella, M., Riggio, G., Rizzo, A., Salvati, E., D'Incalci, M., Staszewsky, L., Frapolli, R., Stevens, M.F., Stoppacciaro, A., et al. (2008). G-quadruplex ligand RHPS4 potentiates the antitumor activity of camptothecins in preclinical models of solid tumors. Clin. Cancer Res. *14*, 7284–7291.

Lipps, H.J., and Rhodes, D. (2009). G-quadruplex structures: in vivo evidence and function. Trends Cell Biol. *19*, 414–422.

Martínez, P., Thanasoula, M., Muñoz, P., Liao, C., Tejera, A., McNees, C., Flores, J.M., Fernández-Capetillo, O., Tarsounas, M., and Blasco, M.A. (2009). Increased telomere fragility and fusions resulting from TRF1 deficiency lead to degenerative pathologies and increased cancer in mice. Genes Dev. *23*, 2060–2075.

Müller, S., Kumari, S., Rodriguez, R., and Balasubramanian, S. (2010). Small-molecule-mediated G-quadruplex isolation from human cells. Nat. Chem. *2*, 1095–1098.

Murat, P., and Balasubramanian, S. (2014). Existence and consequences of G-quadruplex structures in DNA. Curr. Opin. Genet. Dev. *25*, 22–29.

Negrini, S., Gorgoulis, V.G., and Halazonetis, T.D. (2010). Genomic instability–an evolving hallmark of cancer. Nat. Rev. Mol. Cell Biol. *11*, 220–228.

Parkinson, G.N., Lee, M.P., and Neidle, S. (2002). Crystal structure of parallel quadruplexes from human telomeric DNA. Nature *417*, 876–880.

Piazza, A., Boulé, J.B., Lopes, J., Mingo, K., Largy, E., Teulade-Fichou, M.P., and Nicolas, A. (2010). Genetic instability triggered by G-quadruplex interacting Phen-DC compounds in Saccharomyces cerevisiae. Nucleic Acids Res. *38*, 4337–4348.

Ribeyre, C., Lopes, J., Boulé, J.B., Piazza, A., Guédin, A., Zakian, V.A., Mergny, J.L., and Nicolas, A. (2009). The yeast Pif1 helicase prevents genomic instability caused by G-quadruplex-forming CEB1 sequences in vivo. PLoS Genet. *5*, e1000475.

Rodriguez, R., Müller, S., Yeoman, J.A., Trentesaux, C., Riou, J.F., and Balasubramanian, S. (2008). A novel small molecule that alters shelterin integrity and triggers a DNA-damage response at telomeres. J. Am. Chem. Soc. *130*, 15758–15759.

Rodriguez, R., Miller, K.M., Forment, J.V., Bradshaw, C.R., Nikan, M., Britton, S., Oelschlaegel, T., Xhemalce, B., Balasubramanian, S., and Jackson, S.P. (2012). Small-molecule-induced DNA damage identifies alternative DNA structures in human genes. Nat. Chem. Biol. *8*, 301–310.

Rogakou, E.P., Nieves-Neira, W., Boon, C., Pommier, Y., and Bonner, W.M. (2000). Initiation of DNA fragmentation during apoptosis induces phosphorylation of H2AX histone at serine 139. J. Biol. Chem. *275*, 9390–9395.

Salvati, E., Leonetti, C., Rizzo, A., Scarsella, M., Mottolese, M., Galati, R., Sperduti, I., Stevens, M.F., D'Incalci, M., Blasco, M., et al. (2007). Telomere damage induced by the G-quadruplex ligand RHPS4 has an antitumor effect. J. Clin. Invest. *117*, 3236–3247.

Sarkies, P., Reams, C., Simpson, L.J., and Sale, J.E. (2010). Epigenetic instability due to defective replication of structured DNA. Mol. Cell *40*, 703–713.

Schaffitzel, C., Berger, I., Postberg, J., Hanes, J., Lipps, H.J., and Plückthun, A. (2001). In vitro generated antibodies specific for telomeric guanine-quadruplex DNA react with Stylonychia lemnae macronuclei. Proc. Natl. Acad. Sci. USA *98*, 8572–8577.

Schlacher, K., Christ, N., Siaud, N., Egashira, A., Wu, H., and Jasin, M. (2011). Double-strand break repair-independent role for BRCA2 in blocking stalled replication fork degradation by MRE11. Cell *145*, 529–542.

Sfeir, A., Kosiyatrakul, S.T., Hockemeyer, D., MacRae, S.L., Karlseder, J., Schildkraut, C.L., and de Lange, T. (2009). Mammalian telomeres resemble fragile sites and require TRF1 for efficient replication. Cell *138*, 90–103.

Singh, N.P., McCoy, M.T., Tice, R.R., and Schneider, E.L. (1988). A simple technique for quantitation of low levels of DNA damage in individual cells. Exp. Cell Res. *175*, 184–191.

Suwaki, N., Klare, K., and Tarsounas, M. (2011). RAD51 paralogs: roles in DNA damage signalling, recombinational repair and tumorigenesis. Semin. Cell Dev. Biol. *22*, 898–905.

Szüts, D., Marcus, A.P., Himoto, M., Iwai, S., and Sale, J.E. (2008). REV1 restrains DNA polymerase zeta to ensure frame fidelity during translesion synthesis of UV photoproducts in vivo. Nucleic Acids Res. *36*, 6767–6780.

Tacconi, E.M., and Tarsounas, M. (2015). How homologous recombination maintains telomere integrity. Chromosoma *124*, 119–130.

Tahara, H., Shin-Ya, K., Seimiya, H., Yamada, H., Tsuruo, T., and Ide, T. (2006). G-Quadruplex stabilization by telomestatin induces TRF2 protein dissociation from telomeres and anaphase bridge formation accompanied by loss of the 3′ telomeric overhang in cancer cells. Oncogene *25*, 1955–1966.

Tarsounas, M., and Tijsterman, M. (2013). Genomes and G-quadruplexes: for better or for worse. J. Mol. Biol. *425*, 4782–4789.

Tarsounas, M., Muñoz, P., Claas, A., Smiraldo, P.G., Pittman, D.L., Blasco, M.A., and West, S.C. (2004). Telomere maintenance requires the RAD51D recombination/repair protein. Cell *117*, 337–347.

Xu, G., Chapman, J.R., Brandsma, I., Yuan, J., Mistrik, M., Bouwman, P., Bartkova, J., Gogola, E., Warmerdam, D., Barazas, M., et al. (2015). REV7 counteracts DNA double-strand break resection and affects PARP inhibition. Nature *521*, 541–544.

Zeman, M.K., and Cimprich, K.A. (2014). Causes and consequences of replication stress. Nat. Cell Biol. *16*, 2–9.

Zimmermann, M., Kibe, T., Kabir, S., and de Lange, T. (2014). TRF1 negotiates TTAGGG repeat-associated replication problems by recruiting the BLM helicase and the TPP1/POT1 repressor of ATR signaling. Genes Dev. *28*, 2477–2491.

8.3 Original copyright notices

ROYAL SOCIETY OF CHEMISTRY LICENSE TERMS AND CONDITIONS

Jun 08, 2017

This Agreement between Jutta Zimmer ("You") and Royal Society of Chemistry ("Royal Society of Chemistry") consists of your license details and the terms and conditions provided by Royal Society of Chemistry and Copyright Clearance Center.

License Number	4124211427552
License date	Jun 08, 2017
Licensed Content Publisher	Royal Society of Chemistry
Licensed Content Publication	Chemical Society Reviews
Licensed Content Title	Four-stranded nucleic acids: structure, function and targeting of G-quadruplexes
Licensed Content Author	Julian Leon Huppert
Licensed Content Date	May 6, 2008
Licensed Content Volume	37
Licensed Content Issue	7
Type of Use	Thesis/Dissertation
Requestor type	academic/educational
Portion	figures/tables/images
Number of figures/tables/images	1
Format	print and electronic
Distribution quantity	5
Will you be translating?	no
Order reference number	
Title of the thesis/dissertation	Roles of BRCA1 and BRCA2 in DNA Replication and Genome Stability
Expected completion date	Jul 2017
Estimated size	200
Requestor Location	Jutta Zimmer Oxford Institute for Radiation Oncology Old Road Campus Research Building Roosevelt Drive Oxford, OX3 7DQ United Kingdom Attn: Jutta Zimmer
Billing Type	Invoice
Billing Address	Jutta Zimmer Oxford Institute for Radiation Oncology Old Road Campus Research Building Roosevelt Drive

Oxford, United Kingdom OX3 7DQ
Attn: Jutta Zimmer

Total 0.00 USD

Terms and Conditions

This License Agreement is between {Requestor Name} ("You") and The Royal Society of Chemistry ("RSC") provided by the Copyright Clearance Center ("CCC"). The license consists of your order details, the terms and conditions provided by the Royal Society of Chemistry, and the payment terms and conditions.

RSC / TERMS AND CONDITIONS

INTRODUCTION

The publisher for this copyrighted material is The Royal Society of Chemistry. By clicking "accept" in connection with completing this licensing transaction, you agree that the following terms and conditions apply to this transaction (along with the Billing and Payment terms and conditions established by CCC, at the time that you opened your RightsLink account and that are available at any time at .

LICENSE GRANTED

The RSC hereby grants you a non-exclusive license to use the aforementioned material anywhere in the world subject to the terms and conditions indicated herein. Reproduction of the material is confined to the purpose and/or media for which permission is hereby given.

RESERVATION OF RIGHTS

The RSC reserves all rights not specifically granted in the combination of (i) the license details provided by your and accepted in the course of this licensing transaction; (ii) these terms and conditions; and (iii) CCC's Billing and Payment terms and conditions.

REVOCATION

The RSC reserves the right to revoke this license for any reason, including, but not limited to, advertising and promotional uses of RSC content, third party usage, and incorrect source figure attribution.

THIRD-PARTY MATERIAL DISCLAIMER

If part of the material to be used (for example, a figure) has appeared in the RSC publication with credit to another source, permission must also be sought from that source. If the other source is another RSC publication these details should be included in your RightsLink request. If the other source is a third party, permission must be obtained from the third party. The RSC disclaims any responsibility for the reproduction you make of items owned by a third party.

PAYMENT OF FEE

If the permission fee for the requested material is waived in this instance, please be advised that any future requests for the reproduction of RSC materials may attract a fee.

ACKNOWLEDGEMENT

The reproduction of the licensed material must be accompanied by the following acknowledgement:

Reproduced ("Adapted" or "in part") from {Reference Citation} (or Ref XX) with permission of The Royal Society of Chemistry.

If the licensed material is being reproduced from New Journal of Chemistry (NJC), Photochemical & Photobiological Sciences (PPS) or Physical Chemistry Chemical Physics (PCCP) you must include one of the following acknowledgements:

For figures originally published in NJC:

Reproduced ("Adapted" or "in part") from {Reference Citation} (or Ref XX) with permission of The Royal Society of Chemistry (RSC) on behalf of the European Society for Photobiology, the European Photochemistry Association and the RSC.

For figures originally published in PPS:

Reproduced (“Adapted” or “in part”) from {Reference Citation} (or Ref XX) with permission of The Royal Society of Chemistry (RSC) on behalf of the Centre National de la Recherche Scientifique (CNRS) and the RSC.
For figures originally published in PCCP:
Reproduced (“Adapted” or “in part”) from {Reference Citation} (or Ref XX) with permission of the PCCP Owner Societies.

HYPERTEXT LINKS

With any material which is being reproduced in electronic form, you must include a hypertext link to the original RSC article on the RSC’s website. The recommended form for the hyperlink is http://dx.doi.org/10.1039/DOI suffix, for example in the link http://dx.doi.org/10.1039/b110420a the DOI suffix is ‘b110420a’. To find the relevant DOI suffix for the RSC article in question, go to the Journals section of the website and locate the article in the list of papers for the volume and issue of your specific journal. You will find the DOI suffix quoted there.

LICENSE CONTINGENT ON PAYMENT

While you may exercise the rights licensed immediately upon issuance of the license at the end of the licensing process for the transaction, provided that you have disclosed complete and accurate details of your proposed use, no license is finally effective unless and until full payment is received from you (by CCC) as provided in CCC's Billing and Payment terms and conditions. If full payment is not received on a timely basis, then any license preliminarily granted shall be deemed automatically revoked and shall be void as if never granted. Further, in the event that you breach any of these terms and conditions or any of CCC's Billing and Payment terms and conditions, the license is automatically revoked and shall be void as if never granted. Use of materials as described in a revoked license, as well as any use of the materials beyond the scope of an unrevoked license, may constitute copyright infringement and the RSC reserves the right to take any and all action to protect its copyright in the materials.

WARRANTIES

The RSC makes no representations or warranties with respect to the licensed material.

INDEMNITY

You hereby indemnify and agree to hold harmless the RSC and the CCC, and their respective officers, directors, trustees, employees and agents, from and against any and all claims arising out of your use of the licensed material other than as specifically authorized pursuant to this licence.

NO TRANSFER OF LICENSE

This license is personal to you or your publisher and may not be sublicensed, assigned, or transferred by you to any other person without the RSC's written permission.

NO AMENDMENT EXCEPT IN WRITING

This license may not be amended except in a writing signed by both parties (or, in the case of “Other Conditions, v1.2”, by CCC on the RSC's behalf).

OBJECTION TO CONTRARY TERMS

You hereby acknowledge and agree that these terms and conditions, together with CCC's Billing and Payment terms and conditions (which are incorporated herein), comprise the entire agreement between you and the RSC (and CCC) concerning this licensing transaction, to the exclusion of all other terms and conditions, written or verbal, express or implied (including any terms contained in any purchase order, acknowledgment, check endorsement or other writing prepared by you). In the event of any conflict between your obligations established by these terms and conditions and those established by CCC's Billing and Payment terms and conditions, these terms and conditions shall control.

JURISDICTION

This license transaction shall be governed by and construed in accordance with the laws of the District of Columbia. You hereby agree to submit to the jurisdiction of the courts located in the District of Columbia for purposes of resolving any disputes that may arise in connection with this licensing transaction.

LIMITED LICENSE

The following terms and conditions apply to specific license types:

Translation

This permission is granted for non-exclusive world English rights only unless your license was granted for translation rights. If you licensed translation rights you may only translate this content into the languages you requested. A professional translator must perform all translations and reproduce the content word for word preserving the integrity of the article.

Intranet

If the licensed material is being posted on an Intranet, the Intranet is to be password-protected and made available only to bona fide students or employees only. All content posted to the Intranet must maintain the copyright information line on the bottom of each image. You must also fully reference the material and include a hypertext link as specified above.

Copies of Whole Articles

All copies of whole articles must maintain, if available, the copyright information line on the bottom of each page.

Other Conditions

v1.2

Gratis licenses (referencing $0 in the Total field) are free. Please retain this printable license for your reference. No payment is required.

If you would like to pay for this license now, please remit this license along with yourpayment made payable to "COPYRIGHT CLEARANCE CENTER" otherwise you will be invoiced within 48 hours of the license date. Payment should be in the form of a check or money order referencing your account number and this invoice number {Invoice Number}.

Once you receive your invoice for this order, you may pay your invoice by credit card. Please follow instructions provided at that time.

Make Payment To:

Copyright Clearance Center

29118 Network Place

Chicago, IL 60673-1291

For suggestions or comments regarding this order, contact Rightslink Customer Support: customercare@copyright.com or +1-855-239-3415 (toll free in the US) or +1-978-646-2777.

Questions? customercare@copyright.com or +1-855-239-3415 (toll free in the US) or +1-978-646-2777.

AMERICAN ASSOCIATION FOR CANCER RESEARCH LICENSE TERMS AND CONDITIONS

Sep 25, 2017

This Agreement between Jutta Zimmer ("You") and American Association for Cancer Research ("American Association for Cancer Research") consists of your license details and the terms and conditions provided by American Association for Cancer Research and Copyright Clearance Center.

License Number	4195811393410
License date	Sep 25, 2017
Licensed Content Publisher	American Association for Cancer Research
Licensed Content Publication	Cancer Research
Licensed Content Title	A Syngeneic Variance Library for Functional Annotation of Human Variation: Application to *BRCA2*
Licensed Content Author	Tomas Hucl,Carlo Rago,Eike Gallmeier,Jonathan R. Brody,Myriam Gorospe,Scott E. Kern
Licensed Content Date	Jul 1, 2008
Licensed Content Volume	68
Licensed Content Issue	13
Type of Use	Thesis/Dissertation
Requestor type	academic/educational
Format	print and electronic
Portion	figures/tables/illustrations
Number of figures/tables/illustrations	1
Will you be translating?	no
Circulation	5
Territory of distribution	Worldwide
Title of your thesis / dissertation	Roles of BRCA1 and BRCA2 in DNA Replication and Genome Stability
Expected completion date	Oct 2017
Estimated size (number of pages)	250
Requestor Location	Jutta Zimmer Oxford Institute for Radiation Oncology Old Road Campus Research Building Roosevelt Drive Oxford, OX3 7DQ United Kingdom Attn: Jutta Zimmer
Billing Type	Invoice
Billing Address	Jutta Zimmer

Oxford Institute for Radiation Oncology
Old Road Campus Research Building
Roosevelt Drive
Oxford, United Kingdom OX3 7DQ
Attn: Jutta Zimmer

Total 0.00 GBP

Terms and Conditions

American Association for Cancer Research (AACR) Terms and Conditions

INTRODUCTION
The Publisher for this copyright material is the American Association for Cancer Research (AACR). By clicking "accept" in connection with completing this licensing transaction, you agree to the following terms and conditions applying to this transaction. You also agree to the Billing and Payment terms and conditions established by Copyright Clearance Center (CCC) at the time you opened your Rightslink account.

LIMITED LICENSE
The AACR grants exclusively to you, the User, for onetime, non-exclusive use of this material for the purpose stated in your request and used only with a maximum distribution equal to the number you identified in the permission process. Any form of republication must be completed within one year although copies made before then may be distributed thereafter and any electronic posting is limited to a period of one year. Reproduction of this material is confined to the purpose and/or media for which permission is granted. Altering or modifying this material is not permitted. However, figures and illustrations may be minimally altered or modified to serve the new work.

GEOGRAPHIC SCOPE
Licenses may be exercised as noted in the permission process

RESERVATION OF RIGHTS
The AACR reserves all rights not specifically granted in the combination of 1) the license details provided by you and accepted in the course of this licensing transaction, 2) these terms and conditions , and 3) CCC's Billing and Payment terms and conditions.

DISCLAIMER
You may obtain permission via Rightslink to use material owned by AACR. When you are requesting permission to reuse a portion for an AACR publication, it is your responsibility to examine each portion of content as published to determine whether a credit to, or copyright notice of a third party owner is published next to the item. You must obtain permission from the third party to use any material which has been reprinted with permission from the said third party. If you have not obtained permission from the third party, AACR disclaims any responsibility for the use you make of items owned by them.

LICENSE CONTINGENT ON PAYMENT
While you may exercise the rights licensed immediately upon issuance of the license at the end of the licensing process for the transaction, provided that you have disclosed complete and accurate details of your proposed use, no license is finally effective unless and until full payment is received from you, either by the publisher or by the CCC, as provided in CCC's Billing and Payment terms and conditions. If full payment is not received on a timely basis, then any license preliminarily granted shall be deemed automatically revoked and shall be void as if never granted. Further, in the event that you breach any of these terms and conditions, or any of the CCC's Billing and Payment terms and conditions, the license is automatically revoked and shall be void as if never granted. Use of materials as described in a revoked license, as well as any use of the materials beyond the scope of an unrevoked license, may constitute copyright infringement and the publisher reserves the right to take

any and all action to protect its copyright in the materials.

COPYRIGHT NOTICE

You must include the following credit line in connection with your reproduction of the licensed material: "Reprinted (or adapted) from Publication Title, Copyright Year, Volume/Issue, Page Range, Author, Title of Article, with permission from AACR".

TRANSLATION

This permission is granted for non-exclusive world English rights only.

WARRANTIES

Publisher makes no representations or warranties with respect to the licensed material.

INDEMNIFICATION

You hereby indemnify and agree to hold harmless the publisher and CCC, and their respective officers, directors, employees and agents, from and against any and all claims arising out of your use of the licensed material other than as specifically authorized pursuant to this license.

REVOCATION

The AACR reserves the right to revoke a license for any reason, including but not limited to advertising and promotional uses of AACR content, third party usage and incorrect figure source attribution.

NO TRANSFER OF LICENSE

This license is personal to you and may not be sublicensed, assigned, or transferred by you to any other person without publisher's written permission.

NO AMENDMENT EXCEPT IN WRITING

This license may not be amended except in a writing signed by both parties (or, in the case of publisher, by CCC on publisher's behalf).

OBJECTION TO CONTRARY TERMS

Publishers hereby objects to any terms contained in any purchase order, acknowledgement, check endorsement or other writing prepared by you, which terms are inconsistent with these terms and conditions or CCC's Billing and Payment terms and conditions. These terms and conditions together with CCC's Billing and Payment terms and conditions (which are incorporated herein) comprise the entire agreement between you and publisher (and CCC) concerning this licensing transaction. In the event of any conflict between your obligations established by these terms and conditions, and those established by CCC's Billing and Payment terms and conditions, these terms and conditions shall control.

THESIS/DISSERTATION TERMS

If your request is to reuse an article authored by you and published by the AACR in your dissertation/thesis, your thesis may be submitted to your institution in either in print or electronic form. Should your thesis be published commercially, please reapply.

ELECTRONIC RESERVE

If this license is made in connection with a course, and the Licensed Material or any portion thereof is to be posted to a website, the website is to be password protected and made available only to the students registered for the relevant course. The permission is granted for the duration of the course. All content posted to the website must maintain the copyright information notice.

JURISDICTION

This license transaction shall be governed by and construed in accordance with the laws of Pennsylvania. You hereby agree to submit to the jurisdiction of the federal and state courts located in Pennsylvania for purposes of resolving any disputes that may arise in connection with this licensing transaction.

Other Terms and Conditions:

v1.0

Questions? customercare@copyright.com or +1-855-239-3415 (toll free in the US) or +1-978-646-2777.

Copyright Clearance Center RightsLink®

Home | Account Info | Help

Taylor & Francis
Taylor & Francis Group

Journal Reprints

Title: Single-vector inducible lentiviral RNAi system for oncology target validation

Author: Dmitri Wiederschain, Wee Susan, Lin Chen, et al

Publication: Cell Cycle

Publisher: Taylor & Francis

Date: Feb 1, 2009

Copyright © 2009 Taylor & Francis

Logged in as:
Jutta Zimmer

LOGOUT

Thesis/Dissertation Reuse Request

Taylor & Francis is pleased to offer reuses of its content for a thesis or dissertation free of charge contingent on resubmission of permission request if work is published.

BACK | CLOSE WINDOW

Copyright © 2017 Copyright Clearance Center, Inc. All Rights Reserved. Privacy statement. Terms and Conditions.
Comments? We would like to hear from you. E-mail us at customercare@copyright.com

Copyright Clearance Center RightsLink®

Home | Account Info | Help

Logged in as:
Jutta Zimmer
LOGOUT



Title: FANCD2 limits replication stress and genome instability in cells lacking BRCA2

Author: Johanna Michl, Jutta Zimmer, Francesca M Buffa, Ultan McDermott, Madalena Tarsounas

Publication: Nature Structural and Molecular Biology

Publisher: Nature Publishing Group

Date: Jun 20, 2016

Copyright © 2016, Rights Managed by Nature Publishing Group

Author Request

If you are the author of this content (or his/her designated agent) please read the following. If you are not the author of this content, please click the Back button and select an alternative Requestor Type to obtain a quick price or to place an order.

Ownership of copyright in the article remains with the Authors, and provided that, when reproducing the Contribution or extracts from it, the Authors acknowledge first and reference publication in the Journal, the Authors retain the following non-exclusive rights:

a) To reproduce the Contribution in whole or in part in any printed volume (book or thesis) of which they are the author(s).

b) They and any academic institution where they work at the time may reproduce the Contribution for the purpose of course teaching.

c) To reuse figures or tables created by them and contained in the Contribution in other works created by them.

d) To post a copy of the Contribution as accepted for publication after peer review (in Word or Text format) on the Author's own web site, or the Author's institutional repository, or the Author's funding body's archive, six months after publication of the printed or online edition of the Journal, provided that they also link to the Journal article on NPG's web site (eg through the DOI).

NPG encourages the self-archiving of the accepted version of your manuscript in your funding agency's or institution's repository, six months after publication. This policy complements the recently announced policies of the US National Institutes of Health, Wellcome Trust and other research funding bodies around the world. NPG recognises the efforts of funding bodies to increase access to the research they fund, and we strongly encourage authors to participate in such efforts.

Authors wishing to use the published version of their article for promotional use or on a web site must request in the normal way.

If you require further assistance please read NPG's online author reuse guidelines.

For full paper portion: Authors of original research papers published by NPG are encouraged to submit the author's version of the accepted, peer-reviewed manuscript to their relevant funding body's archive, for release six months after publication. In addition, authors are encouraged to archive their version of the manuscript in their institution's repositories (as well as their personal Web sites), also six months after original publication.

v2.0

BACK CLOSE WINDOW

Copyright © 2017 Copyright Clearance Center, Inc. All Rights Reserved. Privacy statement. Terms and Conditions.
Comments? We would like to hear from you. E-mail us at customercare@copyright.com